University of Florence

International Doctorate in Structural Biology

Cycle XXII (2007-2009)

Synthesis of new potential drugs

Ph.D. thesis of

Elisa Dragoni

Tutor	Coordinator
Prof. Cristina Nativi	Prof. Claudio Luchinat

S.S.D. CHIM/03

This thesis has been approved by the University of Florence,
the University of Frankfurt and the Utrecht University.

Index

Chapter 5. Synthesis of high-affinity, water soluble MMPs inhibitors

Chapter 6. Cyclic glycopeptidomimetics through versatile sugar-based scaffold

Chapter 1

Introduction

The continuous demand that the pharmaceutical and biotech companies are facing, has created the need to apply all available techniques to decrease attrition rates, costs and the time to market of new drugs. One of the main goal of the drug discovery process is the identification of a lead compound, that it is the starting point for the development of new candidate drugs.[1]

In the last two decades, the availability of structural information of a macromolecular target opens the door to Structure-Based Drug Design (SBDD).[2] The SBDD exploits the knowledge of the 3D structure of the biological targets and/or their ligands for the design of new lead compounds. In fact, X-ray crystallography and nuclear magnetic resonance (NMR) have been developed to a level where they are now applied routinely. This has had a large impact on the number of experimentally determined molecular structures available. In particular, NMR spectroscopy is greatly esteemed for its ability to elucidate molecular structure, but its greatest potential in drug discovery probably lies in the information that it can reveal about molecular interactions at the atomic level.[3] This trend is now seen both as an alternative and a complement to the more coarse approach exemplified by the application of combinatorial chemistry and high-throughput screening (HTS).

In fact, one of the most common approaches employed up to now to reach this objective is the screening of compounds libraries of small molecules: initial potential hit compounds are easily obtained via, for example, a classic high-throughput screening (HTS). Usually, once found, the most promising hits must be optimized in order to achieve better in vitro activity, selectivity, pharmacodynamic and pharmacokinetic properties, that implicates the synthesis and the testing of compound analogues. This involves a very long iterative process; in fact, even if the achievement of a promising initial compound is quite a efficient process via HTS, the selection of the “wrong” hit (a false positive) to be taken into subsequent steps, may be time consuming and costly.

Therefore, the development of a robust, simple and general technique for hit validation is general needed. Nuclear magnetic resonance (NMR) spectroscopy is a very powerful analytical technique for studying intermolecular interactions and is unique in its ability to provide information on the structural, thermodynamic and kinetic aspects of the binding reaction. It has thus found widespread use in the field of molecular recognition and supramolecular chemistry, a natural consequence of this being its utilization in structure-based drug discovery.

For example, ligand screening methodologies based on NMR spectroscopy are now widely used: this is due to the technical advances with respect to the hardware available and the achievable sensitivity. Perhaps more notably, NMR based approaches offer the benefit of being exquisitely specific and less prone to false positives, a problem that often affects classic spectrophotometric assays.

Another approach, which have the intrinsic advantage of exploring in principle a much larger accessible chemical space than conventional HTS, is the fragment-based drug discovery (FBDD)[3]. This strategy consists of building up a lead compound (typically smaller than 500 daltons) from screening a database of typically 1,000–15,000 smaller molecules (fragments) that are smaller than 300 daltons and have good aqueous solubility. The most common FBDD approaches include X-ray diffraction or NMR spectroscopy as methods for fragment screening, and to guide iterative optimizations through fragment tethering and/or fragment growing.[4]

Metalloproteins[5] represent a group of very interesting targets that has been extensively studied for the development of new candidate drugs. Several of these proteins are important medicinal target for conditions ranging from infection to cancer and metastasis. Many of this proteins present a zinc(II) ion in the active site: different classes of small-molecule inhibitors has been designed to bind this particular ion in the active site of the enzyme.

During my PhD, I have dealt with design, synthesis and evaluation of new Matrix Metalloproteinases (MMPs) inhibitors. Although the role of MMPs in numerous relevant pathologies make them possible pharmacological targets, nevertheless no MMPI is available in the market as drug. In this respect, would be significant the availability of selective drugs with improved water solubility and biodisponibility.

The MMPs, also called matrixins, are a large family of structurally related enzymes that mediate the breakdown of connective tissue, and are important for creating the cellular environments required during development and morphogenesis. They are Ca^{2+}- and Zn^{2+}-dependant enzymes that collectively degrade most of the component of the ECM, including collagen, glycolproteins and proteoglycans, in the normal range of pH.[6] MMPs generally consist of a prodomain, a catalytic domain, a hinge region and a hemopexin domain (Figure 1).

The catalytic domain of MMPs contains two zinc atoms: one of this atoms plays a catalytic role and the other a structural role. Three hystidine coordinates the active-site zinc, and its fourth ligand is a water molecule. They are either secreted from the cell or anchored to the plasma membrane. On the basis of substrate specificity, sequence similarity, and domain organization, vertebrate MMPs can be divided into six group; collagenases (MMP-1, -8, -13, -

18), gelatinases (MMP-2, -9), stromelysins (MMP-3, -10), matrilysins (MMP-7, -26), membrane-type MMPs (MMP-14, -15, -16, -17, -24, -25) and other MMPs (MMP-12, -19, -20).

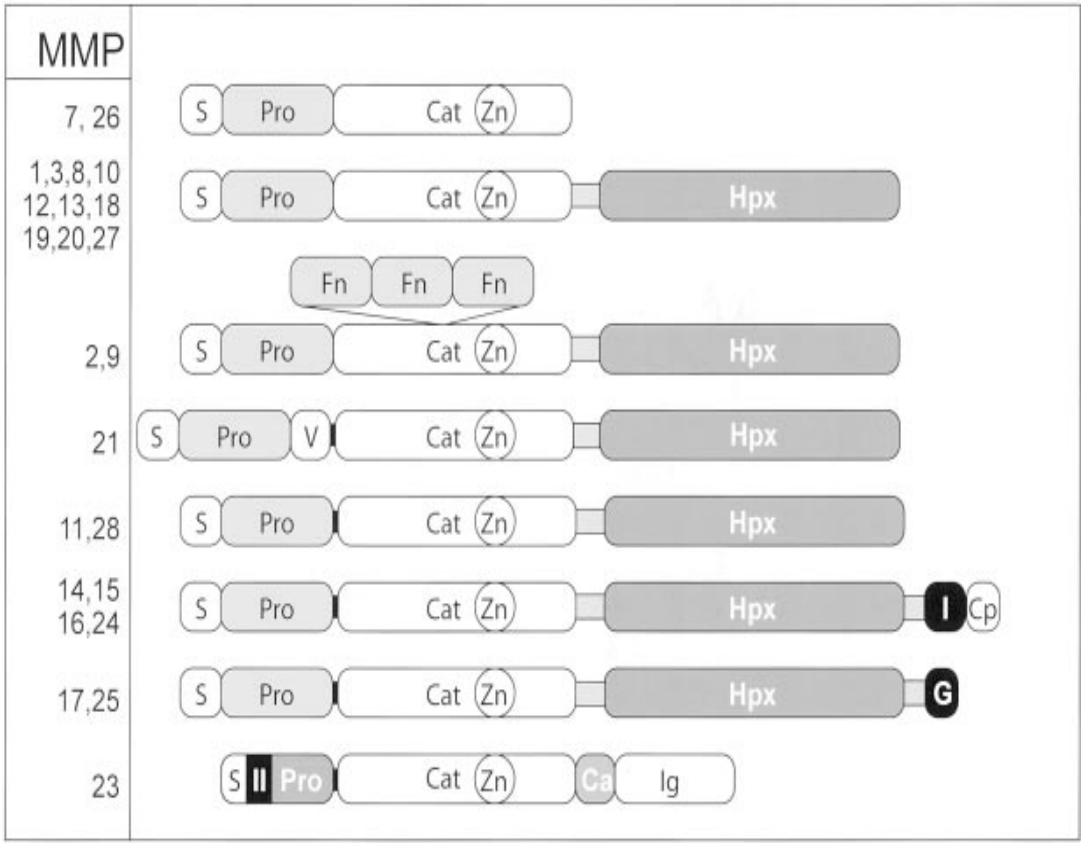

Figure 1. Domain structure of MMPs. The domain organization of MMPs is as indicated: S, signal peptide; Pro, propeptide; Cat, catalytic domain; Zn, active-site zinc; Hpx, hemopexin domain; Fn, fibronectin domain; V, vitronectin insert; I, type I transmembrane domain; II, type II trans membrane domain; G, GPI anchor; Cp, cytoplasmic domain; Ca, cysteine array region; and Ig, IgG-like domain. A furin cleavage site is depicted as a black band between propeptide and catalytic domain.

1.1 MMPs Family

Collagenases

MMP-1, MMP-8, MMP-13, and MMP-18 (*Xenopus*) are in this group.The key feature of these enzymes is their ability to cleave interstitial collagens I, II, and III at a specific site three-fourths from the N-terminus. Collagenases can also digest a number of other ECM and non-ECM molecules.

Gelatinases

Gelatinase A (MMP-2) and gelatinase B (MMP-9) belong to this group. They readily digest the denatured collagens, gelatins. MMP-2, but not MMP-9, digests type I, II, and III collagens: moreover MMP-2 in humans is important for osteogenesis.

Stromelysins

Stromelysin 1 (MMP-3) and stromelysin 2 (MMP-10) both have similar substrate specificities, but MMP-3 has a proteolytic efficiency higher than that of MMP-10 in general. Besides digesting ECM components, MMP-3 activates a number of proMMPs, and its action on a partially processed proMMP-1 is critical for the generation of fully active MMP-1. MMP-11 is called stromelysin 3, but it is usually grouped with “other MMPs” because the sequence and substrate specificity diverge from those of MMP-3.

Matrilysins

The matrilysins are characterized by the lack of a hemopexin domain. Matrilysin 1 (MMP-7) and matrilysin 2 (MMP-26), also called endometase,are in this group. Besides ECM components, MMP-7 processes cell surface molecules such as pro–α-defensin, Fas-ligand, pro–tumor necrosis factor (TNF)-α, and E-cadherin. Matrilysin 2 (MMP-26) also digests a number of ECM components.

Membrane-Type MMPs

There are six membrane-type MMPs (MT-MMPs): four are type I transmembrane proteins (MMP-14, MMP-15, MMP-16, and MMP-24), and two are glycosylphosphatidylinositol (GPI) anchored proteins (MMP-17 and MMP-25). With the exception of MT4-MMP, they are all capable of activating proMMP-2. These enzymes can also digest a number of ECM molecules, and MT1-MMP has collagenolytic activity on type I, II, and III collagens; moreover MT1- MMP also plays an important role in angiogenesis.

Other MMPs

Six MMPs are not classified in the above categories. Metalloelastase (MMP-12) is mainly expressed in macrophages and is essential for macrophage migration. Besides elastin, it digests a number of other proteins. MMP-19 was identified by cDNA cloning from liver and

as a T-cell–derived autoantigen from patients with rheumatoid arthritis (RASI). Enamelysin (MMP-20), which digests amelogenin, is primarily located within newly formed tooth enamel. MMP-22 was first cloned from chicken fibroblasts, and a human homologue has been identified on the basis of EST sequences. The function of this enzyme is not known. MMP-23, also called cysteine array MMP, is mainly expressed in reproductive tissues. The enzyme lacks the cysteine switch motif in the prodomain. It also lacks the hemopexin domain; instead, it has a cysteine-rich domain followed by an immunoglobulin-like domain. One of the last addition to the MMP family is epilysin, or MMP-28, mainly expressed in keratinocytes. Expression patterns in intact and damaged skin suggest that MMP-28 might function in tissue hemostasis and wound repair.

1.2 MMPs structure

Several attempts to design selective inhibitors have been carried out by using the structure-based strategy.[7-9] Although this strategy has been successfully applied in drug discovery against several protein target,[10;11] in case of MMPs the results have been relatively disappointing.

In fact, there is a extensive literature available on the structure of MMPs and their interaction with inhibitors,[12-14] that show the binding mode of several inhibitors in the active site of the enzyme. Moreover, crystal structures are often used in the attempt to highlight subtleties structural differences between the members of the MMP protein family in order to design selective inhibitors.

One of the most distinct structural difference between the MMPs is the relative size and shape of the S_1' pocket.[15] This is clearly evident by the defined S_1' pockets for MMP-1, stromelysin, matrilysin, and neutrophil collagenase.

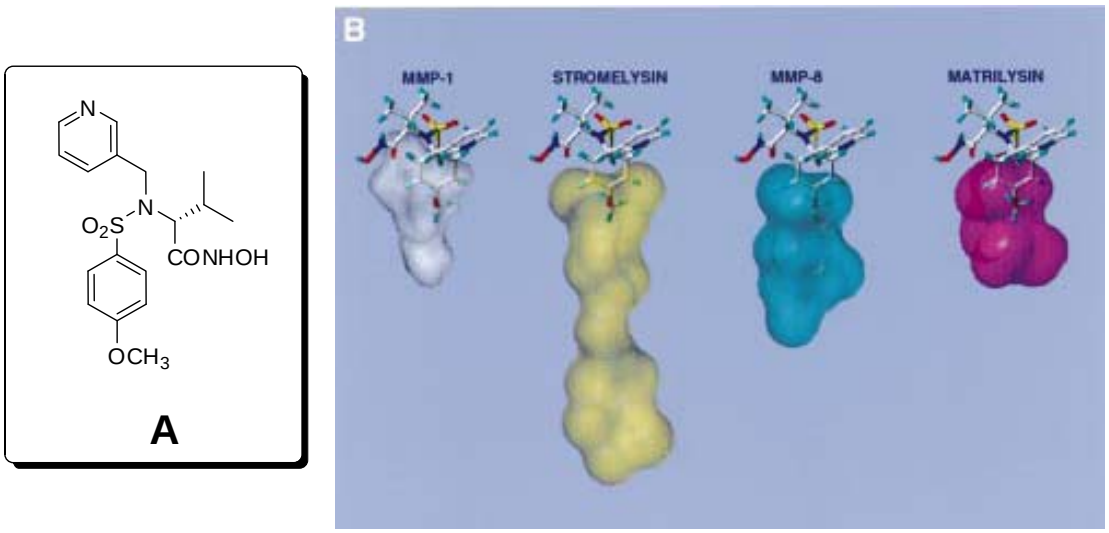

Figure 2. A) Structure of MMI270 (CGS27023A). B) The S_1' pockets of MMP-1, stromelysin (MMP-3), neutrophil collagenase (MMP-8) and matrilysin (MMP-7) with CGS-27023A docked in for comparison.

The large difference in size in the S_1' pockets for MMP-1 and stromelysin is illustrated in Figure 2. CGS-27023A (a broad spectrum MMPs inhibitor) effectively fills the available S_1' pocket for MMP-1, but there is additional space available in the stromelysin S_1' pocket. In fact, the design of stromelysin inhibitors should for example take advantage of this deeper S_1' pocket by using a biphenyl substituent in another series instead of the *p*-methoxyphenyl in CGS-27023A to bind into the S_1' pocket. In addition to the conformational difference between the S_1' pockets, there are some other changes in the sequences between the MMPs in the active site.

Besides the structural differences in the S_1' pocket, the poor results of the structure-based approach in designing of MMPI can be likely due also to the poor knowledge of the dynamical features of these proteins.[16] In fact only few selective MMPI as for example the pyrimidine dicarboxamide MMP-13 inhibitors (Figure 3) have been designed so far. In this molecule the high affinity and selectivity for MMP-13 is achieved by an optimal fit of the inhibitors into the extremely large S_1' cavity and by the large network of interactions that stabilize the protein-ligand adducts. Unfortunately, the promising results obtained with S_1'-targeted in terms of affinity and selectivity, at present, seem difficult to be extended to other MMPs with large S_1' cavities.[17]

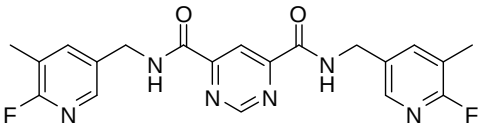

Figure 3. Structure of pyrimidine dicarboxamide MMP-13 inhibitor

Actually, the structural data considered in structure-based drug design result from X-ray structures without taking into account protein flexibility. The detrimental effect of protein flexibility for MMPI selectivity is particularly evident for MMP-1, where the small and shallow S_1' pocket can accommodate a large hydrophobic moiety by reorienting arginine 214,[18] but it has been also observed in MMP-12 where internal conformational adjustments occur upon binding of the inhibitor.[19]

Complementary information can be achieved by NMR structures, where the poor definition of specific protein regions together with dynamic information provide evidence of internal flexibility.[20;21] Recently, the active sites of several MMPs have been structurally characterized by X-ray and NMR and in all investigated proteins exhibits highly similar structural and dynamical features. A comparative analysis carried out on solution and crystal structures of different MMP shows that several regions of the catalytic domain undergo relatively wide and collective motions.[14]

The flexibility of the catalytic domain has been extensively investigated in MMP-12. In this protein the loop regions found disordered in solution show different conformations in the X-ray structures complexed to three different inhibitors. The presence of different conformations is markedly evident for loop L8, forming the S_1' cavity.

In this respect, a further hints to design more potent and selective inhibitors targeted to active site may be obtained from a large number of structures of MMP adducts with a homologous series of ligands, as they can provide information on the extent of the motion of each residue upon binding. This strategy is based on a careful analysis of the structural data, performed on high-resolution crystal structures, and on a detailed thermodynamic characterization of ligand binding.

1.3 Biological functions and regulation of MMPs

Under normal physiological conditions the activities of MMPs are precisely regulated at the level of transcription, activation of the precursor zymogens, interaction with ECM components, and inhibition by endogenous inhibitors.[22] The tissue inhibitors of metalloproteinases (TIMPs) are specific inhibitors of matrixins that participate in controlling the local activities of MMPs in tissues; this inhibitor bind MMPs in a 1:1 stoichiometry (Figure 4).

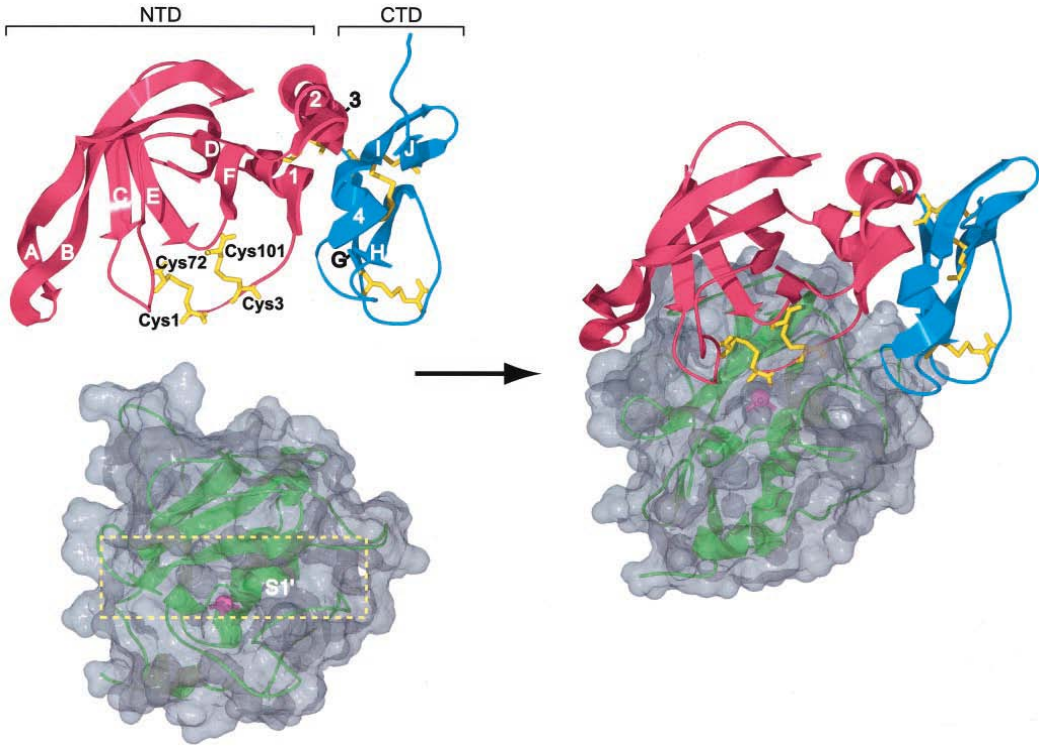

Figure 4. Inhibition of MMP by TIMP: complex of TIMP-2 with catalytic domain of MT1-MMP (1BQQ). On the left, TIMP-2 (top) and the catalytic domain of MT1-MMP (bottom) are shown separately. TIMP-2 is shown as a ribbon diagram. The disulfide bonds stabilizing the protein are shown. The β-stands are labeled A through J; the α-helices are numbered 1 through 4. The catalytic domain of MT1-MMP is shown as a ribbon structure with a transparent surface. The location of the catalytic site cleft is indicated by a dashed rectangle. Within the active-site cleft, the active-site zinc is visible as a pink sphere, and the entrance to the S_1' specificity pocket is labeled. In the complex on the right, the N-terminal cysteine that chelates the active-site zincis clearly visible. The figure was prepared with a Swiss PDB Viewer129 and rendered with POV-Ray.[22]

Four TIMPs (TIMP-1, TIMP-2, TIMP-3, and TIMP-4) have been identified in vertebrates, and their expression is regulated during development and tissue remodeling. Under pathological conditions associated with unbalanced MMP activities, changes of TIMP levels are considered to be important because they directly affect the level of MMP activity.

MMPs are also regulatory molecules, in fact inflammatory cytokine or growth factors can regulate the expression of MMPs, and the cytokine and their receptors can also be substrate for MMP action.

A number of studies[23] have provided evidence for the involvement of the MMPs in normal physiology process as wound repair, epithelial remodeling and angiogenesis. But, when there is an imbalance in one or more of the regulatory processes, what may occur is an overexpression/activation of this proteases. A loss of activity control may lead to the onset of important diseases. At first, the obvious destructive capability of MMPs focused most researches onto diseases that involve breakdown of the connective tissues (arthritis, cancer, periodontal disease), but MMPs are involved in many other pathologies as atherosclerosis, aneurysm, nephritis and fibrosis. Moreover, multiple MMPs are overexpressed in a wide range of tumors, and especially in tumor cells with significant invasive properties. Aggressive cancer cells express many MMPs that have been implicated in growth, invasion and metastasis by degrading surrounded tissue. Angiogenesis around cancer nest also require remodeling of the ECM by proteases: the role of MMPs is particular relevant in early-stage tumors, because their activity is required for tumor proliferation and invasion. Thus, inhibition of MMPs might be a possible approach to reduce tumor malignancy and angiogenesis of metastasis.

1.4 MMPs inhibitors (MMPIs)

Both small molecules (synthetic and natural products) and macromolecular endogenous inhibitors (as TIMPs) have been considered as potential therapies for diseases in which excess MMP activity have been implicated.[24] Unfortunately, the therapeutic use of TIMPs has been limited by the fact that they are proteins: in fact the production, use and administration should be very difficult. The principal approach taken for the identification of synthetic inhibitors is the substrate-based design of peptide derivatives derived from the information of the sequence about the cleavage site; one of the first examples was Marimastat (Figure 5).[25]

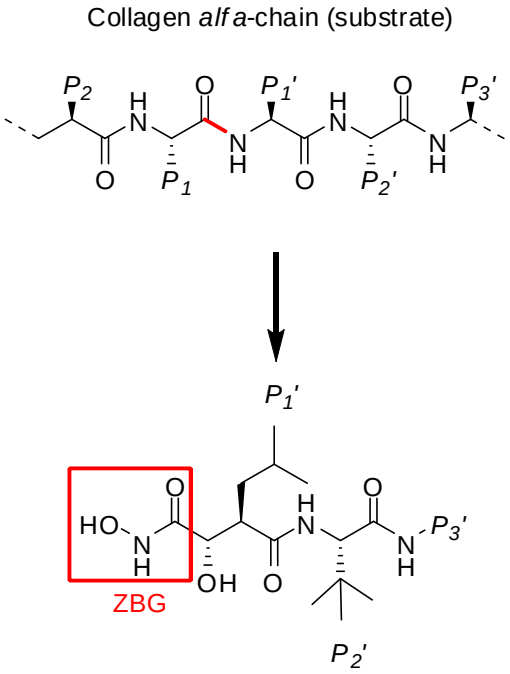

Figure 5. Structure of Marimastat. Many of the inhibitors currently being studied are derived from the peptide structure of the α-chain of type 1 collagen at the point at which collagenases first cleave the molecule (red bond). Marimastat is based on the right-end side of this cleavage site although the chemical groups at the P_1', P_2', P_3' positions are different from the original amino acids residues (Ile-Ala-Gly or Leu-Leu-Ala). The zinc-binding group (ZBG) in this case is an hydroxamate).

The inhibitor binds reversibly at the active site of the MMP in a stereospecific manner. The zinc-binding group, in this case hydroxamic acid (CONHOH), is then positioned to chelate the active site zinc ion. After that, many non-peptide, highly potent inhibitors has been identified and developed; one of the most important classes was represented by the sulfonamide hydroxamate. One of the precursors of this type of inhibitors is NNGH (*N*-isobutyl-N-[4-methoxyphenylsulfonyl]glycyl hydroxamic acid)[26] (Figure 6).

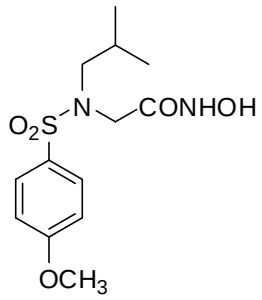

NNGH

Figure 6. Structure of NNGH.

The binding-mode of this inhibitor with MMP-12 has been elucidated through X-ray crystallography;[14] the aromatic moiety interact with the hydrophobic S_1' pocket and the

hydroxamic group is targeted to bind the catalytic zinc ion (Zn1) (Figure 7A). In addition to metal chelation, NNGH is held in the active site by H bonds and hydrophobic interaction. The hydroxamic acid in fact head chelates the zinc ion and is further involved in two H bonds (OH with Glu-219 and NH with Ala-182). Moreover the NNGH sulfonyl oxygen makes an important contribution to inhibitor binding energy by establishing H bonds with Leu 181 (Figure 7B).

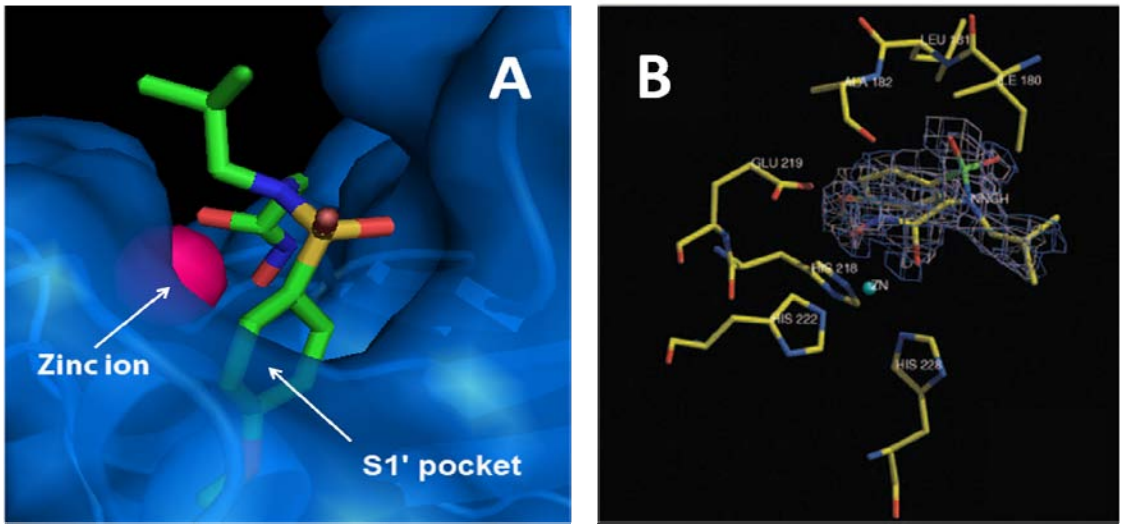

Figure 7. X-ray structure of the catalytic domain of MMP-12 complexed NNGH (A). Only the ligand binding site is shown for clarity. Enlargement of the active site-bound NNGH and its interactions with MMP-12 (B). In B the ligand electron density is also shown.

This aryl-sulfonamide derivatives have been largely exploited to synthesize broad-spectrum MMP inhibitors; these scaffolds in fact present different positions which can be easily functionalized by introducing new functional groups. Moreover many of them present a very high affinity for MMPs. This feature, together with their easy synthetic accessibility and low cost of production, makes these sulfonamide derivatives suitable candidates to design different molecules that should be used for many purposes.

1.5 *In vitro* and *in vivo* studies on MMPIs

One of the most studied MMP inhibitors is the sulfonamidic hydroxamate MMI270 (CGS27023A, Novartis) (Figure 2). This broad-spectrum inhibitor was selected for development based on its superior efficacy in a murine model cancer in comparison of a number of analogues and because it showed a favorable pharmacokinetic profile. In fact MMI270 is one of the first sulfonamidic, orally available inhibitors: additionally it is rapidly absorbed and

eliminated with minimal accumulation on chronic dosing.[27] The hydrosolubility is one of the bigger trouble with this type of inhibitor: in fact high affinity for MMPs is very often achieved by introducing lipophilic substituents, decreasing in this way solubility in water and compromising oral bioavailability.

MMI270 did not show antiproliferative activity against tumor cell lines *in vitro*; however, in rat tumor models of breast and endometrial cancer, it significantly reduced the tumor burden compared with controls and enhanced the activity of cytotoxic and hormonal agents. MMI270 also demonstrated antimetastatic effects *in vivo* and antiangiogenic effects *in vitro*. Very low drug doses were required for antimetastatic effect. In conclusion, the effect of MMI270 has been beneficial in preventing or slowing the formation of lung metastases in a preclinical model. MMI270 was generally well tolerated, but the two main toxicities were rash, generally mild, and musculoskeletal side effects (general myalgia/arthralgia to severe tendonitis with limitation of range of movement in the affected joints).

The musculoskeletal syndrome (MSS) is a side effect very common with non-selective inhibitors; this is probably due to indiscriminate inhibition of all kind of zinc endopeptidases, that are involved in a wide range of normal, physiological processes in which inhibition may cause excessive matrix deposition leading to fibrosis.

The postulate that MMP-1 inhibition alone is responsible for the side effects was dispelled by clinical trials with CP-544439, a hydroxamic acid-based MMP-13 inhibitor that spared MMP-1 but which was otherwise non-selective.[28] This compound still produced MSS despite its lack of activity versus MMP-1. MMP-14 inhibition has also been proposed to cause MSS, but this idea has not yet been clinically evaluated. Moreover, a phase I study had proven that an oral MMP inhibitor, BAY12-9566, that do not inhibit MMP-1 *in vitro* not present musculoskeletal side effects; however, it was not clinically active either.

Unexpected side effects could also result from the inhibition of currently uncharacterized, but essential, MMP-regulated pathways; the activity of ADAMs (adamalysin, a non-MMP metalloproteinases) could also been affected. The dose of broad range inhibitors, on the other hand, could be adjusted so that matrix destruction is prevented without concomitant excessive matrix deposition.[29] Moreover, we don't know actually if the use of specific inhibitor will be possible in a next future: for example, it is not yet known with certainty which enzymes are the key-players in relevant diseases as rheumatoid arthritis or colon carcinoma. Furthermore, the inhibition of one enzyme may merely lead to a compensation by others with similar substrate specificity. This appears to be the case in some MMP gene-knockout studies.[30]

Unfortunately, up to now, *in vivo* studies in animal models and clinical trials frequently gave disappointing results. At present time, the only MMP inhibitor currently on the market is Periostat® (doxycicline, CollaGenex Pharmaceutical Inc., an MMPs' activity inhibitor used for periodontitis); it is a derivative of the antibiotic tetracycline, but it is effective at subantimicrobial doses.

Anyway, because of the high therapeutic potential, the improvement of MMP inhibitors continues as shown by several recent patents and scientific publications. Development of more selective MMP inhibitors lacking serious side-effects (such as MSS) and with good bioavailability is of high importance.[31]

1.6 The aim of the project

In this contest, during my PhD I dealt with the project aimed to design through a structure-based approach new MMPI with better selectivity and bioavailability and new probes to target MMPs in biological samples.

1) In particular I designed and synthesized a biotin chain-terminated inhibitors (BTI) showing high affinity for matrix metalloproteinases (MMPs) on one side and high affinity for avidin through the biotinylated tag on the other. The affinity of the designed BTI toward five different MMPs has been evaluated and the simultaneous formation of a highly stable ternary system Avidin-BTI-MMP clearly assessed. This system will permit the development of new approaches to detect, quantify, or collect MMPs in biological samples, with potential applications in vivo.

2) The dry eye syndrome is a disorder of the tear film due to tear deficiency or excessive evaporation that causes damage to the interpalpebral ocular surface and is associated with symptoms of discomfort. The MMPs (in particular MMP-1, -2, -9 and -13) are highly involved in the pathogenesis of this disease, and they are associated with disruption of corneal epithelial barrier function and corneal surface irregularity. Therefore an important improvement in the treatment of this disease could be the use of a non-selective MMPI conjugated to different type of dendrimers for the development of a new drug delivery system able to sustain the drug release and to remain in the vicinity of the front of the eye for as prolonged period of time. This compounds will be evaluated in the treatment of dry eye syndrome.

3) The lack of selectivity and the poor bioavailability are the two major problem of MMPIs. In particular, a very interesting medicinal target in the MMPs family is the matrylisin (MMP-7), that it is overexpressed in many human cancer and it contributes to the invasive growth of colon carcinoma. Nevertheless, high affinity and selective inhibitors for this particular MMP are not present in literature. In this contest, we had synthesized a new inhibitor that present good water-solubility and an high affinity for MMP-7, that will be tested in vivo against colon cancer, in collaboration with Dr. L. Vannucci of the University of Prague.

4) Moreover I have dealt with the synthesis of a new family of high-affinity, water-soluble MMP inhibitors using a conceptually novel strategy: we replaced a portion of the molecule that was not directly involved in binding with a water-soluble residue. In particular, we had developed novel carbohydrate-based inhibitors that can overcome bioavailability problems. The glycosidic residue was introduced in a suitable location of the molecule, linked through a spacer of appropriate length. This inhibitors are a prototype structure that opens the way to the design of a new class of highly effective MMPIs. Moreover, we had synthesized a new group of MMPIs that presented an hydrophilic residue (for example an alcohol or a diol): we demonstrated not only that inhibiting properties was not be affected by the introduction of this type of residue, but also that the structure modification permitted to modulate the bioavailability, affinity and selectivity of our compounds.

Reference List

[1.] M. Pellecchia, B. Becattini, K. J. Crowell, R. Fattorusso, M. Forino, M. Fragai, D. Jung, T. Mustelin, L. Tautz, *Expert Opinion on Therapeutic Targets* **2004,** *8* 597-611.

[2.] X. Barril, R. Soliva, *Structure-Based Drug Discovery, An Overview* **2006,** 54-96.

[3.] M. Pellecchia, I. Bertini, D. Cowburn, C. Dalvit, E. Giralt, W. Jahnke, T. L. James, S. W. Homans, H. Kessler, C. Luchinat, B. Meyer, H. Oschkinat, J. Peng, H. Schwalbe, G. Siegal, *Nature Reviews Drug Discovery* **2008,** *7* 738-745.

[4.] A. W. Hung, H. L. Silvestre, S. Wen, A. Ciulli, T. L. Blundell, C. Abell, *Angewandte Chemie-International Edition* **2009,** *48* 8452-8456.

[5.] F. E. Jacobsen, J. A. Lewis, S. M. Cohen, *ChemMedChem* **2007,** *2* 152-171.

[6.] M. Seiki, I. Yana, *Cancer sci.* **2003,** *97* 569-574.

[7.] J. J. Li, J. Nahra, A. R. Johnson, A. Bunker, P. O'Brien, W. S. Yue, D. F. Ofwine, C. F. Man, V. Baragi, K. Kilgore, R. D. Dyer, H. K. Han, *Journal of Medicinal Chemistry* **2008,** *51* 835-841.

[8.] C. K. Engel, B. Pirard, S. Schimanski, R. Kirsch, J. Habermann, O. Klingler, V. Schlotte, K. U. Weithmann, K. U. Wendt, *Chemistry & Biology* **2005,** *12* 181-189.

[9.] B. Pirard, *Drug Discovery Today* **2007,** *12* 640-646.

[10.] M. Habeck, *Lancet Oncology* **2002,** *3* 6.

[11.] M. Vonitzstein, W. Y. Wu, G. B. Kok, M. S. Pegg, J. C. Dyason, B. Jin, T. V. Phan, M. L. Smythe, H. F. White, S. W. Oliver, P. M. Colman, J. N. Varghese, D. M. Ryan, J. M. Woods, R. C. Bethell, V. J. Hotham, J. M. Cameron, C. R. Penn, *Nature* **1993,** *363* 418-423.

[12.] I. Bertini, V. Calderone, M. Fragai, C. Luchinat, S. Mangani, B. Terni, *Journal of Molecular Biology* **2004,** *336* 707-716.

[13.] I. Bertini, V. Calderone, M. Fragai, A. Giachetti, M. Loconte, C. Luchinat, M. Maletta, C. Nativi, K. J. Yeo, *Journal of the American Chemical Society* **2007,** *129* 2466-2475.

[14.] I. Bertini, V. Calderone, M. Cosenza, M. Fragai, Y.-M. Lee, C. Luchinat, S. Mangani, B. Terni, P. Turano, *Proc.Natl.Acad.Sci.U.S.A.* **2005,** *102* 5334-5339.

[15.] F. J. Moy, P. K. Chanda, J. M. Chen, S. Cosmi, W. Edris, J. S. Skotnicki, J. Wilhelm, R. Powers, *Biochemistry* **1999,** *38* 7085-7096.

[16.] F. J. Moy, P. K. Chanda, J. Chen, S. Cosmi, W. Edris, J. I. Levin, T. S. Rush, J. Wilhelm, R. Powers, *Journal of the American Chemical Society* **2002,** *124* 12658-12659.

[17.] V. Calderone, M. Fragai, C. Luchinat, C. Nativi, B. Richichi, S. Roelens, *ChemMedChem* **2006,** *1* 598-601.

[18.] B. Lovejoy, A. R. Welch, S. Carr, C. Luong, C. Broka, R. T. Hendricks, J. A. Campbell, K. A. M. Walker, R. Martin, H. Van Wart, M. F. Browner, *Nature Structural Biology* **1999,** *6* 217-221.

[19.] R. Bhaskaran, M. O. Palmier, N. A. Bagegni, X. Y. Liang, S. R. Van Doren, *Journal of Molecular Biology* **2007,** *374* 1333-1344.

[20.] M. Fragai, C. Luchinat, G. Parigi, *Accounts of Chemical Research* **2006,** *39* 909-917.

[21.] K. Lindorff-Larsen, R. B. Best, M. A. DePristo, C. M. Dobson, M. Vendruscolo, *Nature* **2005,** *433* 128-132.

[22.] R. Visse, H. Nagase, *Circ.Res.* **2003,** *92* 827-839.

[23.] M. Mandal, A. Mandal, S. Das, T. Chakraborti, S. Chakraborti, *Mol.Cell.Biochem.* **2003,** *252* 305-329.

[24.] M. Whittaker, C. D. Floyd, P. Brown, A. J. H. Gering, *Chem.Rev.* **1999,** *99* 2735-2776.

[25.] P. H. Brown, *Angiogenesis* **1997,** *1* 142-154.

[26.] L. J. MacPherson, E. K. Bayburt, M. P. Capparelli, B. J. Carroll, R. Goldstein, M. R. Justice, L. Zhu, S. Hu, R. A. Melton, L. Fryer, R. L. Goldberg, J. R. Doughty, S. Spirito, V. Blancuzzi, D. Wilson, E. O'Byrne, V. Ganu, D. T. Parker, *J.Med.Chem.* **1997,** *40* 2525-2532.

[27.] N. C. Levitt, F. A. L. M. Eskens, K. J. O'Byrne, D. J. Propper, L. J. Denis, S. J. Owen, L. Choi, J. A. Foekens, S. Wilner, J. M. Wood, M. Nakajima, D. C. Talbot, W. P. Steward, A. L. Harris, J. Verweij, *Clin.Cancer.Res.* **2001,** *7* 1912-1922.

[28.] L. A. Reiter, K. D. Freeman-Cook, C. S. Jones, G. J. Martinelli, A. S. Antipas, M. A. Berliner, K. Datta, J. T. Downs, J. D. Eskra, M. D. Forman, E. M. Greer, R. Guzman, J. R. Hardink, F. Janat, N. F. Keene, E. R. Laird, J. L. Liras, L. L. Lopresti-Morrow, P. G. Mitchell, J. Pandit, D. Robertson, D. Sperger, M. L. Vaughn-Bowser, D. M. Waller, S. A. Yocum, *Bioorg.Med.Chem.Lett.* **2006,** *16* 5822-5826.

[29.] H. F. Bigg, A. D. Rowan, *Curr.Opin.Pharmacol.* **2001,** *1* 314-320.

[30.] S. D. Shapiro, *Matrix Biol.* **1997,** *15* 527-533.

[31.] G. Dormán, K. Kocsis-Szommer, C. Spadoni, P. Ferdinandy, *Recent Patents on Cardiovascular Drug Discovery* **2007,** *2* 1-9.

Chapter 2

Design, synthesis and evaluation of biotin chain-terminated inhibitors (BTI) of MMPs

2.1 Introduction

The design of molecular probes able to selectively bind biomolecular targets is gaining importance not only for their applications in molecular biology, but also for the development of new techniques for the early stage diagnosis and therapy of several pathologies.[1] Rational drug design driven by structural data is currently applied to speed up the design of new candidate drugs in pharmaceutical research.[2-5] The same approach is even more important to design molecular probes where, besides classical requirements, additive structural and functional features are required. As we have already seen, expression and activation of MMPs are increased in many relevant pathologies, as well as in almost all human cancers, compared to physiological conditions. Furthermore, the degree of overexpression of MMPs in cancer tissues is strictly associated with the level of tumor invasiveness and with its tendency to form metastasis. It is therefore apparent that the development of efficient molecular devices designed to reveal the overexpression of MMPs may be a powerful tool for the early detection of tumors and the assessment of their aggressiveness, as well as of cardiocirculatory problems.[6]

Studies focused on the detection of overexpression of MMPs have already been reported [7] and probes to profile MMPs in tissues synthesized and tested.[8;9] In particular, hydrolyzable, near-infrared fluorescent molecules have been successfully tested in mice to detect fibrosarcoma.[10] Unfortunately, this innovative technique suffers from the serious limitation represented by the limited penetration of light (a few millimeters); such a degree of penetration is only sufficient for the readout of superficial subcutaneous tumors (<10 mm).

An interesting approach to detect overexpression of MMP in atherosclerosis has also been published. Low molecular weight inhibitors, able to interact with the active site of MMPs involved in atherosclerotic plaque disruption, have been targeted with nuclear agents and tested in vivo.[11-13] Although the results reported were extremely encouraging, the approach presented a scarce flexibility, due to experimental difficulties in preparing the targeted inhibitors and to limited availability of suitable nuclear agents.

A significant improvement in the development of MMP-conjugated probes to detect pathological events may be the rational design of biotin-labeled inhibitors,[14] capable of binding to MMPs exclusively and with high affinity. These tagged molecules rely on the well-known avidin-biotin molecular recognition system and could be used in conjunction with commercially available biotin-labeled probes (i.e., radionuclide chelates) to efficiently detect pathological tissues by imaging the local overexpression of MMPs. The use of such molecules

is not limited to in vivo imaging but can be extended to in vitro applications such as MMP purification by using avidin columns or devices.

2.2 Avidin-biotin system

The high affinity binding-pairs biotin/avidin have become an important chemical tool in capture processes for a large number of different application, both *in vitro* and *in vivo*: in fact the specificity of biotin binding to avidin provides the basis for developing assay systems to detect or quantify analytes.

Avidin is a glycoprotein found in egg whites that contains four different identical subunits of 16.400 daltons each, giving an intact molecular weight of approximately 66.000 daltons. Each subunits contains one binding site for biotin, or vitamin H (Figure 8).

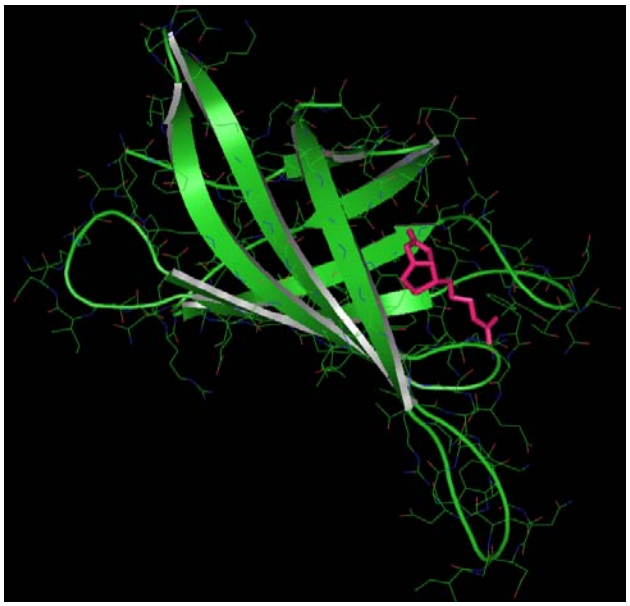

Figure 8. Avidin monomer bound to a molecule of biotin

The biotin interaction with avidin is among the strongest non-covalent affinities known, exhibiting a dissociation constant about 1.3 X 10^{-15} M. Moreover the biospecificity of the interaction is similar to the antibody-antigen or receptor-ligand recognition, but on a much higher level respect to the affinity constants.

The tetrameric structure native structure of avidin is resistant to denaturation under extreme conditions. Even in 8 M urea or 3 M guanidine hydrochloride the protein maintains structural integrity.[15] When biotin is bound to avidin, the interaction promotes even greater stability of the complex. Variations in buffer salts and pH, the presence of denaturants or detergents, and extremes of temperature will not prevent the interaction from occurring. The

strength of non-covalent avidin-biotin interaction along with its resistance to break-down makes it extraordinary useful in bioconjugate chemistry.

A common applications of avidin-biotin biochemistry is in immunoassays: as a matter of fact, the specificity of antibody molecules provides the targeting capability to recognize and bind particular antigen molecules. If there are biotin labeles on the antibody molecule, it creates multiple sites for binding avidin. If avidin is in turn labels with an enzyme, fluorophore etc., then a very sensitive antigen-detection system is created. The simplest assays design, called the labeled avidin-biotin system (LAB), a biotinylated antibody is incubated with its antigen. Next, an avidin-enzyme conjugate is introduced and allow to interact with the available biotin sites. Just as in another ELISA tests, substrate development then provides the chemical detectability necessary to quantify the antigen (Figure 9).

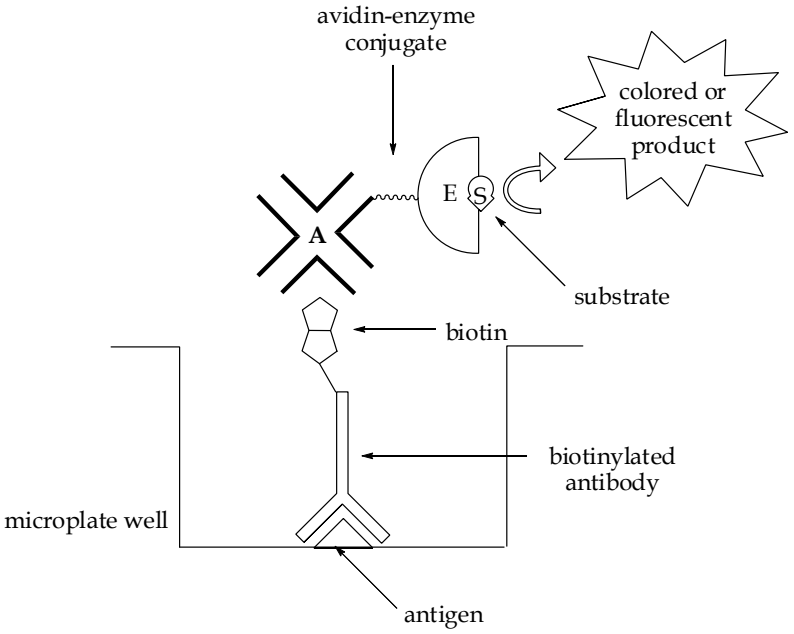

Figure 9. The basic design of the labeled avidin-biotin (LAB) system.

Non-enzyme assays systems can be designed with the avidin-biotin interaction as well; for example employing fluorescently labeled avidin molecules that can be used to detect biotinylated molecule after it has bound its target. The main application of this technique is in cytochemical staining wherein the fluorescent signal is used to localize antigen or receptor in cells. Furthermore, radiolabeled avidin can be employed as a universal detection reagent in radioimmunoassays designs. For example, avidin labeled with ^{125}I can be used to localize biotinylated monoclonal antibody directed against tumor cells *in vivo* for imaging purpose.[16] Besides, cytotoxic substance coupled to avidin can be used to direct cell-killing activity toward

a tumor cell bound, biotinylated monoclonal antibody (or other targeting molecule) for cancer therapy.

2.3 Design of a new biotin chain-terminated inhibitors (BTI)

Capitalizing on our expertise on expression and structural characterization of MMPs[17-19] and on the rational design and synthesis of MMP inhibitors,[20-25] we report the design and synthesis of carboxylic-containing, biotinylated inhibitors able to show high affinity for MMPs and at the same time able to strongly interact with avidin through the biotinylated tag.[26]

In clinical therapy, selectivity of inhibitors for a specific MMP is dramatically important, so much so that the lack of selectivity is believed to have been the main reason for failures of clinical trials in the past. Often, the failure of clinical trials, due to the severity of the side-effects, was related to the chronic adverse effects of nonselective inhibitors (i.e. musculoskeletal syndrome and tendinitis).[27] On the other hand, for the molecules proposed here, selectivity is not an issue as chronic use is not required. Indeed, ideal probes to detect overexpression of MMPs must not be selective inhibitors vs. a specific MMP, but they should instead selectively recognize MMPs among other proteins. These new biotinylated molecules designed to bind to MMPs and to be recognized by avidin might therefore be successfully used in the in vitro collection/purification of MMPs, in the visualization of pathological tissues where MMPs are overexpressed, and to evaluate the aggressiveness of the pathology by monitoring, e.g., radioactivity. Moreover, it might be possible to test in vivo the efficacy of clinical treatments against a specific disease by just monitoring the level of MMPs produced during the therapy. In addition, such molecules can be easily employed for collecting and purifying MMPs from biological samples.

Among all the scaffolds evaluated, molecules **1** and **2** (Figure 10) were selected for their low *K*i values against five different MMPs (see Table 1).

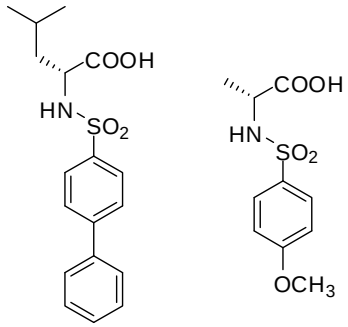

1 **2**

Figure 10. Structure of the selected scaffolds **1** and **2**.

Table 1. Inhibition Constants (*K*i) of the **1** and **2** toward the considered MMPs.

Compound	MMP-1	MMP-7	MMP-8	MMP-12	MMP-13
1	18 ± 2 μM	56 ± 6 μM	31 ± 4 nM	25 ± 2 nM	108 ± 12 nM
2	302 ± 25 μM	80 ± 9 μM	4.6 ± 5 μM	1.4 ± 0.2 μM	2.6 ± 0.3 μM

As zinc binding groups (ZBG), the carboxylic acid was selected despite its relatively weak affinity for the metal ion.[28-30] In this case the choice of a carboxylic acid to replace the most commonly used hydroxamic acid warrants higher stability of the inhibitor under physiological conditions[31] and provides better bioavailability.[32]

In all MMPs, the flexibility of the protein loops forming the active site makes these enzymes able to modify the shape of the catalytic pocket to accommodate ligands with different structures.[33-35] In particular, analyzing the structures available on the protein data bank, it is apparent that the volume of the S1 cavity can be changed to host ligands bearing lipophilic groups of different size. However, in MMP-1 and MMP-7 the S1′ cavity is narrow as well as short "trucked" (MMP-7) such that bulky groups generally do not fit. Therefore, in order to probe all members of the MMP family, two scaffolds, bearing either a linear biphenyl moiety or a shorter methoxyphenyl group, were considered as possible bases for the synthesis of BTIs.

Noteworthy, the two scaffolds exhibit a sizably different selectivity and affinity for the MMPs chosen. In particular, inhibitor **1**, due to the presence of a biphenyl moiety on the sulfonamide sulfur, showed inhibition constants in the nanomolar range. Only for MMP-1 and MMP-7 was the affinity in the low-micromolar range due to the relatively slim size of the S_1' pocket.[36] Although still good, **2** is a weaker MMP inhibitor with micromolar values of *K*i for all the MMPs tested.

Matrix metalloproteinase 12 (MMP-12) performs proteolysis of several ECM components including elastin, laminin, and type IV collagen. The stability of the active MMP-12 catalytic domain in the presence of weak inhibitors, the relatively large S_1' pockets, and the high yield of the ^{15}N-enriched protein in minimal medium make this enzyme an ideal model to evaluate BTI candidates.

To explore the binding mode of the two scaffolds and to properly design the biotin tag derivatives, the two inhibitors were soaked in crystals of MMP-12 and the structure of the complexes solved by X-ray crystallography (Figure 11).

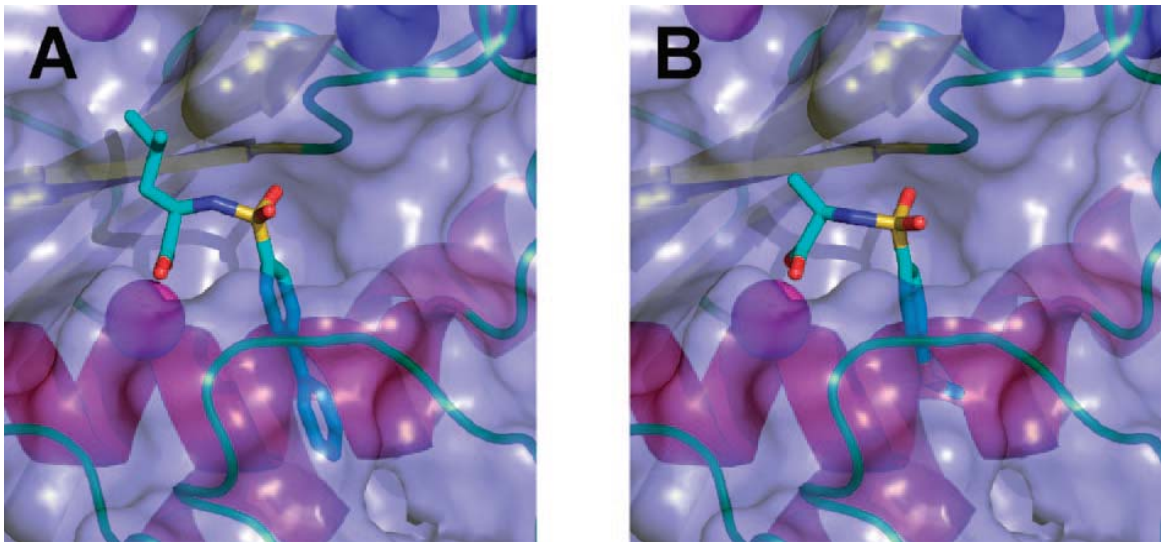

Figure 11. X-ray structure of the catalytic domain of MMP-12 complexed with **1** (A) and with **2** (B). Only the ligand binding site is shown for clarity.

Analysis of the crystal structures revealed that the inhibitors share a similar binding mode, with the catalytic zinc ion coordinated by the oxygens of the free carboxylate, the sulfonyl oxygen H-bonded with the NH of the Ala 182, and the liphophilic groups nested inside the S_1' pocket.

The structural analysis accounts for the larger affinity of **1** for MMP-12 with respect to scaffold **2**, as observed in the enzymatic assays. Indeed, in the MMP-12-**1** complex, larger hydrophobic interactions result from the larger surface-to-surface contact area due to the presence of the biphenyl moiety. More important for the biotin tag inhibitor design was the solvent exposure of the sulfonamide nitrogen revealed by the crystal structures for both ligands. These structural data address the question related to the identification of the position where the tag can be inserted without spoiling the binding affinity.

The structural analysis accounts for the larger affinity of **1** for MMP-12 with respect to scaffold **2**, as observed in the enzymatic assays. Indeed, in the MMP-12-**1** complex, larger hydrophobic interactions result from the larger surface-to-surface contact area due to the presence of the biphenyl moiety. More important for the biotin tag inhibitor design was the solvent exposure of the sulfonamide nitrogen revealed by the crystal structures for both ligands. These structural data address the question related to the identification of the position where the tag can be inserted without spoiling the binding affinity.

A further critical point in developing efficient biotinylated probes for in vivo and in vitro applications is represented by the choice of a suitable linker able to prevent any steric clashes between avidin and the target biomolecule. While a too-short spacer may impair the

ability of the probe to bind both MMP and avidin, the use of a too-long spacer could affect the bioavailability, stability, and solubility of the whole molecule. In particular, a too-long linker can increase the susceptibility of the probe to be split by enzymes such as the biotinidase that can degrade the molecule in vivo. Once more, the availability of the three-dimensional structure of both avidin-biotin complex (present in protein data bank, PDB code: 2avi) and **1**-MMP-12 complex has provided the background information needed for a rational molecular design of the biotin-tagged inhibitors we conceived.

A fourteen-membered spacer was designed to link the biotin residue to **1** (starting from the carboxylic-methyl ester sulfonamide **3**), that is the shorter, synthetically convenient linker allowing the probe to bind both MMP and avidin binding sites (Figure 12).

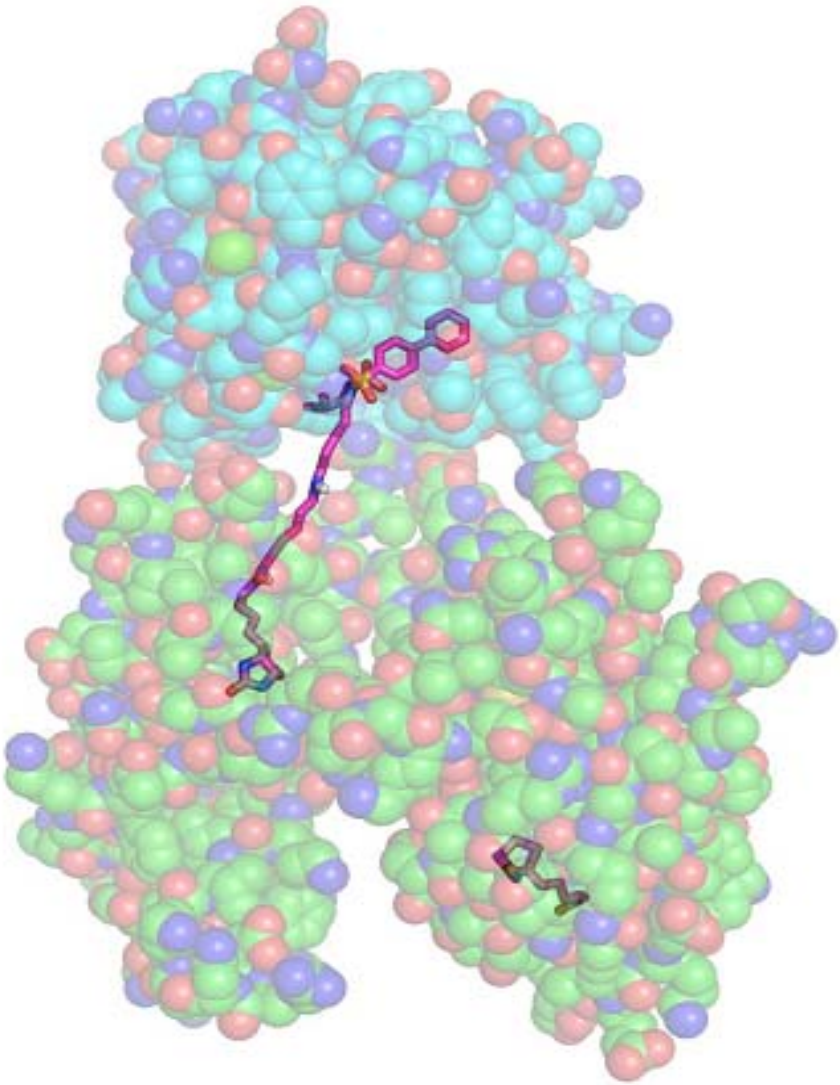

Figure 12. (A) Model of the ternary system Avidin-BTI **4**-MMP generated starting from the avidin-biotin complex (pdb code: 2avi) and compound **1** - MMP-12 adduct, and obtained by linking the biotin moiety to the BTI **1** ligand with the fourteen-membered spacer. Such model, generated by using the program Pymol, was useful in the rational design of linker's length.[37]

The convergent synthesis of biotinylated inhibitor **4** (BTI) was summarized in Scheme 1.

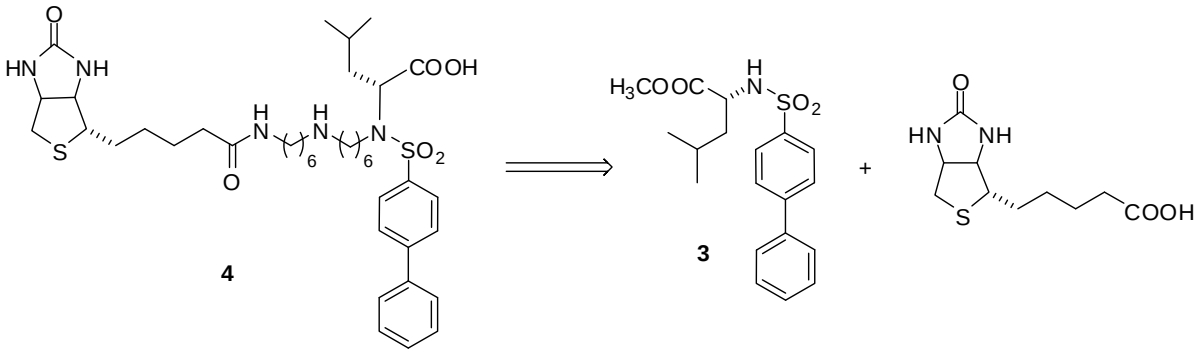

Scheme 1. Retrosynthesis of biotinylated inhibitor **4** (BTI).

2.4 Synthesis of BTI 4 and 10

The synthetical approach that we had undertaken started from biotin, that was first reacted under known procedures[38] with the N-Boc-1,6-diaminohexane **5** to give the amido derivative **6** which, after quantitative removal of *tert*-butyloxy carbonyl protecting group, gave the trifluoroacetylammonium salt **7**. Compound **7** was treated with the bromosulfonamide **8** in the presence of cesium hydroxide, in dimethylformamide as solvent, to give the diastereomerically pure ester **9** in 55% yield. Removal of the methyl ester with lithium hydroxide/water from the latter afforded BTI **4** as a diastereomerically pure compound in 55% yield (Scheme 2).

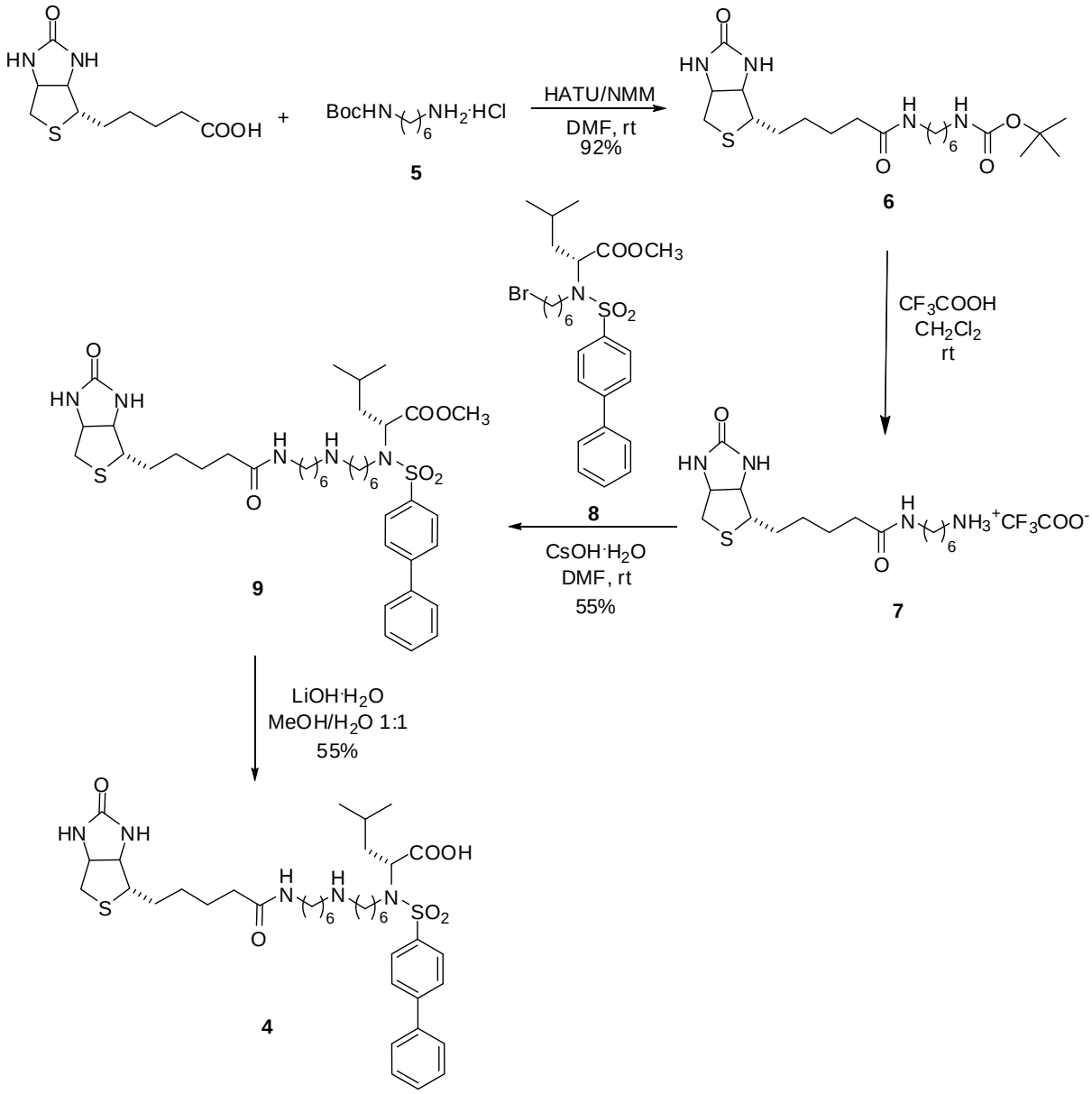

Scheme 2.

Compound **8** was obtained through Mitsunobu reaction starting from the carboxylic-methyl ester sulfonamide **3** and 1-bromo exanol, that it is the second part of the linker; the bromo derivative **8** was obtained with 60% yield (Scheme 3).

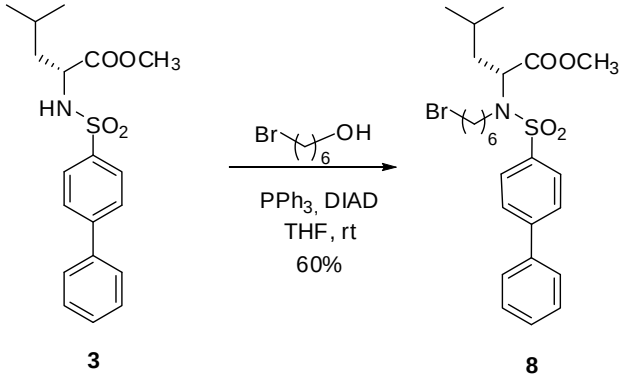

Scheme 3.

Following the synthetic pathway reported for **4**, the biotin-tagged MMP inhibitor **10** was also prepared from **7** and bromosulfonamide **11**, as a diasteromerically pure compound (Scheme 4).

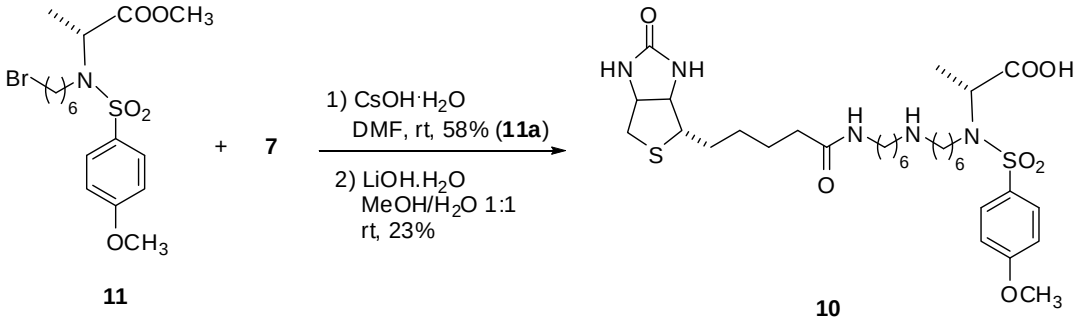

Scheme 4.

2.5 Fluorimetric assays

The affinity properties of the two BTI (**4** and **10**) derivatives toward the selected MMPs were first evaluated by fluorimetric assay (see Experimental Section). The *K*i values are reported in Table 2, in comparison to compound **1** and **2**.

Table 2. Inhibition constants (K_i) of the considered compounds toward the considered MMPs.

Compound	MMP-1	MMP-7	MMP-8	MMP-12	MMP-13
1	18 ± 2 µM	56 ± 6 µM	31 ± 4 nM	25 ± 2 nM	108 ± 12 nM
2	302 ± 25 µM	80 ± 9 µM	4.6 ± 5 µM	1.4 ± 0.2 µM	2.6 ± 0.3 µM
4	25 ± 3 µM	450 ± 50 nM	4 ± 0.5 nM	5 ± 0.6 nM	0.7± 0.2 nM
10	295 ± 40 µM	73 ± 7 µM	8 ± 1 µM	1.6 ± 0.2 µM	1.2 ± 0.1 µM

While BTI **4** had lower *K*i values as compared to the corresponding precursor **1**, BTI **10** exhibited comparable affinity with respect to its precursor **2**. The micromolar *K*i of BTI **10** for all the tested MMPs unambiguously demonstrated that the latter is less interesting as a probe to detect these enzymes *in vivo*, though it might be suitable to collect and purify MMPs from biological samples. Conversely, BTI **4** exhibited a nanomolar affinity for all the MMPs considered (including MMP- 7) except for MMP-1, for which the *K*i was, however, still in the low micromolar range. The molecular details for the observed improved affinity were analyzed by investigating the BTI **4** -MMP-12 complex.

2.6 NMR studies

Several attempts aimed at obtaining the X-ray structure of the biotin tag inhibitors in complex with MMP-12, either by soaking or cocrystallization, failed, probably for steric reasons owing to the tag. Therefore, interaction of compound **1** and of its biotin tag derivative **4** with the catalytic domain of MMP- 12 was further investigated following the chemical shift perturbations on ^{15}N-^{1}H HSQC spectra using ^{15}N-labeled protein samples. The chemical shift is a sensitive indicator of protein-ligand interactions and can be used to identify the binding site when the resonance assignment is available.[39] The complete assignment of the catalytic domain of MMP-12 complexed with the weak inhibitor acetohydroxamic acid is available in our laboratory. Increasing amounts of **1** and **4** were added to 200 μM solutions of the protein up to an equimolar concentration. Although several NH signals were shifted by adding the inhibitors, as many as 134 and 129 cross-peaks belonging to protein adducts with **1** and **4**, respectively, were easily reassigned.

The intensity of signals belonging to NH groups perturbed by the addition of the ligands decreased linearly, while new cross-peaks corresponding to the BTI-bound form of the protein appeared and gradually increased their intensity, in agreement with the effect produced by a slow exchanging ligand (Figure 13).

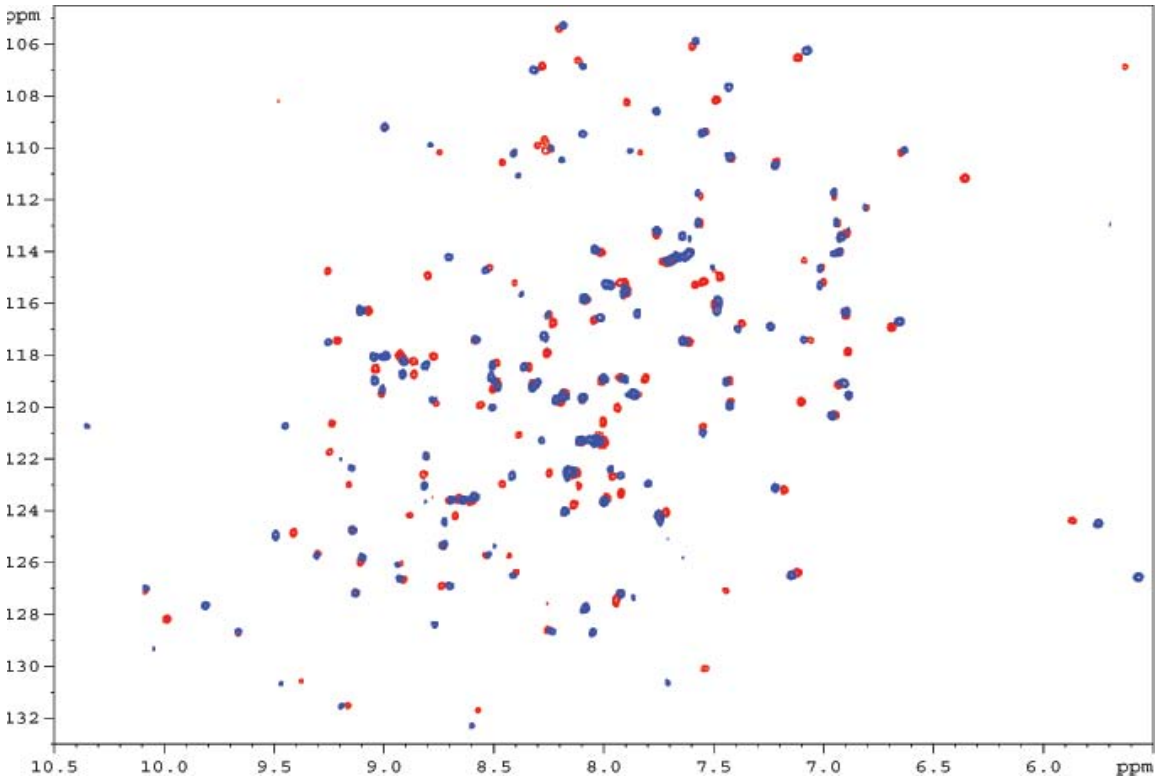

Figure 13. ^{15}N-^{1}H HSQC spectra of catalytic domain of MMP-12 (red) an MMP-12 + BTI **4** (equimolar concentration) (blue).

The binding mode of ligands **1** and **4**, respectively, was analyzed and compared by reporting Garrett values [Δ*δ*(NH)] on a surface representation of the MMP-12 structure (Figure 13). As is evident from Figure 14, for both inhibitors, the region with significant ^{15}N-^{1}H HSQC spectral perturbations involves the catalytic pocket. The analysis of Garrett values rules out relevant additive interactions of the biotinylated tail present in BTI **4** with protein regions outside the catalytic pocket, suggesting a different origin for the observed improved affinity. In addition, a hypothetical binding mode with the biotinylated tail of BTI **4** fitting in the S_1' cavity can be completely excluded by the chemical shift perturbations on the ^{15}N-^{1}H HSQC spectra that are similar for **1** and **4** as well as by the *K*i values of the BTI **10**, which, although biotinylated, showed a low affinity for the enzyme. Likely, extra interactions related to a better fit of **4** into the active site of the enzyme become possible when the fourteen-membered spacer is introduced on BTI **4**. These extra interactions are particularly evident for MMP-7 (Table 1) where the affinity increases by 2 orders of magnitude upon the introduction of the linker.

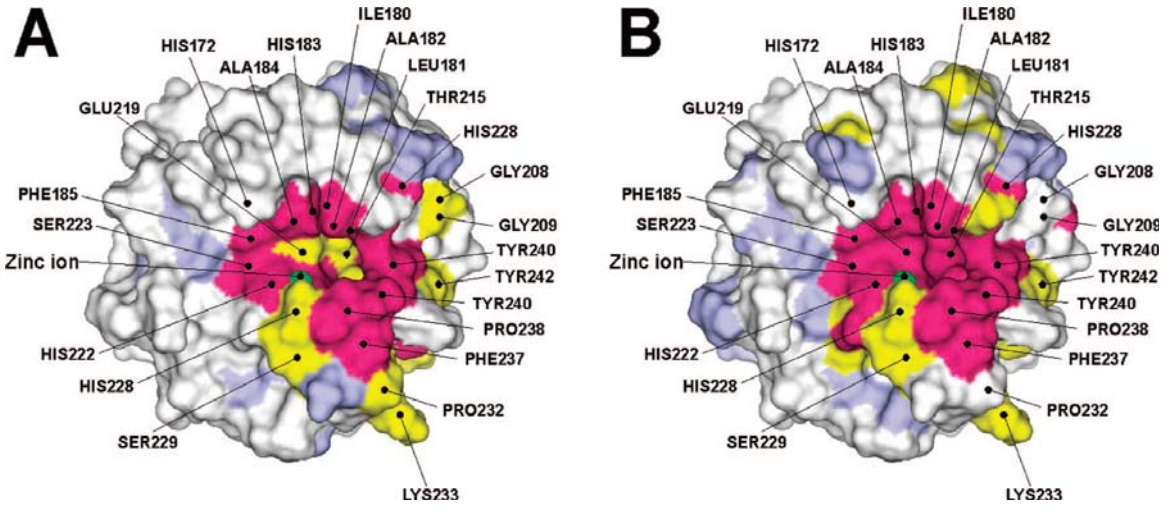

Figure 14. Surface representation of the residues of the catalytic domain of MMP-12 affected by chemical shift perturbation upon the addition of **1** (A) and of **4** (B). Areas of interaction with significant ^{15}N-^{1}H HSQC spectra perturbations are colored-coded according to the Garret values. Magenta, $\Delta\delta$(NH) > 0.1 ppm; Yellow, 0.1 > $\Delta\delta$(NH) > 0.05; Cyan, 0.05 > $\Delta\delta$(NH) > 0.03.

Although a high affinity for the target protein is a basic requirement for the proposed bifunctional ligand to play its role, only the ability of the latter to bind MMP and avidin simultaneously could prove its real efficacy as effective BTI.

Two different approaches based on NMR spectroscopy and on surface plasmon resonance (SPR) were followed to demonstrate the ternary Avidin-BTI-MMP interaction.

Several NMR parameters are strongly influenced by the molecular weight and by the dynamical properties of the investigated macromolecules. Classical NMR experiments such as ^{15}N-^{1}H HSQC usually performed to investigate biomolecules up to 30-40 kDa are inefficient for larger systems due to the fast transverse relaxation rate that broaden the signals beyond the detection threshold.[40] Therefore, NH resonances can act as probes to investigate the formation of large protein-protein complexes.[41] In the present case, the evolution of the NH signals of the ^{15}N MMP-12 catalytic domain complexed with the BTI **4** in ^{15}N-^{1}H HSQC spectra was exploited to monitor the interaction with non labeled avidin, given that the binding of the biotin moiety to one of the four binding sites on the tetrameric avidin should provide a 87 kDa complex. Since multiple binding for each avidin molecule may occur, even larger protein complexes are expected in solution. As shown in Figure 15 (panel D), the addition of an equimolar solution of the 65 kDa avidin to a solution of the ^{15}N-labeled catalytic domain of MMP-12 complexed with the BTI **4** caused the complete disappearance of all NH cross-peaks without any precipitation of the sample.

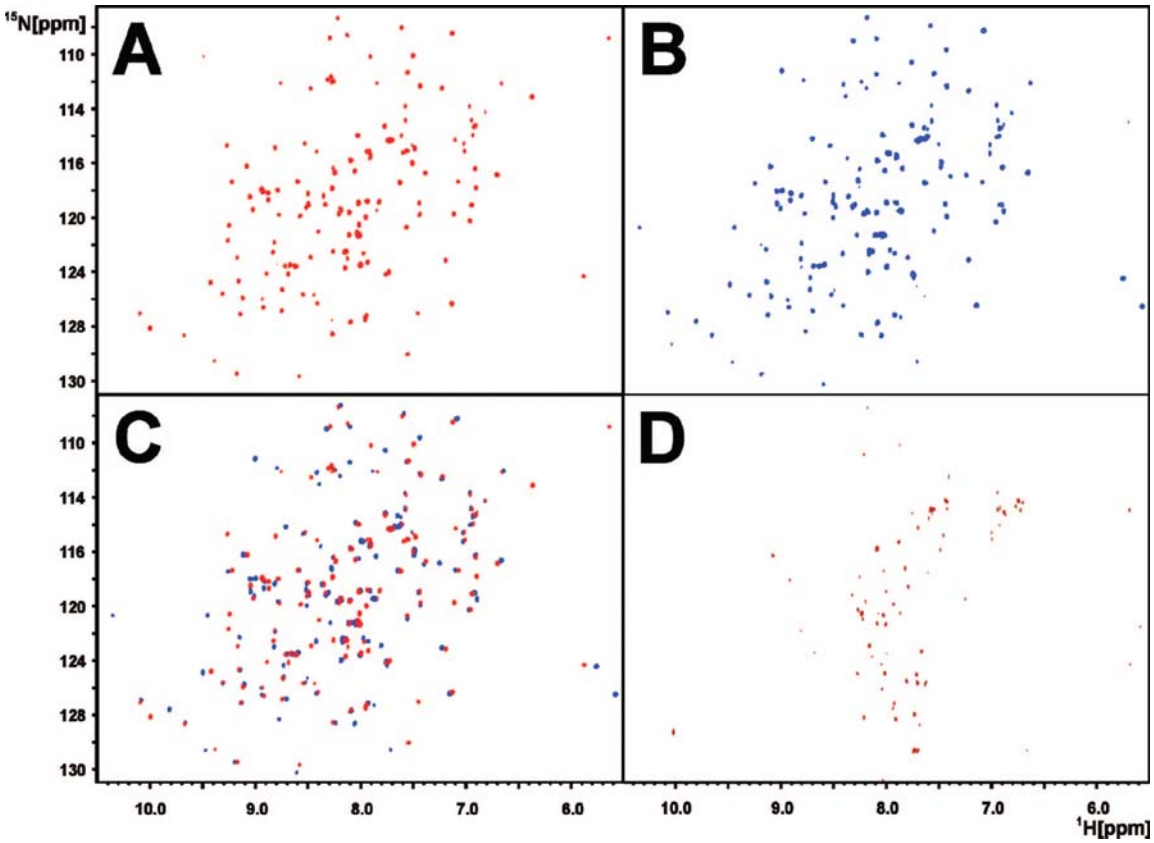

Figure 15. ^{15}N-^{1}H HSQC spectrum of MMP-12 catalytic domain in the absence (A) and in the presence (B) of compound BTI-**4** (equimolar concentration). The two spectra are superimposed to highlight the cross-peak shifts (C). The ternary complex formation Avidin-BTI-MMP is seen in panel D where most of the cross-peaks disappeared.

To exclude the presence of aspecific protein-protein interactions, avidin was added to a solution containing 200 μM of NNGH-inhibited-MMP-12 catalytic domain: in this case, no changes were detected in the HSQC spectra. Therefore, we can reasonably conclude that the strong protein-protein interaction, monitored by the ^{15}N-^{1}H HSQC experiments, is mediated by the BTI **4** which is able to bind MMP-12 and avidin and to prevent, at the same time, an extensive reciprocal reorientation of the complex subunits. Although NMR data allowed us to ascertain that **4** does bind both avidin and MMP-12 simultaneously, the micromolar concentrations used for these experiments do not provide information on how this simultaneous interaction may affect the nanomolar affinity of the inhibitor to MMP-12. Indeed, possible steric effects related to the presence of the hemopexin domain need to be evaluated to understand the real binding capability of the probe toward functionally active enzymes.[42] In this respect, the availability of the active full-length MMP-12 allowed us to ascertain the efficiency of the biotinylated inhibitor to bind simultaneously avidin and the

physiologically active enzyme and to quantify the effect of the hemopexin domain on the affinity constant.

2.7 SPR analysis

Surface plasmon resonance (SPR) is widely applied to investigate protein-protein and protein-ligand interactions. Information on affinity constant, on binding kinetics, as well as on binding enthalpy can be quickly obtained by using small amounts of protein samples. In particular, the sensitivity of the SPR technique permits the investigation of high-affinity interactions and monitoring the formation of ternary complexes. SPR analysis was carried out using a ProteOn XPR36 parallel array biosensor equipped with avidin sensor chips (NLC). This chip has an avidin-coated surface that can be used to immobilize biotinylated molecules.[43]

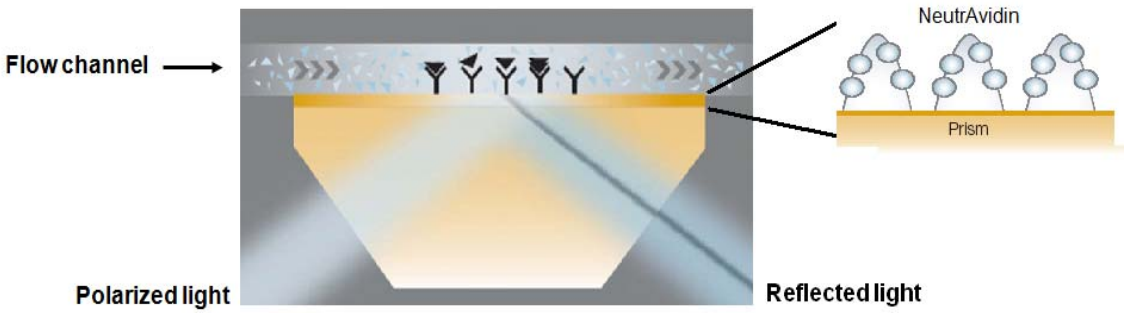

Figure 16. ProteOn NLC Sensor Chip with Neutravidin bound to the polymer layer.

In our study, BTI **4** was immobilized on channels 1-5 of the chip by injecting PBS-T buffered solutions of the biotinylated molecule at different concentrations. The sixth channel was left blank. The assay was performed by injecting solutions of the full-length MMP-12 on the chip channels and fitting the sensorgrams at four different concentrations. The measured K_D (4.76 nM) was comparable to the fluorimetric *K*i measured for **4** vs. the isolated catalytic domain of MMP-12 (BTI **4**-MMP-12 complex) (Figure 16a).

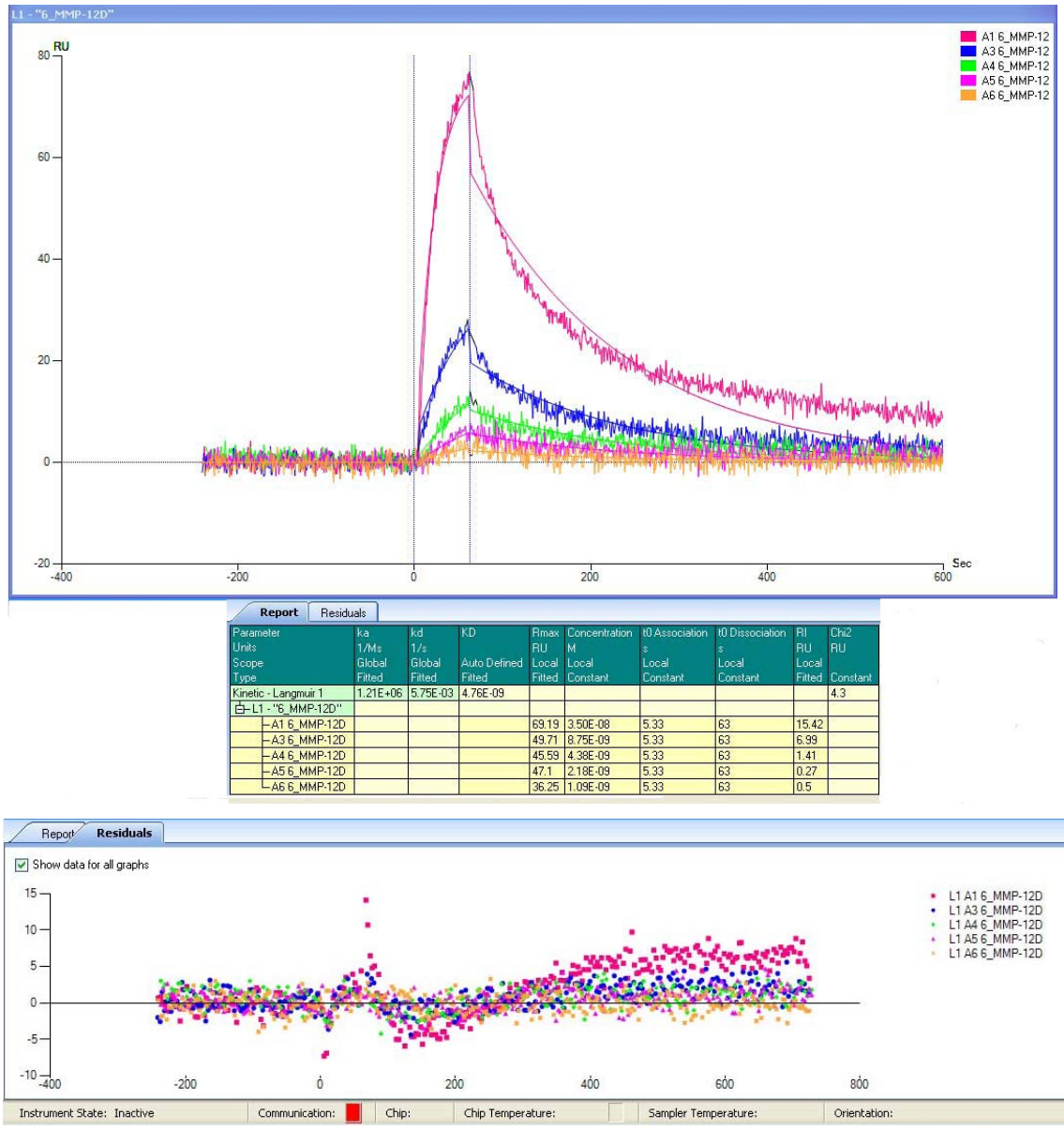

Parameter	ka	kd	KD	Rmax	Concentration	t0 Association	t0 Dissociation	RI	Chi2
Units	1/Ms	1/s		RU	M	s	s	RU	RU
Scope	Global	Global	Auto Defined	Local	Local	Local	Local	Local	
Type	Fitted	Fitted	Fitted	Fitted	Constant	Constant	Constant	Fitted	Constant
Kinetic - Langmuir 1	1.21E+06	5.75E-03	4.76E-09						4.3
L1 - "6_MMP-12D"									
A1 6_MMP-12D				69.19	3.50E-08	5.33	63	15.42	
A3 6_MMP-12D				49.71	8.75E-09	5.33	63	6.99	
A4 6_MMP-12D				45.59	4.38E-09	5.33	63	1.41	
A5 6_MMP-12D				47.1	2.18E-09	5.33	63	0.27	
A6 6_MMP-12D				36.25	1.09E-09	5.33	63	0.5	

Figure 16a. SPR Sensorgram of BTI **4** vs. MMP-12, calculation of K_D and plot of the residuals.

2.8 Purification of MMPs from biological fluids

The employment of bifuctional ligand BTI **4** for the selective collection of matrix metalloproteinases from biological fluids has been evaluated by using a monomeric avidin-bound column (Pierce). An amount of 2.50 mg of BTI **4** was dissolved in 8.1 mL of Tris-buffer, and the solution (50 uL) was mixed with the same volume of an equimolar sample of MMP-12 (0.4 mM) dissolved into Tris buffer; 25 uL of the mixture so obtained was added to 50 uL of a solution of carbonic anhydrase from erythrocytes (0.1 mM in Tris-buffer). A monomeric avidin-bound column (0.6 mL of settled gel) was loaded with the solution of BTI **4**, MMP-12,

and carbonic anhydrase; then, it was first eluted with 1.4 mL of Tris-buffer and subsequently with a solution of NNGH (1 mM, Tris buffer). Relying on the strong avidin-biotin interaction, the column blocked BTI **4**-MMP-12 complex, while carbonic anhydrase was completely washed out. Addition of nanomolar inhibitor NNGH displaced BTI **4** complexed to MMP-12, and the latter was so eluted and separated from carbonic anhydrase (Figure 17).

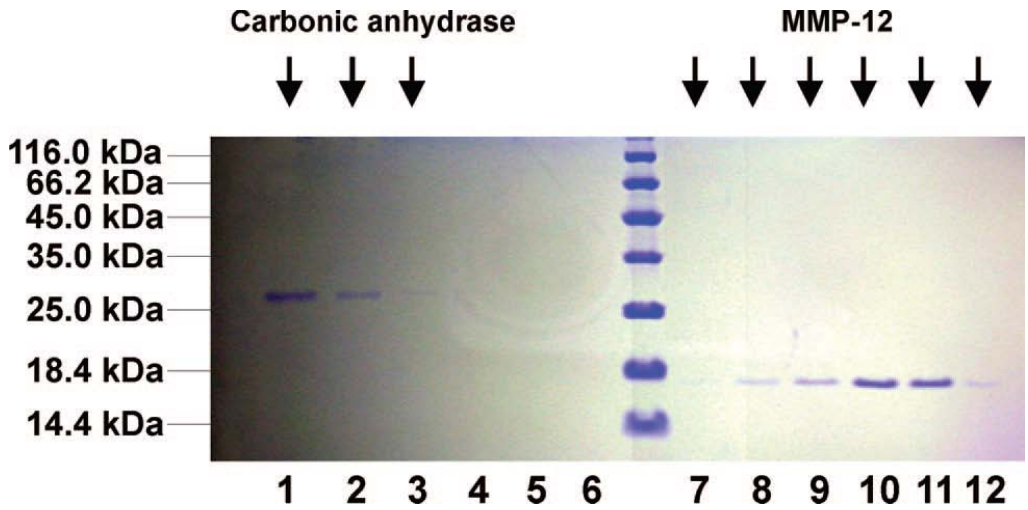

Figure 17. SDS PAGE analysis of the fractions shows an effective chromatographic separation of MMP-12 and carbonic anhydrase loaded on a monomeric avidin-bound column.

Reference List

[1.] B. N. G. Giepmans, S. R. Adams, M. H. Ellisman, R. Y. Tsien, *Science* **2006,** *312* 217-224.

[2.] T. L. Blundell, H. Jhoti, C. Abell, *Nat.Rev.Drug Discovery* **2002,** *1* 45-54.

[3.] S. L. Johnson, M. Pellecchia, *Curr.Top.Med.Chem.* **2006,** *6* 317-329.

[4.] W. Jahnke, M. J. Blommers, C. Fernandez, C. Zwingelstein, R. Amstutz, *ChemBioChem* **2005,** *6* 1607-1610.

[5.] D. Heckmann, A. Meyer, L. Marinelli, G. Zahn, R. Stragies, H. Kessler, *Angew.Chem., Int.Ed.* **2007,** *46* 3571-3574.

[6.] C. Bremer, C. H. Tung, A. Bogdanov, R. Weissleder, *Radiology* **2002,** *222* 814-818.

[7.] M. Lepage, W. C. Dow, M. Melchior, Y. You, B. Fingleton, C. C. Quarles, C. Pepin, J. C. Gore, L. M. Matrisian, J. O. McIntyre, *Mol.Imaging* **2007,** *6* 393-403.

[8.] A. David, D. Steer, S. Bregant, L. Devel, A. Makaritis, F. Beau, A. Yiotakis, V. Dive, *Angew.Chem., Int.Ed.* **2007,** *46* 3275-3277.

[9.] A. Saghatelian, N. Jessani, A. Joseph, M. Humphrey, B. F. Cravatt, *Proc.Natl.Acad.Sci.U.S.A.* **2004,** *101* 10000-10005.

[10.] C. Bremer, C. H. Tung, R. Weissleder, *Nat.Med.* **2001,** *7* 743-748.

[11.] A. Faust, B. Waschkau, J. Waldeck, C. Holtke, H. J. Breyholz, S. Wagner, K. Kopka, W. Heindel, M. Schafers, C. Bremer, *Bioconjugate Chem.* **2008,** *19* 1001-1008.

[12.] S. Wagner, H. J. Breyholz, M. P. Law, A. Faust, C. Holtke, S. Schroer, G. Haufe, B. Levkau, O. Schober, M. Schafers, K. Kopka, *J.Med.Chem.* **2007,** *50* 5752-5764.

[13.] S. Wagner, H. J. Breyholz, A. Faust, C. Holtke, B. Levkau, O. Schober, M. Schafers, K. Kopka, *Curr.Med.Chem.* **2006,** *13* 2819-2838.

[14.] E. Dragoni, V. Calderone, M. Fragai, R. Jaiswal, C. Luchinat, C. Nativi, *Bioconjugate Chemistry* **2009,** *20* 719-727.

[15.] Hermanson, G. T. Bioconjugate techniques (Avidin-Biotin Systems). Academic Press.

[16.] G. Paganelli, P. Riva, G. Deleide, A. Clivio, F. Chiolerio, G. A. Scassellati, M. Malcovati, A. G. Siccardi, *Int.J.Cancer, Supp.* **1988,** *2* 121-125.

[17.] I. Bertini, V. Calderone, M. Fragai, C. Luchinat, M. Maletta, *Angew.Chem., Int.Ed.* **2006,** *45* 7952-7955.

[18.] I. Bertini, V. Calderone, M. Fragai, C. Luchinat, S. Mangani, B. Terni, *Angew.Chem., Int.Ed.* **2003,** *42* 2673-2676.

[19.] I. Bertini, V. Calderone, M. Fragai, C. Luchinat, S. Mangani, B. Terni, *J.Mol.Biol.* **2004,** *336* 707-716.

[20.] I. Bertini, V. Calderone, M. Fragai, A. Giachetti, M. Loconte, C. Luchinat, M. Maletta, C. Nativi, K. Yeo, *J.Am.Chem.Soc.* **2007,** *129* 2466-2475.

[21.] I. Bertini, M. Fragai, Y.-M. Lee, C. Luchinat, B. Terni, *Angew.Chem., Int.Ed.* **2004,** *43* 2254-2256.

[22.] V. Calderone, M. Fragai, C. Luchinat, C. Nativi, B. Richichi, S. Roelens, *ChemMedChem* **2006,** *1* 598-601.

[23.] I. Bertini, M. Fragai, A. Giachetti, C. Luchinat, M. Maletta, G. Parigi, K. Yeo, *J.Med.Chem.* **2005,** *48* 7544-7559.

[24.] M. Fragai, C. Nativi, B. Richichi, C. Venturi, *ChemBioChem* **2005,** *6* 1345-1349.

[25.] C. Mannino, M. Nievo, F. Machetti, A. Papakyriakou, M. Fragai, A. Guarna, *Bioorg.Med.Chem.* **2006,** *14* 7392-7403.

[26.] E. Dragoni, V. Calderone, M. Fragai, R. Jaiswal, C. Luchinat, C. Nativi, *Bioconjugate Chem.* **2009,** *20* 719-727.

[27.] H. F. Bigg, A. D. Rowan, *Curr.Opin.Pharmacol.* **2001,** *1* 314-320.

[28.] A. Agrawal, D. Romero-Perez, J. A. Jacobsen, F. J. Villarreal, S. M. Cohen, *ChemMedChem* **2008,** *3* 812-820.

[29.] D. T. Puerta, S. M. Cohen, *Curr.Top.Med.Chem.* **2004,** *4* 1551-1573.

[30.] S. Pikul, N. E. Ohler, G. Ciszewski, M. C. Laufersweiler, N. G. Almstead, B. De, M. G. Natchus, L. C. Hsieh, M. J. Janusz, S. X. Peng, T. M. Branch, S. L. King, Y. O. Taiwo, G. E. Mieling, *J.Med.Chem.* **2001,** *44* 2499-2502.

[31.] X. Q. Wang, Y. C. Choe, C. S. Craik, J. A. Ellman, *Bioorg.Med.Chem.Lett.* **2002,** *12* 2201-2204.

[32.] F. Auge, W. Hornebeck, M. Decarme, J. Y. Laronze, *Bioorg.Med.Chem.Lett.* **2003,** *13* 1783-1786.

[33.] I. Bertini, V. Calderone, M. Cosenza, Y.-M. Lee, C. Luchinat, S. Mangani, B. Terni, P. Turano, *J.Mol.Biol.* **2007,** *374* 1333-1344.

[34.] L. Devel, V. Rogakos, A. David, A. Makaritis, F. Beau, P. Cuniasse, A. Yiotakis, V. Dive, *J.Biol.Chem.* **2006,** *281* 11152-11160.

[35.] A. Tochowicz, K. Maskos, R. Huber, R. Oltenfreiter, V. Dive, A. Yiotakis, M. Zanda, W. Bode, P. Goettig, *J.Mol.Biol.* **2007,** *371* 989-1006.

[36.] B. Lovejoy, A. R. Welch, S. Carr, C. Luong, C. Broka, R. T. Hendricks, J. A. Campbell, K. A. M. Walker, R. Martin, H. Van Wart, M. F. Browner, *Nat.Struct.Biol.* **1999,** *6* 217-221.

[37.] DeLano, W. L. The PyMOL Molecular Graphics System. 2002.

[38.] G. Sabatino, M. Chinol, G. Paganelli, S. Papi, M. Chelli, G. Leone, A. M. Papini, A. De Luca, M. Ginanneschi, *J.Med.Chem.* **2003,** *46* 3170-3173.

[39.] A. Canales-Mayordomo, R. Fayos, J. Angulo, R. Ojeda, M. Martin-Pastor, P. M. Nieto, M. Martin-Lomas, R. Lozano, G. Gimenez-Gallego, J. Jimenez-Barbero, *J.Biomol.NMR* **2006,** *35* 225-239.

[40.] M. Pellecchia, P. Sebbel, U. Hermanns, K. Wuthrich, R. Glockshuber, *Nat.Struct.Biol.* **1999,** *6* 336-339.

[41.] L. D'Silva, P. Ozdowy, M. Krajewski, U. Rothweiler, M. Singh, T. A. Holak, *J.Am.Chem.Soc.* **2005,** *127* 13220-13226.

[42.] I. Bertini, V. Calderone, M. Fragai, R. Jaiswal, C. Luchinat, M. Melikian, E. Mylonas, D. Svergun, *J.Am.Chem.Soc.* **2008,** *130* 7011-7021.

[43.] T. Bravman, V. Bronner, K. Lavie, A. Notcovich, G. A. Papalia, D. G. Myszka, *Anal.Biochem.* **2006,** *358* 281-288.

Chapter 3

Development of new dendrimeric MMPI as alternative drug delivery system for the Dry-Eye Syndrome (DES).

3.1 Introduction

Dry eye is a common disease affecting a significant percentage of the population: it is defined as "a disorder of the tear film due to tear deficiency or excessive evaporation that causes damage to the interpalpebral ocular surface and is associated with symptoms of discomfort."[1] Here I report a classification scheme (Figure 18) that stratifies patients with dry eye from those with decreased aqueous tear production by the lacrimal glands to those with increased evaporative loss.

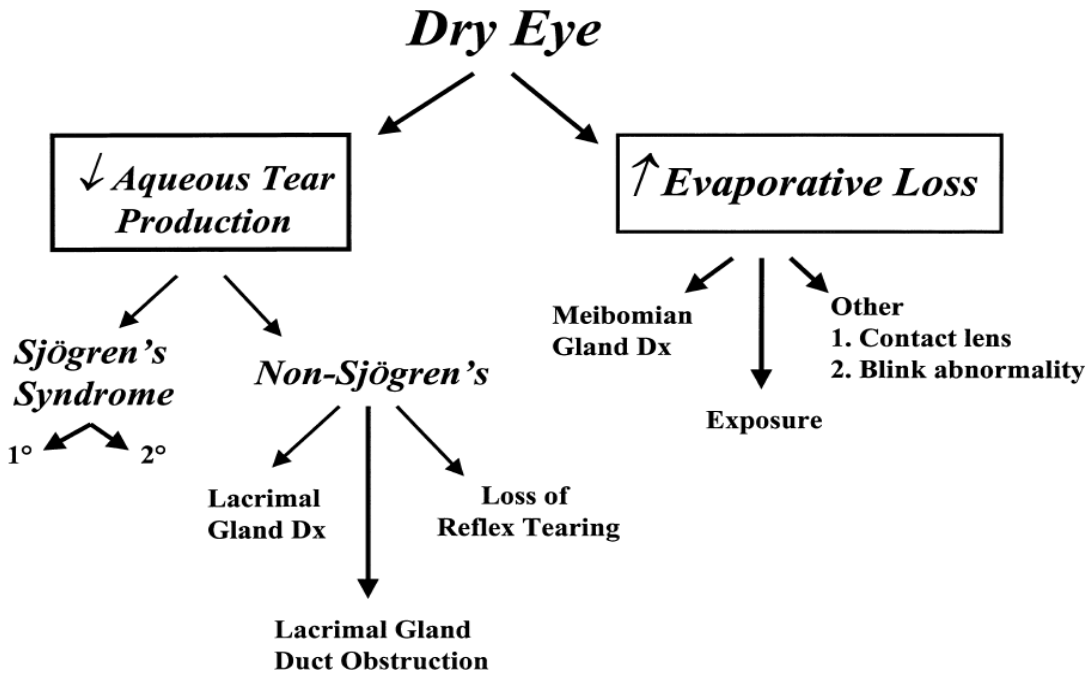

Figure 18. Diagnostic classification scheme for dry eye disease proposed by the National Eye Institute/Industry Workshop.

Dry eye syndrome could have many causes. One of the most common reason for dryness is simply the normal aging process. As we grow older, our bodies produce less oil – 60% less at age 65 then at age 18. This is more pronounced in women, who tend to have drier skin then men. The oil deficiency also affects the tear film. Without as much oil to seal the watery layer, the tear film evaporates much faster, leaving dry areas on the cornea. Many other factors, such as hot, dry or windy climates, high altitudes, air-conditioning and cigarette smoke also cause dry eyes. Many people also find their eyes become irritated when reading or working on a computer. Stopping periodically to rest and blink keeps the eyes more comfortable. Contact lens wearers may also suffer from dryness because the contacts absorb the tear film, causing proteins to form on the surface of the lens. Certain medications, thyroid conditions, vitamin A deficiency, and diseases such as Parkinson's and Sjögren's can also cause

dryness. Women frequently experience problems with dry eyes as they enter menopause because of hormonal changes.

3.2 Tear film structure and composition

The precorneal tear film consists of three separate layers: mucus, water, and oil. Imaging studies performed in rodents and humans indicate that the mucus, protein, and aqueous components in the precorneal tear film combine to form a hydrated gel (Figure 19)[1].

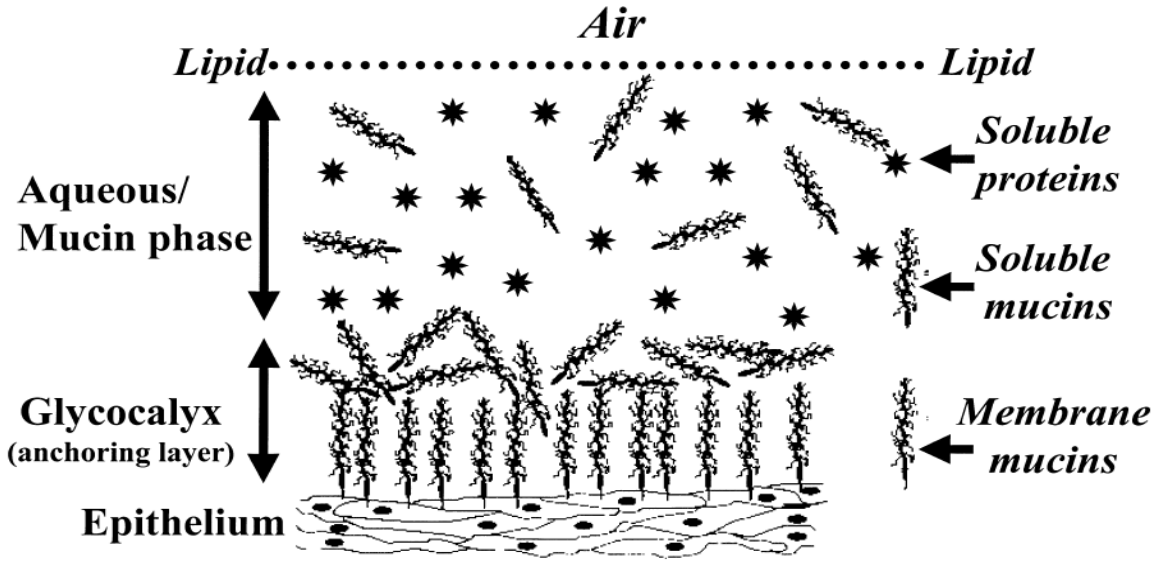

Figure 19. Proposed structure of precorneal tear film that consists of a superficial lipid layer, a middle aqueous/mucin phase that contains soluble mucins, aqueous fluid, electrolytes, and proteins that are secreted by the lacrimal glands, and ocular surface epithelium. This layer is anchored to the underlying superficial corneal epithelium by chemical attractions to the epithelial membrane mucins (glycocalyx).

- The innermost layer is the thinnest. It is a layer of mucin (or mucus). This very thin layer of mucus is produced by the cells in the conjunctiva (the clear skin that lines the eye). The mucus helps the overlying watery layer to spread evenly over the eye.

- The middle (or aqueous) layer is the largest and the thickest. This layer is essentially a very dilute saltwater solution. The lacrimal glands under the upper lids and the accessory tear glands produce this watery layer. This layer's function is to keep the

eye moist and comfortable, as well as to help flush out any dust, debris, or foreign objects that may get into the eye. Defects of the aqueous layer are the most common cause of dry eye syndrome.

- The most superficial layer is a very thin layer of lipids (fats or oils). These lipids are produced by the meibomian glands and the glands of Zeis (oil glands in the eyelids). The main function of this lipid layer is to help decrease evaporation of the watery layer beneath it.

3.3 Dry Eye Syndrome symptoms and pathogenesis

The most common symptoms of the dry eye syndrome are the follows:

- Dry, gritty/scratchy, or filmy feeling in the eyes
- Burning or itching in the eyes
- Redness of the eyes
- Blurred vision
- A sensation of having a foreign body in the eyes
- Light sensitivity

Symptoms seem to worsen in dry climates, in windy conditions, with higher temperatures, with lower humidity, with prolonged use of your eyes (for example, reading, watching TV), and toward the end of the day. Sometimes a symptom of DES may actually be intermittent excessive tearing with DES. When the eye becomes slightly dry and irritated, it may initiate reflex tearing with production of a large amount of tears all at once to try to get moist and comfortable again. Unfortunately, the eye can only handle so many tears at any one time; the rest pour over your eyelids and down the cheeks. Those tears do not help the eyes and are wasted. A short time later, the eyes will become slightly dry and irritated again, and the whole process may repeat itself.

An exact mechanism for the development of these pathologic changes has not been elucidated. The severity of DES worsens as aqueous tear secretion decreases and as the ability to reflex tear in response to sensory stimulation is lost. Ocular surface epithelial function and differentiation may be adversely affected by the increase in tear film osmolarity that occurs in dry eye. Trauma to a poorly lubricated and unprotected ocular surface from environmental

factors and blinking may be another contributing factor because DES is most severe in the exposure zone that is subjected to these stresses. If DES represents a chronic wound-healing response, then it may be perpetuated, in part, by reduced levels of lacrimal gland-secreted growth factors in the tear fluid.

Inflammation may represent another important causative factor for DES. Decreased aqueous tear production and tear clearance leads to chronic inflammation of the ocular surface, that it is responsible in part of the ocular surface epithelial disease and irritation symptoms. Increased levels of inflammatory cytokines (as IL-1β and TNF-α) and concentrations and activities of MMPs have been detected in the tear fluid and/or conjunctival epithelia of patients with DES.[2;3] As a matter of fact, IL-1β and TNF-α upregulate production of gelatinase A and B (MMP-2 and MMP-9), collagenases (MMP-1, -8 and -13), and stromelysins (MMP-3).[4-6]

Increased levels of MMP-3 and -9 have been detected in the tear fluid of patients with keratoconjunctivitis sicca (KCS).[7;8] Among the MMPs, MMP-9 has been found to be of central importance in cleaving epithelial basement membrane components and tight junction proteins (such as ZO-1 and occludin) that maintain corneal epithelial barrier function.[9] Expression of MMP-9 by the ocular surface epithelia in normal healthy eyes is low.

Increased production of MMP-9 by the corneal epithelium has been found in the eyes of individuals with sterile corneal ulceration: moreover increased MMP-9 activity has been associated with disruption of corneal epithelial barrier function and corneal surface irregularity in an experimental murine model of dry eye. MMP-9 knockout mice showed significantly less alteration of epithelial barrier function in response to experimental desiccating stress than did wild-type mice, and this protective effect was abrogated by topical application of MMP-9 to the ocular surface.[10] Furthermore, Solomon et al.[3] found increased activity of MMP-9 in the tear fluid of patients with Sjögren's syndrome.

Very interesting results had been obtained with the use of the doxycycline (a tetracycline antibiotic) for DES. This compound is in fact well recognized for its therapeutic efficacy in treating ocular surface disease, such as rosacea and sterile corneal ulceration. Doxycycline has been found to decrease the production and activity of IL-1β and MMP-9[6] in the human corneal epithelium.

But, unfortunately, the only treatments available up to now are palliative and provide insufficient relief for many patients, particularly those with chronic moderate to severe disease. These patients are at increased risk of ocular surface damage and ocular infection, as

well as being subjected to chronic ocular discomfort and visual difficulties, in fact healing dry eye problems is important not only for comfort, but also for the health of the cornea.

One of the few and the elective approach to treating DES is the use of artificial tears, but some of these products are watery and alleviate the symptoms temporarily; others are thicker and adhere to the eye longer. Preservative-free tears are recommended because they are the most soothing and have fewer additives that could potentially irritate. In fact the frequent use of artificial tear solutions that are preserved with benzalkonium chloride may be toxic to the ocular surface epithelium[1]. To avoid the risk of preservative toxicity to the abnormal ocular surface epithelium of eyes with DES, there has been an increase in trend over the past decade to use unit-dose nonpreserved artificial tears in patients who must frequently instill artificial tears to control their irritation symptoms. As a matter of fact, ocular delivery is one of the most interesting and challenging endeavors faced by the researchers, because of the critical and pharmacokinetically specific environments that exists in the eye.

3.4 Design of a dendrimeric MMPI as new drug delivery system

On the basis of this data, to improve the treatment of this disease we resolved to use a sulfonamidic MMPs inhibitor, **12**, to develop a drug delivery system able to sustain the drug release and to remain in the vicinity of the FOTE (Front Of The Eye) for a prolonged period of time.

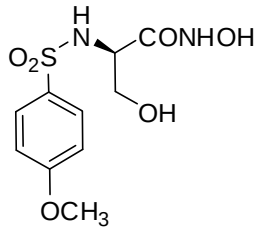

12

Figure 20. Structure of **12.**

To accomplish that we decided to use dendrimers. Dendrimers are macromolecular compounds made up of a series of branches around an inner core[11]. They are attracting systems for drug delivery because of their easiness of preparation and functionalization and their ability to display multiple copies of surface groups for biological recognition processes.

In ocular drug delivery dendrimers had shown several potential advantages. Easily administered as eye drops with a good patient compliance, they had demonstrated a prolonged residence time at the ocular surface after instillation and they could protect the drug loaded against metabolic enzymes. Moreover dendrimers can be tailored or modified into biocompatible compounds with low cytotoxicity.

Dendrimers are classified and designed according to the surface terminating groups quality (for example aminic, carboxylic and hydroxylic groups) and quantity: the number of these surface terminating group, and consequently the molecular weight of the macromolecule, rises with the higher generation (Figure 21)[12].

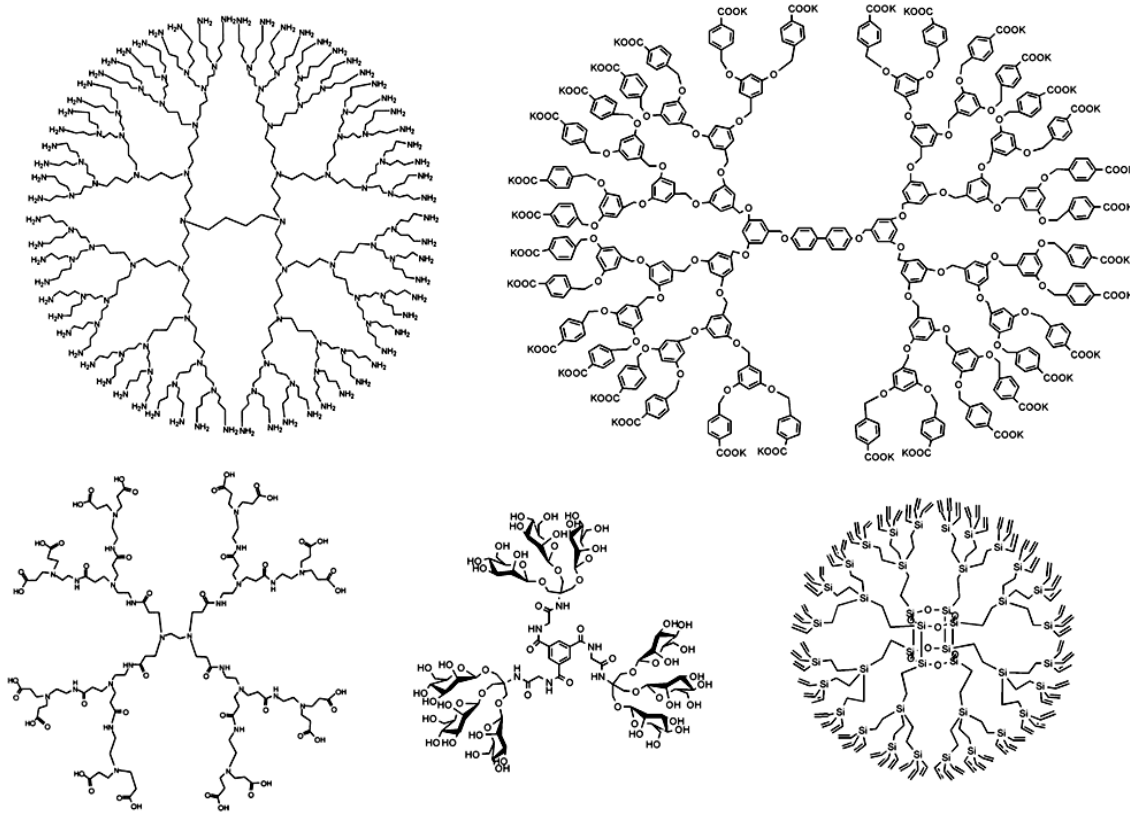

Figure 21. Different type of dendrimers.

Polyamidoamine (PAMAM) dendrimers are the most common class of dendrimers suitable for many materials science and biotechnology applications. They presents a very high stability; moreover substituted and low generation PAMAM dendrimers are in general non-toxic and non-immunogenic compounds.

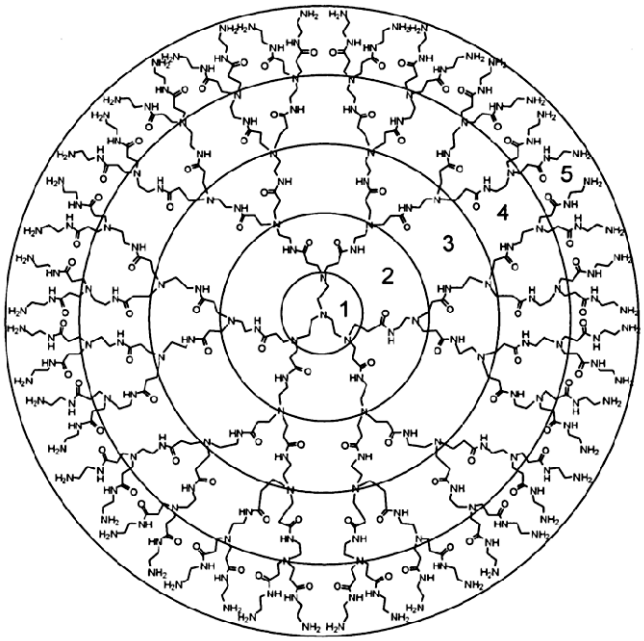

Figure 22. General structure of polyamido amine dendrimers (PAMAM, Starburst™) (G5). Each generation is marked with a circle.

Most common PAMAM dendrimers consist of alkyl-diamine core and tertiary amine branches (Figure 23), but they are commercially available in different generations, with different core types and different functional surface groups.

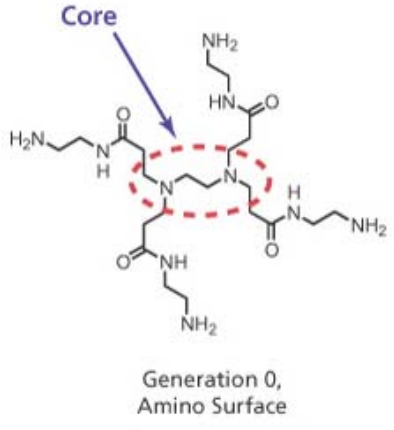

Figure 23. Amino surface PAMAM dendrimer.

In particular, PAMAM dendrimers with amino surface consist of polar, highly reactive primary amine surface groups. The surfaces of these dendrimers are cationic and can be derivatized, either through ionic interactions with negatively charged molecules, or using many well-known reagents for covalent functionalization of primary amines. Thanks to these characteristics, PAMAM are easily coupled with carboxylic activated groups.

Following this strategy, we projected the synthesis of an high-reactive, key intermediate to link our inhibitor **12** to the dendrimer. As docking point of the linker we chosen the sulfonamidic nitrogen for the same rationale seen before (see Chapter 1).

3.5 Synthesis and Fluorimetric assays

First of all, the sulfonamide of D-serine methyester **13** was transformed, under standard conditions, into the corresponding *tert*butyldimethylsilyl ether **14**, then it was reacted with the first part of the linker under Mitsunobu condition to give compound **15**. Acidic removal of silylether protecting group afforded compound **16**: this compound had been hydrogenated to deprotect the aminic group, but the reaction afforded a mixture of compound **17** and a cyclic side-product in a 1:1 ratio.

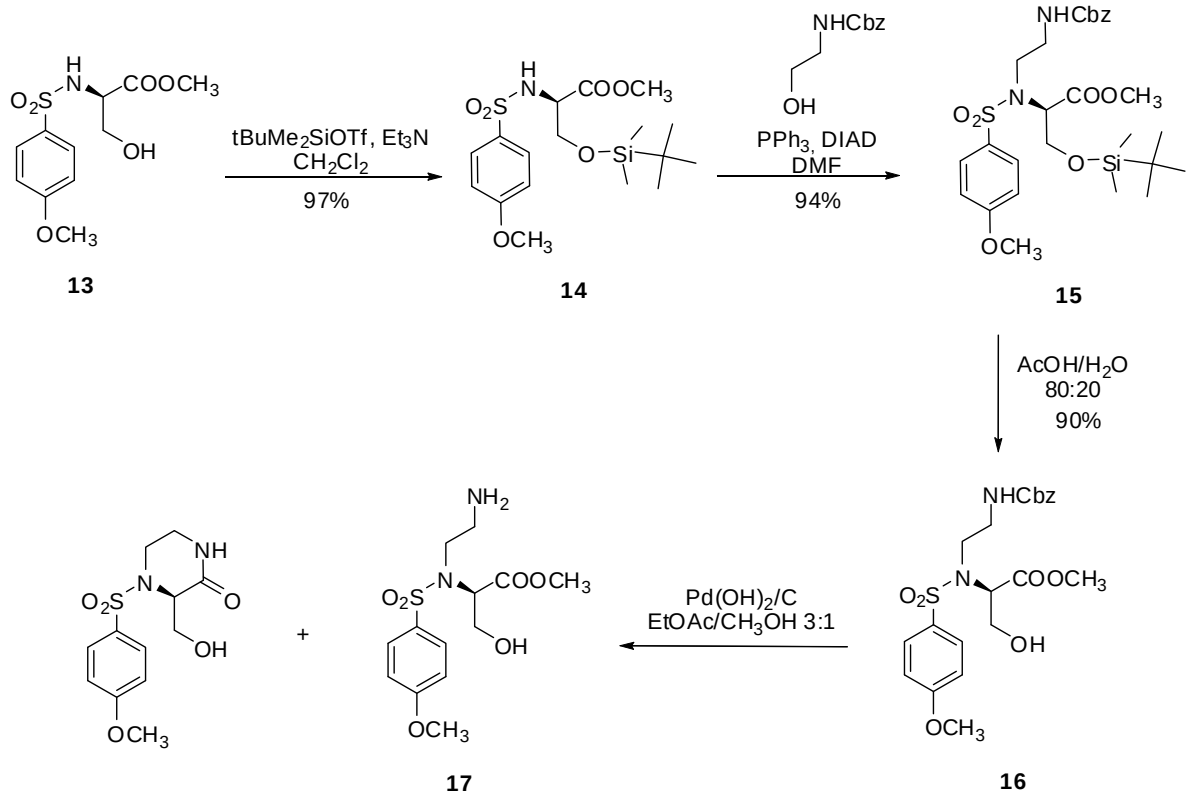

Scheme 5.

After the achievement of **17** we had to find a conjugation method to effect the covalent linkage of our inhibitor to the PAMAM dendrimer. We had to chose a coupling reaction that would ideally proceed in near quantitative yield. To achieve this objective we selected the homobifunctional reagent, adipate 4-nitrophenyl diester **18**, which was readily

synthesized from commercially available adipoyl chloride. Reaction of adipoyl chloride with 4-nitrophenol in pyridine gave **18** in 70% yield, as shown in Scheme 6.

The efficient coupling methods that use this type of homobifunctional reagent affords reproducible conjugation in high yields under mild conditions.[13]

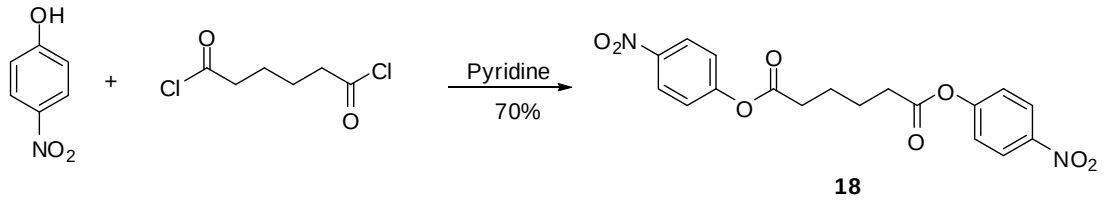

18

Scheme 6. Synthesis of adipate 4-nitrophenyl diester **18**.

The mixture of compound **17** and the cyclic side product had been reacted with **18** to give the activated ester **19**, that has been coupled with a small dendron (PAMAM-2) to afford compound **20** in a good yield (64%) (Scheme 7).

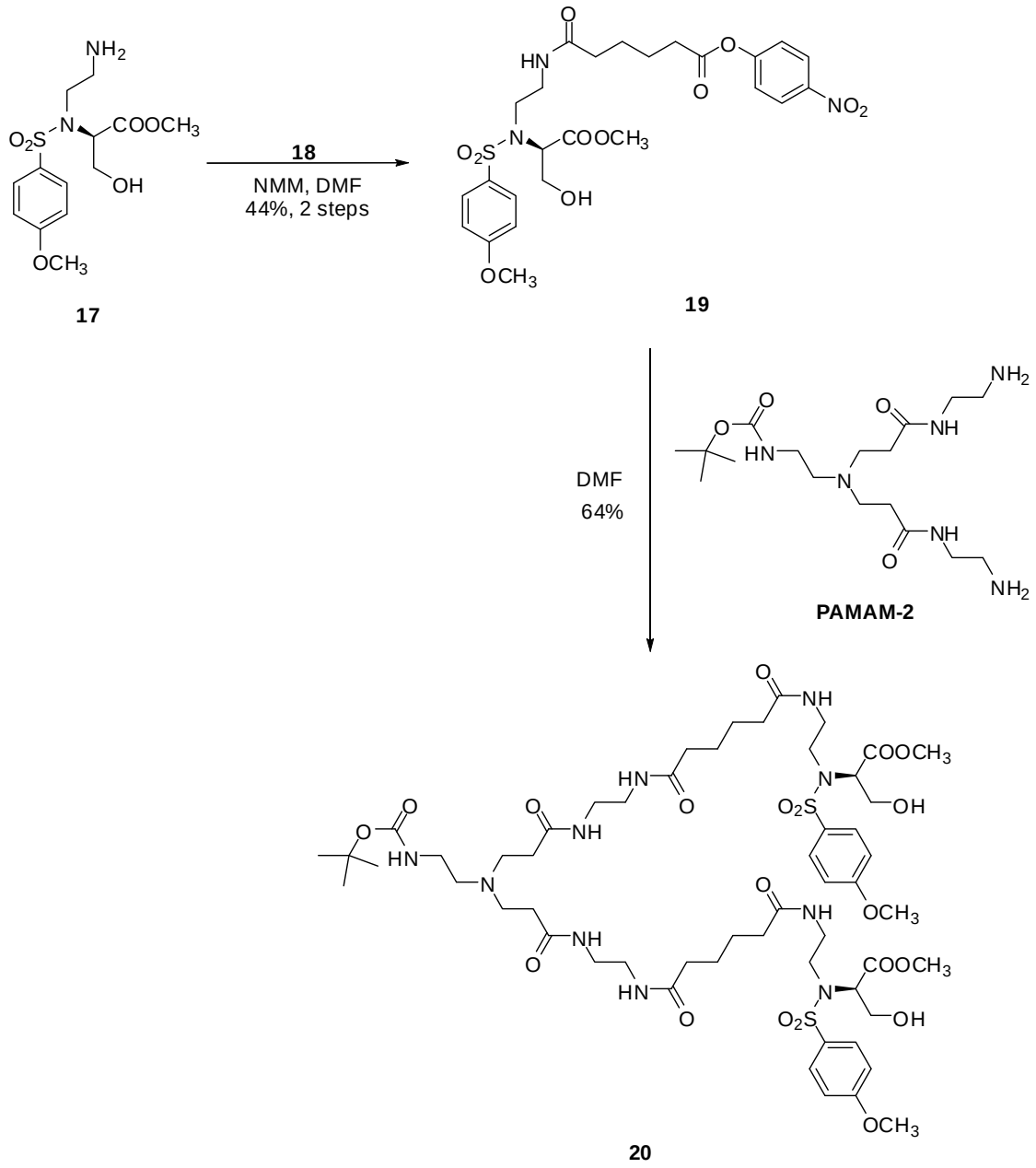

Scheme 7.

Compound **20** was directly transformed into the corresponding hydroxamic acid **21** by reaction with hydroxylamine hydrochloride and potassium hydroxide, in methanol as solvent.

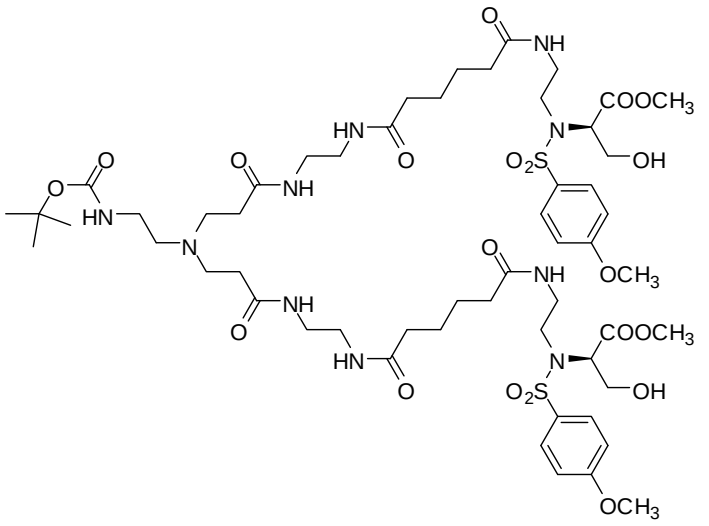

20

$NH_2OH{\cdot}HCl$, KOH
CH_3OH
67%

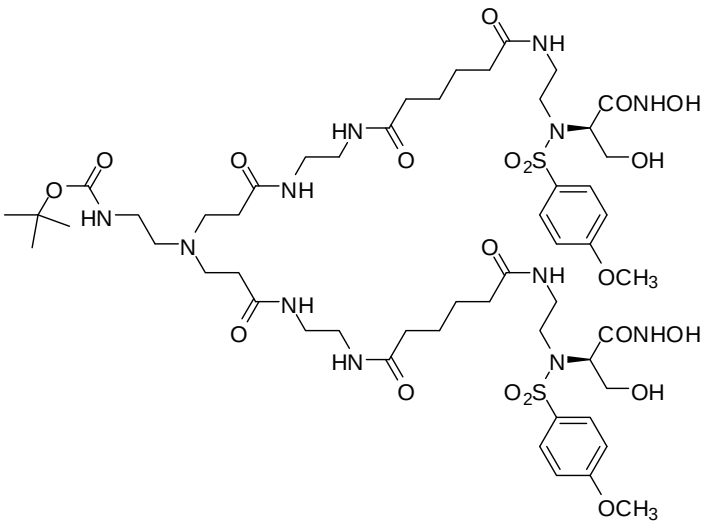

21

Scheme 8.

To rationalize the influence of the position and length of the linker vs. the interaction of our inhibitor with MMPs, we synthesized **22** as reference compound, starting from **15**. These compound had been deprotected through hydrogenation ad reprotected as acetyl to mimic an amidic bond to give compound **23**. Acidic removal (CH_3COOH/H_2O 80:20) of silylether protecting group on **23** afforded **24**, that was treated with hydroxylamine

hydrochloride and potassium hydroxide in methanol to form hydroxamic acid **22** in 45% yield (Scheme 9).

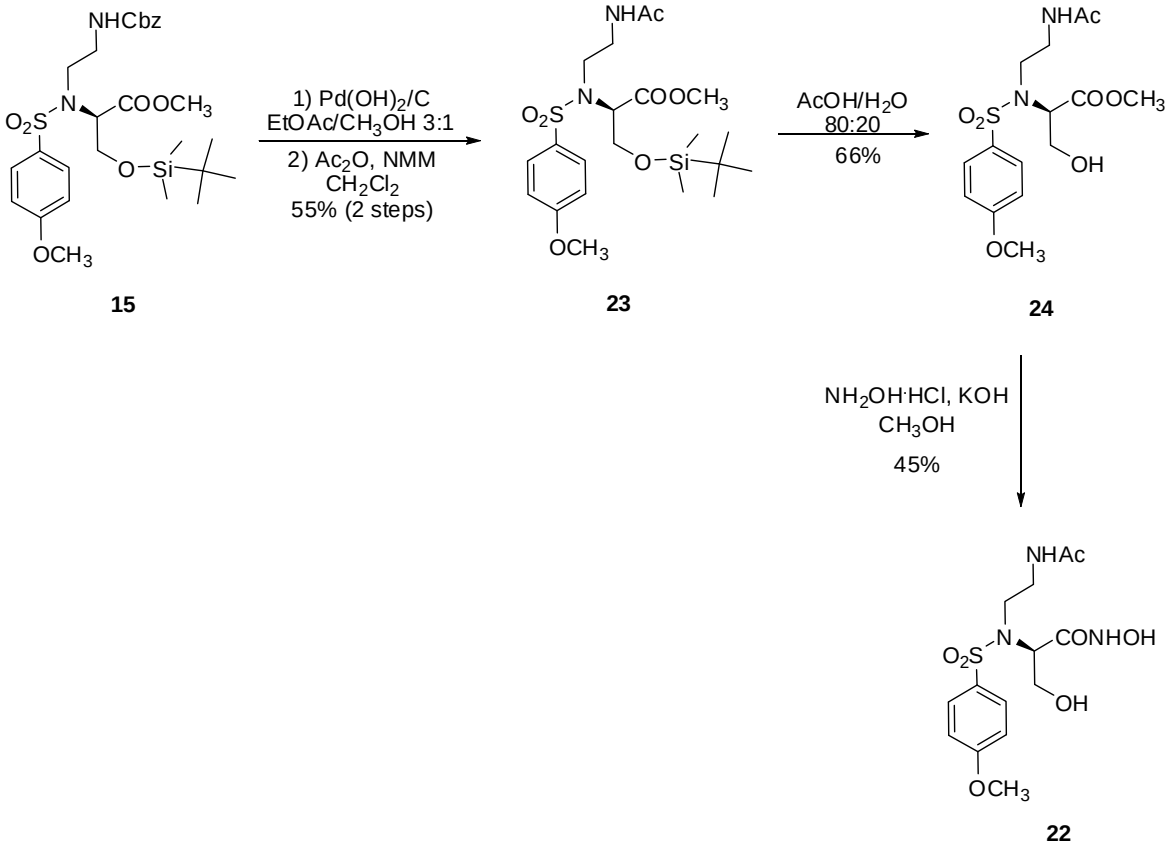

15 **23** **24** **22**

Scheme 9.

The affinity properties of **22** and PAMAM dendron **21** toward the selected MMPs were evaluated by fluorimetric assay. The *K*i values are reported in Table 3, in comparison to **12**.

Table 3. Inhibition constants (K_i) of inhibitors **22**, **21**, **12** toward different MMPs.

Compound	MMP-1	MMP-2	MMP-7	MMP-9	MMP-12	MMP-13
21	940 nM	182 nM	14.8 µM	119 nM	172 nM	190 nM
22	44.0 nM	7.20 nM	147 nM	36.0 nM	19.0 nM	23.3 nM
12	143 nM		823 nM	18.0 nM	8.89 nM	2.20 nM

As we can notice from the data of compound **22**, the insertion of the linker on the sulfonamidic nitrogen of **12** gave a little increase in the affinity for MMP-1 and -7 and a little decrease for MMP-12 and -13, but to sum up the K_i remained very similar. While, if we consider **22** dendron the affinity vs. all the MMPs decreased very much.

Our hypothesis for this reduction in the inhibition constants was that the linker (which connected the inhibitor to the dendron) was too short, and this diminished the affinity for MMPs.

To understand this, we synthesized a new dendron, that presented a longer linker (by the addition of three methylene residues). With the same strategy seen before, we obtained compound **25**, that was evaluated by fluorimetric assays; K_i values are reported in Table 4.

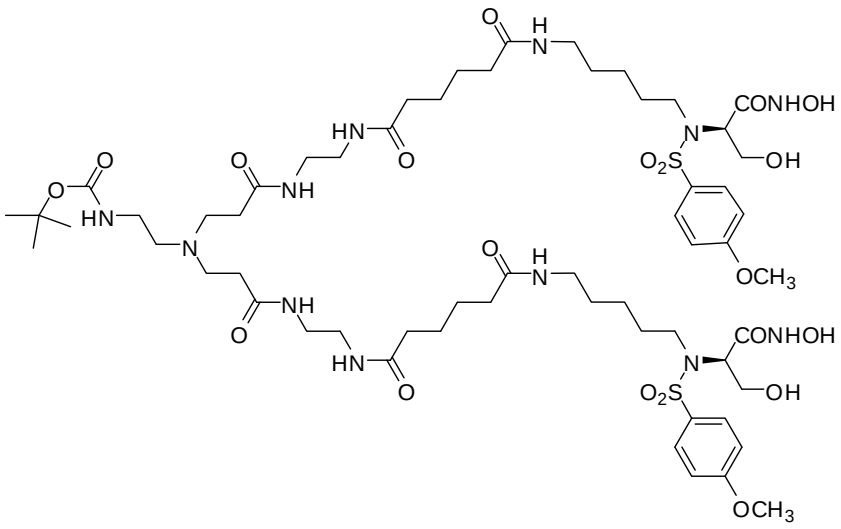

25

Figure 24. Structure of **25**.

Table 4. Inhibition constants (K_i) of **25** toward different MMPs.

Compound	MMP-1	MMP-2	MMP-7	MMP-9	MMP-12	MMP-13
25	286 nM	32.0 nM	7.40 µM	18.0 nM	45.0 nM	115 nM

As we had hypnotized, in this case the affinity vs. all the MMPs greatly increased with respect to **21** dendron; probably, a longer linker was more suitable for the interaction with MMPs. In particular, the affinity vs. MMP-1, -2, -9 and -13, that are directly involved in the pathogenesis of the dry eye syndrome, was in the low nanomolar range.

For the synthesis of **25** we started from **14** and we introduced the first part of the linker through Mitsunobu reaction to obtain **26**, that after deprotection of the oxydrilic (**27**) and of the aminic groups (**28**) had been linked with **18** to give **29**.

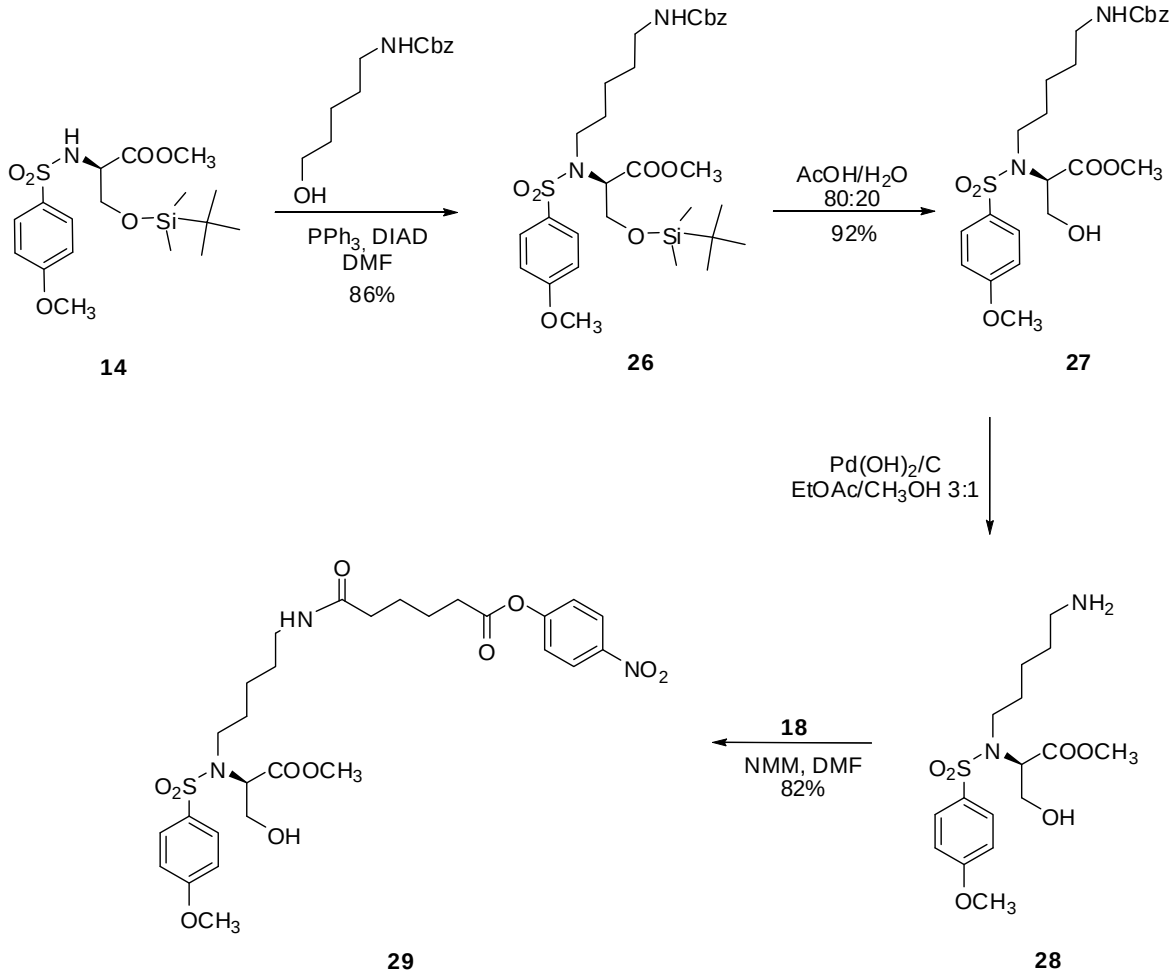

Scheme 10.

Compound **29** had been coupled with PAMAM-2 to give compound **30**, that was treated with hydroxylamine hydrochloride and potassium hydroxide in methanol to form hydroxamic acid **25.**

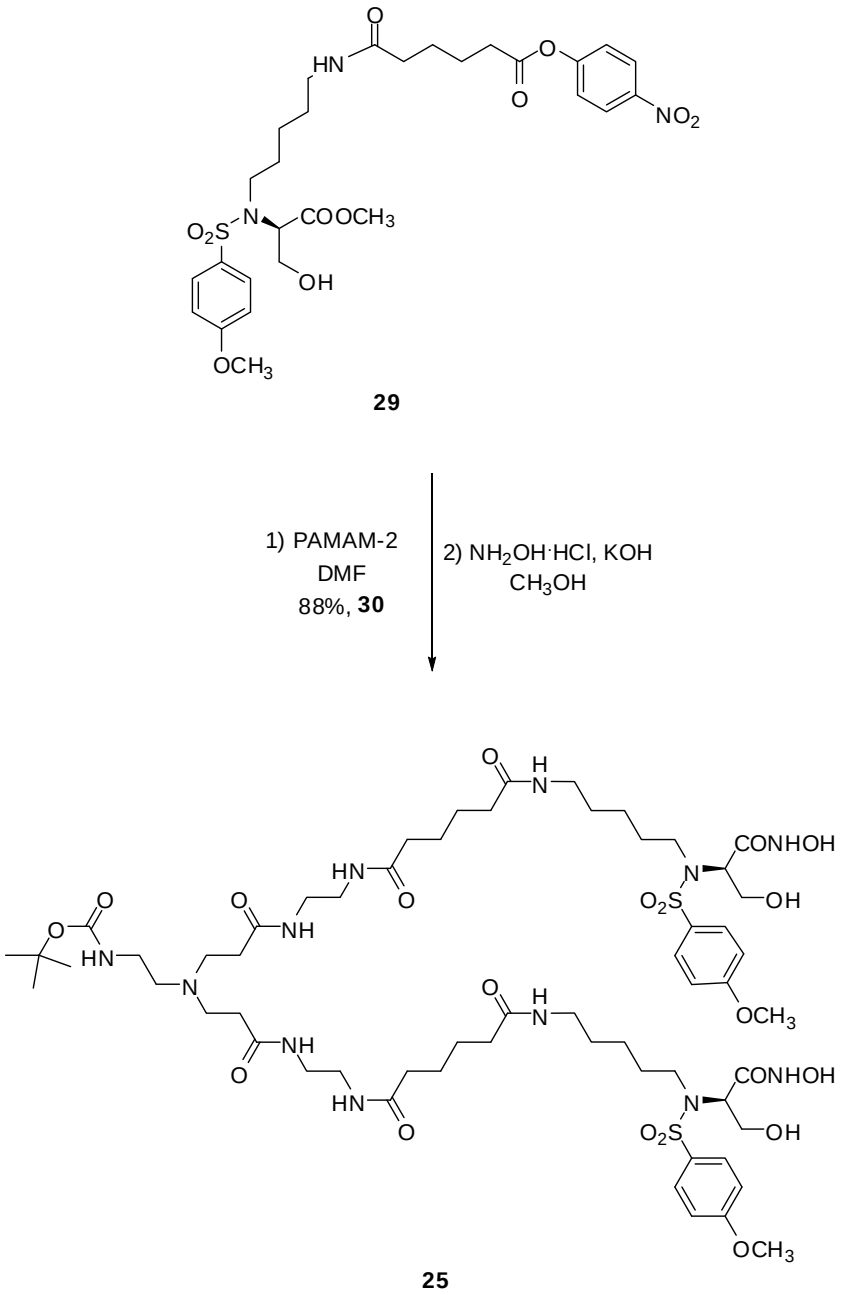

29

25

Scheme 11.

In parallel to this, we synthesized a little dendrimer called TETRAM, started from **29**: in this case we employed as zinc binding group a carboxylic acid instead of an hydroxamic acid.

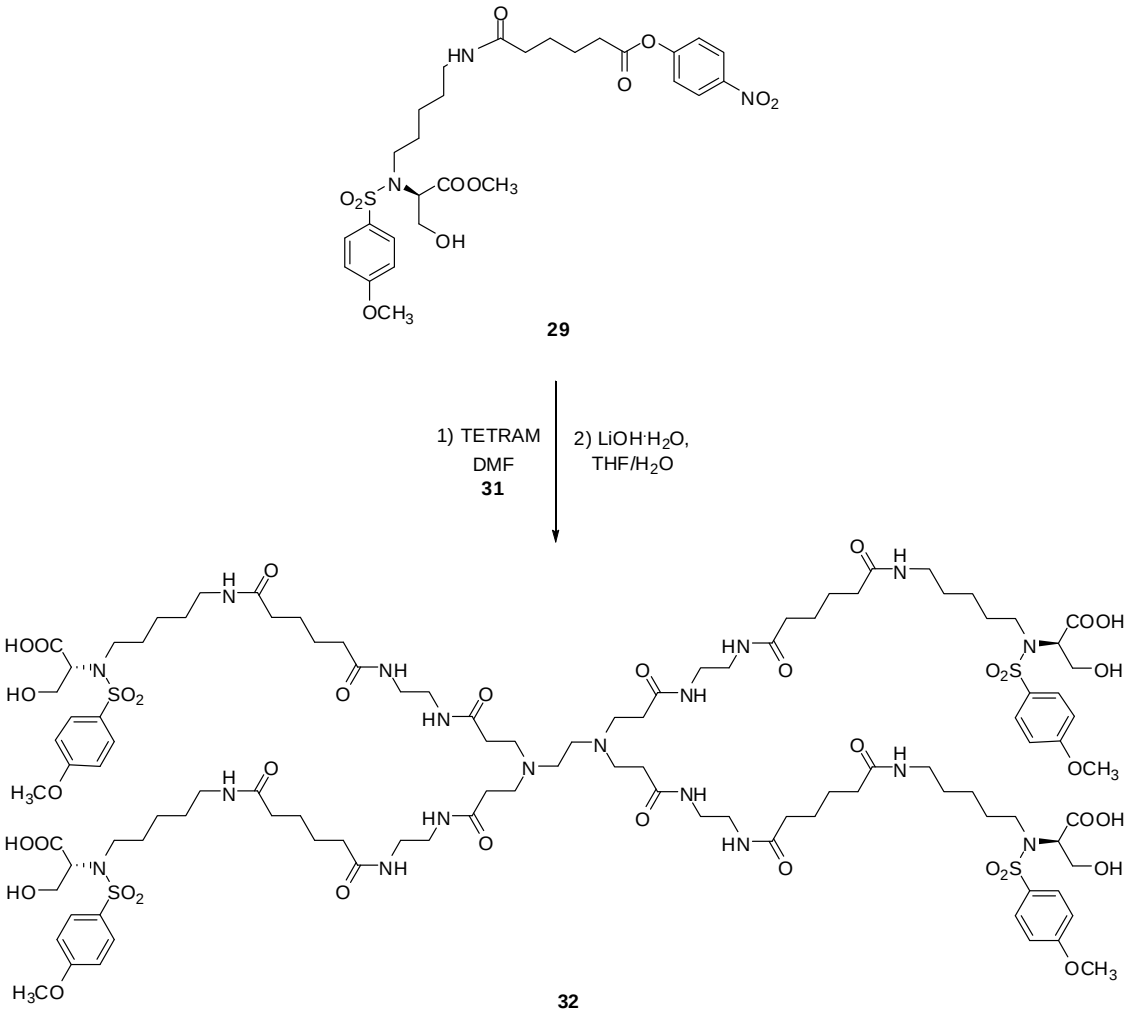

29

32

Scheme 12.

As reference compound for **32** we use compound **33**.

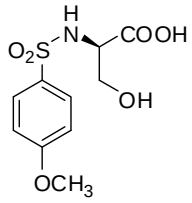

33

Figure 25. Structure of compound **33**.

The affinity properties of the two compounds (**32** and **33**) toward the selected MMPs were evaluated by fluorimetric assay. The *K*i values are reported in Table 5.

Table 5. Inhibition constants (K_i) of inhibitors **32** and **33** toward different MMPs.

Compound	MMP-1	MMP-2	MMP-7	MMP-9	MMP-12	MMP-13
32	132 µM	3.20 µM	300 µM	1.00 µM	1.72 µM	2.12 µM
33	101 µM		146 µM		3.90 µM	

This is a remarkable result: in the case of TETRAM, there was not a decrease in the affinity of the inhibitor vs. MMPs at all.

All these compounds will be evaluated as drug delivery system for the Dry Eye Syndrome.

Reference List

[1.] S. C. Pflugfelder, A. Solomon, M. E. Stern, *Cornea* **2000,** *19* 644-649.

[2.] S. C. Pflugfelder, D. Jones, Z. H. Ji, A. Afonso, D. Monroy, *Current Eye Research* **1999,** *19* 201-211.

[3.] A. Solomon, D. Dursun, Z. G. Liu, Y. H. Xie, A. Macri, S. C. Pflugfelder, *Investigative Ophthalmology & Visual Science* **2001,** *42* 2283-2292.

[4.] R. M. Corrales, M. E. Stern, C. S. De Paiva, J. Welch, D. Q. Li, S. C. Pflugfelder, *Investigative Ophthalmology & Visual Science* **2006,** *47* 3293-3302.

[5.] D. Q. Li, T. Y. Shang, H. S. Kim, A. Solomon, B. L. Lokeshwar, S. C. Pflugfelder, *Investigative Ophthalmology & Visual Science* **2003,** *44* 2928-2936.

[6.] D. Q. Li, B. L. Lokeshwar, A. Solomon, D. Monroy, Z. G. Ji, S. C. Pflugfelder, *Experimental Eye Research* **2001,** *73* 449-459.

[7.] L. Sobrin, Z. G. Liu, D. C. Monroy, A. Solomon, M. G. Selzer, B. L. Lokeshwar, S. C. Pflugfelder, *Investigative Ophthalmology & Visual Science* **2000,** *41* 1703-1709.

[8.] D. Q. Li, S. C. Pflugfelder, *Ocular Surface* **2005,** *3* S198-S202.

[9.] S. Chotikavanich, C. S. De Paiva, D. Q. Li, J. J. Chen, F. Bian, W. J. Farley, S. C. Pflugfelder, *Investigative Ophthalmology & Visual Science* **2009,** *50* 3203-3209.

[10.] S. C. Pflugfelder, W. Farley, L. H. Luo, L. Z. Chen, C. S. De Paiva, L. C. Olmos, D. Q. Li, M. E. Fini, *American Journal of Pathology* **2005,** *166* 61-71.

[11.] S. K. Sahoo, F. Diinawaz, S. Krishnakumar, *Drug Discovery Today* **2008,** *13* 144-151.

[12.] J. Vandervoort, A. Ludwig, *Nanomedicine* **2007,** *2* 11-21.

[13.] X. Y. Wu, C. C. Ling, D. R. Bundle, *Organic Letters* **2004,** *6* 4407-4410.

Chapter 4

Design, synthesis and evaluation of new inhibitors of MMP-7

4.1 Introduction

Matrilysin (MMP-7) is a member of the MMP gene family and, after being activated, has a broad proteolytic activity against a variety of extracellular matrix substrates, including collagens, proteoglycans, elastin, laminin, fibronectin, and casein. Compared with other MMPs, matrilysin is distinguished by its low molecular mass (28 kDa) and its lack of a C-terminal domain; this C-terminal domain is found to be present in almost all of the MMPs except MMP-7 and MMP-23, and seems to regulate the enzyme activity. Matrilysin was identified first in postpartum rat uterus, and has been detected in several normal tissues, such as endometrium, bronchial mucosa, monocytes, and mesangial cells.[1]

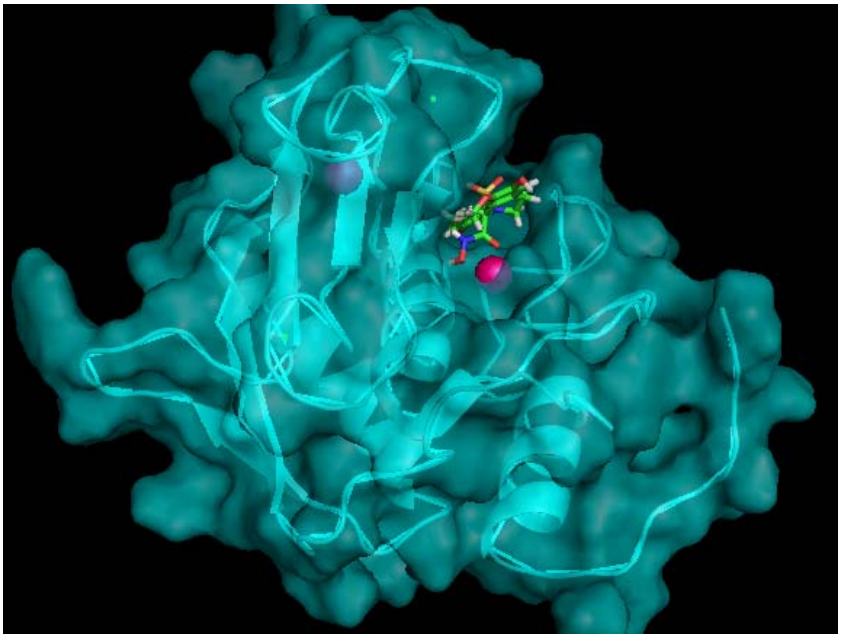

Figure 26. Structure of MMP-7 complexed with a sulfonamidic inhibitor (Zheng, X.H. et all, **2009**, pdb code: 2ddy).

MMP-7 has been specifically implicated as an important facilitator of tissue remodeling due to its ability to cleave a variety of known substrates, including many ECM proteins and the latent forms of other MMPs.[2] It is notable that MMP-7 is produced predominantly by cells of epithelial origin, whereas most other MMPs are generally expressed by the underlying stromal cells including those residing in connective tissues or by migratory cells of the immune system.

Overexpression of MMP-7 has been directly correlated with enhanced tumorigenicity and tumor cell invasion using *in vitro* model systems. For tumor systems in which MMP-7 activity is known to modulate the course of the disease, MMP-7 is secreted even in the

earliest stages. Small, benign "precancerous" lesions, for example, exhibit MMP-7 secretion well before these lesions would be clinically detectable. Furthermore, analysis of MMP-7 expression in human neoplasia revealed that enzyme mRNA appeared in the surrounding normal tissue in only a few isolated cases, suggesting highly specific enzyme expression in the immediate tumor vicinity. The larger and more progressed these tumors become, the higher the MMP-7 levels tend to be. Moreover, intestinal tumorigenesis is suppressed in mice lacking matrilysin.[3] In addition, approximately 80% of spontaneous tumors analyzed express matrilysin . Taken together, these findings suggest that inhibition of matrilysin activity in human colorectal cancers may provide a protective effect.

Furthermore, MMP-7 has proven to have diagnostic and prognostic value, as expression is associated with poor outcome in esophageal, colon, and pancreatic cancers. In human colon carcinomas, it has been reported that expression of MMP-7 correlates with poor prognosis, advanced Dukes stage, liver metastasis and depth of invasion. In addition, cell line studies have shown that overexpression of MMP-7 increases the invasiveness and metastatic potential of colon cancer cells, and that an antisense oligonucleotide against MMP-7 suppresses liver metastasis. These results suggest a significant role for MMP-7 in tumor invasion and metastasis even at late stages of colon cancer progression.[4]

Nevertheless selective inhibitors for MMP-7 are not present in the literature, and almost all inhibitors synthesized up to now have a very high affinity for other MMPs (such as MMP-12 and MMP-13 for example) and a lower affinity for MMP-7; this is due to its relatively slim size of the S_1' pocket.

4.2 Design, synthesis and evaluation of new MMP-7 inhibitors.

In this contest we dealt with the design and synthesis of a new MMP-7 inhibitor that contains a sulphonamidic and a peptidic portion, conceived on specific aminoacidic sequences recognized by MMP-7: only after the cleavage operated by matrilysin in a specific region (where the MMP-7 was overexpressed) our pro-inhibitor should be opened and only in this form it should inhibit the protein. Cantley et al.[5] published a paper with some peptidic sequence selectively cleaved by MMP-7 (see Table 6):

Table 6. Kinetics of cleavage for a series of substituted peptides based on the predicted optimal cleavage motif for MMP-7.

Peptide sequence	***V*max/*K*M**
VPLS-LTMG	100 ± 13
GPLS-LTMG	60 ± 10
GVLS-LTMG	31 ± 3
GGLS-LTMG	2.8 ± 0.6
VPQS-LTMG	40 ± 10
VPLS-ITMG	52 ± 7
VPL**S-LA**MG	22 ± 3
VPLS-LDMG	9 ± 2
VPLS-LTGG	31 ± 4

We firstly synthesized the sulphonamidic inhibitor that contained the aminoacid serine (that it is the first aminoacid before the cleavage operated by MMP-7): on this derivate we had to introduce the aminoacids for recreating the proper sequence recognized by MMP-7. To do this we synthesized **33** (only a mild inhibitor), that has as zinc-binding group a carboxylic acid.

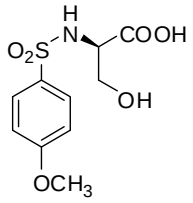

33

Figure 27. Structure of compound **33.**

This molecule had been modified (substitution of the OH of the serine with an aminic group), and after the achievement of derivate **34** starting from the L-serinemethylester hydrochloride we added the other two aminoacids of the highlighted sequence in Table 6 that was positioned after the cleavage operated by MMP-7 (an alanine and a leucine) to obtain compound **35**.

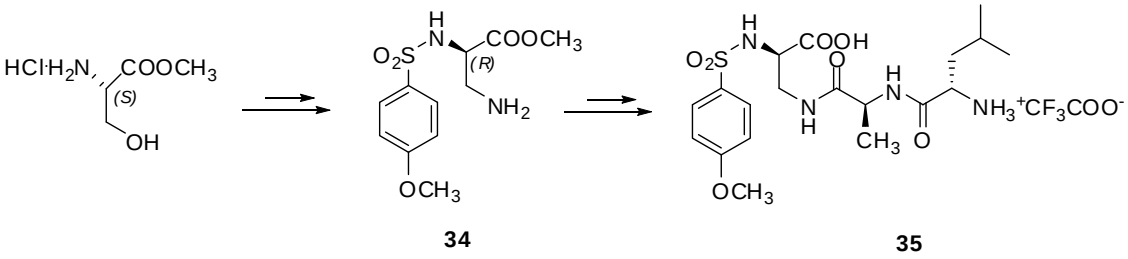

34 **35**

Scheme 13. Synthesis of compound **35**

The synthesis of compound **35** was optimized and afforded the desired compound in a very good yield (35% on 11 steps). We started from L-serine methyl ester, that was firstly selectively benzylated on the aminic group (compound **36**)[6] and then mesylated on the oxydrilic group to obtain the intermediate **37**. The reaction of compound **37** with sodium azide was performed under optimized conditions (CH_3CN/DMF 4:1, 60 °C); a single product was isolated in 75% yield whose structure was determined to be (*R*)-methyl α-azido-*β*-*N*,*N*-dibenzyl propionate (**38**). Methyl *N*,*N*-dibenzyl-*β*-azido alanate (**39**) resulting from the formal direct nucleophilic substitution of mesylate by azide was not detected in the crude product by ^{1}H NMR analysis (Scheme 14).

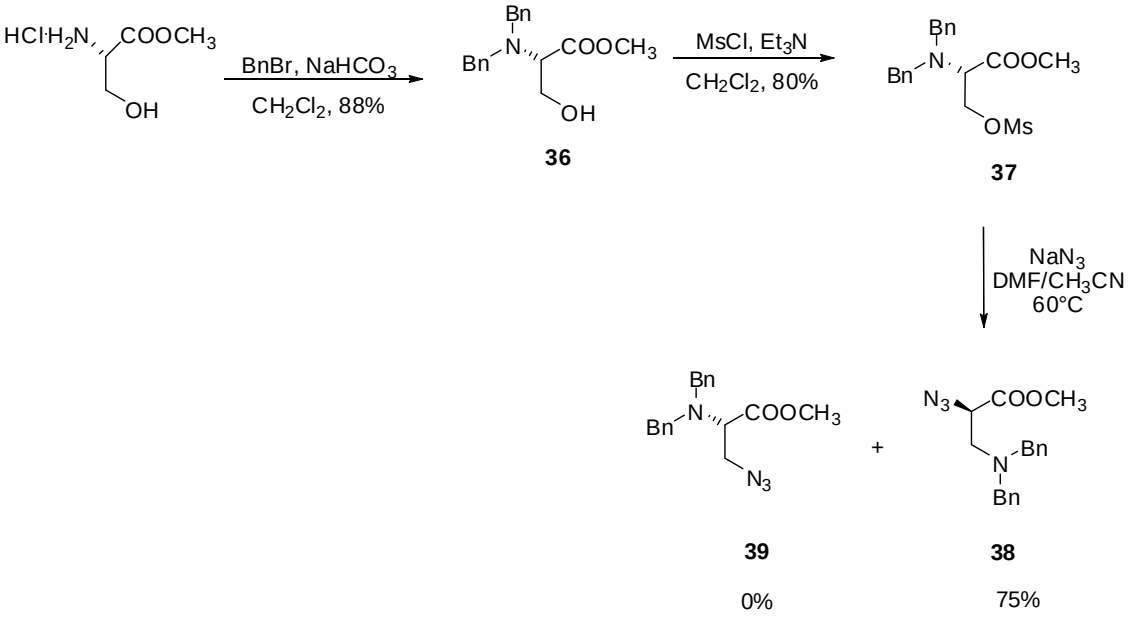

36 **37** **39** **38**

0% 75%

Scheme 14.

Staudinger reduction of the azide **38** gave the diamine **40** in 94% yield. This compound was been reacted with *p*-metoxybenzensulfonyl chloride to obtain compound **41**, that was deprotected to give the aminic derivative **34** in quantitative yield.

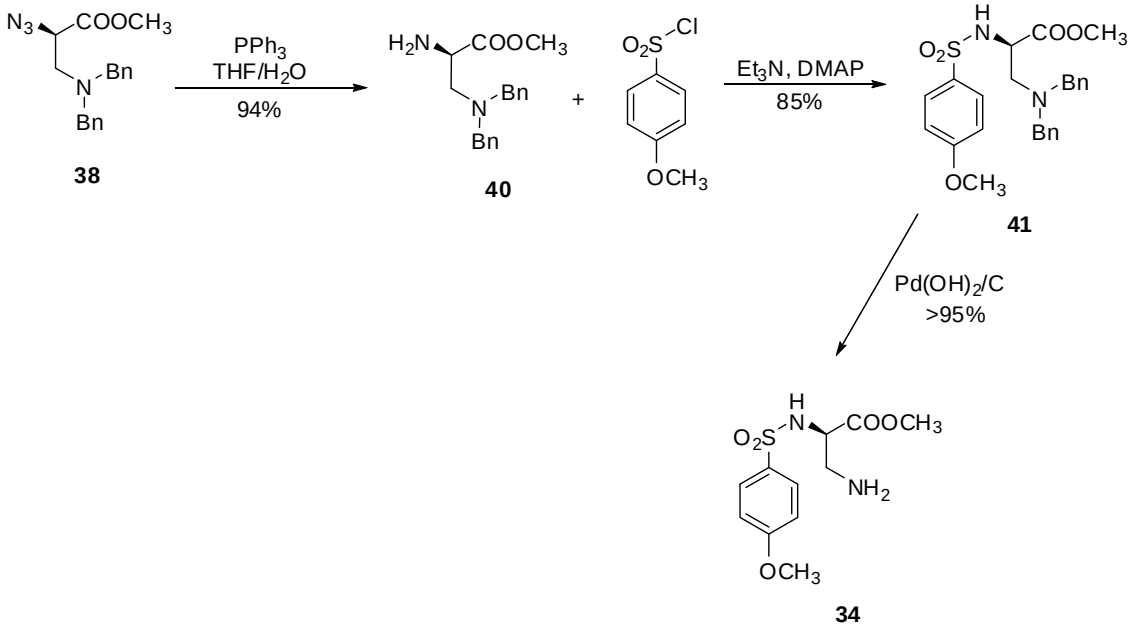

Scheme 15.

After the achievement of compound **34**, we proceeded with the addition of the two amminoacid positioned after the cleavage operated by MMP-7: an alanine and a leucine. Compound **34** had been coupled to a Boc-L-alanine-OH to obtain compound **42**, that was quantitatively deprotected (compound **43**) and then coupled with the next aminoacid, a Boc-L-leucine-OH to give compound **44** (Scheme 16).

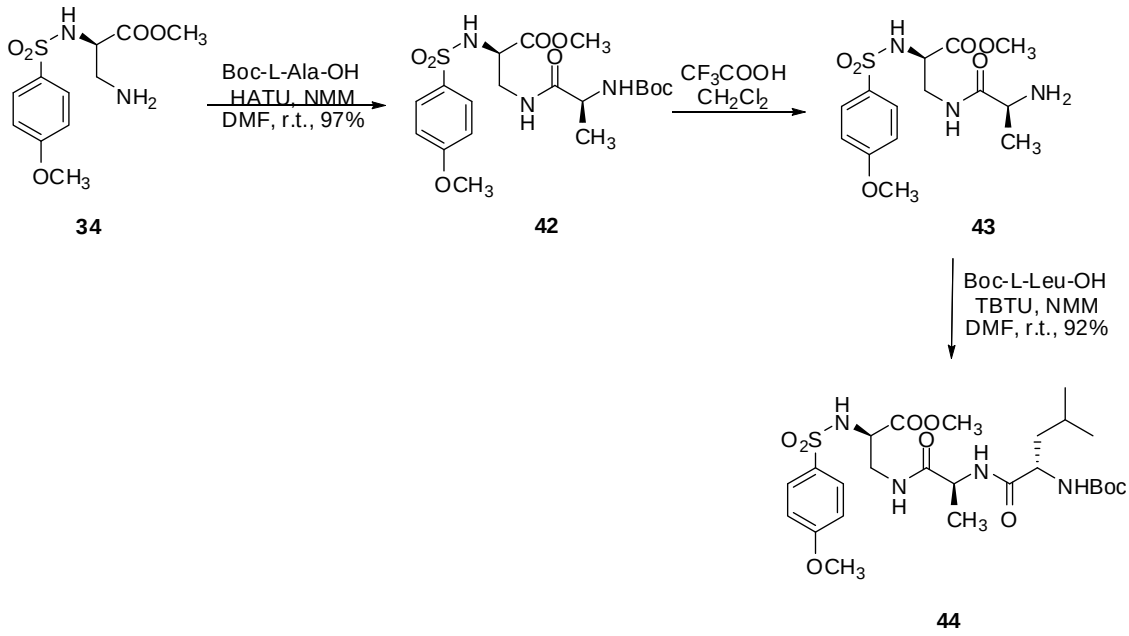

34 **42** **43** **44**

Scheme 16.

Methyl ester of compound **44** had been hydrolyzed to give the free carboxylic acid **45**: following deprotection of the *tert*-butoxycarbonyl group gave compound **35**.

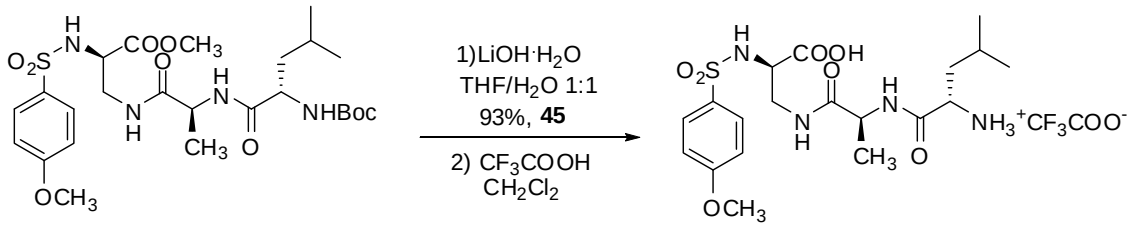

44 **35**

Scheme 17.

The derivate **35** was the "active form" of the inhibitor, that after cyclization of the free aminic group of the leucine with the carboxylic group of the serine recreated the sequence recognized by MMP-7 (VPL**S-LA**MG). If the matrilysin should cleave the cyclic inhibitor, the carboxylic group of the serine (that it is the zinc-binding group) will be revealed and we will have the active form of the inhibitor. After the coupling reaction what we obtained is not the cyclic monomer of **35** (compound **46**), but the dimer (compound **47**).

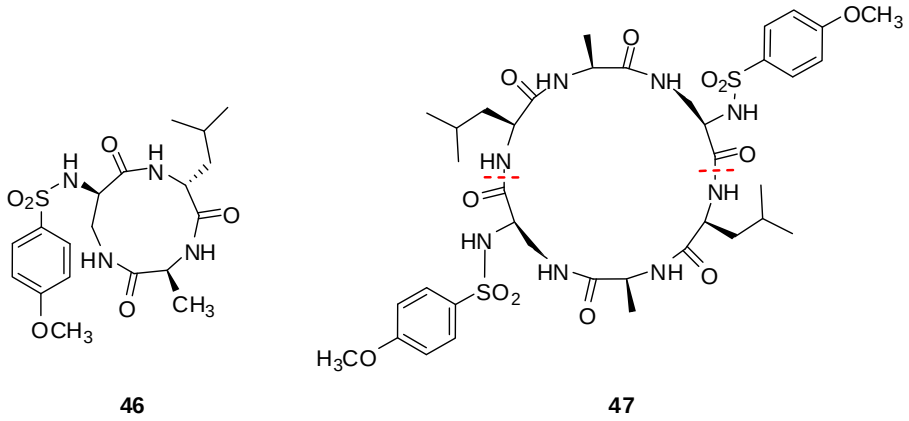

46 **47**

Figure 28. Structure of compounds **46** and **47**

However we tried to employ dimer **47**: in this case MMP-7 should cleave in two different points (shown in red) to give two desired monomers, that was the real inhibitors. On compound **47** we performed kinetic studies by fluorimetric assays to understand if MMP-7 should be able to cleave the cycle as we have hypothesized. The dimer **47** was incubated with MMP-7 for 10', 30', 1h, 12h, 24h and the K_i were measured. Since K_i didn't change evidently during the investigation period, these data suggested us that probably the dimer was not recognized by the protein and it was not cleaved by MMP-7.

On the other hand, the interaction between **35** and **33** vs. different MMPs had been investigated by fluorimetric assays to understand the influence of the aminoacidic chain. The results are shown in Table 7.

Table 7. Inhibition constants (K_i) of **33** and **35** vs. different MMPs

Compound	MMP-1	MMP-7	MMP-8	MMP-12
33	101 uM	146 uM		3.90 uM
35	11.2 uM	2.60 uM	6.80 uM	0.30 uM

An interesting result was the increased affinity of **35** for MMP-7 compared with **33**, while the enhancement for MMP-12 and MMP-1 is lower. Probably the addition of

the peptidic chain gave an extra-interaction with the protein, and in particular with MMP-7. Moreover **35** is well water-soluble (~100 mg/mL).

To better comprehend the importance of peptidic chain in the interaction with MMP-7, we also synthesized another compound presenting a different aminoacidic sequence (VPQ**S-LT**MG). The synthesis was made as describe above starting from compound **34**. In this case we performed the coupling with Boc-Thr(Bn)-OH (compound **48**): after the quantitative deprotection of *tert*-butoxycarbonyl group we coupled the same aminoacid used before, a Boc-L-leucine-OH (compound **49**).

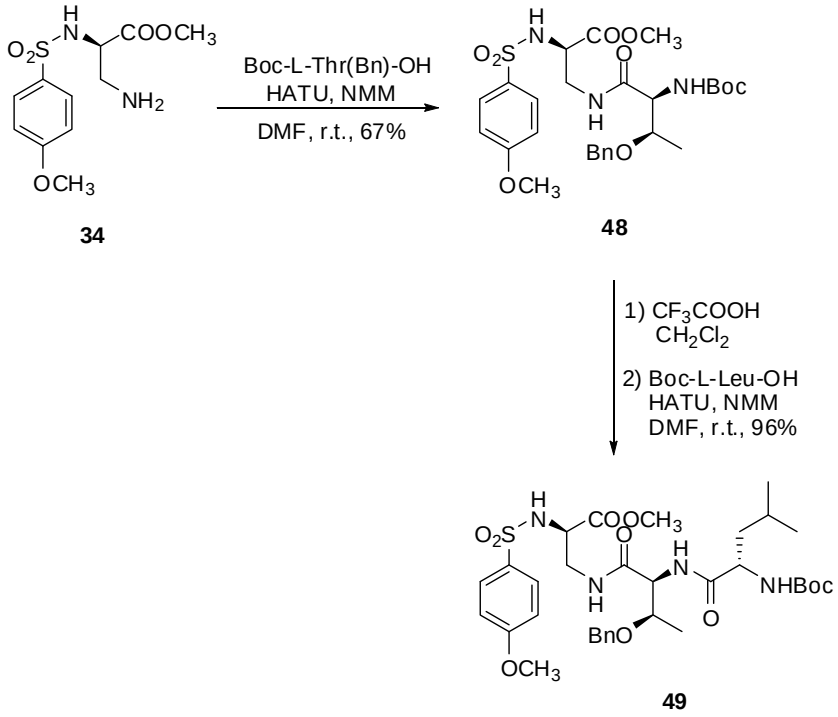

34 **48** **49**

Scheme 18.

Lateral chain of the aminoacid threonine of compound **49** was deprotected using $Pd(OH)_2/C$ to give compound **50**, that was reacted with $LiOH \cdot H_2O$ in a mixture THF/H_2O 1:1 and then with CF_3COOH to give the final product **51**.

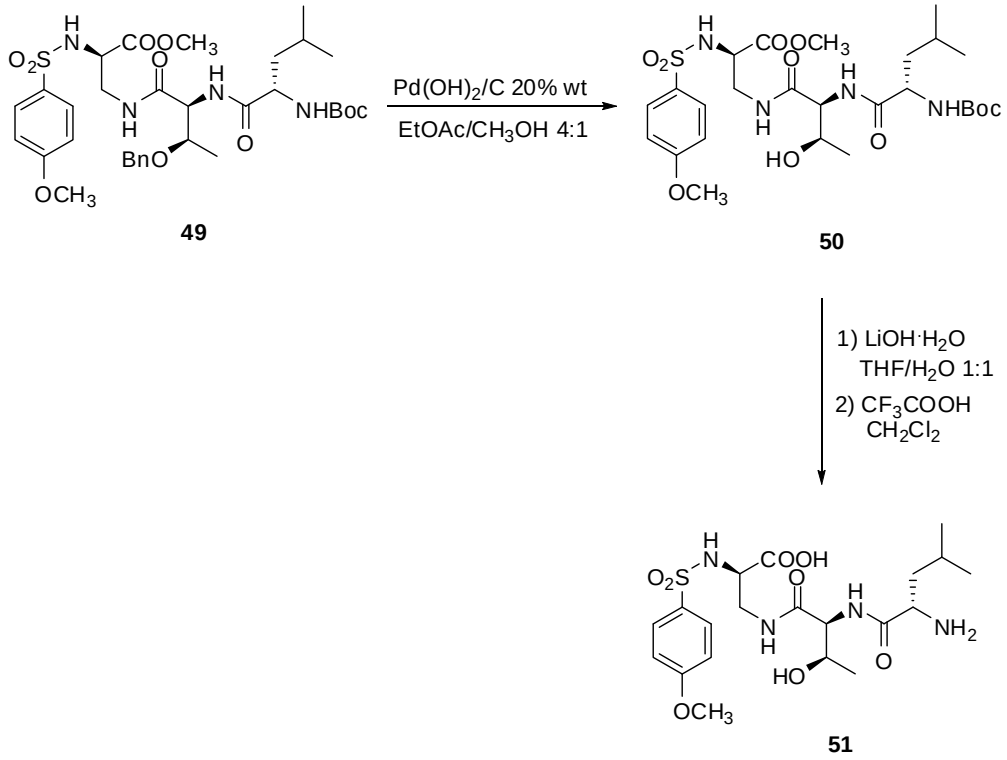

49 **50** **51**

Scheme 19.

Compound **51** had been tested vs. different MMPs. The results are shown in Table 8 in comparison with compound **35**.

Table 8. Inhibition constants (K_i) of **31** and **35** vs. different MMPs.

Compound	MMP-1	MMP-7	MMP-12
51	21.1 uM	38.0 uM	1.21 uM
35	11.2 uM	2.60 uM	0.30 uM

As we can notice, the K_i of compound **51** vs. MMP-7 is lower compared to **35**: probably the substitution of a lipophilic and little aminoacid as alanine with a threonine was not efficient for the interaction with the protein. Moreover the K_i does not change markedly in the case of MMP-1 and MMP-12, while for MMP-7 it is more than one order of magnitude: this was probably due to a specific interaction of the aminoacidic chain of compound **35** with the protein.

Considering that compound **35** presented a good affinity for MMP-7 even if it presents a carboxylic acid as zinc binding group, we synthesized the hydroxamic derivate **52** starting from compound **44**; in this case we performed the synthesis of the

hydroxamic acid (compound **53**) and then we deprotected the amino-group of the leucine to obtain the final product **52**.

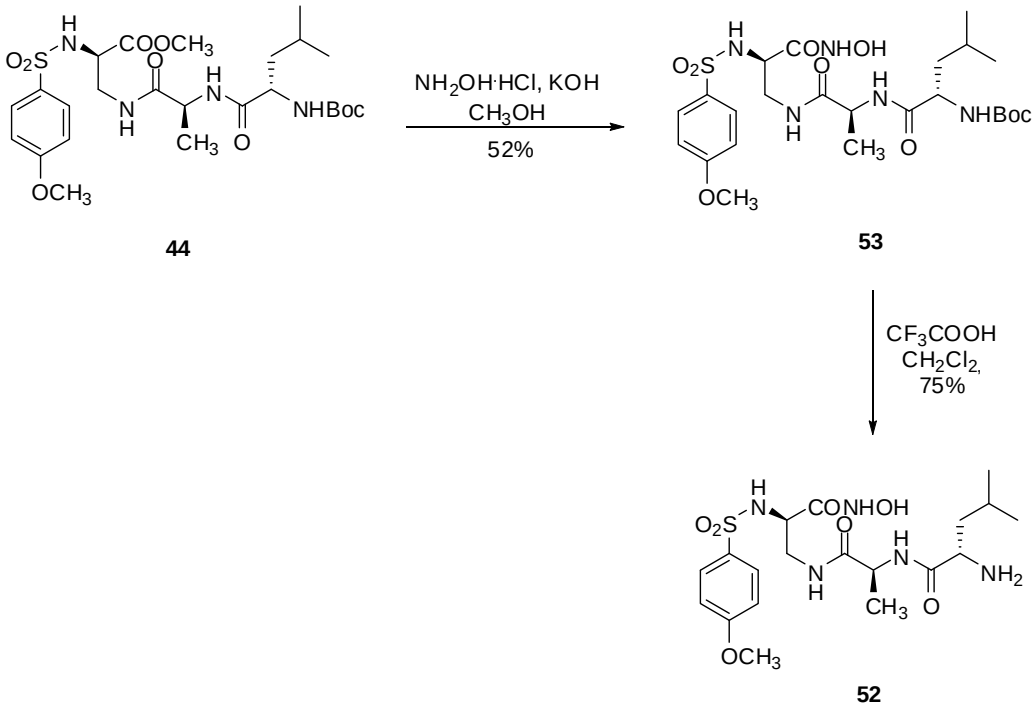

44 **53** **52**

Scheme 20.

In this case we needed a compound as reference to understand if the aminoacidic chain gave an extra-interaction with MMP-7 as we had seen for compound **35**. To do this we had chosen compound **54** (Figure 29), that should mimic the interaction of the inhibitor with MMPs in the absence of the aminoacidic chain.

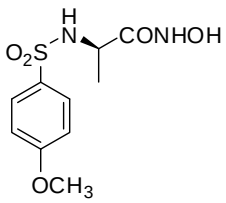

54

Figure 29. Structure of compound **54.**

Compound **52** and **54** had been tested vs. different MMPs (Table 9).

Table 9. Inhibition constants (K_i) of **52** and **54** vs. different MMPs.

Compound	MMP-1	MMP-7	MMP-12
52	135 nM	562 nM	10.5 nM
54	183 nM	3.20 uM	6.00 nM

The inhibition constant of compound **52** vs. MMP-7 is remarkable: it was indeed one of the best MMP-7 inhibitors that we have synthesized, and it presentes a very good water-solubility (~100 mg/mL). Moreover, the synthesis was optimized and proceeded with very good yields (15% in 11 steps). For all this reasons compound **52** was chosen to be tested against colon cancer, in collaboration with Dr. L. Vannucci of the University of Prague.

What is more the comparison between K_i values of compound **52** and **34** supported the hypothesis that the aminoacidic chain gave an extra interaction selectively with MMP-7 and did not influence the affinity for the other MMPs. In fact the affinity of compound **52** vs. MMP-7 was almost six-time better than **54**, while the inhibition constants for other MMPs remained almost unvaried.

Reference List

[1.] Y. Adachi, M. Yamamoto, F. Itoh, Y. Hinoda, Y. Okada, K. Imai, *Gut* **1999,** *45* 252-258.

[2.] C. L. Wilson, L. M. Matrisian, *Int J Biochem Cell Biol* **1996,** *28* 123-136.

[3.] C. L. Wilson, K. J. Heppner, P. A. Labosky, B. L. M. Hogan, L. M. Matrisian, *Proc.Natl.Acad.Sci.U.S.A.* **1997,** *94* 1402-1407.

[4.] T. Kitamura, K. Biyajima, M. Aoki, M. Oshima, M. M. Taketo, *Lab.Invest.* **2009,** *89* 98-105.

[5.] B. E. Turk, L. L. Huang, E. T. Piro, L. C. Cantley, *Nat.Biotechnol.* **2001,** *19* 661-667.

[6.] C. Couturier, J. Blanchet, T. Schlama, J. Zhu, *Org.Lett.* **2006,** *8* 2183-2186.

Chapter 5

Synthesis of high-affinity, water soluble MMPs inhibitors.

5.1 Introduction

To date, poor oral bioavailability of MMPIs remains the most frequent cause for failure in clinical drug development. Indeed, up to now, only very few of the plethora of potentially useful MMPIs reported[1-3] are water soluble.[4-6] Indeed, solubility in water is required for maintaining high drug levels in plasma, which is essential for treatments relying on oral administration. Doses of drug higher than those based on intrinsic efficacy must be administered because of limited bioavailability. High doses, in turn, exacerbate the adverse effects of modest selectivity by causing indiscriminate inhibition of other zinc endopeptidases.

Furthermore, MMP-related pathologies are usually chronic and any plausible pharmacological scheme would require long term treatment, during which time lipophilic drugs tend to accumulate in tissues and thereby enhance side effects. High lipophilicity also increases binding affinity to human serum albumin (HSA). Strong binding to HSA has an adverse effect on bioavailability by increasing the half-life in vivo and preventing the drug from reaching the target site. To date, poor oral bioavailability of MMPIs remains the most frequent cause for failure in clinical drug development. Consequently, alternative routes of administration[7] as well as new hydrophilic inhibitors were explored.

However, high affinity for MMPs is often achieved by introducing lipophilic substituents on suitable binding scaffolds, thereby decreasing solubility in water and compromising oral bioavailability,[3] as we can see in the case of NNGH (Figure 30).

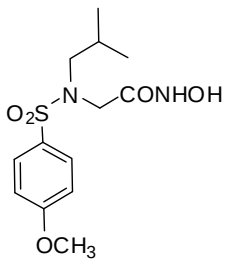

NNGH

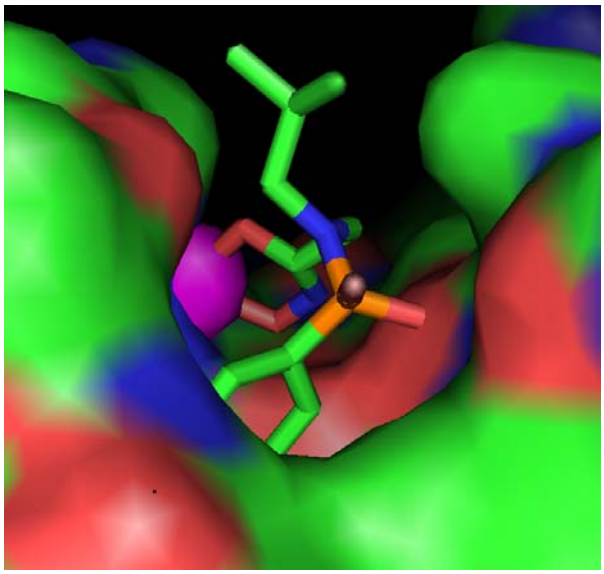

Figure 30. Structure of NNGH and X-ray structure of the catalytic domain of MMP-12 complexed NNGH.

N-Isobutyl-N-(4-methoxyphenylsulfonyl)glycyl hydroxamic acid (NNGH)[8] is one of the most prominent representatives of a family of inhibitors possessing nanomolar affinity for several MMPs.[9] The NNGH family of inhibitors suffers from the major drawbacks discussed before, and is therefore inadequate for most applications. The published X-ray crystallographic structure of the NNGH–MMP-12 complex[10] allowed us to ascertain that the interaction of the inhibitor with the active site of the enzyme involves binding of the hydroxamate moiety to the catalytic Zn ion and binding of the aromatic group to the S_1' subsite., while the isopropyl group on the sulfonamide nitrogen atom points away from the shallow S_2' pocket and does not directly participate in binding.

In an effort to overcome the limitations of NNGH, this structural information was used to prepare a new family of MMPI, whereby the isopropyl group was replaced with a hydrophilic moiety. The leading concept in designing of this compounds was to replace a portion of the molecule not directly involved in binding with a water-soluble residue in the hope that its inhibiting properties would not be affected. It must be emphasized that the addition a hydrophilic residue to this type of inhibitors is unprecedented in the NNGH family.

The extensive NMR and X-ray studies to elucidate the binding interactions between functional groups in the inhibitors and their corresponding subsites in the enzymes[1] have provided the basis to effectively design new analogues with potentially more favorable interactions and enhanced solubility in water.

5.2 Carbohydrate-Containing Inhibitor of Matrix Metalloproteinases.

Capitalizing on this structural information, we recently reported[11] the water soluble inhibitor **55** (see Figure 31), whereby the isopropyl group was replaced with a glucosylated N-hydroxyethyl chain obtaining a carbohydrate-based inhibitor.

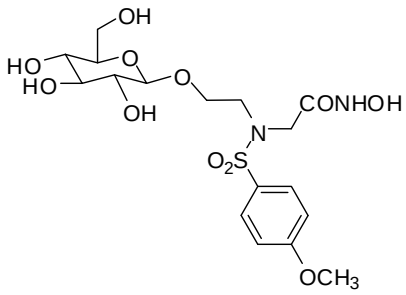

55

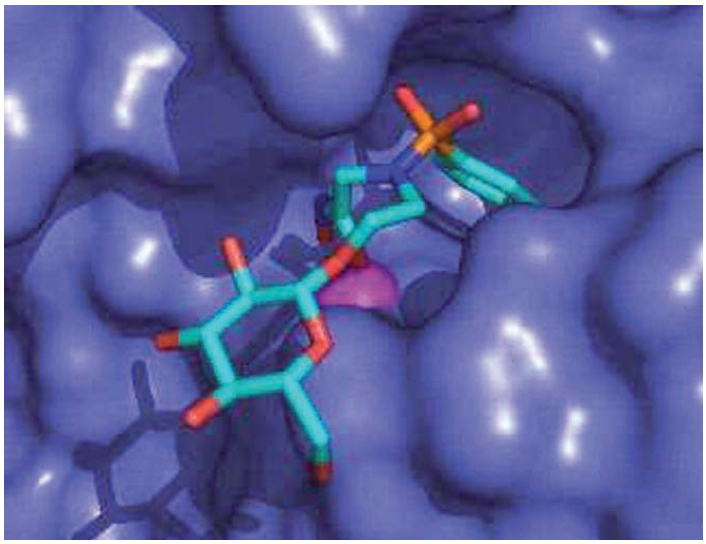

Figure 31. X-ray structure of **55** complexed with MMP-12. Only the active site region is shown for clarity.

Glucoside **55** is a new carbohydrate-based inhibitor, unprecedented in the NNGH family, that displays nanomolar affinity toward several MMPs. Compound **55** is water soluble (> 30 mM) and does not appreciably interact with HSA. A distinct advantage of **55** is the modular adaptivity of the design to the desired hydrophilicity, which can be appropriately tuned to specific applications by simply varying the number and the nature of substituents on the carbohydrate residue. This type of glycosilated compounds can be used to target the inhibitor versus particular tissues, decreasing in prospective the side effects and increasing the efficacy.

This inhibitors was synthesized through a general synthetic pathway. Starting from compound **56**,[11] we synthesized a group of carbohydrate-based inhibitors; here we reported in particular the synthesis of compound **57**, that present as saccharidic mojety an N-Ac glucosamine. The synthetic patway, which produces the glycosidic β isomer exclusively, has been specifically devised as a general method easily amenable to the preparation of the desired derivatives and it was similar for all the compounds presented.

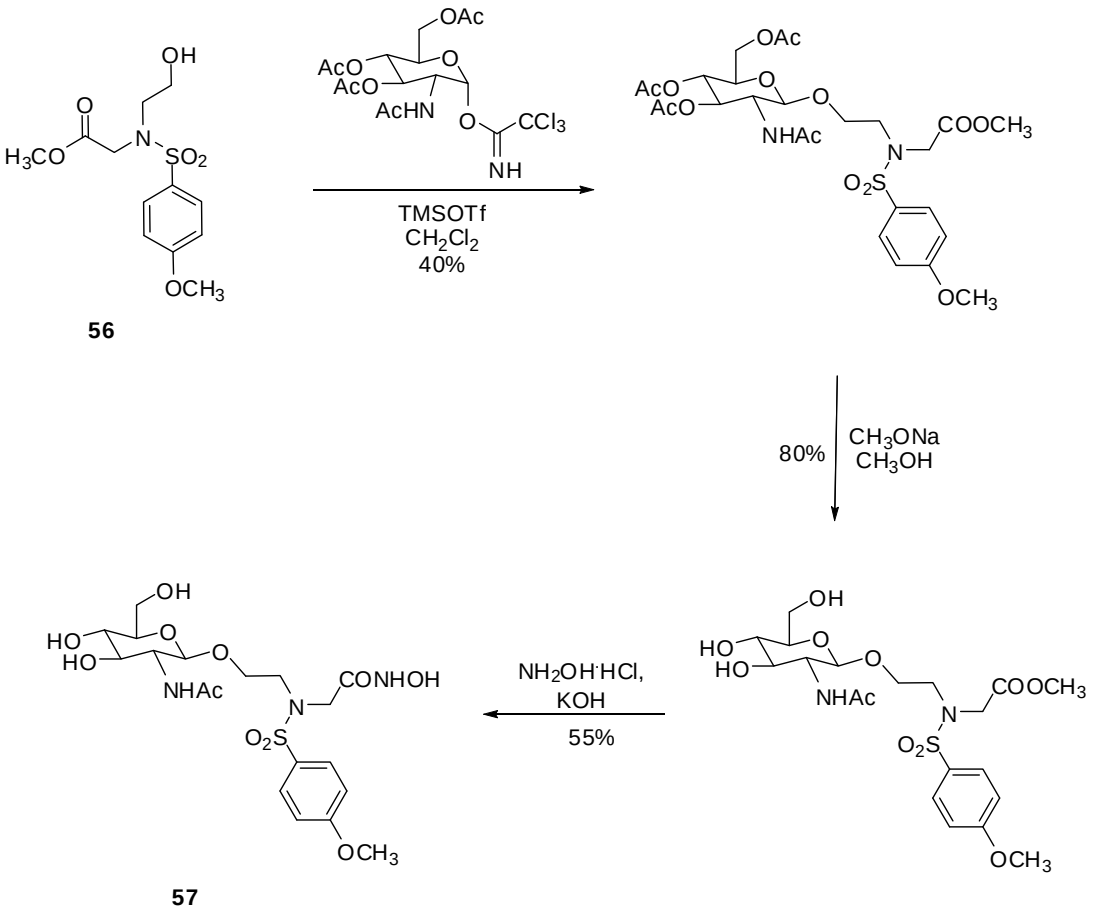

Scheme 21.

Additionally, we synthesized another two derivates, that presented a galactose and a lactose moiety. The structures of compounds **58** and **59** are shown in Figure 32.

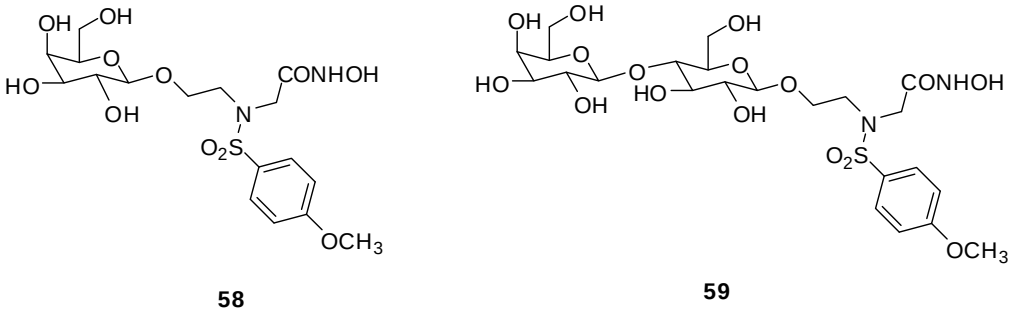

Figure 32. Structures of compounds **58** and **59.**

The affinity properties of **57** and **59** derivatives toward the selected MMPs were evaluated by fluorimetric assay, while the assays on compound **58** are in progress. The *K*i values are reported in Table 10, in comparison to compound **55**.

Table 10. Inhibition Constants (*K*i) of the **55**, **57** and **59** toward the considered MMPs.

Compound	MMP-1	MMP-2	MMP-7	MMP-12	MMP-13
55	286 nM		2.00 μM	14.3 nM	1.70 nM
57	450 nM	31.5 nM	3.20 μM	18.0 nM	20.5 nM
59	420 nM	34.0 nM	5.20 μM	14.0 nM	16.5 nM

As expected, the inhibition constants vs. all the MMPs remain practically the same for all the compounds, direct evidence of the lack of significant participation in binding of the carbohydrate moiety that was demonstrated from the X-ray crystal structure of the MMP-12–**55** complex (Figure 31). The structure is strictly analogous to that of the complex with NNGH,[10] with the hydroxamate moiety chelated to the penta-coordinated Zn and the methoxyphenyl moiety nested inside the S_1' pocket; all the other contacts to the amino acid residues are similarly conserved. Most noteworthy, the glucose residue protrudes out of the protein toward the solvent region located between two symmetry-related protein molecules in the crystal. The lack of strong interactions with the protein residues causes an increased mobility of the glucose moiety, reflected in the lower definition of some of the corresponding atoms, which nonetheless refine to an acceptable B-factor (25 $Å^2$ versus 15–20 $Å^2$ for well-defined atoms).

5.3 High-Affinity, Water soluble Inhibitors of Matrix Metalloproteinases

Then, following the same leading concept seen for carbohydrate-containing inhibitors, we additionally reported the synthesis and binding assessment of a family of low molecular weight, efficiently prepared, water-soluble inhibitors. Low nanomolar affinities were assessed for these new inhibitors to some relevant MMPs such as: MMP-12, implicated in the development of emphysema,[12] MMP-13 involved in rheumatoid arthritis,[13] MMP-9 iperexpressed in diabetic retinopathy[14] and MMP-1, engaged in skin damages.[15]

Synthesis. Non-natural, commercially available, GlyOMe **60**, D-SerOMe **61**, and D-ThrOMe **62** were reacted with solfenylchloride in the presence of triethylamine and dimethylaminopyridine in dichloromethane as solvent to give sulfonamides **63**, **13** and **64** in high yield (90-97%) (Scheme 22).

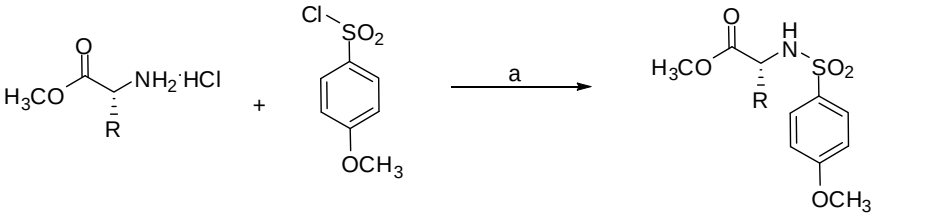

60 R = H
61 R = CH_2OH
62 R = $CH(CH_3)OH$

63 R = H
13 R = CH_2OH
64 R = $CH(CH_3)OH$

a) Et_3N, DMAP, CH_2Cl_2, rt, overnight, 90-97 %

Scheme 22.

The sulfonamide of glycine methylester **63** was reacted with ethylene oxide and methyliodide[11] to afford compound **56** which was directly transformed into the corresponding hydroxamic acid **65** by reaction with hydroxylamine hydrochloride and potassium hydroxide, in methanol as solvent (Scheme 23). Compound **63** was also reacted with enantiopure glycerine dimethylacetal **66** under Mitzunobu conditions, to give methylester **67**. Acidic removal (CH_3COOH/H_2O 80:20) of acetal protecting group on **67** afforded a mixture of the desired dihydroxyl derivative **68** and lactone **69**; the latter obtained by intramolecular trans-esterification.

The non-easily separable mixture of **68** and **69** was treated with hydroxylamine hydrochloride and potassium hydroxide in methanol to form hydroxamic acid **70** as white solid in 45% yield (Scheme 23).

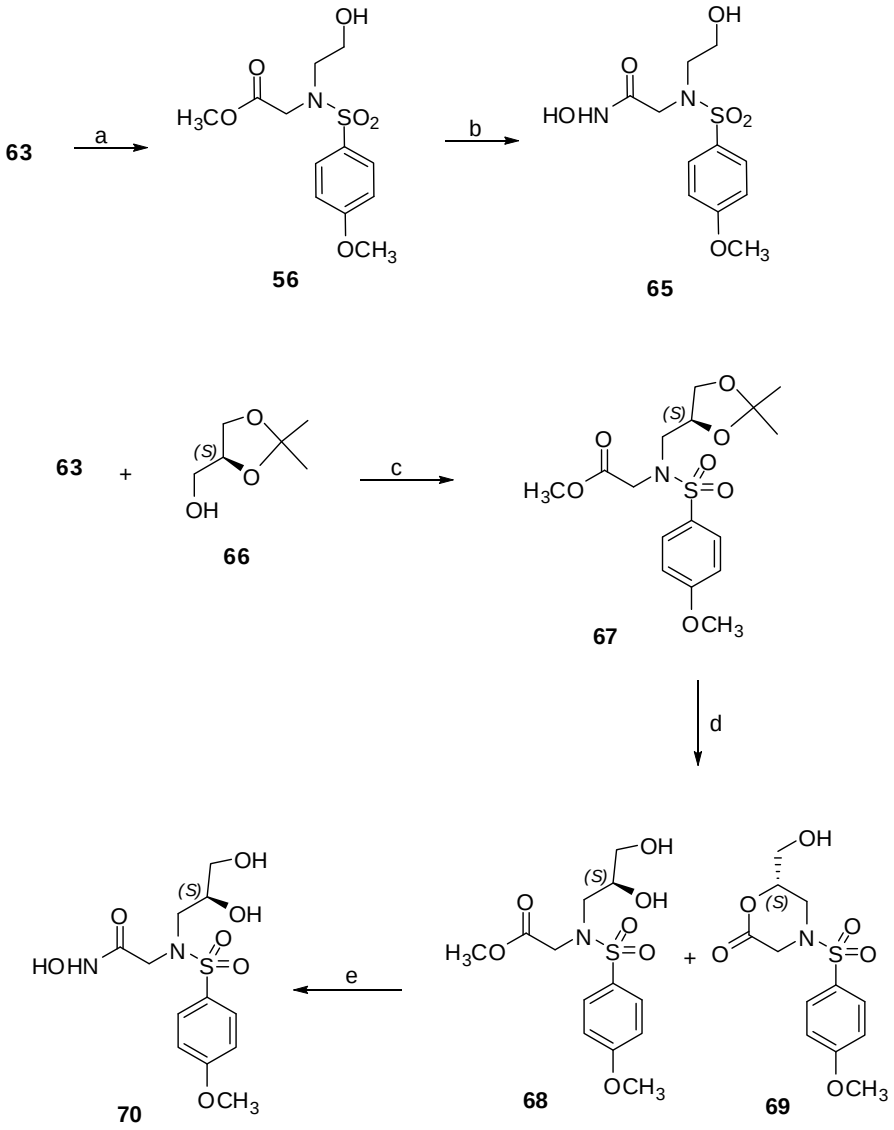

a)[11], 64%; b) $NH_2OH{\cdot}HCl$, KOH, CH_3OH, rt, 1h + 6h, 38%; c) PPh_3, DIAD, THF, rt, overnight, 87%; d) CH_3COOH/H_2O 80:20, 60 °C, 4h, 75%, (**68** + **69**); e) $NH_2OH{\cdot}HCl$, KOH, CH_3OH, rt, 1h + 18h, 45% (after HPLC purification).

Scheme 23

To explore the binding mode of the compound **70** it was soaked in crystals of MMP-12 and the structure of the complexes solved by X-ray crystallography (Figure 33).

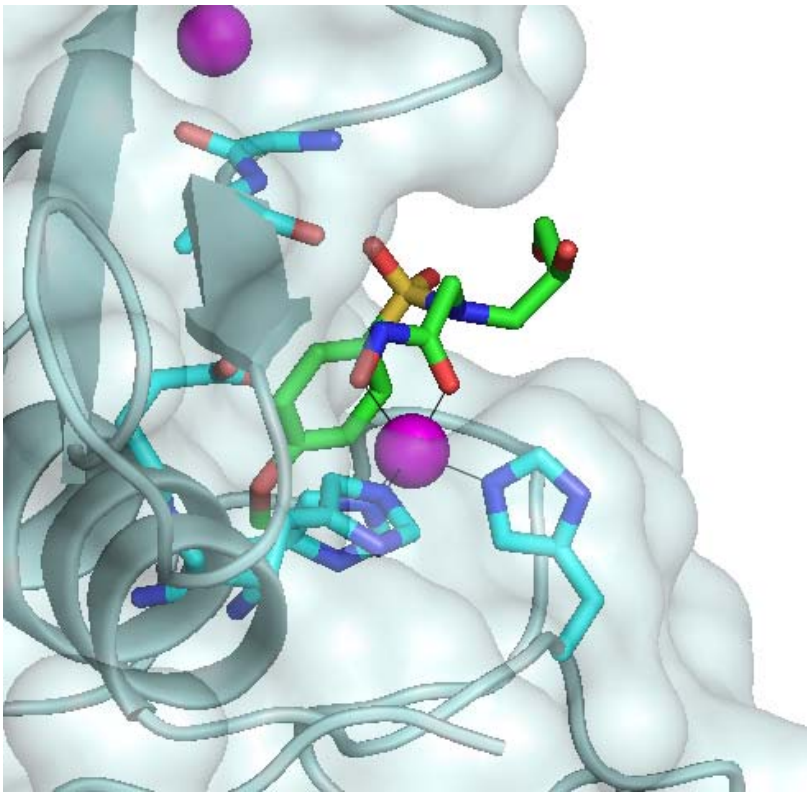

Figure 33. X-ray structure of the catalytic domain of MMP-12 complexed with **70**. Only the ligand binding site is shown for clarity.[16]

As we have seen for compound **55**, also in this case the binding is due to hydrophobic interactions of **70** with the S_1' pocket through the aromatic moieties. The hydrophilic residue located outside the protein does not appear to contribute to binding, while the hydroxamic acid is oriented toward the catalytic zinc ion.

For the synthesis of a more soluble analogues of compound **70**, the sulfonamide of serine methyester **13** was firstly transformed, under standard conditions, into the corresponding *tert*butyldimethylsilyl ether **14** then reacted with acetal **66** as reported above, to give compound **71** (Scheme 24).

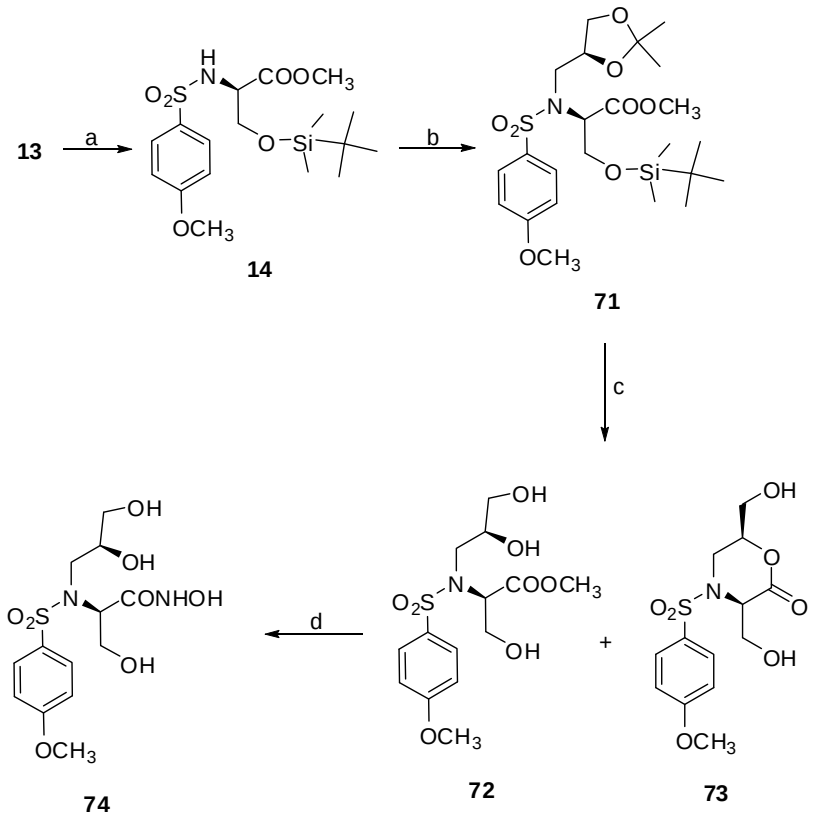

a) $tBuMe_2SiOTf$, Et_3N, rt, 20h, 97%; b) **66**, PPh_3, DIAD, THF, rt, overnight, 85%; c) CH_3COOH/H_2O 80:20, 60 °C, 90%, (**72** + **73**); e) $NH_2OH \cdot HCl$, KOH, CH_3OH, rt, 1h + 15h, 50% (after HPLC purification).

Scheme 24

Acidic removal of silylether and acetal protecting groups afforded a mixture of tri-hydroxyl derivative **72** and lactone **73** which was treated with hydroxylamine hydrochloride and potassium hydroxide to form the expected hydroxamic acid **74** in 50% yield (Scheme 24).
In parallel to this, we synthesized the corresponding biphenyl derivative of compound **70**, starting from **60** and biphenylsolfenylchloride, to give the sulfonamidic derivative **75**.This compound was reacted under Mitsunobu conditions with **66** to give compound **76**. Acidic removal (CH_3COOH/H_2O 80:20) of acetal protecting group on **76** afforded a mixture of the compound **77** and lactone **78** as we have seen before; this mixture was treated with hydroxylamine hydrochloride and potassium hydroxide to give the corresponding hydroxamic acid **79**.

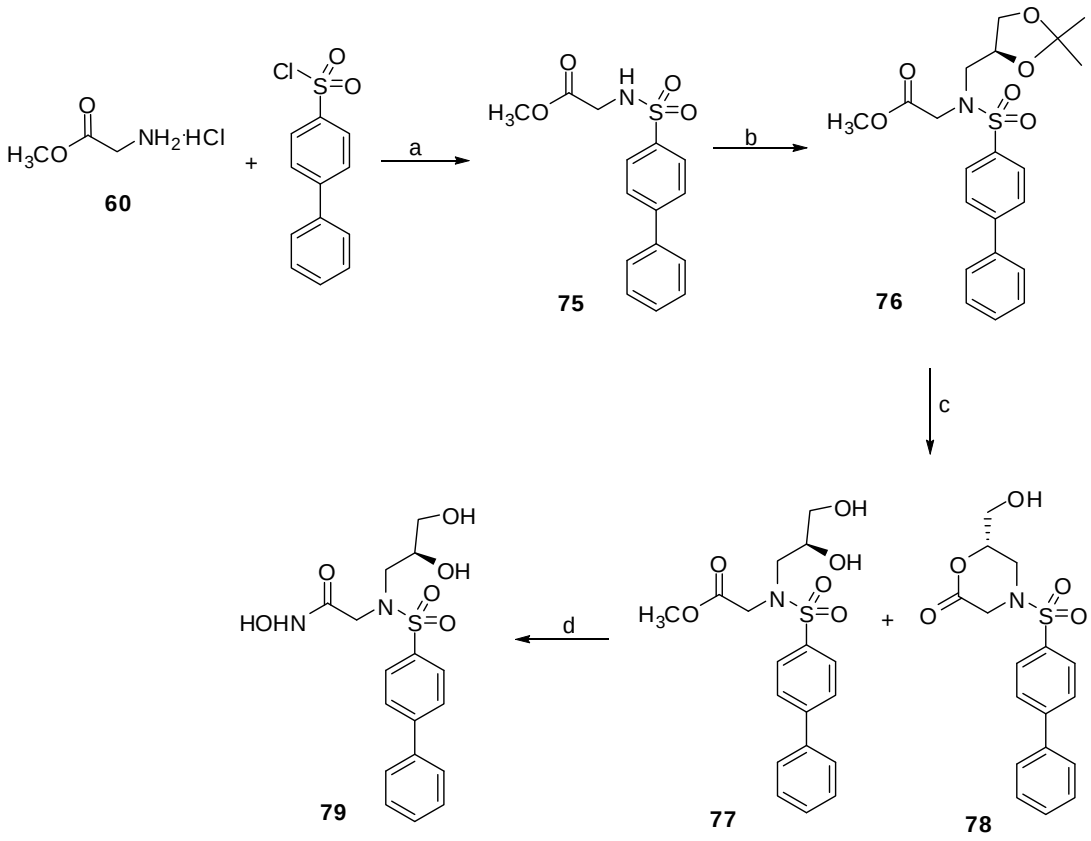

a) Et_3N, DMAP, CH_2Cl_2, rt, overnight, 81%; b) **66**, PPh_3, DIAD, THF, rt, overnight, 64%; c) CH_3COOH/H_2O 80:20, 60 °C, 56%, (**77** + **78**); e) $NH_2OH \cdot HCl$, KOH, CH_3OH, rt, 0.5h + 2h, 54%.

Scheme 25.

Treatment of sulfonamide of serine methylester **13** and of threonine methylester **63**, with hydroxylamine and potassium hydroxide in methanol as solvent afforded the hydroxamic acids **12** and **80** (Scheme 26).

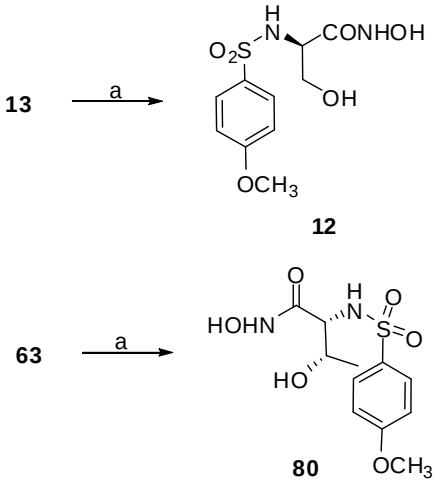

a) $NH_2OH \cdot HCl$, KOH, CH_3OH, rt, 1h + 20h, 47% (**12**); 1h + 18h, 36% (**80**).

Scheme 26.

Derivatives **12** and **80**, as well as hydroxamic acids **65**, **70**, **74** and **78** are soluble in water and stable as solid or in solution, at room temperature for several months at pH = 7 and 8.5. The same good stability was observed at pH = 4.5 with the only exception of derivative **74** which tends to degrade forming the corresponding carboxylic acid.

In order to improve inhibitors selectivity, *para*-methoxybenzyl residue on scaffold **62** was replaced by *para*-fluorobenzyl- and biphenyl-moieties. Therefore, the *para*-fluorosolfonamide of glycine methyester **81** and the biphenylsolfenamide of glycine methylester **75** were prepared reacting, ester **60** with *para*-fluorosolfenylchloride and biphenylsolfenylchloride respectively (Scheme 27).

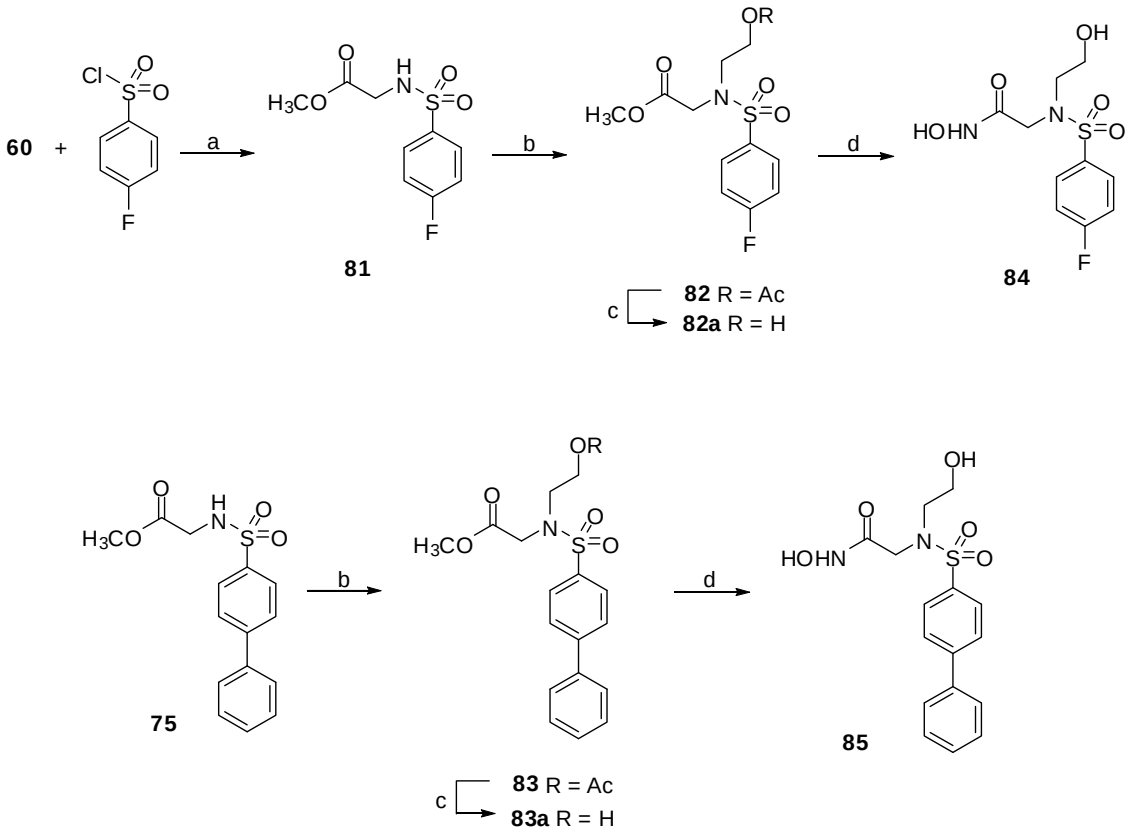

a) Et_3N, DMAP, CH_2Cl_2, rt, overnight, 89% (**81**); 81% (**75**); b) $AcOCH_2CH_2Br$, NaH, DMF, 0 °C – rt, 18h, (**82**); 36h (**83**); c) CH_3ONa, CH_3OH, 1h, 50% (**82a**); 40% (**83a**) e) $NH_2OH{\cdot}HCl$, KOH, CH_3OH, rt, 1h + 18h, 72% (**84**); 48% (**85**).

Scheme 27.

The sulfonamidic nitrogen has been alkylated using sodium hydride and 2-bromoethyl acetate (**82** and **83**), then the alcoholic moiety has been deprotected (compounds **82a** and **83a** respectively). Compound **82a** and **83a** was treated with hydroxylamine hydrochloride and potassium hydroxide to give the corresponding hydroxamic acid **84** and **85**.

The affinity properties of all this derivatives toward the selected MMPs were evaluated by fluorimetric assays. The *K*i values are reported in Table 11.

Table 11. Inhibition Constants (*K*i, nM) of **65**, **70**, **74**, **79**, **12**, **80**, **84**, **85** toward the considered MMPs.

Compound	MMP-1	MMP-7	MMP-8	MMP-9	MMP-12	MMP-13	MMP-20
65	128	1500	13.0		8.00	1.00	
70	160	9000	24.0	14.0	8.00	3.60	30.0
74	32.0	344	8.00		7.00	1.70	18.4
79	742	4000	48.0		60.0	18.0	116
12	143	823	9.00	18.0	6.00	2.20	25.7
80	287	984	10.0		11.0	2.90	
84	151	3000	172		40.0	46.0	
85	67.0	1600	4.60		31.0	2.70	

As we can notice from Table 11, all the compounds evaluated presented a very good affinity for several MMPs. This is an ulterior proof that the substitution of the lipophylic group on the sulfonamidic nitrogen with an hydrophilic moiety not only doesn't invalidate the binding with MMPs, that remains in the nanomolar range for the majority of MMPs, but permits of synthesize new inhibitors with an enhanced water-solubility and bioavailability.

Reference List

[1.] M. Whittaker, C. D. Floyd, P. Brown, A. J. H. Gering, *Chem.Rev.* **1999,** *99* 2735-2776.

[2.] J. W. Skiles, N. C. Gonnella, A. Y. Jeng, *Current Medicinal Chemistry* **2001,** *8* 425-474.

[3.] J. W. Skiles, N. C. Gonnella, A. Y. Jeng, *Current Medicinal Chemistry* **2004,** *11* 2911-2977.

[4.] T. Masuda, Y. Nakayama, *Journal of Medicinal Chemistry* **2003,** *46* 3497-3501.

[5.] M. Fragai, C. Nativi, B. Richichi, C. Venturi, *ChemBioChem* **2005,** *6* 1345-1349.

[6.] H. Moriyama, T. Tsukida, Y. Inoue, H. Kondo, K. Yoshino, S. I. Nishimura, *Bioorganic & Medicinal Chemistry Letters* **2003,** *13* 2741-2744.

[7.] K. Lindorff-Larsen, R. B. Best, M. A. DePristo, C. M. Dobson, M. Vendruscolo, *Nature* **2005,** *433* 128-132.

[8.] L. J. MacPherson, E. K. Bayburt, M. P. Capparelli, B. J. Carroll, R. Goldstein, M. R. Justice, L. Zhu, S. Hu, R. A. Melton, L. Fryer, R. L. Goldberg, J. R. Doughty, S. Spirito, V. Blancuzzi, D. Wilson, E. O'Byrne, V. Ganu, D. T. Parker, *J.Med.Chem.* **1997,** *40* 2525-2532.

[9.] S. Hanessian, N. Moitessier, C. Gauchet, M. Viau, *Journal of Medicinal Chemistry* **2001,** *44* 3066-3073.

[10.] I. Bertini, V. Calderone, M. Cosenza, M. Fragai, Y.-M. Lee, C. Luchinat, S. Mangani, B. Terni, P. Turano, *Proc.Natl.Acad.Sci.U.S.A.* **2005,** *102* 5334-5339.

[11.] V. Calderone, M. Fragai, C. Luchinat, C. Nativi, B. Richichi, S. Roelens, *ChemMedChem* **2006,** *1* 598-601.

[12.] V. Lagente, C. Le Quement, E. Boichot, *Expert Opinion on Therapeutic Targets* **2009,** *13* 287-295.

[13.] H. Takaishi, T. Kimura, S. Dalal, Y. Okada, J. D'Armiento, *Current Pharmaceutical Biotechnology* **2008,** *9* 47-54.

[14.] S. J. Giebel, G. Menicucci, P. G. McGuire, A. Das, *Laboratory Investigation* **2005,** *85* 597-607.

[15.] K. K. Dong, N. Damaghi, S. D. Picart, N. G. Markova, K. Obayashi, Y. Okano, H. Masaki, S. Grether-Beck, J. Krutmann, K. A. Smiles, D. B. Yarosh, *Experimental Dermatology* **2008,** *17* 1037-1044.

[16.] I. Bertini, V. Calderone, M. Fragai, A. Giachetti, M. Loconte, C. Luchinat, M. Maletta, C. Nativi, K. J. Yeo, *Journal of the American Chemical Society* **2007,** *129* 2466-2475.

Chapter 6

Cyclic glycopeptidomimetics through versatile sugar-based scaffold.

6.1 Introduction

Most biological processes are controlled by molecular interactions that involve peptides and proteins.[1] Drug discovery processes often start by identifying peptides that interact with a specific receptor or enzyme by using well-established combinatorial peptide chemistry approaches. In some fortunate cases, bioactive peptides have been used directly as therapeutic agents; however, in general, they are not suitable as drugs because of their well-documented pharmacokinetic problems (susceptible to proteolysis, poor oral availability and rapid excretion by the liver and kidney). The conversion of bioactive peptides into more drug-like molecules has often been approached systematically by identifying the key elements responsible for activity in terms of essential amino acid residues and their presentation in space. Bioactive molecules derived from such strategies are commonly labelled as peptidomimetics and, as suggested by the name, aim to closely resemble the peptides from which they originated.

Peptidomimetic concepts and synthetic strategies were increasingly investigated from 1980 onwards. Approaches have varied greatly, from peptide-like templates, such as pseudopeptides, peptoids, retroinverso peptides and cyclic peptides, to using organic scaffolds that bear little resemblance to the peptide backbone.

Carbohydrates represent a natural source for stereodiverse scaffolds, which, through orthogonal protection and modular chemistries, enable medicinal chemists to systematically alter shapes and surface properties of molecules to suit selected targets. The opportunity to create molecular diversity in a modular, systematic and tailored way (structurally and functionally) is unique to carbohydrates. It is self evident that such approaches are not limited to mimicking peptides. Molecular diversity can be tailored, at least in principle, to any target. We have applied this concept in the development of a α-O-linked glycohomoglutamate,[2] easily obtained as distereomerically pure compound by chemo-, regio- and stereoselective cycloaddition between glycals and aspartic acid derivative, as versatile, multifunctionalized scaffold in the synthesis of cyclic SAA-peptidomimetics (Figure 34).

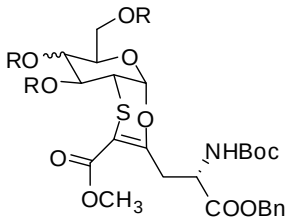

Figure 34. General structure of the α-O-linked glycohomoglutamate

In particular, during my PhD I synthesized several compounds characterized by small peptide sequences linked to the sugar-based scaffold. The role played by the scaffold is orienting the aminoacidic residues in the space. We thus obtained a compound which showed some, although limited, activity in the binding assay at the human tachykinin NK_2 receptor.[3] By changing the aminoacidic chain, we have obtained good results with the synthesis of a new cyclic SAA that presents a nanomolar affinity vs. NK_2 receptor (unpublished results).

Moreover we had demonstrated that the pyranose ring of a more rigid derivative of our scaffold retains the $^4C_1$ chair conformation,[4] maintaining biomimetic properties as documented by combined molecular modeling and NMR spectroscopic analyses. In fact the sugar part of our molecules retains bioactivity for the different lectins investigated. For these reasons, our scaffold can be considered a promising candidates for further exploitation of this type of derivatives to give O-glycans for lectin blocking and vaccination. Concerning this research topic during my PhD I performed the synthesis and characterization of the all the molecules used for NMR binding studies.

Reference List

[1.] G. T. Le, G. Abbenante, B. Becker, M. Grathwohl, J. Halliday, G. Tometzki, J. Zuegg, W. Meutermans, *Drug Discovery Today* **2003,** *8* 701-709.

[2.] F. Venturi, C. Venturi, F. Liguori, M. Cacciarini, M. Montalbano, C. Nativi, *Journal of Organic Chemistry* **2004,** *69* 6153-6155.

[3.] M. Altamura, E. Dragoni, A. S. Infantino, L. Legnani, S. B. Ludbrook, G. Menchi, L. Toma, C. Nativi, *Bioorganic & Medicinal Chemistry Letters* **2009,** *19* 3841-3844.

[4.] J. Jimenez-Barbero, E. Dragoni, C. Venturi, F. Nannucci, A. Ardà, M. Fontanella, S. Andrè, F. J. Canada, H.-J. Gabius, C. Nativi, *Chemistry-A European Journal* **2009,** *15* 10423-10431.

Bioorganic & Medicinal Chemistry Letters 19 (2009) 3841–3844

Contents lists available at ScienceDirect

Bioorganic & Medicinal Chemistry Letters

journal homepage: www.elsevier.com/locate/bmcl

Cyclic glycopeptidomimetics through a versatile sugar-based scaffold

Maria Altamura [a], Elisa Dragoni [b,e], Angela Simona Infantino [b], Laura Legnani [c], Steve B. Ludbrook [d], Gloria Menchi [b], Lucio Toma [c], Cristina Nativi [b,e,*]

[a] Menarini Ricerche S.p.A., via dei Sette Santi 1, I-50131 Firenze, Italy
[b] Dipartimento di Chimica Organica, Universita' di Firenze, via della Lastruccia, 13-Polo Scientifico e Tecnologico, Sesto F.no, I-50019 Firenze, Italy
[c] Dipartimento di Chimica Organica, Universita' di Pavia, via Taramelli 10, I-27100 Pavia, Italy
[d] Dept of Screening and Compound Profiling, GlaxoSmithKline R&D, New Frontiers Science Park, Harlow, Essex CM19 5AW, UK
[e] CERM, Universita' di Firenze, via Sacconi, 6-Polo Scientifico e Tecnologico, Sesto F.no, I-50019 Firenze, Italy

ARTICLE INFO

Article history:
Received 16 February 2009
Revised 31 March 2009
Accepted 3 April 2009
Available online 9 April 2009

Keywords:
Glycopeptides
Peptidomimetics
Sugar aminoacids
Tachykinins
Integrins

ABSTRACT

Cyclic peptidomimetics are attracting structures to obtain a distinct, bioactive conformation. Even more attractive are sugar-containing cyclic peptidomimetics which present turn structures induced by the pyranose ring when incorporated in cyclic peptides. The use of a new and versatile saccharidic scaffold to achieve sugar-based peptidomimetics is here reported together with the successful synthesis of diastereomerically pure cyclic SAA peptidomimetics **15** and **16**.

Low bioavailability, poor stability towards peptidases and rapid excretion displayed by a large number of peptides of therapeutic and biological interest, prompted an intensive search for peptidomimetics.[1–3] As a matter of fact, peptidomimetics molecules, are expected to have the same therapeutic effects as their peptide counterparts, with the added advantages of metabolic stability and bioavailability.

A possible approach of such peptidomimetics is to replace the peptide, or part of the peptide, by a scaffold that distributes in the space the epitopes. Ideally, an attractive scaffold should easily be available as chiral, enantiomerically pure, building block. It should be highly functionalized to introduce various side chains and its flexibility or rigidity could be modulated. Therefore, the use of sugars as scaffolds in mimetic synthesis is a strategy that has been widely studied and which still draws attention.[4–6]

Sugar derivatives can be incorporated in the peptide backbone or in the side chains; modification of peptide skeleton by introducing carbohydrate derivatives is documented leading to a real improvement of the properties of the peptides. Moreover, because of the presence of pyranose ring, sugar aminoacids (SAAs) have been found to introduce turn structures when incorporated in linear or cyclic peptides.[5]

Cyclization of peptides affords structure of special interest to obtain a distinct, bioactive conformation, and several SAAs have been used as building blocks for peptide scaffolds and conformational restrained peptido-mimetics.[2,7] Indeed, this approach has been successfully evaluated for biologically active, cyclic RGD peptides[3] or cyclic peptides with the β-turn motif of somatostatin, containing tetrapeptide Phe-D-Trp-Lys-Thr.[2,8]

Consequently, efficient syntheses and availability of suitable saccharidic scaffolds allowing the systematic modification of the amino acids and the carbohydrate residues, as well as the size of the macrocycle, remain a challenging and attracting target to fully exploit the potential of such hybride structure, in the search of new active compounds.

We report herein the use of the α-O-linked glycohomoglutamate **1**, (Scheme 1), easily obtained as distereomerically pure compound by chemo-, regio- and stereoselective cycloaddition between glucal **2** and aspartic acid derivative **3**,[9] as versatile, multifunctionalized scaffold in the synthesis of cyclic SAA-peptidomimetics **15** and **16** (Scheme 2).

Scaffold **1,** characterized by two orthogonally protected carboxyls, a protected α-amino function and a selectively functionalized monosaccharidic unit, was successfully employed to obtain the monosilyl derivative **4** which, in turn, was oxidized with TEMPO/BAIB to give the glucuronic derivative **5** (see Scheme 1) in 54% yield. No sulfoxide derivative **6** was observed under these reaction conditions (see Supplementary data).[10] Condensation reactions

* Corresponding author.
E-mail address: cristina.nativi@unifit.it (C. Nativi).

0960-894X/$ - see front matter © 2009 Elsevier Ltd. All rights reserved.
doi:10.1016/j.bmcl.2009.04.008

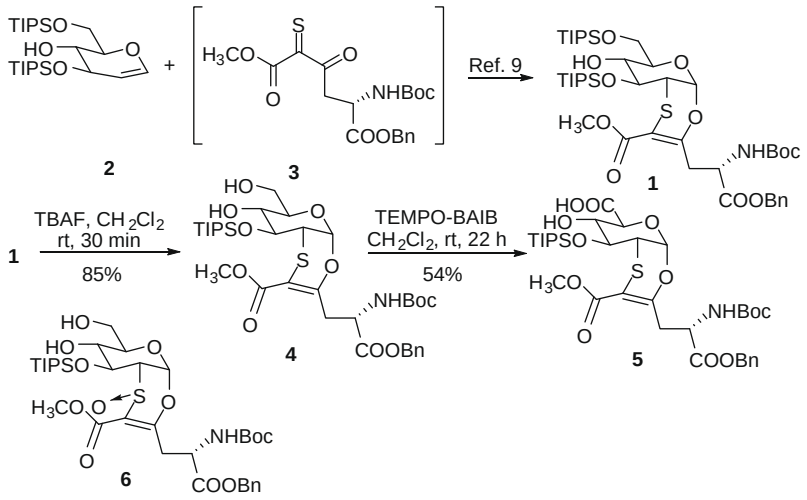

Scheme 1. Synthesis of scaffold **5** and structure of cyclo SAA peptidomimetics **15** and **16**.

between **5** and **7** as well as between **5** and **8** were performed using standard conditions (see Supplementary data) affording respectively compounds **9** and **10** (Scheme 2). Peptidic chains **7** and **8** as well as SAA derivatives **9** and **10** have been obtained relying on standard solid-phase strategy, using 2-chlorotrityl resin. Removal of the resin, gave linear glycopeptides **11** (62%, over 10 steps) and **12** (25%, over 11 steps) which were treated with trifluoroacetic acid to take off the Boc protecting group quantitatively affording derivatives **13** and **14**, as trifluoroacetic salts. Intramolecular condensation of the latter, and suitable deprotection, gave the cyclo glycopeptides: *cyclo*(SAA**5**-Ala-Phe-Phe-Phe-Ala) **15**, and *cyclo*(SAA**5**-Glu-Ile-Leu-Asp-Val) **16**, (see Supplementary data) which were prepared to be tested as tachykinin NK_2 receptor ligand and integrin ($\alpha4\beta1$) inhibitor respectively (Scheme 2).

In a previous paper[11] we have shown how insertion of aromatic groups on a suitable sugar derived scaffold can mimic the structure of highly active tachykinin NK_2 antagonists such as the small monocyclic pseudopeptide **17**[12] (Fig. 1).

Indeed, some of the compounds we obtained showed binding affinities at the human tachykinin NK_2 receptor at submicromolar concentrations, while molecular dynamics calculations indicated that the structures of **17** and that of one of the best sugar derived compounds were quite well superimposable. As tachykinin NK_2 antagonists continue to raise interest as potential new drugs for the therapy of gastrointestinal and CNS diseases,[13] we turned our attention to the synthesis of compounds in which small peptide sequences, containing aromatic aminoacids (Phe) and alanine residues as chiral spacers, are linked to the sugar derived rigid scaffold **5** in order to distribute the aromatic moieties in suitable space regions. We thus synthesized compound **15** which showed some, although limited, activity in the binding assay at the human tachykinin NK_2 receptor. Affinity of compound **15** at the human NK_2 receptor was determined in binding experiments by using membranes of Chinese Hamster Ovary (CHO) cells stably transfected with the human NK_2 receptor.[14] The compound was tested for its ability to displace the radioligand [^{125}I]-neurokinin A (0.15 nM) after 30 min incubation at room temperature, resulting in 25% inhibition of the radioligand binding at 10 μM concentration.

Capitalizing on this encouraging result, further work is ongoing in order to increase the biological activity through the modulation of the peptide sequence assisted by molecular dynamics calculations.

It is known that a requisite for a good recognition by NK_2 receptors is the presence of two close aromatic rings in the axial position about the backbone ring.[15] We performed a preliminary modeling study of compound **15** to locate its allowed conformations;[16] the molecule showed a high degree of conformational flexibility and several populated geometries. Among them, two significant conformations show two of the three phenyl rings oriented in the same region of the space, though they do not belong to adjacent aminoacidic residues as in **17**. These conformations, reported in Figure 2, are stabilized by a β-turn motif and support the potential interest in such cyclic glycopeptidic structures.

Integrins are a family of membrane-spanning adhesion receptors composed of non- covalently linked α and β subunits which combine to give a wide amount of heterodimers. In recent years antagonists of very late antigen-4 (VLA4, also known as integrin $\alpha4\beta1$) have shown great promise in treating inflammatory disorders.[17–19] VLA4 recog-

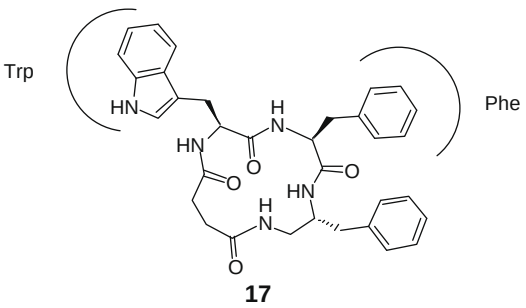

Figure 1. Structure of compound **17**.

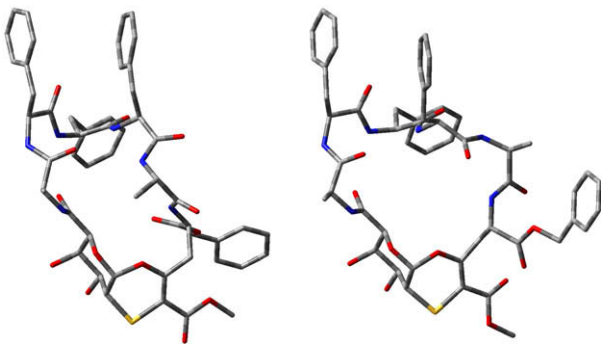

Figure 2. 3D plot of representative conformations for compound **15**.

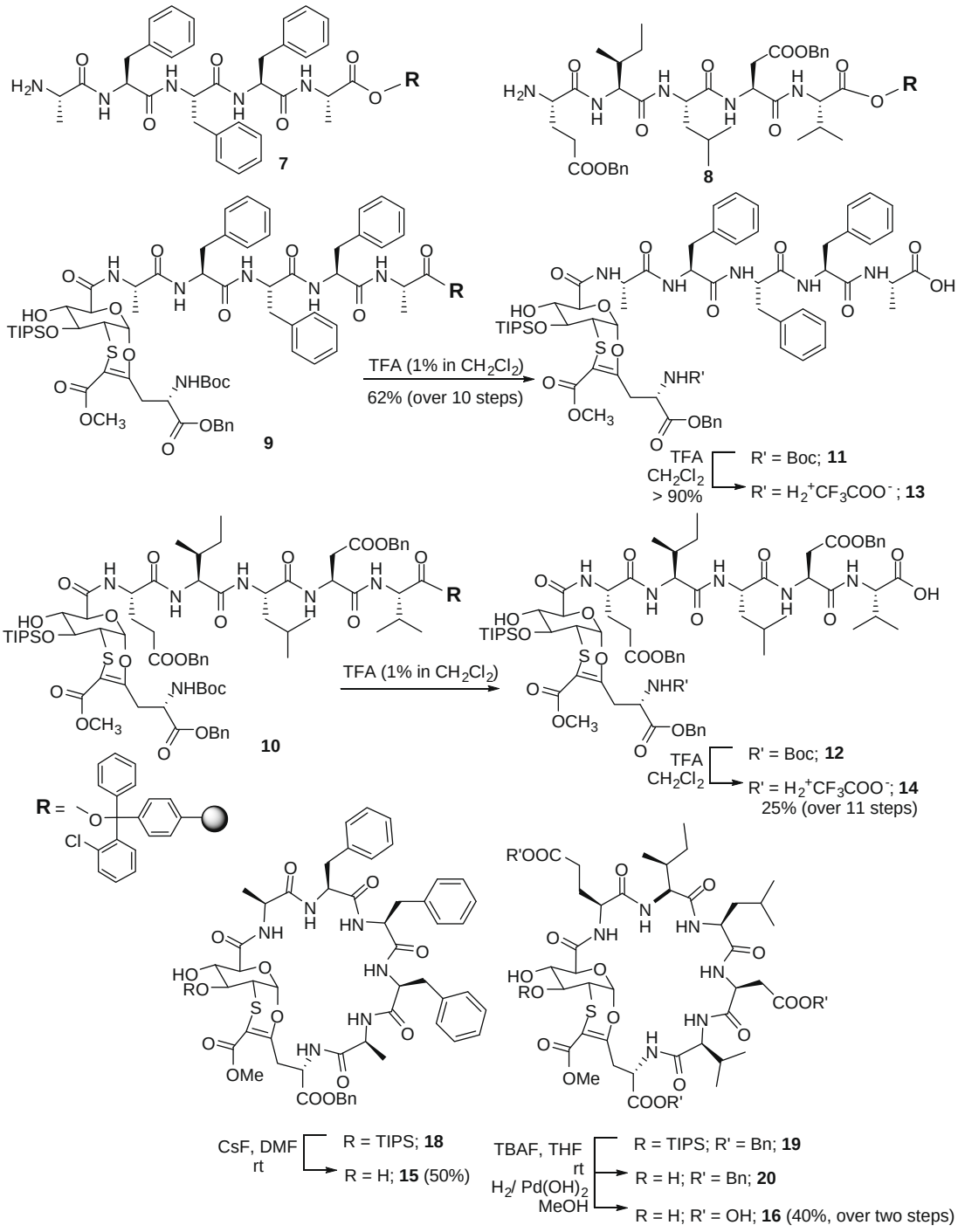

Scheme 2. Synthesis of open-chain SAA peptides **13** and **14**.

nizes polypeptide domains containing the Glu-Ile-Leu-Asp-Val aminoacid sequence whose specificity and efficacy is determined by the contest (flanking residues, conformational presentation, etc.). A number of peptidomimetics have been proposed as anti-VLA4 agents and in this contest the cyclo SAA peptidomimetic **16** was prepared and tested for inhibitory activity against $\alpha4\beta1$ integrin by assessing ability to inhibit the adhesion of U937 and Jurkat cells to a VCAM-1 coated surface[20] demonstrating a lack of inhibition of these processes up to a concentration of 100 μM.

In summary, the monosaccharidic scaffold **5**, efficiently obtained as diastereomerically pure compound, was successfully used to synthesize cyclic SAA peptidomimetics. As suggested by molecular calculations, a pentapeptidic sequence should well fit to form macrocyclic structures, therefore biologically engaging compounds **15** and **16** were prepared as single diastereoisomers. *Cyclo*(SAA**5**-Ala-Phe-Phe-Phe-Ala) **15** was tested as tachykinin NK_2 ligand, showing some, although limited, activity which can likely be rationalized on the basis of a correct orientation of its phenyl groups. *Cyclo*(SAA**5**-Glu-Ile-Leu-Asp-Val) **16**, however, did not exhibit activity against $\alpha4\beta1$ integrin. Relying on the versatility and potentials of the scaffold **5** we propose herein, assisted by molecular modeling studies, further work is ongoing to prepare an array of cyclic SAA peptidomimetics containing proper peptidic chains to interact with specific biological targets.[21]

Acknowledgments

We thank Dr. A. Triolo and Dr. E. Libralesso (Menarini Ricerche) for helpful discussions on MS and NMR spectra and Ente Cassa di Risparmio di Firenze for Ph.D. grant of E.D.

Supplementary data

Supplementary data associated with this article can be found, in the online version, at doi:10.1016/j.bmcl.2009.04.008.

References and notes

1. (a) Hanessian, S.; McNaughton-Smith, G.; Lombart, H.-G.; Lubell, W. D. *Tetrahedron* **1997**, *53*, 12789; (b) Hanessian, S.; Auzzas, L. *Acc. Chem. Res.* **2008**, *41*, 1241. and references cited therein.
2. Graf von Roedern, E.; Lohof, E.; Hessler, G.; Hoffmann, M.; Kessler, H. *J. Am. Chem. Soc.* **1996**, *118*, 10156.
3. For recent reviews see: (a) Gruner, S. A. W.; Locardi, E.; Lohorf, E.; Kessler, H. *Chem. Rev.* **2002**, *102*, 491; (b) Schweizer, F. *Angew. Chem., Int. Ed.* **2002**, *41*, 231; (c) Cipolla, L.; Peri, F.; La Ferla, B.; Redaelli, C.; Nicotra, F. *Curr. Org. Synth.* **2005**, *2*, 153.
4. (a) Lohof, E.; Plaker, E.; Mang, C.; Burkhart, F.; Dechantsreiter, M. A.; Haubner, R.; Wester, H. J.; Schwaiger, M.; Holzemann, G.; Goodman, S. L.; Kessler, H. *Angew. Chem., Int. Ed.* **2000**, *39*, 2761; (b) Locardi, E.; Stockle, M.; Gruner, S.; Kessler, H. *J. Am. Chem. Soc.* **2001**, *123*, 8189.
5. (a) van Well, R. M.; Marinelli, L.; Altona, C.; Erkelens, K.; Siegal, G.; van Raaij, M.; Llamas-Saiz, A. L.; Kessler, H.; Novellino, E.; Lavecchia, A.; van Boom, J. H.; Overhand, M. *J. Am. Chem. Soc.* **2003**, *125*, 10822; (b) El Oualid, F.; Burm, B. E. A.; Leroy, I. M.; Cohen, L. H.; van Boom, J. H.; van den Elst, H.; Overkleeft, H. S.; van der Marel, G. A.; Overhand, M. *J. Med. Chem.* **2004**, *47*, 3920.
6. Chakraborty, T. K.; Srinivasu, P.; Tapadar, S.; Mohan, B. K. *Glycoconjugate J.* **2005**, *22*, 83.
7. Haubner, R.; Finsinger, D.; Kessler, H. *Angew. Chem., Int. Ed.* **1997**, *36*, 1374.
8. Burgess, K.; Feng, Y. *Chemtracts: Org. Chem.* **1997**, *10*, 1054.
9. Venturi, F.; Venturi, C.; Liguori, F.; Cacciarini, M.; Montalbano, M.; Nativi, C. *J. Org. Chem.* **2004**, *69*, 6153.
10. van den Bos, L. J.; Codée, J. D. C.; Van der Toorn, J. C.; Boltje, T. J.; van Boom, J. H.; Overkleeft, H. S.; van der Marel, G. A. *Org. Lett.* **2004**, *6*, 2165.
11. Capozzi, G.; Giannini, S.; Menichetti, S.; Nativi, C.; Giolitti, A.; Patacchini, R.; Perrotta, E.; Altamura, M.; Maggi, C. A. *Bioorg. Med. Chem. Lett.* **2002**, *12*, 2263.
12. Giannotti, D.; Perrotta, E.; Di Bugno, C.; Nannicini, R.; Harmat, N. J. S.; Giolitti, A.; Patacchini, R.; Renzetti, A. R.; Rotondaro, L.; Giuliani, S.; Altamura, M.; Maggi, C. A. *J. Med. Chem.* **2000**, *43*, 4041.
13. Quartara, L.; Altamura, M. *Curr. Drug Targets* **2006**, *7*, 975.
14. See Ref. 11 and references cited therein.
15. Siahaan, T. J.; Lutz, K. *J. Pharm. Biomed. Anal.* **1994**, *12*, 65.
16. Modeling studies were performed through the exploration of the conformational space with a random search approach at an empirical level. All the located conformations were re-optimized within the density functional approach at the B3LYP/6-31G(d) level. Then, the energy was recalculated using a continuum solvent model (PCM) to take into account the effect of water.
17. Lin, K.-C.; Castro, A. C. *Curr. Opin. Chem. Biol.* **1998**, *2*, 453.
18. Belvisi, L.; Bernardi, A.; Colombo, M.; Manzoni, L.; Potenza, D.; Scolastico, C.; Giannini, G.; Marcellini, M.; Riccioni, T.; Castorina, M.; LoGiudice, P.; Pisano, M. *Bioorg. Med. Chem.* **2006**, *14*, 169.
19. Owen, R. M.; Carlson, C. B.; Xu, J.; Mowery, P.; Fasella, E.; Kiessling, L. L. *Chem BioChem* **2007**, *8*, 68.
20. Green, P. M.; Ludbrook, S. B.; Miller, D. D.; Horgan, C. M. T.; Barry, S. T. *FEBS Lett.* **2001**, *503*, 75.
21. The computational approach described for **15** was also applied to virtual c*yclo*(SAA**5**-Arg-Gly-Asp), that contains the RGD motif usually known to confer affinity for the αvβ3 integrin receptor when the tripeptide moiety assumes a kinked conformation. Calculations showed that the desired conformation is largely populated though this analog exhibits a certain degree of conformational freedom.

DOI: 10.1002/chem.200901077

α-*O*-Linked Glycopeptide Mimetics: Synthesis, Conformation Analysis, and Interactions with Viscumin, a Galactoside-Binding Model Lectin

Jesús Jiménez-Barbero,*[a] Elisa Dragoni,[b, c] Chiara Venturi,[a, b, c] Federico Nannucci,[b] Ana Ardá,[a] Marco Fontanella,[a] Sabine André,[d] Francisco Javier Cañada,[a] Hans-Joachim Gabius,[d] and Cristina Nativi*[b, c]

Abstract: Efficient cycloaddition of a silylidene-protected galactal with a suitable heterodiene yielded the basis for a facile diastereoselective route to a glycopeptide-mimetic scaffold. Its carbohydrate part was further extended by β1–3-linked galactosylation. The pyranose rings retain their $^4C_1$ chair conformation, as shown by molecular modeling and NMR spectroscopy, and the typical *exo*-anomeric geometry was observed for the disaccharide. The expected bioactivity was ascertained by saturation-transfer-difference NMR spectroscopy by using the galactoside-specific plant toxin viscumin as a model lectin. The experimental part was complemented by molecular docking. The described synthetic route and the strategic combination of computational and experimental techniques to reveal conformational properties and bioactivity establish the prepared α-*O*-linked glycopeptide mimetics as promising candidates for further exploitation of this scaffold to give *O*-glycans for lectin blocking and vaccination.

Keywords: carbohydrates · drug design · glycoproteins · lectins · molecular modeling · NMR spectroscopy

Introduction

Protein glycosylation, which rivals phosphorylation in its frequency, imparts a series of distinct properties to a carrier backbone. They range from changes in physicochemical parameters, such as solubility and protection from proteolytic degradation, to adding versatile docking sites for the receptors that read the sugar-encoded information.[1] A characteristic of secretory or polarized epithelia, and also encountered in different cell-surface glycoproteins, is the presence of mucin-type O-glycosylated positions linked to serine/threonine residues via an α-*N*-D-acetylgalactosamine (GalNAc) moiety that are often subject to intimate structural control.[2] When clustered together and arranged in repeats, the resulting glycoproteins are referred to as mucins. They can form a highly stable viscoelastic gel over epithelial cell surfaces, thus providing a protective barrier against external agents. Equally importantly, their glycan part can mediate cell adhesion and attachment processes that initiate bacterial infection or leukocyte infiltration into inflamed tissue, here recruiting the sialomucins CD34 or GLYCAM-1 and PSGL-1 as ligands for the C-type lectins of the selectin group.[3] Since these recognition processes with *O*-glycans extend to other lectin classes, such as adhesion/growth-regulatory galectins and to clinically relevant events in the metastatic cascade, it is a challenge to develop bioactive mimetics that would also be useful as vaccines against mucin-based tumor-associated antigens.[4] Towards this end, we directed our efforts to the diastereoselective synthesis of mucin-like scaffolds, which maintain the key structural features of such natural glycoproteins and present suitable functional groups

[a] Prof. Dr. J. Jiménez-Barbero, Dr. C. Venturi, Dr. A. Ardá, Dr. M. Fontanella, Prof. Dr. F. J. Cañada
Chemical and Physical Biology
Centro de Investigaciones Biológicas, CSIC
Ramiro de Maeztu 9, 28040 Madrid (Spain)
Fax: (+34) 915-360-432
E-mail: jjbarbero@cib.csic.es

[b] Dr. E. Dragoni, Dr. C. Venturi, Dr. F. Nannucci, Prof. Dr. C. Nativi
Dipartimento di Chimica Organica
via della Lastruccia, 13, 50019 Sesto F.no, Firenze (Italy)
Fax: (+39) 055-4573570
E-mail: cristina.nativi@unifi.it

[c] Dr. E. Dragoni, Dr. C. Venturi, Prof. Dr. C. Nativi
CERM, University of Florence
via Sacconi, 6, 50019 Sesto F.no, Firenze (Italy)

[d] Dr. S. André, Prof. Dr. H.-J. Gabius
Tierärztliche Fakultät, Lehrstuhl für Physiologische Chemie
Ludwig-Maximilians-Universitaet
Veterinaerstrasse 13, 80539 München (Germany)
Fax: (+49) 89-2180-2290

Supporting information for this article is available on the WWW under http://dx.doi.org/10.1002/chem.200901077.

for the insertion of a saccharidic moiety and one or two peptidic chains or a peptidic chain and a carrier, as required for generating synthetic vaccines against tumor-associated glycopeptide antigens.[5] Since the synthesis of naturally occurring glycopeptides is tedious, often ending up in diastereomeric mixtures, one focus in this area is glycopeptide mimetics.[6] As an added advantage, the latter can have improved stability against chemical and enzymatic hydrolysis and, depending on the type of substitution, improved bioavailability compared to natural materials.

In the course of the rational design of glycopeptidomimetics, it is mandatory for these neoglyco derivatives to retain bioactivity, that is, the capacity to serve as ligands for specific receptors. Thus, synthetic products need to be rigorously controlled by respective assays, in our case tested against a plant lectin with affinity to galactosides including the Thomsen–Friedenreich antigen, which is often present in mucins, or its Galβ1–3Gal derivative as a model.[7] Viscumin, also referred to as *Viscum album* agglutinin (VAA), is a potent biohazard akin to ricin, whose toxicity can be neutralized by suitable inhibitors competing with the cognate cell-surface glycans.[8] This perspective has made the toxin a model for drug design, for example, applying library approaches in search of new binding partners.[9] In a more general context, the strategy of combining preparative synthesis of glycopeptide mimetics with affinity testing will not only explore this substrate class as potential source for new pharmaceuticals but also enable us to gain insights into structural aspects of the recognition process, which have relevance for understanding and exploiting lectin–carbohydrate interactions.[10]

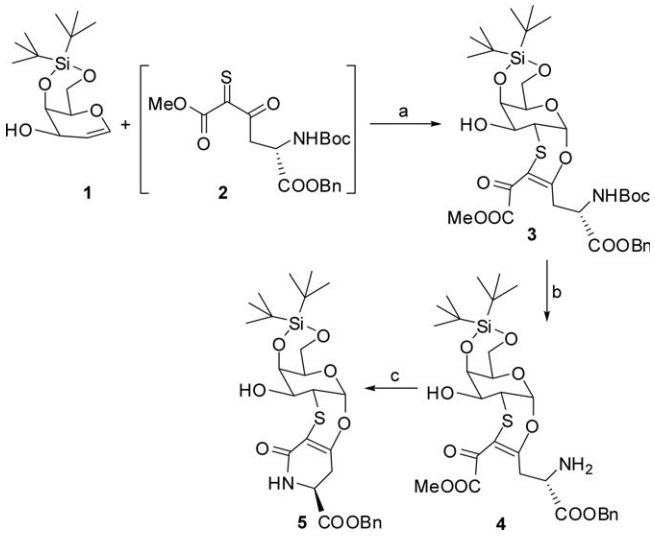

Scheme 1. Synthesis of α-*O*-galactosyl scaffold **5**. a) pyridine, $CHCl_3$, 45 °C, 24 h, 70 %;[11] b) CF_3COOH, CH_2Cl_2, RT; c) triethylamine, $CHCl_3$, 40 °C, 40 h, 65 % (over two steps).

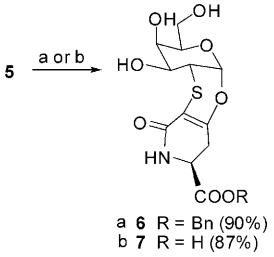

Scheme 2. Synthesis of deprotected scaffolds **6** and **7**. a) HF/pyridine (70 %), CH_2Cl_2, 0 °C, 1 h, 90 %; b) HF/pyridine (70 %), CH_2Cl_2/MeOH, RT, 4.5 h, 87 %.

Results and Discussion

Synthesis: The entirely diastereoselective synthesis of glycopeptide scaffolds that preserve the natural α-*O*-glycosyl linkage is based on an efficient cycloaddition between galactal **1**, as electron-rich dienophile, and homoglutamate **2**, as electron-poor diene[11] (Scheme 1).

The attack of the heterodiene **2** exclusively on the bottom (α) face of the dienophile **1** resulted in the α-*O*-glycosyl derivative **3** as the single diastereomer, in a 70 % yield. Treatment of **3** with trifluoroacetic acid enabled removal of the *tert*-butoxycarbonyl group without affecting the silylidene protecting group on the galactose moiety, leading to the amino derivative **4**. Under basic conditions, compound **4** underwent cyclization to give the tricyclic lactam **5** in a 65 % yield (calculated over two steps). Galactosyl amino acid **5** is a versatile scaffold that presents an α-glycosyl linkage and decorated with three hydroxyls and one carboxylic group.

Treatment of scaffold **5** with hydrogen fluoride/pyridine (70 %) in dichloromethane and methanol at room temperature facilitated the removal of the silylidene and benzyl ester protecting groups to produce unprotected scaffold **7** as a diastereometrically pure compound, in one step and in 87 % (Scheme 2).

Under these reaction conditions, first the removal of silylidene occurred, followed by nucleophilic cleavage of the benzyl ester. In fact, if the deprotection reaction is stopped after one hour instead of four, the benzyl derivative **6** was isolated in 90 % yield. Focusing our attention on the development of a synthetically convenient compound for tests as a bioactive ligand, with perspectives for application as a vaccine against α-Tn and α-TF antigens, we started with scaffold **5** to prepare the glycopeptide mimetic **8**, its sugar part then extended to the disaccharide **9** (Scheme 3).

After selective removal of benzyl ester under standard conditions (90 %), scaffold **5** was transformed into derivative **10** (Scheme 4). It presents a free carboxylic residue that is suitable for the introduction of a serine moiety. Indeed, the serine methyl ester was treated with **10** in the presence of *O*-(7-azabenzotriazol-1-yl)-*N*,*N*,*N*′,*N*′-tetramethyluronium hexafluorophosphate (HATU) and *N*-methylmorpholine (NMM) at room temperature and in dimethylformamide as solvent to give the glycopeptide mimetic **11** in 93 % yield.

Removal of the silylidene protecting group, as reported above, followed by deprotection of the serine carboxylic residue, with lithium hydroxide/water, in tetrahydrofuran/water

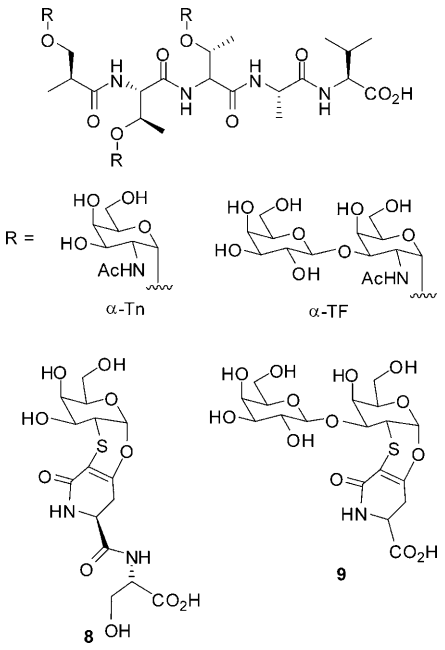

Scheme 3. Structure of α-Tn, α-TF, and scaffolds **8** and **9**.

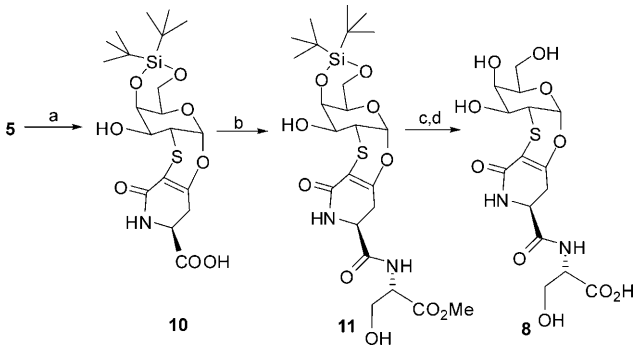

Scheme 4. Synthesis of scaffold **8**. a) $Pd(OH)_2/C$ (20%), H_2, EtOAc/CH_2Cl_2, RT, 2 h, 90%; b) Ser(OMe), *N*,*N*-dimethylformamide, NMM, HATU, RT, 2 h, 93%; c) HF/pyridine (70%), CH_2Cl_2, RT, 2 h; d) LiOH/H_2O (0.04 M), THF/H_2O, 0 °C, 1.5 h, 39% (over two steps).

as solvent at 0 °C (39%, calculated over two steps), afforded the fully unprotected building block **8**.

Glycosylation, under Schmidt's conditions, of scaffold **5** with the glycosyl donor **12**[12] then gave the disaccharide **13**, as single β-diastereoisomer in 75% yield (Scheme 5). Deacetylation under standard conditions, in methanol as solvent, resulted in the disaccharide **14** as a methyl ester (60%). The latter was then treated with HF/pyridine and lithium hydroxide to obtain the completely unprotected disaccharide **9** in 56% yield (calculated over two steps). This product was further studied to evaluate its conformational properties.

Conformational analysis in solution by NMR spectroscopy and molecular modeling: Analysis of the vicinal proton–proton coupling constants (Table 1) for the pyranose rings of **7** and **8** indicates the exclusive presence of the $^4C_1$ chair conformation, as for natural galactosides.[13] Indeed, most of the NMR parameters regarding the shape of the bicyclic moieties of these compounds were very similar, thus indicating no influence from the presence of the Ser moiety in **8**. Results obtained from MM3*-based molecular mechanics calculations[14] also support these observations, with the $^4C_1$ chair form being more than 3 kJ mol^{-1} more stable than the $^1S_3$ skew-boat conformation and much more stable than the alternative $^1C_4$ chair conformer. The major difference concerns the orientation around the C5–C6 torsion angle. For **7**, the observed $J_{H5,H6a}$ and $J_{H5,H6b}$ values (4.6 and 10.1 Hz) are in agreement with a major conformation of this torsion, in contrast to the equilibrium usually observed for galactoside derivatives.[15] On the other hand, the observed intermediate values (4.5 and 7.9 Hz) for **8** are accounted for by the expected *gt*:*tg* conformational distribution. For **8**, the $J_{\alpha\beta}$ and $J_{\alpha\beta'}$ values are also on an intermediate level (4.0, 5.0 Hz); this indicates the existence of an equilibrium around the Cα–Cβ lateral chain. Molecular dynamics simulations (5 ns with the MM3* force field) were performed (Figures 1 and 2 and Supporting Information). The results disclose that the chair conformer is very stable, with basically no fluctuations. Moreover, motion around the pseudoglycosidic Φ (H1′-C1′-O-C2) and Ψ (C1′-O-C2-C3) angles is also rather restricted for both molecules, with values centered around +80° and 180°. However, fluctuations take place around the region containing the nitrogen atom, defined by torsions $\phi 1$ and $\phi 2$, giving rise to two geometries (Figure 2).

The first conformer (A) is defined by $\phi 1$ (defined as C1-C2-C3-N4) $\approx +48°$ and $\phi 2$ (defined as C2-C3-N4-C5) $\approx -35°$. The second one (B) is defined by $\phi 1$, $\phi 2$ angles around −45° and +35°, respectively (Figures 1 and 2). Comparison of the expected couplings with those experimentally

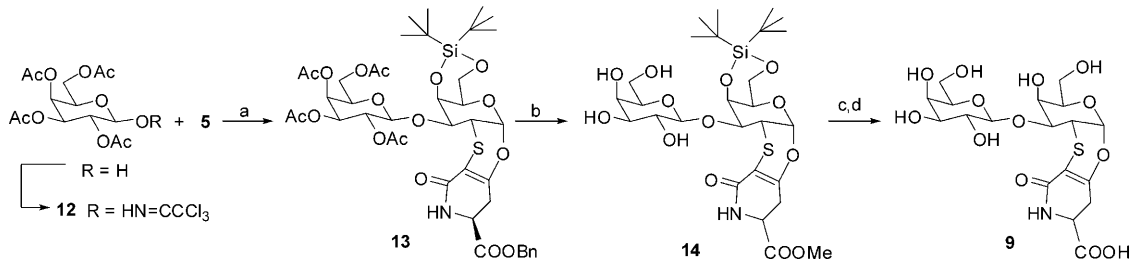

Scheme 5. Synthesis of scaffold **9**. a) CH_2Cl_2 at −30 °C then TMSOTf at RT, 2.5 h; Et_3N (Ph 7), 75%; b) CH_3ONa, CH_3OH, 0 °C, 1 h, 60%; c) HF/Py (70%), RT, 2 h, d) LiOH, H_2O (Ph 10), RT, 2 h then H_3PO_4 (Ph 7), 56% (over two steps).

Table 1. Chemical shifts and coupling constants of compounds **7** and **8**, measured in D_2O (500 MHz, 298 K, phosphate buffer: 20 mM, pH 5.8). The theoretical values (J_{theor}) were obtained by applying the generalized Karplus equation proposed by Altona to the geometries calculated by the MM3*-based calculations. The *gt* conformer around the C5–C6 torsion was employed.

	Compound **7**				Compound **8**			
Atom	δ (ppm) D_2O	J [Hz] (exp)	J [Hz] theor (Conf A)	J [Hz] theor (Conf B)	δ (ppm) D_2O	J [Hz] (exp)	J [Hz] theor (Conf A)	J [Hz] theor (Conf B)
H1′	5.74	1′/2′ 3.0	2.6	2.6	5.80	2.9	1.4	1.5
H2′	3.42	2′/3′ 11.3	11.4	11.4	3.48	11.3	10.9	10.9
H3′	3.75	3′/4′ 3.1	2.8	2.8	3.77	2.7	2.2	2.3
H4′	3.96	4′/5′ <1	0.8	0.8	4.02	<1	0.2	0.3
H5′	4.12	5′/6′a 4.6	2.0	2.3	4.15	4.5	4.7	1.6
H6′a	3.70	5′/6′b 10.1	9.7	10.4	3.73	7.9	10.5	9.8
H6′b	3.65				3.72			
H_{2a}	2.87	2a/3 5.3	5.0	5.1	3.11	5.5	4.0	5.0
H_{2b}	2.67	2b/3 7.7	11.0	1.8	2.82	6.5	11.3	1.7
H_3	4.05				4.39			
$H_{\beta,\beta'}$ Ser					3.89	α,β 5.0	1.0	10.7
H_α					4.43	α,β′ 4.0	2.4	4.5
HN	7.21 (H_2O)				7.67 (H_2O)			
HN-Ser					8.22			

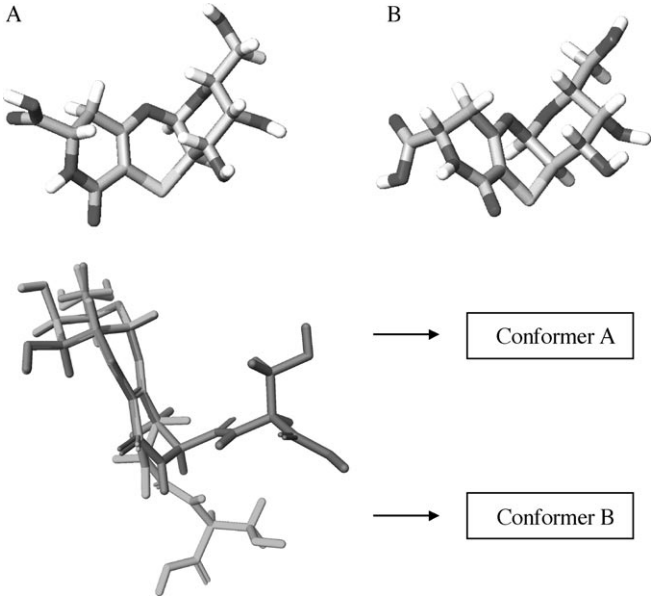

Figure 1. A) The two major conformers of **7** (A and B) according to the experimental NMR data and MM3*-based molecular mechanics and dynamics calculations. This orientation of the lactam defines the two geometries by the MD. B) Superimposition of the two major conformers of **8** according to the experimental NMR data and MM3*-based molecular mechanics and dynamics calculations. This orientation of the lactam defines the two geometries, which show rather different spatial orientations of the Ser moiety. The additional mobility at the Ser moiety is not defined here, although it is manifested in the NMR data.

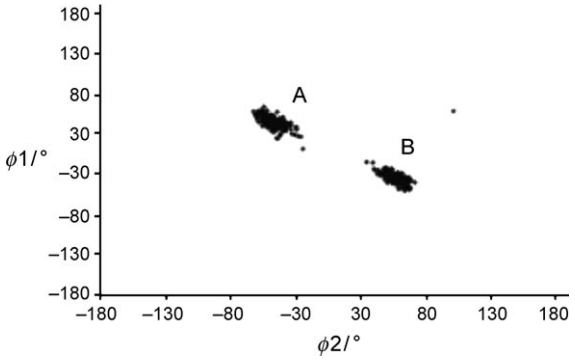

Figure 2. Plot of the $\phi1/\phi2$ values sampled during the 5 ns MD simulations performed for **8** with the MM3* force field and the GB/SA solvent model. The data for **7** are basically identical.

observed for the C2–C3 fragment enabled us to deduce that both conformers are present in solution to a significant extent, with an approximate A/B ratio of 40:60 for **7** and 50:50 for **8**. Overall, this slight 10% shift of the conformational equilibrium is almost negligible considering the ΔG parameter. Calculation of the expected J values for the ensemble deduced from the MD simulations enabled us to quantitatively explain the experimental observations (Table 1) and NOEs (Supporting Information).[16,17]

Next, the conformational behavior of the Galβ1–3Gal analogue **9** was investigated. In this case, a mixture of stereoisomers at the α-carbon of the amino acid was obtained. Nonetheless, its presence does not preclude testing the bioactivity, so a qualitative conformational analysis of both isomers was performed. The coupling constant data (see Table 2) revealed that both galactose residues adopt the usual $^4C_1$ chair geometry. The existence of a inter-residual Gal H1′–Gal H3 NOE indicated the presence of a typical *exo*-anomeric geometry[18] around the glycosidic linkage. Chemical shift and coupling constant data, as deduced from analysis of the 2D ^{1}H NMR spectra, are given in Table 2. With this information, molecular-mechanics calculations were performed for both diastereomers, and the expected coupling constants were compared to those experimentally observed. Since the two H_α protons for both diastereomers can be distinguished in the ^{1}H NMR spectrum, the couplings to the corresponding H_β could easily be measured. The values range between 5.1 and 7.9 Hz (Table 2), thus indicating that a conformational equilibrium, similar to that de-

Table 2. Chemical shifts and coupling constants of compound **9**, measured in D_2O (500 MHz, 298 K, phosphate buffer: 20 mM, pH 5.8).

Proton	δ (ppm)	*J* [Hz]	Proton	δ (ppm)	*J* [Hz]
H-1	5.74	$J_{1,2}=2.7$	H-1′	4.48, 4.45 for both isomers	$J_{1'2'}=7.6$ and 7.9, for both isomers
H-2	3.57	$J_{2,3}=11.1$	H-2′	3.55	–
H-3	3.95	$J_{3,4}=3.2$	H-3′	3.61	–
H-4	4.16	–	H-4′	3.82	$J_{3',4'}=3.5$
H-5	4.14	–	H-5′	4.16	–
CH_2-6	3.75	–	CH_2-6′	3.65	–
H-α (*R*, *S*)	4.05, 3.96	$J_{\alpha,\beta1}=6.7$, $J_{\alpha,\beta2}=7.9$ $J_{\alpha,\beta1'}=5.1$, $J_{\alpha,\beta2'}=6.9$	H-β, H-β′ (*R*, *S*)	2.92–2.65	overlapping

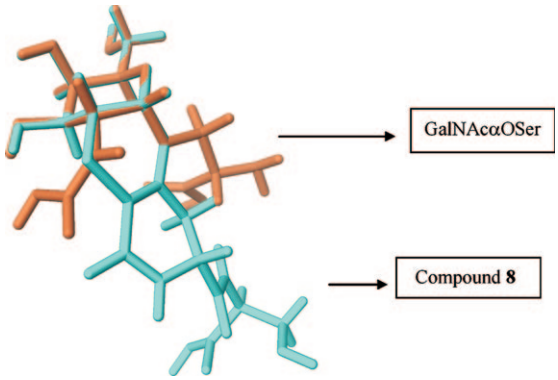

Figure 4. Superimposition of the major conformer of **8** with that of GalNAcαOSer. The positions of chair constituents perfectly match each other. Different orientations of the polar groups of both compounds are evident, although the existing flexibility might let them occupy similar regions of the conformational space.

scribed above for **7** and **8**, is also present. A view of the major MM3*-based conformers, which are in agreement with the experimental data, is given in Figure 3.

Thus, in principle, and according to their conformational behavior in solution, compounds **7–9** can act as mimetics of the natural glycopeptides, with *exo*-anomeric orientation for the corresponding *Φ* glycosidic linkage of **9**. Indeed, a superimposition of compound **8** with GalNAcαOSer (Figure 4) illustrates a remarkable match of the chairs and the positions of the polar groups of both compounds. To test whether this similarity will in fact translate into bioactivity, we proceeded to perform interaction studies with the plant-toxin-reactive β1–3-linked galactosides.[7,19]

Interaction with viscumin: Saturation transfer difference (STD) NMR spectra[20] of **7** and **8** in the presence of the galactoside-specific viscumin (VAA) were recorded (Figure 5). Two molar ratios for the **7**/VAA or **8**/VAA mixture were tested, that is, 20:1 and 50:1. Major saturation transfer to the protons in the pyranose ring was observed, followed by minor transfer to H3 at the lactam ring, with basically no transfer to H2 at this fragment. Thus, the recognition mainly involved the galactose moiety. Moreover, competitive STD experiments with lactose, a common ligand for VAA known to enter the lectin sites, were performed. It was shown that both **7** and **8** competed with lactose for the contact site; this underscored their bioactivity as lectin ligands.

Further STD NMR assays[21] on **9** in the presence of viscumin were also performed (Figure 6). As above for the interactions between **9** and this receptor, but now with ligand/receptor molar ratios between 30:1 and 200:1, major saturation transfer to the protons in both galactopyranose rings was observed, especially for the nonreducing end. No transfer to the amino acid protons was evidenced even after long saturation times; this indicates intimate contact of the lectin to the sugar moiety of **9.** Again, competition experiments with lactose revealed that both molecules target the same binding site in the lectin.

To rationalize the interaction on the molecular level, the low-energy conformers of **7–9**, as deduced from NMR experiments, were docked into the lectin sites by the program AUTODOCK. Two sites are known in the lectin dimer, charac-

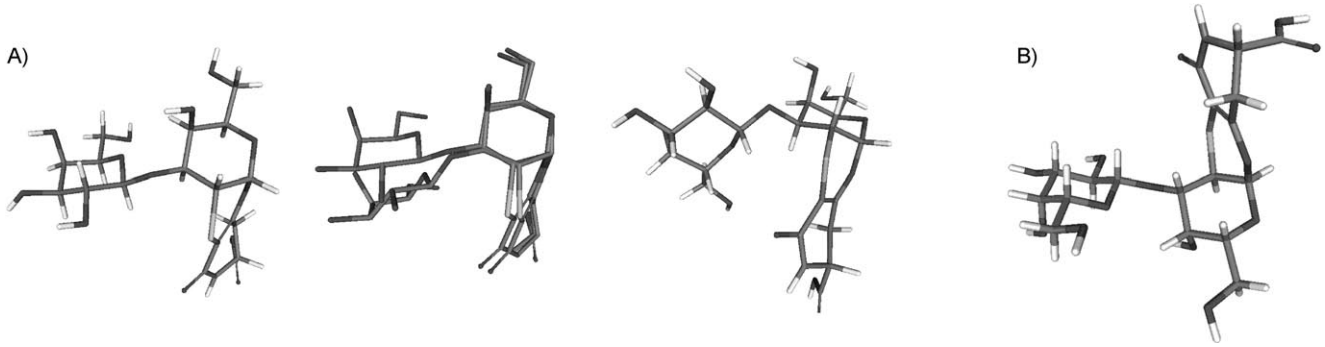

Figure 3. A) The major conformers of **9** (*R* configuration for Cα) according to the experimental NMR data and MM3*-based molecular mechanics and dynamics calculations. The orientation around the glycosidic linkage is defined by the *exo*-anomeric effect, while, according to MD simulations, mobility is allowed for *Ψ* angle, with a concomitant effect on the lactam ring. A superimposition of the two conformers shown left and right is given in the central. This moiety, in turn, may also adopt the two geometries shown in Figure 1, for **7** and **8**. B) The major conformer of **9** (*S* configuration for Cα) according to the experimental NMR data and MM3*-based molecular mechanics and dynamics calculations.

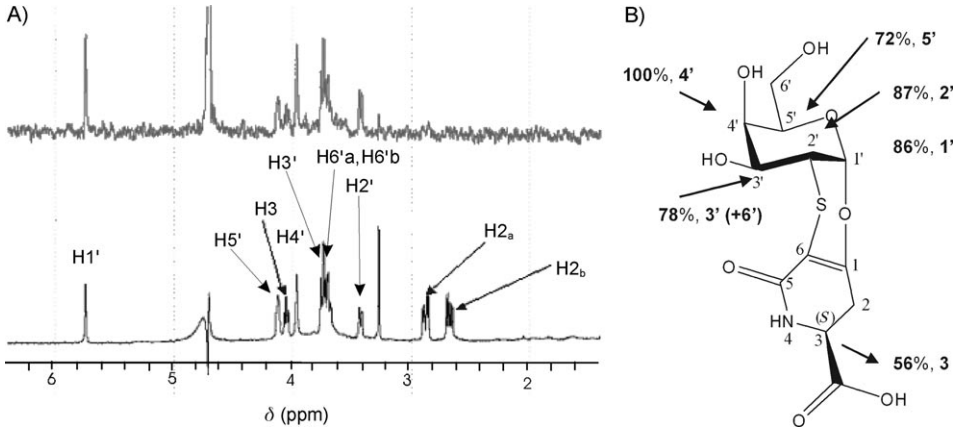

Figure 5. A) Compound **7** interacts with viscumin, inhibitable by lactose, via the galactose epitope and with similar affinity, that is in the millimolar range. The concentration of the protein was 25 μM. The bottom part shows the 500 MHz ^{1}H NMR spectrum of **7**. At the top is the STD spectrum of **7** (2 s saturation time) in the presence of VAA. The **7**/VAA molar ratio is 50:1. The off-resonance frequency was set at 50 ppm, while the on-resonance frequency was established at −0.5 ppm. B) The STD percentages assigned to the particular hydrogens. The 78% value below H3′ Gal corresponds to the addition of H3′ and both H6′ protons.

terized by the central presence of Trp38 in the 1α subdomain and by Tyr249 in the 2γ subdomain.[22] With emerging insights into pH-dependent changes when comparing the crystal structure obtained at acidic pH with experimental binding data under physiological condition, a slight modification of the architecture of the site in the 2γ subdomain was inferred.[22,23] The $^4C_1$ conformer fitted very well, especially in the Trp binding site when geometry A was employed for the lactam ring. The superimposition of the Gal rings of **8** and **9** of the AUTODOCK solution with that of lactose in the X-ray structure was excellent. In contrast, AUTODOCK did not find a lactose-type structure for the other site in viscumin for **8**, although manual docking could be acceptable. Conformer B of **8**, on the other hand, could not be accommodated at either site (Figure 7) due to steric repulsion of the carboxy group with the protein backbone's side chains. For geometry A, the two methylene H2a and H2b protons were oriented outside of the protein, thus precluding their contact, as inferred from the STD experiments. Therefore, there is a perfect match between the molecular modeling results and the experimental data for bound **8**. A similar conclusion was deduced for the docking of **9**, although in this case the extension of the additional galactose moiety permitted docking for any conformer at the lactam ring as well as retaining conformational flexibility at the interglycosidic torsion angles (Figure 8). Indeed, the docked structure perfectly explains the experimental STD data for the galactose hydrogens (with the obvious limitations arising from overlapping) and the lack of STD effect for protons at the lactam moiety). These computational data thus establish a structural concept for the experimental data obtained by STD NMR experiments.

Conclusion

The presented facile synthetic route not only afforded diastereoselectivity, but also a product that maintains the biomimetic conformational properties of the resulting scaffold, as documented by combined molecular modeling and NMR spectroscopic analyses. The sugar part retains bioactivity for

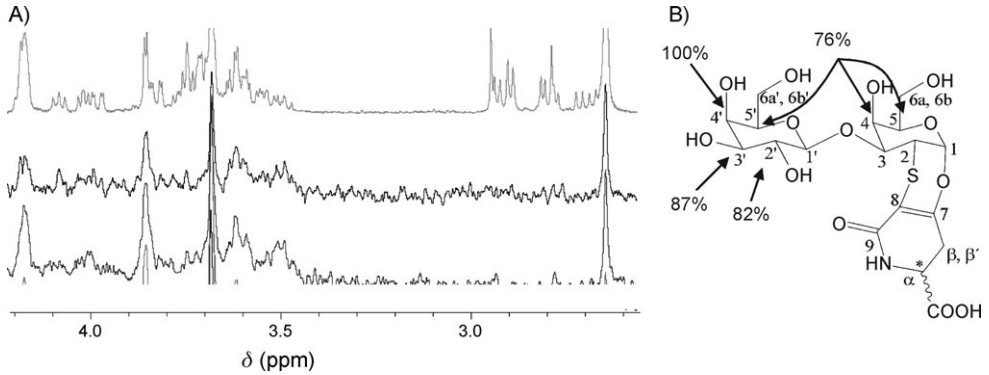

Figure 6. Compound **9** interacts with viscumin, mainly through the nonreducing galactose moiety, as can be observed in the STD spectra, and in the molecular scheme, where the key STD percentages are given. The concentration of the protein was ca. 15 μM. The experiments were performed at 298 K, in 20 mM phosphate buffer at pH 5.8. A) An expanded view of the sugar region with a superimposition of the regular 500 MHz ^{1}H NMR spectrum of **9** (top) onto two STD spectra recorded with 100:1 and 50:1 molar ratios of ligand/VAA, which yielded analogous results. The off-resonance frequency was set to 50 ppm, while the on-resonance frequency was established at −0.5 ppm. B) The STD percentages for **9**. The 76% value corresponds to the addition of H4 and H5 of the reducing Gal unit, and H5′ of the nonreducing Gal. Negligible STD effects on the protons of the lactam moiety are observed, independently of the diastereomer at the amino acid chiral center.

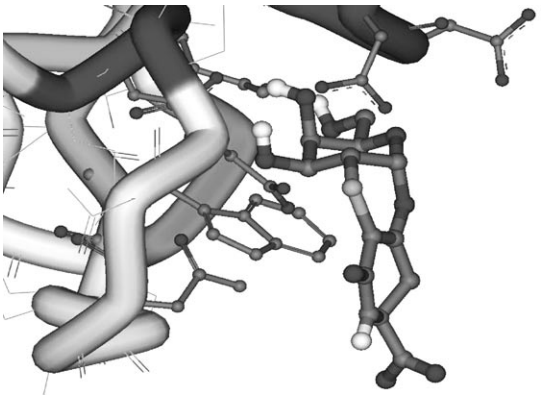

Figure 7. The putative binding mode of compound **8** in complex with viscumin, according to AUTODOCK calculations. The expansion of the lectin's Trp site shows interaction with **8** in the preferred A-type conformation. The methylene protons are not in contact with the polypeptide, in agreement with the STD observations, which mainly indicate transfer to the Gal protons. The side chains of the key amino acids interacting through hydrogen bonds or van der Waals contacts with **8** are shown in ball and stick form.

the tested model lectin, so this synthetic scaffold is suitable to present functionally potent docking sites for clinically relevant human lectins, such as the selectins mentioned in the introduction. The selectivity for the prepared Galβ1–3Gal sugar moiety among the adhesion/growth-regulatory galectins, with preference for galectins-3 and -9, encourages further testing at this level of structural complexity, at which formation of a C-glycoside could even afford a nonhydrolyzable galectin ligand.[24]

Experimental Section

Molecular modeling: The low-energy conformers were calculated by using the MM3* force field,[13] in MAESTRO.[25] The six-membered ring *cis*-fused to the pseudogalactose moiety through C1 and C2 is rather rigid. Therefore, only a low level of flexibility remains for the lactam moiety. Two torsion angles were evaluated to account for the six-membered ring's shape, namely for **8**, torsion angle $\phi 1$ is defined as N4-C3-C2-C1 and $\phi 2$ as C5-N4-C3-C2. For all the molecules, the molecular-dynamics simulations were performed by using the MM3* force field. A temperature of simulation of 300 K was employed with a time step of 1.5 fs and an equilibration time of 100 ps. The total simulation time for each compound was 5 ns. In all the molecular-mechanics and -dynamics calculations, the GB/SA solvation model for water was used.[26] For **9**, different initial geometries of the Φ/Ψ glycosidic linkages were used, with *syn* or *anti* conformers for both Φ and Ψ angles. Also, the two possible epimers at the chiral centre of the amino acid were used as starting geometries, as well as the two possible geometries of the lactam ring, previously deduced for **7** and **8** (see text).

For the C5–C6 torsion of the Gal moieties, only the *gt* geometry (ω, defined as C4-C5-C6-O4 ca. 180°) was considered, since it has been demonstrated to be the major one for galactose derivatives (O4 in axial orientation).[15,27]

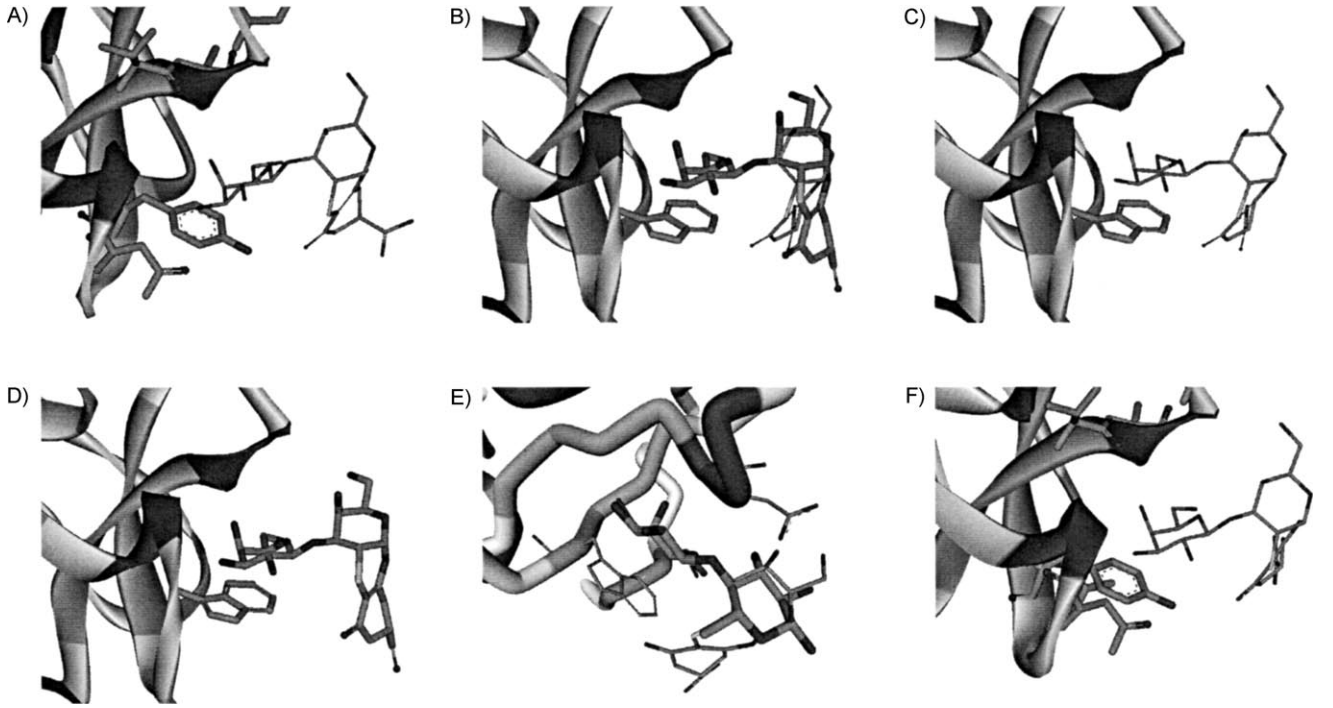

Figure 8. Different possibilities for the binding mode of compound **9** to VAA, according to AUTODOCK calculations. The expansion of the Trp site of VAA is shown in panels (B)–(E). The Tyr site is outlined in panels (A) and (F), with the two different possible epimers of the lactam ring. There is not any hindrance for the recognition of any of them. Panel (B) shows a superimposition of two conformers around the glycosidic torsion angles of the disaccharide, while panels (C) and (D) depict the two geometries separately. Panel (E) presents a superimposition of the pose shown in (C) with the crystallographic binding mode of lactose, showing a good match. All these structures perfectly match the experimental STD data, which are mainly observed at the Gal moiety, with no transfer to the lactam hydrogens. Indeed, the methylene protons point outside the polypeptide chain. The side chains of the key amino acids interacting through hydrogen bonds or van der Waals contacts with **9** are shown as sticks.

NMR experiments with free compound: ^{1}H NMR spectra were recorded on Bruker Avance 500 spectrometers in D_2O with concentrations of 5 mM. Chemical shifts are reported in ppm with external TSP (2,2,3,3-tetradeutero-3-trimethylsilylpropionic acid, 0 ppm) as reference. Vicinal proton–proton coupling constants were estimated from first-order analysis.

2D TOCSY experiments (30 and 70 ms mixing times) were performed by using a data matrix of 256×2K to digitize a spectral width of 5000 Hz. Eight scans were used per increment, with a relaxation delay of 2 s. 2D NOESY (600 and 1000 ms) and 2D T-ROESY experiments (400 and 500 ms) used the standard sequences. Distances were estimated from NOESY/ROESY experimental data by using the isolated spin-pair approximation[28] for the data with decreased mixing time and averaging. Estimated errors were below 10%.

A comparison between the observed NOEs and those derived computationally for the different conformations was performed by using a full-relaxation-matrix approach, with a home-made program, which is available from the authors upon request.[27] For all molecules, an average effective correlation time of 150 ps was estimated for the best adjustment of the observed and calculated cross peaks.

Interaction studies with viscumin: The lectin was isolated from extracts of dried mistletoe leaves, with affinity chromatography on lactosylated Sepharose 4B as a crucial step. The purity and quaternary structure were ascertained by one- and two-dimensional gel electrophoresis, gel filtration and ultracentrifugation; carbohydrate-dependent activity was tested by hemagglutination as well as solid-phase/cell assays.[29] The binding of the different compounds was evaluated by STD experiments, which were performed without saturation of the residual HDO signal for molar ratios of 20:1 and 50:1 of compound/VAA for **8**, and of 30:1 and 200:1 of compound/VAA for **9**. The concentration of the protein was 25 μM. A series of Gaussian-shaped pulses of 50 ms each was employed with a total saturation time for the protein envelope of 2 s and a maximum $B1$ field strength of 60 Hz. An off-resonance frequency of $\delta = 40$ ppm and an on-resonance frequency of $\delta = -1.0$ ppm (protein aliphatic signals region) were applied. Competition experiments with lactose were also performed. In these cases, a threefold excess of lactose relative to **8** was added to the solution containing the VAA/**8** mixture, and the STD experiment was repeated. For the other compounds, analogous experiments were performed. In all cases, a decrease in the STD signals of the mimetic compound was observed, thus indicating competition for the same binding sites.

For the VAA/**8** and VAA/**9** samples, exchange-transferred NOE experiments (trNOE)[30] were performed by using selective 1D experiments with the double pulse field-gradient spin-echo (DPFGSE) module.[31] Measurements were performed on a freshly prepared ligand/lectin mixture, with mixing times of 100 and 200 ms, at an approximately 20:1 molar ratio of ligand/protein for **8** and 40:1 for **9**. The ligand concentration of 2 mM was kept in all cases. No purging spin-lock period was employed to remove the NMR signals of the macromolecule background. Strong negative NOE cross peaks were observed, in contrast to the free state; this indicated binding of the sugars to the lectin preparation.

Docking calculations: The conformers of **8** and **9** (as observed by NMR) were docked into the two carbohydrate-binding sites of VAA in the 1α and 2γ subdomains of the B-subunit of VAA (PDB ID: 1PUM). The different conformational possibilities of compounds **8** and **9** (see text) were used as input geometries for AUTODOCK 3.0 simulations[32] with the multiple Lamarckian genetic algorithm. Only local searches were performed centered around the two known lectin sites of viscumin. Grids of probe-atom interaction energies and electrostatic potential were generated by the AutoGrid program present in AUTODOCK 3.0. Grid spacings of 0.6 and 0.375 Å were used for the global and local searches, respectively. For each calculation, 100 docking runs were performed on a population of 200 individuals and an energy evaluation number of 3×10^6.

Acknowledgements

This work was supported by a grant from the Ministry of Science and Innovation of Spain (CTQ2006-10874-C02-01/BQU) and by an EC Marie Curie Research Training Network grant (MCRTN-CT-2005-19561). The authors thank the Ente Cassa di Risparmio di Firenze for a PhD grant to E.D.

[1] a) N. Sharon, H. Lis in *Glycosciences: Status and Perspectives* (Eds.: H.-J. Gabius, S. Gabius), Chapman & Hall, London, **1996**, pp. 133–162; b) G. Reuter, H.-J. Gabius, *Cell. Mol. Life Sci.* **1999**, *55*, 368–422; c) O. Seitz, *ChemBioChem* **2000**, *1*, 214–246; d) H.-J. Gabius, H.-C. Siebert, S. André, J. Jiménez-Barbero, H. Rüdiger, *ChemBioChem* **2004**, *5*, 740–764; e) T. Buskas, S. Ingale, G.-J. Boons, *Glycobiology* **2006**, *16*, 113R–136R; f) C. Zuber, J. Roth in *The Sugar Code. Fundamentals of Glycosciences* (Ed.: H.-J. Gabius), Wiley-VCH, Weinheim, **2009**, in press.

[2] a) M. A. Hollingsworth, B. J. Swanson, *Nat. Rev. Cancer* **2004**, *4*, 45–60; b) C. Robbe, C. Capon, B. Coddeville, J.-C. Michalski, *Biochem. J.* **2004**, *384*, 307–316; c) H.-J. Gabius, *Crit. Rev. Immunol.* **2006**, *26*, 43–79; d) G. Theodoropoulos, K. L. Carraway, *J. Cell. Biochem.* **2007**, *102*, 1103–1116; e) L. Royle, E. Matthews, A. Corfield, M. Berry, P. M. Rudd, R. A. Dwek, S. D. Carrington, *Glycoconjugate J.* **2008**, *25*, 763–773; f) G. Patsos, A. Corfield in *The Sugar Code. Fundamentals of Glycosciences* (Ed.: H.-J. Gabius), Wiley-VCH, Weinheim, **2009**, in press.

[3] a) S. D. Rosen, *Annu. Rev. Immunol.* **2004**, *22*, 129–156; b) H. C. Hang, C. R. Bertozzi, *Bioorg. Med. Chem.* **2005**, *13*, 5021–5034; c) F. Corzana, J. H. Busto, G. Jimenez-Oses, M. Garcia de Luis, J. L. Asensio, J. Jiménez-Barbero, J. M. Peregrina, A. Avenoza, *J. Am. Chem. Soc.* **2007**, *129*, 9458–9467; d) H.-J. Gabius, *Biochem. Soc. Trans.* **2008**, *36*, 1491–1496; e) R. Schwartz-Albiez in *The Sugar Code. Fundamentals of Glycosciences* (Ed.: H.-J. Gabius), Wiley-VCH, Weinheim, **2009**, in press.

[4] a) I. Brockhausen, J. Schutzbach, W. Kuhns, *Acta Anat.* **1998**, *161*, 36–78; b) A. M. Wu, J. H. Wu, J.-H. Liu, T. Singh, S. André, H. Kaltner, H.-J. Gabius, *Biochimie* **2004**, *86*, 317–326; c) I. Brockhausen, *EMBO Rep.* **2006**, *7*, 599–604.

[5] D. Dziadek, D. Kowalczyk, H. Kunz, *Angew. Chem.* **2005**, *117*, 7798–7803; *Angew. Chem. Int. Ed.* **2005**, *44*, 7624–7630.

[6] a) A. Dondoni, A. Marra, *Chem. Rev.* **2000**, *100*, 4395–4422; b) H. Herzner, T. Reipen, M. Shultz, H. Kunz, *Chem. Rev.* **2000**, *100*, 4495–4538.

[7] a) R. T. Lee, H.-J. Gabius, Y. C. Lee, *Carbohydr. Res.* **1994**, *254*, 269–276; b) O. E. Galanina, H. Kaltner, L. S. Khraltsova, N. V. Bovin, H.-J. Gabius, *J. Mol. Recognit.* **1997**, *10*, 139–147; c) M. Gilleron, H.-C. Siebert, H. Kaltner, C.-W. von der Lieth, T. Kožár, K. M. Halkes, E. Y. Korchagina, N. V. Bovin, H.-J. Gabius, J. F. G. Vliegenthart, *Eur. J. Biochem.* **1998**, *252*, 416–427; d) H.-J. Gabius, *Biochimie* **2001**, *83*, 659–666; e) M. Jiménez, J. L. Sáiz, S. André, H.-J. Gabius, D. Solís, *Glycobiology* **2005**, *15*, 1386–1395.

[8] a) S. André, P. J. C. Ortega, M. A. Perez, R. Roy, H.-J. Gabius, *Glycobiology* **1999**, *9*, 1253–1261; b) S. André, B. Liu, H.-J. Gabius, R. Roy, *Org. Biomol. Chem.* **2003**, *1*, 3909–3916; c) S. André, H. Kaltner, T. Furuike, S.-I. Nishimura, H.-J. Gabius, *Bioconjugate Chem.* **2004**, *15*, 87–98; d) S. André, F. Sansone, H. Kaltner, A. Casnati, J. Kopitz, H.-J. Gabius, R. Ungaro, *ChemBioChem* **2008**, *9*, 1649–1661.

[9] a) S. André, Z. Pei, H.-C. Siebert, O. Ramström, H.-J. Gabius, *Bioorg. Med. Chem.* **2006**, *14*, 6314–6326; b) S. André, C. E. P. Maljaars, K. M. Halkes, H.-J. Gabius, J. P. Kamerling, *Bioorg. Med. Chem. Lett.* **2007**, *17*, 793–798.

[10] a) D. Solís, J. Jiménez-Barbero, H. Kaltner, A. Romero, H.-C. Siebert, C.-W. von der Lieth, H.-J. Gabius, *Cells Tissues Organs* **2001**, *168*, 5–21; b) D. Solís, A. Romero, M. Menéndez, J. Jiménez-Barbero in *The Sugar Code. Fundamentals of Glycosciences* (Ed.: H.-J. Gabius), Wiley-VCH, Weinheim, **2009**, in press.

[11] F. Venturi, C. Venturi, F. Liguori, M. Cacciarini, M. Montalbano, C. Nativi, *J. Org. Chem.* **2004**, *69*, 6153–6155.
[12] G. Grundler, R. R. Schmidt, *Liebigs Ann. Chem.* **1984**, 1826.
[13] *NMR Spectroscopy of Glycoconjugates* (Eds.: J. Jiménez-Barbero, T. Peters), Wiley-VCH, Weinheim, **2002**.
[14] N. L. Allinger, Y. H. Yuh, J. H. Lii, *J. Am. Chem. Soc.* **1989**, *111*, 8551–8566.
[15] K. Bock, J. O. Duus, *J. Carbohydr. Chem.* **1994**, *13*, 513–543.
[16] D. Neuhaus, M. P. Williamson in *The Nuclear Overhauser Effect in Structural and Conformational Analysis*, VCH, Weinheim, **1989**.
[17] A. Poveda, J. L. Asensio, M. Martin-Pastor, J. Jiménez-Barbero, *J. Biomol. NMR* **1997**, *10*, 29–43.
[18] J. L. Asensio, F. J. Cañada, A. Garcia-Herrero, M. T. Murillo, A. Fernandez-Mayoralas, B. A. Johns, J. Kozak, Z. Zhu, C. R. Johnson, J. Jiménez-Barbero, *J. Am. Chem. Soc.* **1999**, *121*, 11318–11329.
[19] R. T. Lee, H.-J. Gabius, Y. C. Lee, *J. Biol. Chem.* **1992**, *267*, 23722–23727.
[20] M. Mayer, B. Meyer, *J. Am. Chem. Soc.* **2001**, *123*, 6108–6117.
[21] J. Angulo, B. Langpap, A. Blume, T. Biet, B. Meyer, N. R. Krishna, H. Peters, M. M. Palcic, T. Peters, *J. Am. Chem. Soc.* **2006**, *128*, 13529–13538.
[22] M. Jiménez, S. André, H.-C. Siebert, H.-J. Gabius, D. Solís, *Glycobiology* **2006**, *16*, 926–937.
[23] M. Jiménez, S. André, C. Barillari, A. Romero, D. Rognan, H.-J. Gabius, D. Solís, *FEBS Lett.* **2008**, *582*, 2309–2312.
[24] a) J. L. Asensio, J. F. Espinosa, H. Dietrich, F. J. Cañada, R. R. Schmidt, M. Martin-Lomas, S. André, H.-J. Gabius, J. Jiménez-Barbero, *J. Am. Chem. Soc.* **1999**, *121*, 8995–9000; b) I. Pelletier, T. Hashidate, T. Urashima, N. Nishi, T. Nakamura, M. Futai, Y. Arata, K.-i. Kasai, M. Hirashima, J. Hirabayashi, S. Sato, *J. Biol. Chem.* **2003**, *278*, 22223–22230; c) H. Lahm, S. André, A. Hoeflich, H. Kaltner, H.-C. Siebert, B. Sordat, C.-W. von der Lieth, E. Wolf, H.-J. Gabius, *Glycoconjugate J.* **2004**, *20*, 227–238.
[25] *Maestro, A powerful, all-purpose molecular modelling environment*, Schrodinger LLC, **2005**.
[26] W. C. Still, A. Tempzyk, R. Hawley, T. Hendrickson, *J. Am. Chem. Soc.* **1990**, *112*, 6127–6129.
[27] M. Martin-Pastor, J. L. Asensio, J. Jiménez-Barbero, *Int. J. Biol. Macromol.* **1995**, *17*, 137–148.
[28] J. W. Keepers, T. L. James, *J. Magn. Reson.* **1984**, *57*, 404–426.
[29] a) H.-J. Gabius, *Anal. Biochem.* **1990**, *189*, 91–94; b) H.-J. Gabius, H. Walzel, S. S. Joshi, J. Kruip, S. Kojima, V. Gerke, H. Kratzin, S. Gabius, *Anticancer Res.* **1992**, *12*, 669–676; c) J. M. Alonso-Plaza, M. A. Canales, M. A. Jiménez, J. L. Roldán, A. Garcia-Herrero, L. Iturrino, J. L. Asensio, F. J. Cañada, A. Romero, H.-C. Siebert, S. André, D. Solís, H.-J. Gabius, J. Jiménez-Barbero, *Biochim. Biophys. Acta Gen. Subj.* **2001**, *1568*, 225–236; d) H.-J. Gabius, F. Darro, M. Remmelink, S. André, J. Kopitz, A. Danguy, S. Gabius, I. Salmon, R. Kiss, *Cancer Invest.* **2001**, *19*, 114–126; e) J. C. Manning, K. Seyrek, H. Kaltner, S. André, F. Sinowatz, H.-J. Gabius, *Histol. Histopathol.* **2004**, *19*, 1043–1060; f) V. García-Aparicio, M. Sollogoub, Y. Blériot, V. Colline, S. André, J. L. Asensio, F. J. Cañada, H.-J. Gabius, P. Sinaÿ, J. Jiménez-Barbero, *Carbohydr. Res.* **2007**, *342*, 1918–1928; g) L. He, S. André, V. M. Garamus, H.-C. Siebert, C. Chi, B. Niemeyer, H.-J. Gabius, *Glycoconjugate J.* **2009**, *26*, 111–116.
[30] For further recent examples in the carbohydrate field, see: a) R. S. Houliston, N. Yuki, T. Hirama, N. H. Khieu, J.-R. Brisson, M. Gilbert, H. C. Jarrell, *Biochemistry* **2007**, *46*, 36–44; b) T. Haselhorst, H. Blanchard, M. Frank, M. J. Kraschnefski, M. J. Kiefel, A. J. Szyczew, J. C. Dyason, F. Fleming, G. Holloway, B. S. Coulson, M. von Itzstein, *Glycobiology* **2007**, *17*, 68–81.
[31] K. Stott, J. Stonehouse, J. Keeler, T.-L. Hwang, A. J. Shaka, *J. Am. Chem. Soc.* **1995**, *117*, 4199–4200.
[32] a) G. M. Morris, D. S. Goodsell, R. S. Halliday, R. Huey, W. E. Hart, R. K. Belew, A. J. Olson, *J. Comput. Chem.* **1998**, *19*, 1639–1647; b) M. Kolympadi, M. Fontanella, C. Venturi, S. André, H.-J. Gabius, J. Jiménez-Barbero, P. Vogel, *Chem. Eur. J.* **2009**, *15*, 2861–2873.

Received: April 23, 2009
Published online: September 11, 2009

Conclusions

and general remarks.

In summary, during my PhD, thanks to structure-based design we developed a potent biotin probe to bind matrix metalloproteinases for possible application *in vitro* and *in vivo*. The enzymatic assay demonstrated a nanomolar to low micromolar (MMP-1) affinity of our BTI **4** not only for MMP-12 but also for all the MMPs investigated. Furthermore, the evolution of the ^{15}N-^{1}H HSQC spectra upon the addition of unlabeled avidin to solution of ^{15}N MMP-12 clearly showed that the fourteen-member spacer used to link the biotin unit to carboxylic aryl sulfonamide inhibitor **1** ensures the simultaneous binding of the two proteins without permitting large interprotein mobility. SPR analyses clearly showed the ability of **4** to bind the functional active enzyme MMP-12 and avidin side-by-side. This simultaneous interaction did not affect negatively the nanomolar affinity of inhibitor **4** for MMP-12, given that the SPR data nicely reproduced the fluorimetric values measured for the BTI **4**-MMP-12 complex.

We developed a new drug delivery system for the Dry-Eye Syndrome (DES), a pathology affecting a significant percentage of the population, especially people older than 40 years of age. We introduce on a appropriate carrier (in our case different PAMAM dendrimers) a broad-spectrum inhibitor of matrix metalloproteinases, in order to inhibit the activity of MMPs that are deeply implicated in the corneal damage that occurs in consequence of DES. Our drug delivery systems should be able to sustain the drug release and to remain in the vicinity of the FOTE (Front Of The Eye) for a more prolonged period of time with respect to the inhibitor itself.

We designed and synthesized a new water-soluble inhibitor that could be easily prepared on a multigram scale and presented a very good affinity for MMP-7, that it is one of the matrix metalloproteinases that has a critical role in tumour invasion, and is often expressed in gastrointestinal cancers. Moreover, it presents a fundamental role in the early tumor development. For these reasons compound **52** will be tested against colon cancer, in collaboration with Dr. L. Vannucci of the University of Prague.

Finally, we reported a family of new high-affinity MMP inhibitors that was designed and synthesized by using a conceptually novel strategy whereby a glycosidic residue was introduced on a suitable MMPI. These new carbohydrate-based inhibitors, unprecedented in the NNGH family, display nanomolar affinity toward several MMPs and do not appreciably interact with HSA. These inhibitors are a prototype structure that open the way to the design of a new class of highly effective MMPIs. Moreover we had synthesized and tested a new group of high affinity, low molecular weight MMPIs. These inhibitors presented an hydrophilic residue, that has been appropriately inserted to the sulfonamidic nitrogen in order to modulate bioavailability, selectivity and affinity of our compounds.

Experimental section

Abbreviations

Ac:	Acetyl
AcOH:	Acetic acid
Bn:	Benzyl
BnBr	Benzyl bromide
DBU:	1,8-Diazabicyclo[5.4.0]undec-7-ene
DIAD:	Di*iso*propyl azodicarboxylate
DMAP:	4-(Dimethylamino)pyridine
DMF:	N,N-dimethylformamide
DMSO:	Dimethylsulfoxide
Et_2O:	Diethyl ether
Et_3N:	Triethylamine
EtOH:	Ethanol
EtOAc:	Ethyl acetate
i-PrOH:	*Iso*propanol
MsCl	Methanesulfonyl chloride
MeOH:	Methanol
NMM	N-methyl morpholine
Py:	Pyridine
PPh_3:	Triphenylphosphine
TBAI:	Tetrabutylammonium iodide
TBAF:	Tetrabutylammonium fluoride
TBDMSOTf:	*tert*-butyldimethylsilyl trifluoromethanesulfonate
THF:	Tetrahydrofuran
TFA:	Trifluoroacetic acid

General Remarks.

All reagents were commercially available and used as received. All reactions, when anhydrous conditions were needed, were performed under nitrogen atmosphere. Dry solvents were prepared before use.

SPR data were obtained using a BioRad ProteOn XPR36. Melting points were uncorrected and were recorded on Melting Point Büchi 510. Optical rotations were determined with Jasco DIP-370 polarimeter. Elemental analysis were performed with Elementar analyzer 2400 serie II Perkin-Elmer NMR spectra were recorded using a Varian Gemini 200, Varian Mercury 400 spectrometer, and a Brucker 700 spectrometer (HSQC). Notations s, d, t, q, m, b, a indicate respectively singlet, doublet, triplet, quadruplet, multiplet, broad, apparent.

Protein Cloning, Expression and Purification

The cDNA encoding the catalytic domain of the MMP-12 (G106-G263) was cloned into the pET21a (Novagen) using the restriction enzymes *Nde I* and *Xho I* (New England BioLabs). One additional Methionine at position 105 was present in the final expression product. The expression vector encoding for the protein was transformed into competent *Escherichia coli* BL21 (DE3) Gold strain and colonies were selected for Ampicillin resistance. Bacteria were grown in LB medium containing 50 µg/mL Ampicillin in a shaker flask at 37°C. Protein expression was induced with 0.5 mM IPTG at an OD600 = 0.6 and cell growth was continued for a further 5 hours. For expression of ^{15}N and ^{13}C-enriched protein, the bacteria were grown in minimal medium containing ^{15}N enriched $(NH_4)_2SO_4$ and ^{13}C enriched glucose (Cambridge Isotope Laboratories). Cells were harvested by centrifugation, resuspended in a buffer containing 25% Sucrose, 50 mM Tris-HCl (pH 8), 0.1 M NaCl, 0.2 M EDTA, 1 mM DTT. 5-10 mg. Lysozyme was added to the resulting suspension and stirred for 15-20 min. at 4°C. A buffer containing 2% Triton, 50 mM Tris-HCl (pH 8), 0.1 M NaCl, 0.2 M EDTA, 1 mM DTT was added and sonicated (7-8 30-seconds cycles) and centrifuged at 40000 rpm for 20 min. at 4°C. The pellets were washed with 50 mM Tris, 5 mM EDTA, 1 mM DTT (pH 8) and centrifuged. The resulting inclusion bodies were solublized in 8 M Urea, 20 mM Sodium Acetate (pH 5). The insoluble material was removed by centrifuging at 9000 rpm for 10 min. Protein molecular weight and purity was checked on 15% Gel by SDS-PAGE.

Protein was purified with Ion Exchange chromatography using HiTrap SP column using a gradient of NaCl up to 350mM (6 M Urea, 20 mM Sodium Acetate, pH 5). The purified protein was refolded by serial dilution method. The protein was diluted to a final concentration of 0.10 mg/mL in 4 M Urea, 20 mM Tris-HCl, 10 mM $CaCl_2$, 0.1 mM $ZnCl_2$, 0.3 M NaCl (pH 7.2), dialysed overnight

against same buffer (4 M Urea, 20 mM Tris-HCl, pH 7.2, 10 mM $CaCl_2$, 0.1mM $ZnCl_2$, 0.3M NaCl) successively followed by two steps with Buffer B (2 M Urea, 20 mM Tris pH 7.2, 10 mM $CaCl_2$, 0.1 mM $ZnCl_2$, 0.3 M NaCl) for 8 hours, then finally 3 step of 8 hours each with Buffer C (20 mM Tris pH 7.2, 10 mM $CaCl_2$, 0.1mM $ZnCl_2$, 0.3M NaCl,). The protein solution was concentrated up to 5 ml and purified by size exclusion chromatography using High Load™ 16/60 Superdex™ 75 (Amersham Biosciences) and eluted with 20 mM Tris pH 7.2, 10 mM $CaCl_2$, 0.1 mM $ZnCl_2$, 0.3 M NaCl and 0.2 M AHA. The eluted fractions were checked for purity on 15% Gel by SDS-PAGE and elution fractions containing protein were pooled and concentrated.

Crystallization, Data Collection and X-ray Structure Determination

Crystals of human MMP-12, already containing AHA from the refolding process, grew at 20° C from a 0.1 M Tris-HCl, 30% PEG 8000, 200 mM AHA, solution at pH 8.0 using the vapor diffusion technique. The final protein concentration was about 14 mg/mL.

The complexes have been obtained through soaking MMP-12-AHA crystals with a solution containing the inhibitor itself.

The data were measured in-house, using a PX-Ultra copper sealed tube source (Oxford Diffraction). All the datasets were collected at 100 K and the crystals used for data collection were cryo-cooled without any cryo-protectant treatment. The crystals of all complexes had a mosaicity ranging from 0.6° to 0.8° and diffracted to a maximum resolution of 1.7 Å. All the soaked adducts crystallize in the C2 space group with one molecule in the asymmetric unit.

The data were processed in all cases using the program MOSFLM [1] and scaled using the program SCALA [2] with the TAILS and SECONDARY corrections on (the latter restrained with a TIE SURFACE command) to achieve an empirical absorption correction. Table 1 shows the data collection and processing statistics for all datasets.

The structures of the all adducts were solved using the molecular replacement technique; the model used was that of a molecule of human MMP-12 (1Y93) from where the inhibitor, all water molecules and ions were omitted. The correct orientation and translation of the molecule within the crystallographic unit cell was determined with standard Patterson search techniques [3;4] as implemented in the program MOLREP [5;6]. The refinement was carried out using REFMAC [7] and for the metal ions anisotropic B-factors were also refined. In between the refinement cycles the models were subjected to manual rebuilding by using XtalView [8]. The same program has been used to fit the two inhibitors in the electron density. Water molecules have been added by using the standard procedures within the ARP/wARP suite [9]. The stereochemical quality of the refined models was

assessed using the program Procheck [10]. The Ramachandran plot for all structures is of very good quality.

Table 12. X-ray data collection and refinement statistics.

	1	**2**
Space group	C2	
Cell dimensions (Å, °)	a= 51.18 b= 60.55 c= 54.43 β = 115.90	a= 51.15 b= 60.58 c= 54.38 β = 115.76
Resolution (Å)	30.2 – 1.9	30.2 – 1.9
Unique reflections	11585 (1553)	11350 (1226)
Overall completeness (%)	98.0 (91.3)	95.7 (71.6)
R_{sym}	0.06 (0.17)	0.07 (0.17)
Multiplicity	6.5 (3.4)	5.2 (2.0)
I/(σI)	11.2 (4.6)	12.2 (5.2)
B-factor from Wilson plot ($Å^2$)	8.73	7.87
R_{cryst} / R_{free}	0.16 / 0.20	0.22 / 0.27
Protein atoms	1238	1238
Ions	5	5
Ligand atoms	23	17
Water molecules	163	123
RMSD bonds (Å)	0.01	0.02
RMSD angles (°)	1.61	2.30
Average B-factor ($Å^2$)	9.04	6.48

Fluorimetric Assays

To assess the binding properties of compounds **1, 2**, **4** and **10** their abilities to inhibit the hydrolysis of fluorescence-quenched peptide substrate Mca-Pro-Leu-Gly-Leu-Dpa-Ala-Arg-NH_2 (Biomol, Inc.) [11] were tested. The analyses were carried out at 298 K in 50 mM HEPES buffer, containing 10 mM $CaCl_2$, 0.05% Brij-35, at pH 7, using 1 nM of MMP catalytic domains and 1 µM of peptide. The experiments were performed with peptide concentration much lower than *K*i. The fluorescence ($excitation_{max}$ 328 nm; $emission_{max}$ 393 nm) was measured for 3 minutes after the addition of the substrate using a Varian Eclipse fluorimeter. Fitting of rates as a function of inhibitor concentration provided the *K*i values.

Synthesis of compound 1.

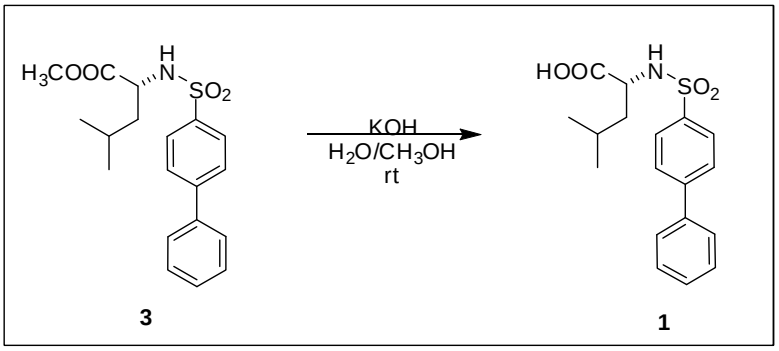

To a solution of **3** (500 mg, 1.38 mmol) in 15 mL of CH_3OH a solution of KOH (1.00 g, 17.90 mmol) in 7 mL of H_2O was added. After 72 h at room temperature, HCl (36%, H_2O) was added (pH=1); the precipitate formed was filtered and washed several times with water to give **1 (**463mg, 97%) as a crystalline white solid.

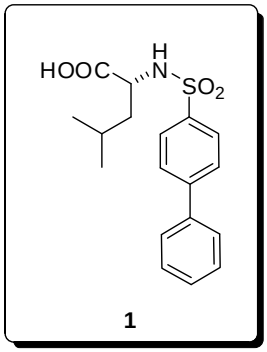

M.p. 129-130 °C. **$[\alpha]^{25}_D$** -15.6 (c 1.13, CH_3OH). **Anal.** Calcd for $C_{18}H_{21}NO_4S$: C, 62.23; H, 6.09; N, 4.03. Found: C, 61.61; H, 6.10; N, 3.99. **^{1}H NMR** (200 MHz, $CDCl_3$); δ 7.93-7.88 (part AA' of an AA'MM' system, J_{AM} = 8.4 Hz, 2H), 7.79-7.75 (part MM' of an AA'MM' system, J_{AM} = 8.4 Hz, 2H), 7.68-7.34 (m, 5H), 3.90-3.82 (m, 1H), 1.81-1.68 (m, 1H), 1.54-1.46 (m, 2H), 0.90 (d, *J* = 7.0 Hz, 3H), 0.83 (d, *J* = 6.2 Hz, 3H) ppm. **^{13}C NMR** (50 MHz, CD_3OD): δ 173.97, 145.04, 139.34, 139.17, 128.62, 127.97, 127.33; 126.94; 126.79, 54.46, 41.84, 24.31, 22.02, 20.44 ppm.

Synthesis of compound 2.

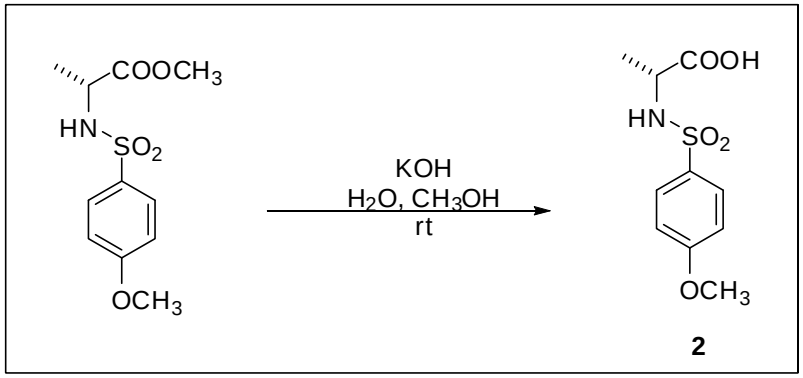

To a solution of (R)-methyl 2-(4-methoxyphenylsulfonamido)propanoate (500 mg, 1.18 mmol) in 1 mL of CH_3OH a solution of KOH (1M, H_2O; 304 mg, 5.43 mmol) was added. After 72 h, HCl (25%, H_2O) was added (pH=1). The CH_3OH was removed in vacuo and the acqueous phase was extracted with AcOEt (2 x). The organic layer was dried over anhydrous Na_2SO_4 and the solvent was removed in vacuo to give **2 (**426 mg, 90%) as a white solid.

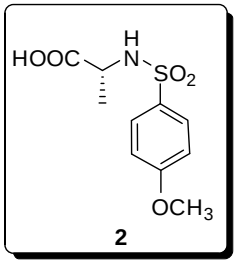

M.p. 90-92 °C. **$[\alpha]^{25}_D$** +17.0 (c 0.34, CH_3OH). **Anal.** Calcd for $C_{10}H_{13}NO_5S$: C, 46.32; H, 5.05; 5.40. Found; C, 46.67; H, 5.51; N, 5.77. **^{1}H NMR** (200 MHz, CD_3OD) δ 7.83-7.78 (part AA' of an AA'MM' system, J_{AM} = 8.8 Hz, 2H), 7.08-7.04 (part MM' of an AA'MM' system, J_{AM} = 8.8 Hz, 2H), 3.88 (s, 3H), 3.62 (q, *J* = 7.4 Hz, 1H), 1.31 (d, *J* = 7.4 Hz, 3H) ppm. **^{13}C NMR** (50 MHz, CD_3OD) 176.68, 162.81, 132.02, 128.82, 113.81, 54.91, 52.54, 19.08 ppm.

Synthesis of compound 3.

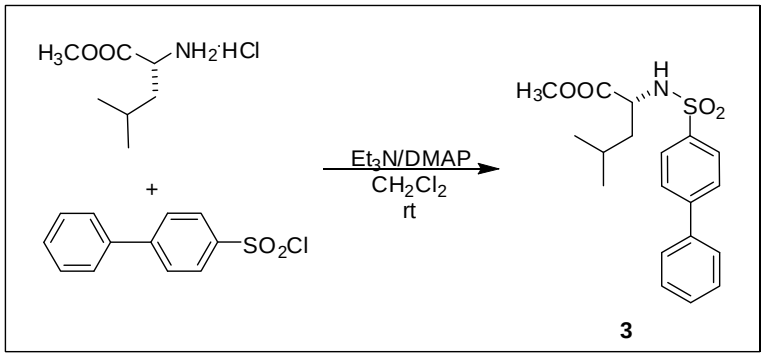

A solution of D-leucine methyl ester hydrochloride (3.00 g, 16.5 mmol) in CH_2Cl_2 (80 mL) was cooled to 0°C, triethylamine (6.85 mL, 49.5 mmol) and a catalytic amount of DMAP were added. The mixture was stirred at room temperature for 10 min, then biphenyl-4-sulfonyl chloride (4.17 g, 16.5 mmol) was added. The reaction was stirred at room temperature for 4.5 h. The mixture was

neutralized with HCl (3%, H_2O) and washed with brine (3x). The organic layer was dried over anhydrous Na_2SO_4 and the solvent was removed in vacuo to give 8.00 g of a pale yellow solid. The crude material was purified by flash chromatography on silica gel (petroleum ether/$CHCl_3$/EtOAc 2:5:1) to give **3** as a white solid (5.38 g, 90% yield).

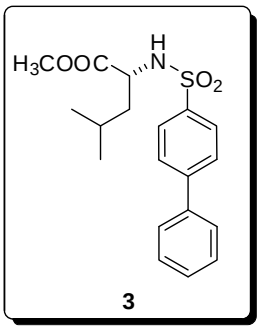

3

M.p. 135-137 °C. **$[\alpha]^{25}_D$** +1.85 (c 0.87, $CHCl_3$). **Anal.** for $C_{19}H_{23}NO_4S$ Calcd: C, 63.13; H, 6.41; N, 3.88. Found: C, 63.23; H, 6.11; N, 3.84. **^{1}H NMR** (200 MHz, $CDCl_3$) δ 7.93-7.89 (part AA' of an AA'MM' system, J_{AM} = 8.4 Hz, 2H), 7.73-7.69 (part MM' of an AA'MM' system, J_{AM} = 8.4 Hz, 2H), 7.64-7.44 (m, 5H), 5.07 (d, *J* = 10.2 Hz, 1H), 4.05-3.93 (m, 1H), 3.43 (s, 3H), 1.89-1.72 (m, 1H), 1.59-1.48 (m, 2H), 0.93 (d, *J* = 3.2 Hz, 3H); 0.90 (d, *J* = 2.8 Hz, 3H) ppm. **^{13}C NMR** (50 MHz,$CDCl_3$): 172.49, 145.64, 139.09, 138.03, 129.02, 128.49, 127.80, 127.47, 127.20, 54.52, 52.43, 42.52, 24.51, 22.90, 21.63 ppm.

Synthesis of compound 4: (2*R*)-4-Methyl-2-(N-(((5-((4*S*)-2-oxohexahydro-1H-thieno[3,4-d]imidazol-4yl) pentanamido) methylamino)methyl)biphenyl-4-ylsulfonamido)pentanoic acid.

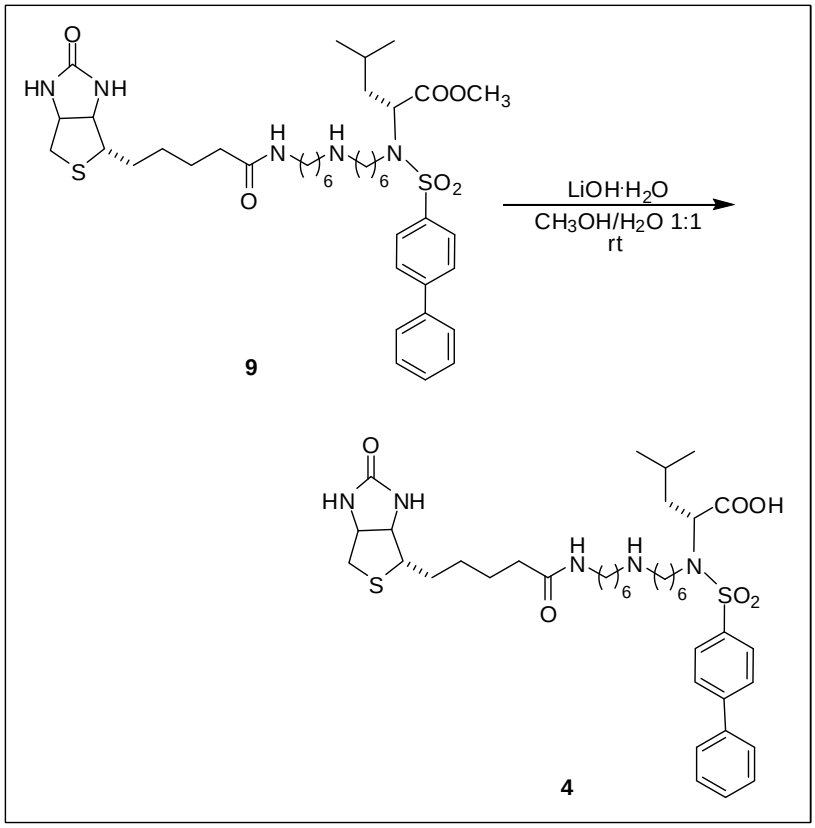

9

4

To a solution of **9** (143 mg, 0.18 mmol) in 2.80 mL of THF/H_2O 1:1, $LiOH{\cdot}H_2O$ (15.1 mg, 0.36 mmol) was added and the mixture was stirred for 6 h at rt, then H_3PO_4 1M was added (pH=5); the solvent was removed in vacuum and the solution was lyophilized. The solid obtained was re-dissolved in AcCN/H_2O 3:1 and purified by a reversed-phase semi-preparative HPLC to give of compound **4** (76.0 mg, 55%).

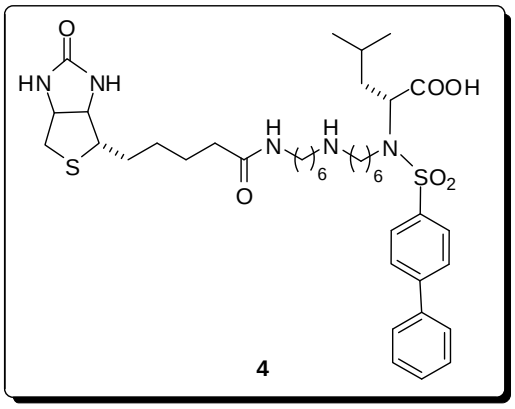

4

M.p.: 119-121 °C. **[α]$^{25}_D$** +38.19 (c 0.33, CH_3OH). **ESI-MS** $[M+H]^+$ calcd 772.41. Found 772.54. **^{1}H NMR (**400 MHz, CD_3OD) δ 7.96-7.38 (m, 9H), 4.49-4.46 (part A of an ABMN system, J_{AB} = 8.0 Hz, J_{AM} = 4.4 Hz, 1H), 4.41-4.37 (m, 1H), 4.30-4.27 (part B of an ABX system, J_{AB} = 8.0 Hz, J_{BX} = 4.6 Hz, 1H), 3.49-3.38 (m, 1H), 3.29-3.14 (m, 4H), 2.93-2.88 (m, 5H), 2.71-2.68 (part N of an AMN system, J_{MN} = 12.8 Hz, 1 H), 2.19 (t, *J* = 7.2 Hz, 2H), 1.88-1.22 (m, 25H), 0.93 (at, *J* = 6.4 Hz, 6H) ppm. **^{13}C NMR** (50 MHz, CD_3OD) δ 176.04, 174.39, 164.51, 144.75, 139.22, 128.64, 127.94, 127.79, 126.80, 126.76, 62.07, 61.02, 60.31, 55.72, 47.51, 45.04, 40.31, 39.77, 38.79, 35.54, 30.38, 28.96, 28.51, 28.27, 26.12, 25.92, 25.68, 25.56, 24.81, 22.17, 21.16.

Synthesis of compound 6: tert-Butyl(5-((4*S*)-2-oxohexahydro-1H-thieno[3,4-d]imidazol-4-yl) pentanamido) methylcarbamate.

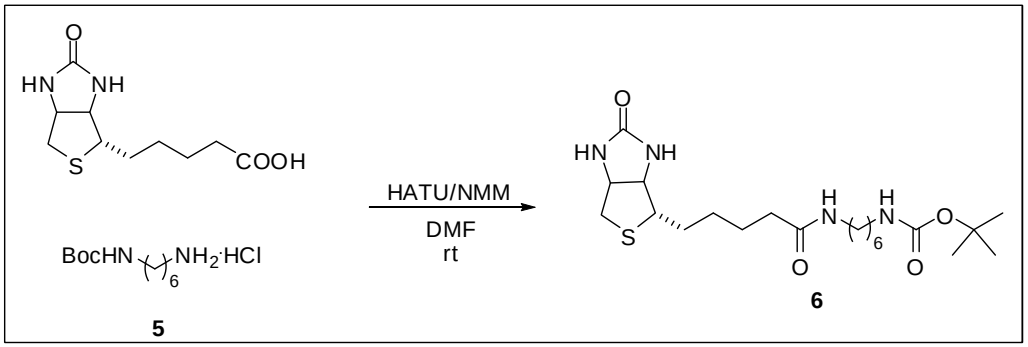

5 **6**

A suspension of N-Boc-1,6-diaminohexane hydrochloride **5** (310 mg, 1.23 mmol) and NMM (0.14 mL, 1.23 mmol) in dry DMF (3 mL) was added to a slurry of D-biotin (300 mg, 1.23 mmol) and NMM (0.14 mL, 1.23 mmol) in dry DMF (10 mL) and the mixture was stirred at rt for 10 min. A solution of HATU (468 mg, 1.23 mmol) in dry DMF (3 mL) was added and the mixture was stirred for 3.5 h. The reaction mixture was diluited with 20 mL of CH_2Cl_2 and washed with water: the organic layer was dried over anhydrous Na_2SO_4 and the solvent was removed in vacuo to give a yellow pale

oil. Part of DMF was removed in vacuum to give 2.20 g of a yellow solid. The crude material was purified by flash column chromatography on silica gel (CH_2Cl_2/CH_3OH 6:1) to give **6** as a white solid (500 mg, 92% yield).

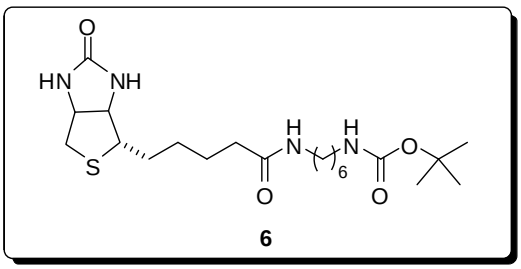

6

M.p. : 174-175 °C; **^{1}H NMR** (200 MHz, $CDCl_3$) δ 6.17-6.07 (m, 2H), 4.70-4.56 (m, 1H), 4.55-4.49 (part A of an ABMN system, J_{AB} = 8.0 Hz, J_{AM} = 4.4 Hz, 1H), 4.36-4.29 (part B of ABX system, J_{AB} = 8.0 Hz, J_{BX} = 4.6 Hz, 1H), 3.24-3.10 (m, 5H), 2.97-2.71 (part MN of an AMN system, J_{MN} = 12.4 Hz, J_{AM} = 4.4 Hz, 2H), 2.22 (t, *J* = 7.0 Hz, 2H), 1.48-1.25 (m, 23H) ppm. **^{13}C NMR** (50 MHz, $CDCl_3$) δ 173.80, 163.62, 155.91, 62.11, 60.56, 55.56, 40.56, 39.70, 35.65, 30.06, 29.87, 29.27, 28.61, 28.18, 28.09, 26.39, 26.25, 25.84 ppm.

Synthesis of compound 7: (5-((4*S*)-2-Oxohexahydro-1H-thieno[3,4-d]imidazol-4yl)pentanamido) methanaminium.

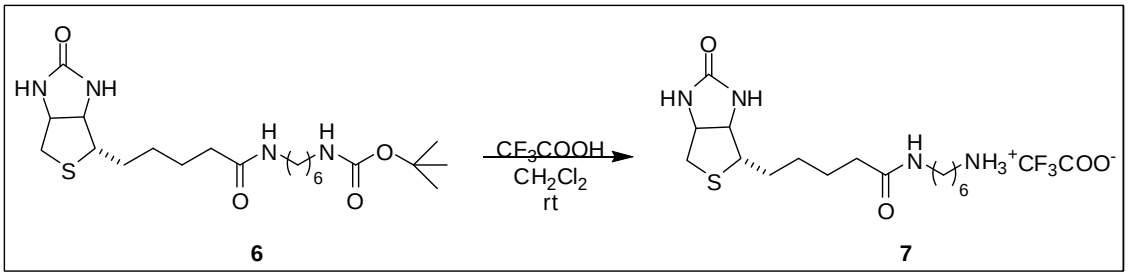

6 **7**

A solution of CF_3COOH (1.90 mL, 23.8 mmol) in dry CH_2Cl_2 (6.20 mL) was added to a suspension of **6** (480 mg, 1.08 mmol) in dry CH_2Cl_2 (4.6 mL). After 1.5 h, 10 mL of toluene were added and solvent was removed in vacuum to give pale yellow oil. The oil was repeatedly washed with CH_3OH and $CHCl_3$; the compound **7** (490 mg, >90%) so obtained was used without any further purification.

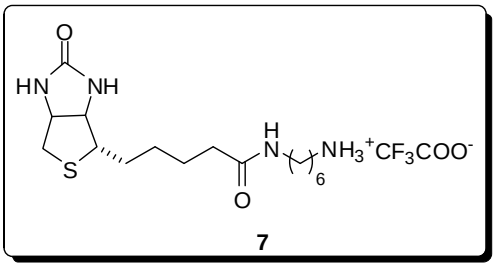

7

^{1}H-NMR (200 MHz, CD_3OD); δ 4.53-4.47 (part A of an ABMN system, J_{AB} = 8.0 Hz, 1H), 4.33-4.27 (part B of an ABX system, J_{AB} = 8.0 Hz, J_{BX} = 4.4 Hz, 1H), 3.23-3.14 (m, 3H), 3.00-2.87 (m, 5H), 2.73-2.67 (part M of an AMN system, J_{MN} = 12.4 Hz, 1H), 2.20 (t, *J* = 7.2 Hz, 2H), 1.72-1.40 (m, 12H) ppm. **^{13}C NMR** (50 MHz, CD_3OD): 174.45,

164.54, 159.90, 62.07, 60.32, 55.74, 39.77, 39.40, 38.79, 35.54, 28.87, 28.53, 28.27, 27.24, 26.12, 25.75, 25.69 ppm.

Synthesis of compound 8: *R*)-Methyl2-(N-(bromomethyl)biphenyl-4-ylsulfonamido)-4 methylpentanoate.

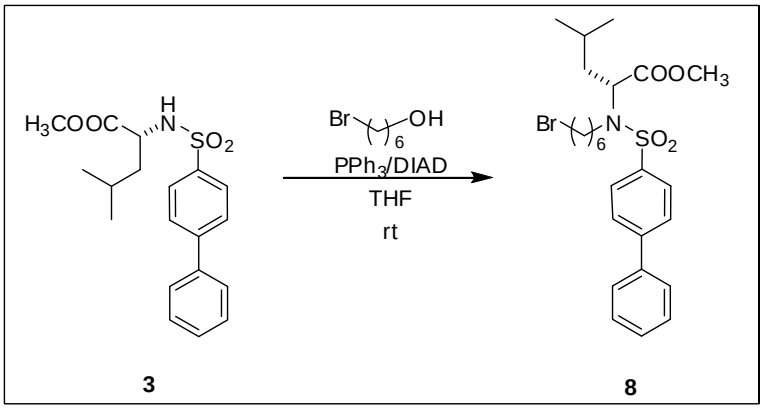

To a solution of **3** (600 mg, 1.66 mmol), 6-bromo-1-hexanol (450 mg, 2.49 mmol) and triphenilphosphine (872 mg, 3.32 mmol) in 17 mL of dry THF, 0.65 mL of DIAD (1.66 mmol) were added drop-wise, in 1 h. The reaction was stirred at rt for 43 h, and then the solvent was removed in vacuo to give yellow oil. After crystallization of the betainic side product (EtOAc/ciclohexane 1:8) the filtrate was concentrated in vacuum and the residue (3.20 g) was purified twice by flash column chromatography on silica gel (petroleum ether/EtOAc 6:1 then CH_2Cl_2) to give pure **8** as a white solid (515 mg, 60% yield).

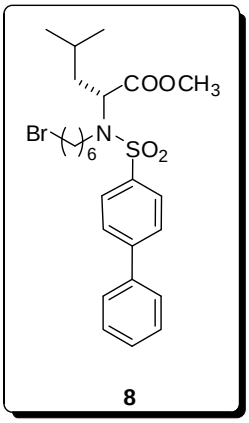

M.p.: 59-61 °C. **$[\alpha]^{25}_D$** +47.4 (c 1.13, $CHCl_3$). **ESI-MS** $[M+H]^+$ calcd 524.14. Found 524.11. **^{1}H NMR** (200 MHz, $CDCl_3$) δ 7.90-7.86 (part AA' of an AA'MM' system, J_{AM} = 8.8 Hz, 2H), 7.72-7.68 (part MM' of an AA'MM' system, J_{AM} = 8.8 Hz, 2H), 7.65-7.40 (m, 5H), 4.63-4.55 (dd, 1H, *J* = 5.6 Hz, *J* = 6.0 Hz), 3.46 (s, 3H), 3.40 (t, *J* = 6.8 Hz, 2H), 3.30-3.06 (m, 2H), 1.97-1.17 (m, 11H), 0.99-0.94 (m, 6H) ppm. **^{13}C NMR** (50 MHz, $CDCl_3$) δ 171.66, 145.27, 139.23, 138.26, 128.97, 128.38, 127.88, 127.26, 127.20, 58.09, 51.96, 45.95, 39.59, 33.86, 32.75, 31.19, 27.86, 26.36, 24.63, 22.99, 21.73 ppm.

Synthesis of compound 9: (2*R*)-Methyl-4-methyl-2-(*N*-(((5-((4*S*)-2-oxohexahydro-1*H*thieno[3,4-*d*]imidazol-4-yl)pentanamido)methylamino)methyl) biphenyl-4-ylsulfonamido)pentanoate.

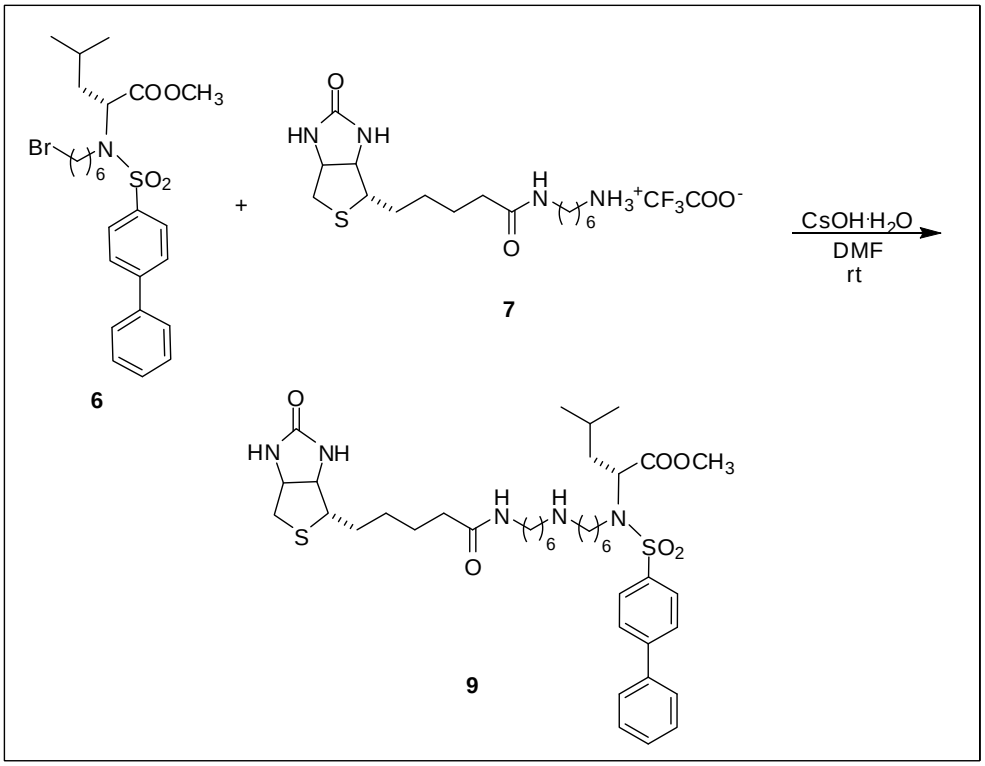

To a solution of **7** (236 mg, 0.69 mmol) in dry DMF (4 mL) were added 4 Å activated pellets molecular sieves (400 mg). The mixture was stirred at rt for 1 h. Cesium hydroxide monohydrate previously dried at 120 °C for 24 h (116 mg, 0.69 mmol) was added, and the solution was allowed to stir for 30 min. TBAI (250 mg, 0.69 mmol) and compoud **8** (360 mg, 0.69 mmol) was finally added and the mixture was stirred for 48 h. The crude material was purified by flash column chromatography on silica gel (CH_2Cl_2/CH_3OH 6:1) to give **9** (300 mg, 55%) as a pale yellow solid.

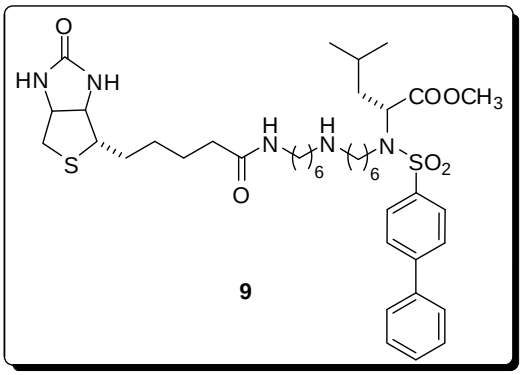

M.p.: 129-131 °C. **ESI-MS** $[M+H]^+$ calcd 786.42. Found 786.50. **^{1}H NMR** (200 MHz, CD_3OD) δ 7.91-7.41 (m, 9H), 4.58-4.48 (m, 2H), 4.34-4.28 (part B of an ABX system, J_{AB} = 7.8 Hz, J_{BX} = 4.4 Hz, 1H), 3.43 (s, 3H), 3.26-3.14 (m, 4H), 3.04-2.74 (m, 6H) , 2.21 (t, *J* = 7.0 Hz, 2H), 1.73-1.29 (m, 25H), 0.95 (ad, 6H, *J* = 5.4 Hz) ppm. **^{13}C NMR** (50 MHz, $CDCl_3$) δ 174.45, 171.45, 164.47, 145.45, 138.97, 138.03, 128.71, 128.15, 127.70, 127.05, 126.80, 62.07, 60.32, 58.13, 55.72, 51.14, 47.60, 45.71, 39.79, 39.26, 38.73, 35.54, 30.97, 28.94, 28.50, 28.27, 26.18, 26.06, 25.94, 25.84, 25.69, 24.42, 21.93, 20.58 ppm.

Synthesis of compound 10: (2*R*)-2-(4-Methoxy-N-(((5-((4*S*)-2-oxohexahydro-1H-thieno[3,4-d]imidazol-4yl)pentanamido)methylamino)methyl)phenylsulfonamido) propanoic acid.

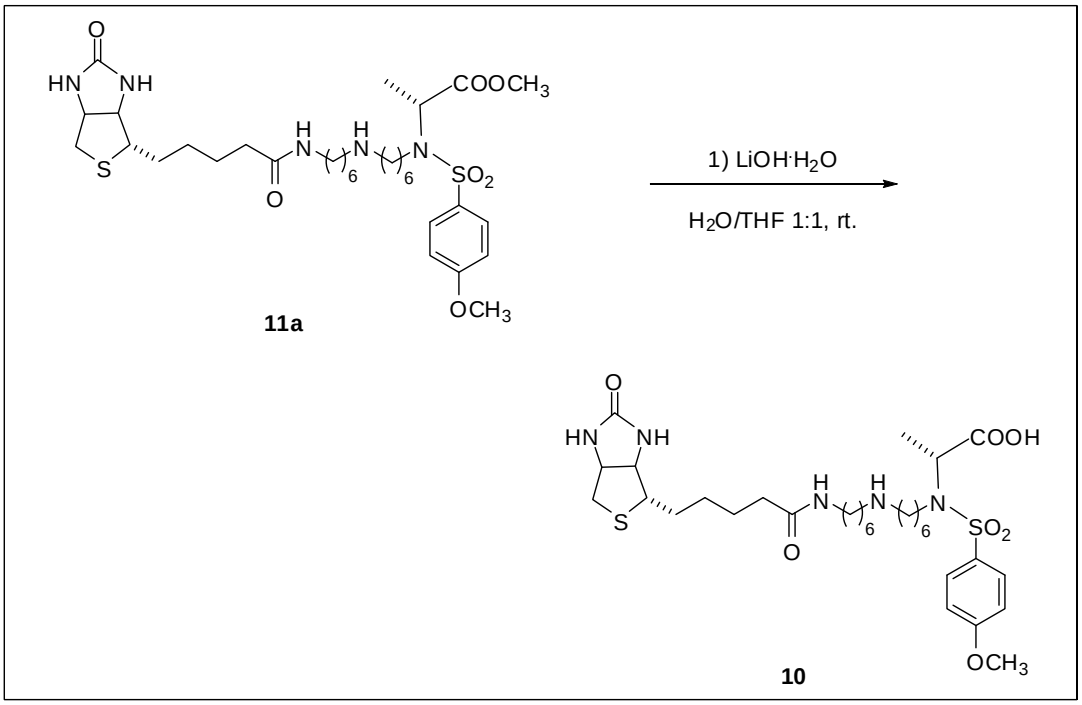

To a solution of **11a** (229 mg, 0.33 mmol) in 4.80 mL of CH_3OH/H_2O 1:1, $LiOH{\cdot}H_2O$ (28.0 mg, 0.66 mmol) was added and the mixture was stirred for 19 h at rt. A solution of H_3PO_4 (1M, H_2O) was added (pH=5), the solvent was removed in vacuum and the crude was lyophilized. The solid obtained was re-dissolved in AcCN/ H_2O 3:1 and purified by a reversed-phase semi-preparative HPLC to give compound **10** (53.0 mg, 23%) as white solid.

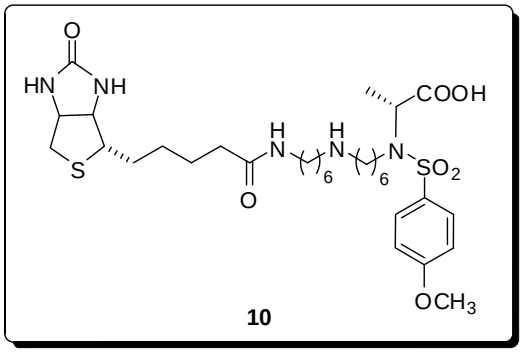

M.p. 93-94 °C. **ESI-MS** $[M+H]^+$ calcd 698.35. Found 698.30. **^{1}H NMR** (200 MHz, CD_3OD) δ 7.78-7.70 (part AA' of an AA'MM' system, J_{AM} = 9.2 Hz, 2H); 6.95-6.94 (part MM' of an AA'MM' system, J_{AM} = 9.2 Hz, 2H); 4.58-4.47 (m, 2H); 4.38-4.32 (part B of an ABX system, J_{AB} = 7.8 Hz, J_{BX} = 4.4 Hz, 1H); 3.88 (s, 3H); 3.55 (s, 3H); 3.26-3.14 (m, 5H); 3.03-2.87 (m, 5H); 2.72-2.69 (part N of an AMN system, J_{MN} = 12.6 Hz, 1 H); 2.20 (t, J = 7.0 Hz, 2H); 1.72-1.29 (m, 25 H) ppm. **^{13}C NMR** (50 MHz,CD_3OD) δ 173.27, 171.80, 163.50, 162.71, 131.39, 129.28, 114.03, 68.21, 61.99, 60.22, 55.72, 55.18, 52.49, 52.26, 45.45, 40.70, 38.06, 35.78, 30.84, 29.85, 28.94, 28.15, 28.07, 26.33, 26.25, 26.03, 25.80, 23.16, 16.83 ppm.

Synthesis of compound 11.

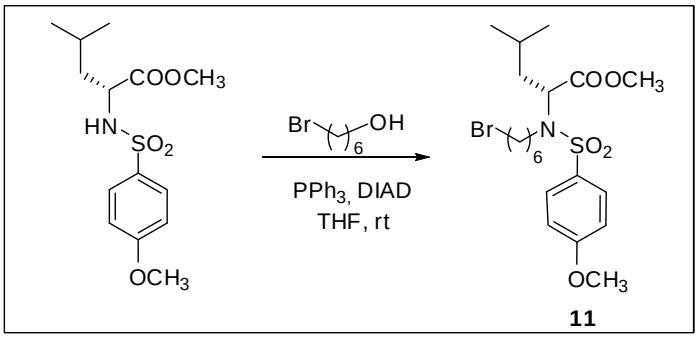

11

To a solution of (R)-methyl 2-(4-methoxyphenylsulfonamido)propanoate (1.00 g, 3.60 mmol), 6-bromo-1-hexanol (0.99 g, 3.60 mmol) and triphenilphosphine (1.93 g, 7.32 mmol) in 37 mL of dry THF, DIAD (1.44 mL, 7.32 mmol) were added dropwise in 1 h. The reaction was stirred at room temperature for 16.5 h, then the solvent was removed in vacuo to give 5.00 g of a yellow oil. After removal of crystalin betain (EtOAc/ciclohexane 1:8) the filtrate was concentrated in vacuo and the residue (4.10 g) was purified by flash chromatography on silica gel (CH_2Cl_2/CH_3OH 30:1) to give **11** (1.03 g, 64%) as a colourless oil.

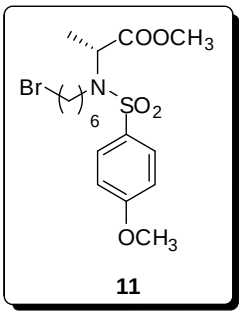

11

$[\alpha]^{25}_D$ +37.5 (c 0.41, $CHCl_3$). **Anal.** Calcd for $C_{17}H_{26}BrNO_5S$: C, 46.79; H, 6.01; N, 3.21. Found: C, 46.83; H, 5.84; N, 3.32. **^{1}H NMR** (200 MHz, $CDCl_3$); δ 7.78-7.73 (part AA' of an AA'MM' system, J_{AM} = 8.8 Hz, 2H), 6.98-6.94 (part MM' of an AA'MM' system, J_{AM} = 8.8 Hz, 2H), 4.62 (q, *J* = 7.0 Hz, 1H), 3.87 (s, 3H), 3.57 (s, 3H), 3.39 (t, *J* = 6.6 Hz, 2H), 3.31-3.01 (m, 2H), 1.90-1.21 (m, 8H), 1.41 (d, *J* = 7.0 Hz, 3H) ppm. **^{13}C NMR** (50 MHz, $CDCl_3$) δ 171.87, 162.63, 131.64, 129.32, 113.92, 55.71, 55.13, 52.25, 45.66, 33.92, 32.75, 30.85, 27.85, 26.21, 16.80 ppm.

Synthesis of compound 11a: (2*R*)-Methyl-2-(4-methoxy-*N*-(((5-((4*S*)-2-oxohexahydro-1*H*thieno[3,4-*d*]imidazol-4-yl)pentanamido) methylamino)methyl)phenyl sulfonamido)propanoate.

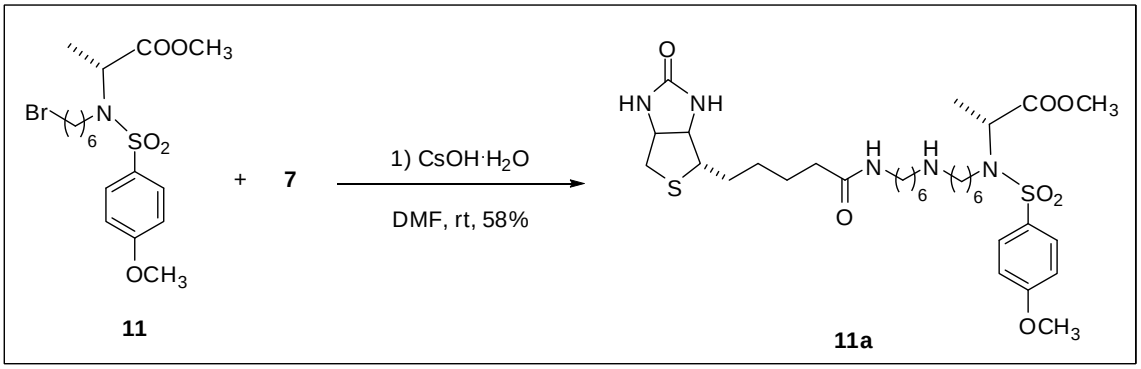

11 **11a**

To a solution of **7** (170 mg, 0.50 mmol) in dry DMF (2 mL) 4 Å activated pellets molecular sieves (280 mg) were added and the mixture was gently stirred at room temperature for 1 h. Cesium hydroxide monohydrate previously dried at 120 °C for 24 h (84 mg, 0.50 mmol) was added, and the reaction mixture was allowed to stir for 30 min. A solution of **11** (218 mg, 0.50 mmol) and TBAI (182 mg, 0.50 mmol) in DMF (1 mL) were finally added and the mixture was stirred for 48 h at room temperature. The crude material obtained was purified by flash chromatography on silica gel (CH_2Cl_2/CH_3OH 6:1) to give **11a** (200 mg, 58%) as a pale yellow solid.

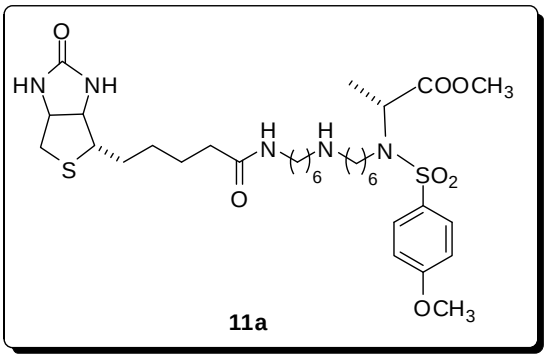

11a

M.p.: 93-94 °C. **ESI-MS** $[M+H]^+$ calcd 698.35. Found 698.30. **^{1}H NMR** (200 MHz, CD_3OD) δ 7.78-7.70 (part AA' of an AA'MM' system, J_{AM} = 9.2 Hz, 2H); 6.95-6.94 (part MM' of an AA'MM' system, J_{AM} = 9.2 Hz, 2H); 4.58-4.47 (m, 2H); 4.38-4.32 (part B of an ABX system, J_{AB} = 7.8 Hz, J_{BX} = 4.4 Hz, 1H); 3.88 (s, 3H); 3.55 (s, 3H); 3.26-3.14 (m, 5H); 3.03-2.87 (m, 5H); 2.72-2.69 (part N of an AMN system, J_{MN} = 12.6 Hz, 1 H); 2.20 (t, J = 7.0 Hz, 2H); 1.72-1.29 (m, 25 H) ppm. **^{13}C NMR** (50 MHz,CD_3OD) δ 173.27, 171.80, 163.50, 162.71, 131.39, 129.28, 114.03, 68.21, 61.99, 60.22, 55.72, 55.18, 52.49, 52.26, 45.45, 40.70, 38.06, 35.78, 30.84, 29.85, 28.94, 28.15, 28.07, 26.33, 26.25, 26.03, 25.80, 23.16, 16.83 ppm.

Synthesis of compound 12.

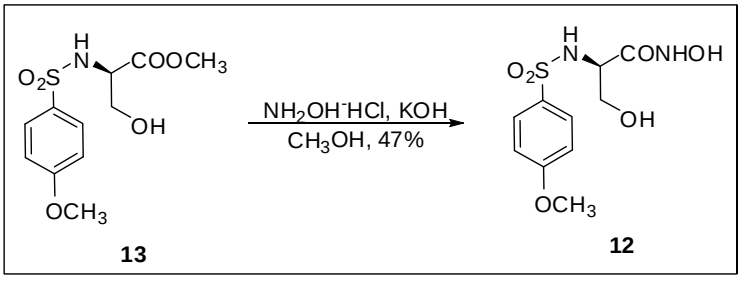

13 **12**

A suspension of KOH (78.0 mg, 1.40 mmol) and $NH_2OH{\cdot}HCl$ (77.0 mg, 1.12 mmol) in CH_3OH (1 mL) was stirred at room temperature for 1h, then a solution of **13** (80.0 mg, 0.28 mmol) in CH_3OH (1 mL) was added. The reaction mixture was stirred for 20 h then concentrated to dryness. The crude product was dissolved in EtOAc, washed with a mixture CH_3COOH/H_2O 1:1 and dried over Na_2SO_4. Concentration of the solvent under vacuum afford a crude product which was purified by flash column chromatography on silica gel (CH_2Cl_2/CH_3OH 6:1) to afford **12** (38.0 mg, 47%) as a pale yellow solid.

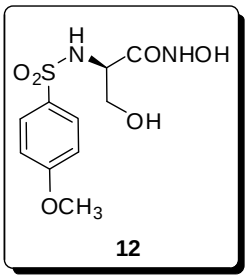

12

M.p.: 134-136 °C. **[α]$^{25}_{D}$** -22.1 (c 0.24, CH_3OH). **Anal.** for $C_{10}H_{14}N_2O_6S$ calcd: C, 41.37; H, 4.86; N, 9.65. Found: C, 40.94; H, 4.92; N, 9.12. **^{1}H NMR** (200MHz, CD_3OD): δ 7.83-7.81 (AA' part of an AA'MM' system, J_{AM} = 9.2 Hz, 2H), 7.09-7.07 (MM' part of an AA'MM' system, J_{AM} = 9.2 Hz, 2H), 3.90 (s, 3H), 3.72-3.69 (X part of an ABX system, J_{XA} = 2.8 Hz, J_{XB} = 3.4 Hz, 1H), 3.61-3.57 (A part of an ABX system, J_{AX} = 2.6 Hz, J_{AB} = 5.6 Hz, 1H), 3.56-3.53 (B part of an ABX system, J_{BX} = 3.4 Hz, J_{AB} = 5.6 Hz, 1H). **^{13}C NMR** (50MHz, CD_3OD): δ 168.7, 164.5, 133.2, 130.2, 115.2, 63.3, 57.6, 56.1.

Synthesis of compound 13.

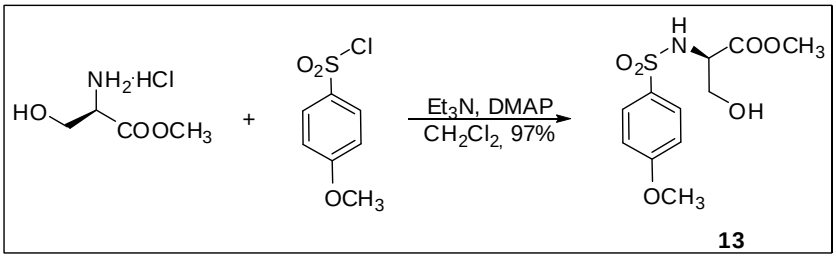

13

To a stirred suspension of **61** (1.00 g, 6.42 mmol) in CH_2Cl_2 (35 mL) 2.66 mL of NEt_3 (19.3 mmol) were added at 0°C. The suspension was stirred at room temperature for 30', cooled to 0°C then *para*-toluen sulphonyl chloride (1.33 g, 6.42 mmol) and DMAP (catalytic amount) were added. The reaction mixture was stirred at room temperature for 3 h then diluted with CH_2Cl_2. The mixture was neutralized with HCl (3%, H_2O) and washed with brine (3x). The organic phase was dried over Na_2SO_4 and the solvent was removed in vacuum. The crude product was used without further purification to afford **13** (1.80 g, 97%) as a pale yellow solid.

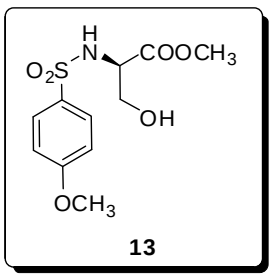

13

M.p.: 93-95 °C. **[α]$^{25}_{D}$** -8.38 (c 0.37, $CHCl_3$). **Anal.** for $C_{11}H_{15}NO_6S$ calcd: C, 45.67; H, 5.23; N, 4.84. Found: C, 46.07; H, 5.50; N, 4.90. **^{1}H NMR** (200MHz, $CDCl_3$): δ 7.81-7.76 (AA' part of an AA'MM' system, J_{AM} = 8.8 Hz, 2H), 6.98-6.94 (MM' part of an AA'MM' system, J_{AM} = 8.8 Hz, 2H), 5.94 (d, J = 7.8 Hz, 1H), 4.00-3.83 (m, 3H). 3.84 (s, 3H), 3.59 (s, 3H), 2.95 (bs, 1H). **^{13}C NMR** (50MHz, $CDCl_3$): δ 170.0, 162.7, 130.6, 129.0, 113.9, 63.3, 57.3, 55.4, 52.6.

Synthesis of compound 14.

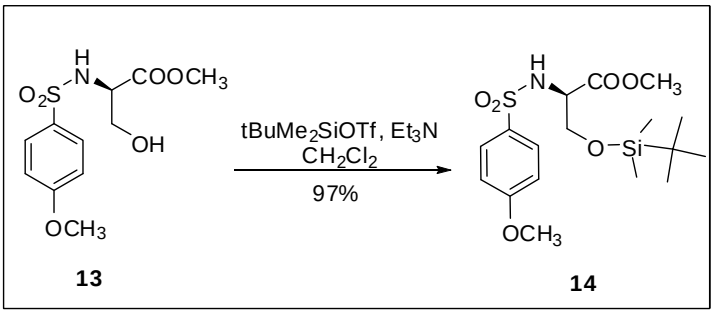

A solution of **13** (1.00 g, 3.46 mmol) in CH_2Cl_2 (15 mL) was cooled to 0°C. NEt_3 (0.72 mL, 5.19 mmol) and *t*$BuMe_2SiOTf$ (1.03 mL, 4.50 mmol) were added. The reaction mixture was heated to room temperature and stirred for 20 h, then diluted with CH_2Cl_2 (15 mL). The mixture was neutralized with HCl (3%, H_2O) and then was washed with brine (2x). The organic phase was dried over Na_2SO_4. Evaporation of solvent gave the crude product (1.40 g) which was purified by flash column chromatography on silica gel (petroleum ether/EtOAc 5:2) to afford **14** (1.35 g, 97%) as a colourless oil.

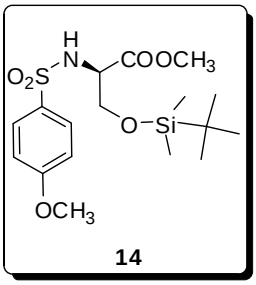

$[\alpha]^{25}_D$ -9.41 (c 0.17, $CHCl_3$). **Anal.** for $C_{17}H_{29}NO_6SSi$ calcd: C, 50.59; H, 7.24; N, 3.47. Found: C, 50.40; H, 7.52; N, 3.59. **^{1}H NMR** (200 MHz, $CDCl_3$): δ 7.78-7.73 (AA' part of an AA'MM' system, J_{AM} = 8.8 Hz, 2H), 6.95-6.91 (MM' part of an AA'MM' system, J_{AM} = 8.8 Hz, 2H), 5.39 (d, *J* = 9.0 Hz, 1H), 4.05-3.72 (m, 3H), 3.83 (s, 3H), 3.53 (s, 3H), 0.80 (s, 9H), -0.02 (s, 3H), -0.04 (s, 3H). **^{13}C NMR** (50 MHz, $CDCl_3$): δ 170.0, 162.8, 131.6, 129.2, 114.1, 64.6, 57.6, 55.7, 52.5, 25.8, 18.3, -5.3, -5.5.

Synthesis of compound 15

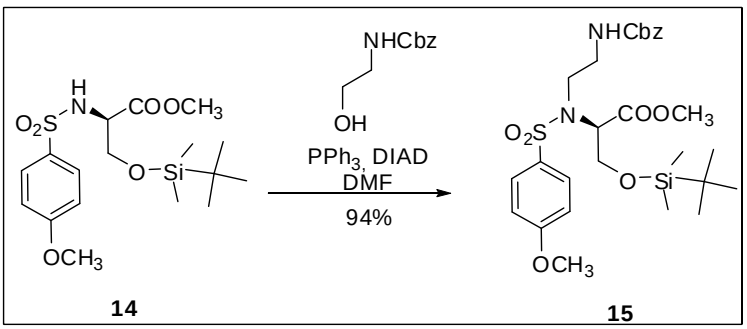

To a solution of **14** (555 mg, 1.38 mmol), N-Z-ethanolamine (322 mg, 1.65 mmol) and triphenilphosphine (434 mg, 1.65 mmol) in 13 mL of dry THF, 0.33 mL of DIAD (1.65 mmol) were

added drop-wise, in 1 h. The reaction was stirred at room temperature for 18 h, and then the solvent was removed in vacuo to give an yellow oil. After crystallization of the betainic side product (EtOAc/ciclohexane 1:8) the filtrate was concentrated in vacuum and the residue (1.80 g) was purified twice by flash column chromatography on silica gel ($CHCl_3$/EtOAc 15:1) to give pure **15** as an oil (750 mg, 94% yield).

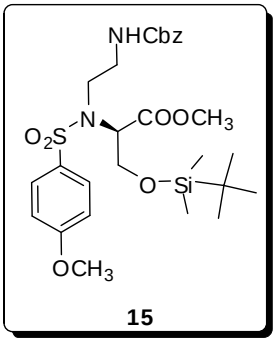

15

[α]$^{25}_{D}$ +21.8 (c 0.33, $CHCl_3$). **ESI-MS**. $[M+Na]^+$ calcd 603.22. Found 603.25. $[M+K]^+$ calcd 619.19. Found 619.17. **^{1}H NMR** (200 MHz, $CDCl_3$): δ 7.75-7.70 (AA' part of an AA'MM' system, J_{AM} = 8.8 Hz, 2H), 7.38-7.26 (m, 5H), 6.95-6.90 (MM' part of an AA'MM' system, J_{AM} = 8.8 Hz, 2H), 5.80-5.65 (m, 1H), 5.16-5.10 (A part of an AB system, J_{AB} = 12.2 Hz, 1H), 5.08-5.02 (B part of an AB system, J_{AB} = 12.2 Hz, 1H), 4.66-4.61 (dd, *J* = 4.4 Hz, *J* = 6.6 Hz, 1H), 4.12-3.80 (m, 2H), 3.85 (s, 3H), 3.58 (s, 3H), 3.56-3.41 (m, 4H), 0.82 (s, 9H), 0.04 (s, 3H), 0.02 (s, 3H). **^{13}C NMR** (50 MHz, $CDCl_3$): δ 169.7, 162.8, 156.4, 136.7, 130.9, 129.4, 128.4, 128.00, 127.9, 114.0, 66.6, 62.4, 61.7, 55.7, 52.4, 46.1, 41.3, 25.8, 18.2, -5.3, -5.5.

Synthesis of compound 16

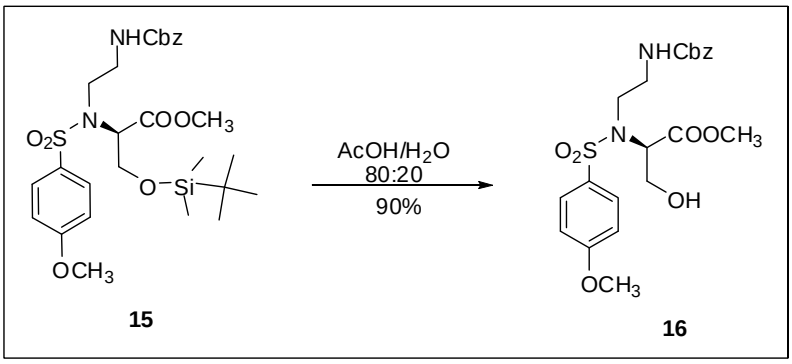

15 **16**

A solution of **15** (330 mg, 0.57 mmol) in 10 mL of a mixture AcOH/H_2O 80:20 was left to stir at 60°C for 5.5 h then toluene (15 mL) was added. Concentration of the solvent under vacuum gave a crude product (300 mg) which was purified by a flash column chromatography on silica gel (petroleum ether/EtOAc 1:2) to afford **16** (240 mg, 90% yield) as a colourless oil.

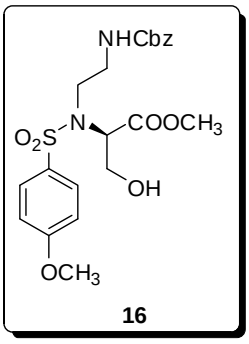

16

[α]$^{25}_{D}$ +42.6 (c 0.23, $CHCl_3$). **ESI-MS**. $[M+Na]^+$ calcd 489.13. Found 489.17. $[M+K]^+$ calcd 505.10. Found 505.08. **^{1}H NMR** (200 MHz, $CDCl_3$): δ 7.76-7.68 (AA' part of an AA'MM' system, J_{AM} = 8.8 Hz, 2H), 7.36-7.26 (m, 5H); 6.97-6.89 (MM' part of an AA'MM' system, J_{AM} = 8.8 Hz, 2H), 5.63-5.54 (m, 1H), 5.14-5.08 (A part of an AB system, J_{AB} = 12.2 Hz, 1H), 5.08-5.01 (B part of an AB system, J_{AB} = 12.2 Hz, 1H), 4.61-4.56 (dd, *J* = 4.4 Hz, *J* = 6.6 Hz, 1H), 4.19-3.84 (m, 2H), 3.83 (s, 3H), 3.59-3.36 (m, 4H), 3.52 (s, 3H), 1.96 (bs, 1H). **^{13}C NMR** (50 MHz, $CDCl_3$): δ 169.5, 162.9, 157.0, 136.3, 130.5, 129.5, 128.4, 128.1, 128.0, 114.1, 67.0, 62.1, 55.7, 52.5, 46.3, 41.6.

Synthesis of compound 17.

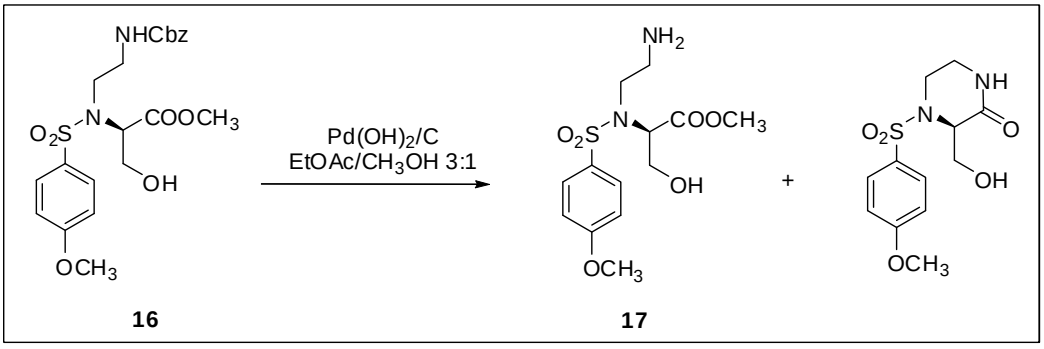

16 **17**

To a solution of **16** (410 mg, 0.88 mmol) in EtOAc/CH_3OH 3:1 (6 mL) $Pd(OH)_2$/C 20% wt. was added (205 mg, 50% wt.). The mixture was stirred at room temperature for 17 h, then was filtrated on Celite®. Evaporation of the solvent under reduced pressure gave the crude product that was used without further purification (**17**/cyclic side product 1:1) (quantitative yield).

Synthesis of compound 18.

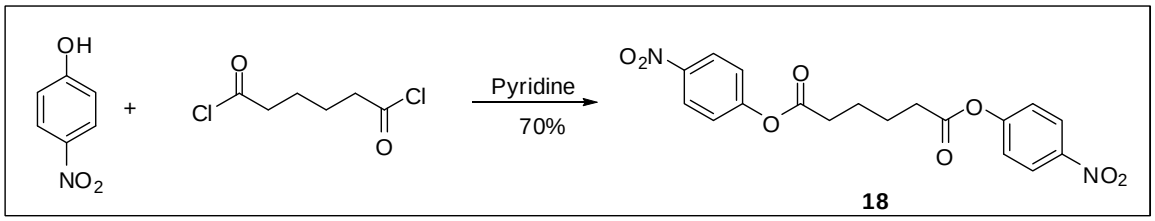

18

To a solution of 4-nitrophenol (1.20 g, 8.60 mmol) in pyridine (17 mL) adipoyl chloride (0.80 g, 4.30 mmol) was added. The solution was left to stir for 15 h, then diluted with then diluted with CH_2Cl_2 (200 mL). The mixture was washed with H_2O (2 x 30 mL), then the organic layer was dried over anhydrous Na_2SO_4 and the solvent was removed in vacuo to give a crude product (1.70 g) that was

purified by a flash column chromatography on silica gel ($CHCl_3$) to afford **18** (1.20 g, 70% yield) as a white solid.

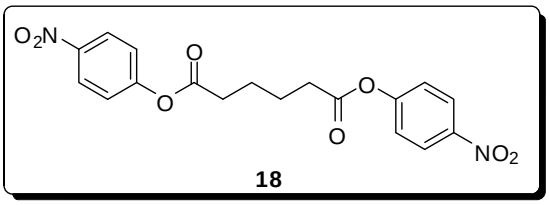

18

M.p. 108-110 °C. **^{1}H NMR** (400 MHz, $CDCl_3$): δ 8.29-8.26 (part AA' of an AA'MM' system, J_{AM} = 9.2 Hz, 2H), 7.30-7.28 (part MM' of an AA'MM' system, J_{AM} = 9.2 Hz, 2H), 2.74-2.67 (m, 4H), 1.94-1.90 (m, 4H). **^{13}C NMR** (50 MHz,$CDCl_3$): 170.5, 155.2, 145.3, 125.2, 122.3, 34.0, 24.1 ppm.

Synthesis of compound 19

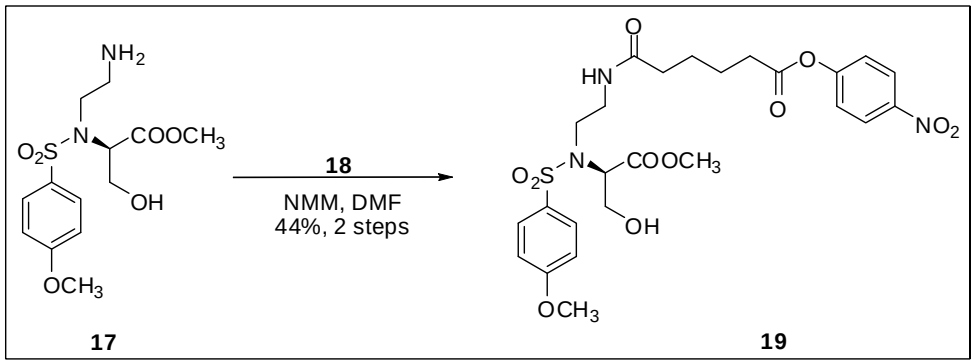

17 **19**

To a solution of the crude mixture **17** + cylic side product (0.52 mmol) in DMF (10 mL), NMM (43.0 µL, 0.39 mmol) and **18** (504 mg, 1.30 mmol) were added. The yellow solution was left to stir for 15 h, then DMF was removed. The crude product was redissolved in CH_2Cl_2 (100 mL) and washed with a saturated solution of $NaHCO_3$ (3 x 20 mL). The organic layer was dried over anhydrous Na_2SO_4 and the solvent was removed in vacuo to give a crude product (400 mg) that was purified by a flash column chromatography on silica gel ($CHCl_3$ then $CHCl_3$/CH_3OH 15:1) to afford **19** (132 mg, 44% yield in two steps) as a pale yellow oil.

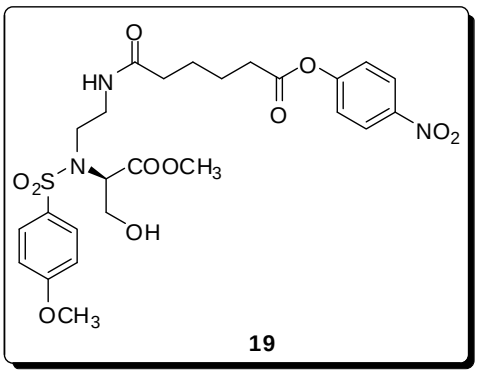

19

$[\alpha]^{25}_D$ +20.6 (c 0.51, $CHCl_3$). **ESI-MS**. $[M+Na]^+$ calcd 604.16. Found 604.25. $[M+K]^+$ calcd 620.13. Found 620.08. **^{1}H NMR** (200 MHz, $CDCl_3$): δ 8.30-8.21 (AA' part of an AA'MM' system, J_{AM} = 9.2 Hz, 2H), 7.75-7.68 (AA' part of an AA'MM' system, J_{AM} = 8.6 Hz, 2H), 7.31-7.27 (MM' part of an AA'MM' system, J_{AM} = 9.2 Hz, 2H), 7.00-6.92 (MM' part of an AA'MM' system, J_{AM} = 8.6 Hz, 2H), 6.49 (bt, 1H), 4.62-4.57 (m, 1H), 4.11-3.95 (m, 2H), 3.87 (s, 3H), 3.77-3.34 (m, 4H), 3.52 (s, 3H), 2.68-2.61 (m, 2H),

2.34-2.27 (m, 2H), 1.84-1.77 (m, 4H). **^{13}C NMR** (50 MHz, $CDCl_3$): δ 173.5, 170.9, 169.4, 163.0, 155.3, 130.5, 129.4, 125.1, 122.4, 114.1, 62.2, 62.0, 55.7, 52.5, 45.9, 39.9, 36.1, 34.1, 24.8, 24.4.

Synthesis of compound 20

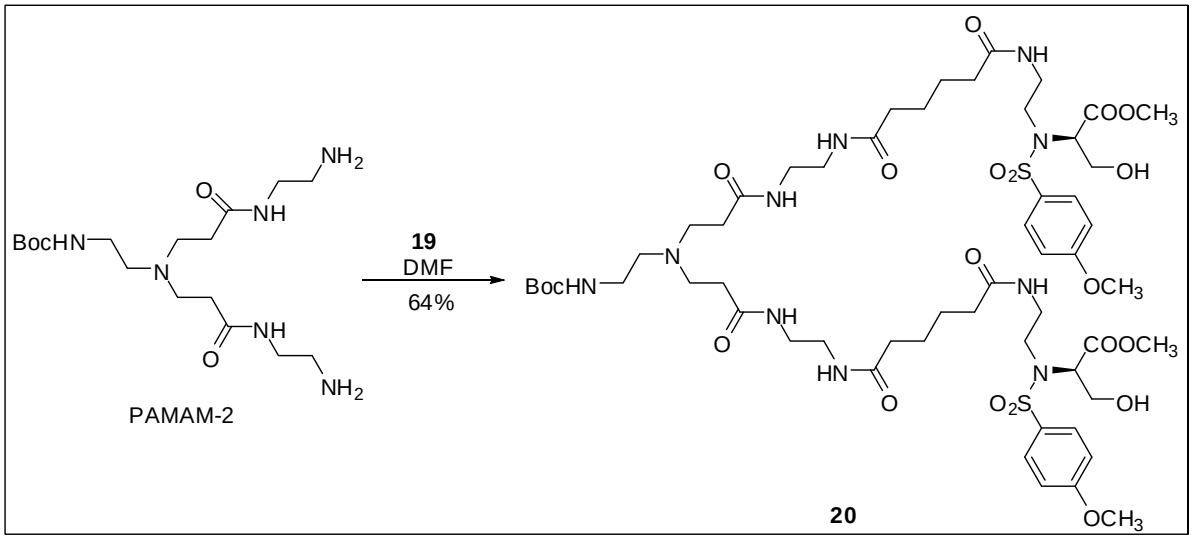

To a solution of **19** (60.0 mg, 0.10 mmol) in 0.9 mL of DMF was added dropwise a solution of PAMAM-2 (20.0 mg, 0.05 mmol) in 0.6 mL of DMF. The yellow solution was left to stir for 15.5 h, then DMF was removed. The crude product (120 mg) was purified by a flash column chromatography on silica gel ($CHCl_3$/CH_3OH 10:1 then 4:1) to afford **20** (41.0 mg, 64%) as a colourless oil.

^{1}H NMR (200 MHz, $CDCl_3$): δ 7.90-7.77 (m, 2H), 7.73-7.69 (AA' part of an AA'MM' system, J_{AM} = 8.8 Hz, 4H), 7.50-7.35 (m, 2H), 6.98-6.93 (MM' part of an AA'MM' system, J_{AM} = 8.8 Hz, 4H), 5.80-6.68 (m, 1H), 5.22-5.10 (m, 2H), 4.66-4.61 (m, 2H), 4.10-3.85 (m, 4H), 5.85 (s, 6H), 3.62-3.08 (m, 18H), 3.47 (s, 6H), 2.76-2.12 (m, 20H), 1.63 (bs, 8H), 1.41 (bs, 9H). **^{13}C NMR** (50 MHz, $CDCl_3$): δ 174.0, 173.9, 173.4, 169.4, 163.0, 156.2, 130.4, 129.5, 114.1, 62.5, 61.5, 55.7, 52.4, 50.1, 45.8, 40.2, 39.7, 39.5, 36.0, 28.6, 25.2, 25.0.

Synthesis of compound 21.

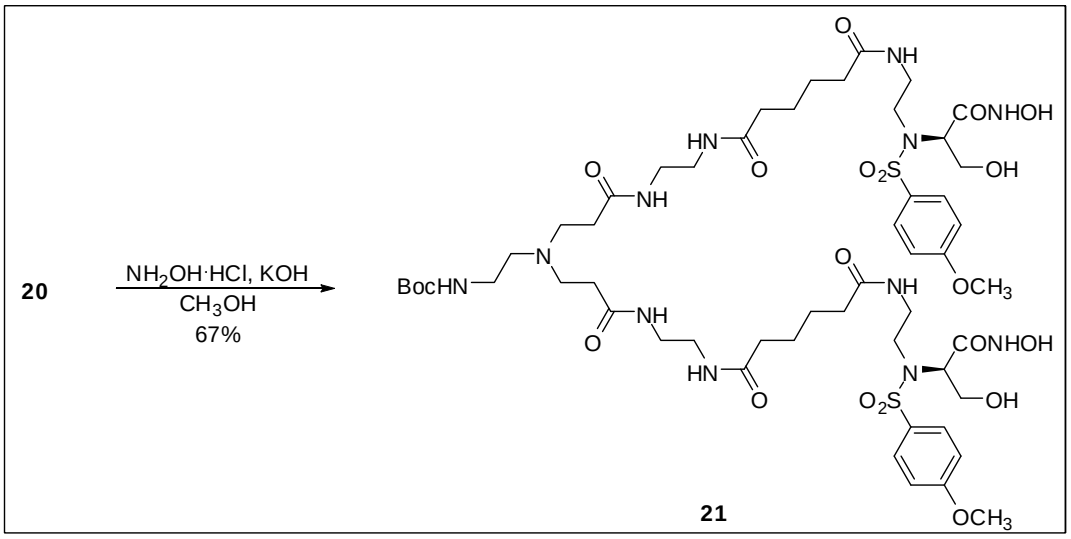

A suspension of KOH (19.0 mg, 0.34 mmol) in 300 µL of CH_3OH was refluxed for 15', then $NH_2OH{\cdot}HCl$ (16.0 mg, 0.23 mmol) was added and the suspension was stirred at 40 °C for 5'. This suspension was added to **20**, and reaction mixture was stirred for 1 h then was filtered and concentrated to dryness. The crude product which was purified by a column chromatography on Sephadex LH-20 resin (CH_3OH, 0.1% CF_3COOH) to afford **21** (14.0 mg, 67%) as a white solid.

ESI-MS. $[M+H-2H_2O]^+$ calcd 1238.53. Found 1238.97. $[M+Na-2H_2O]^+$ calcd 1261.52. Found 1260.98.

Synthesis of compound 22.

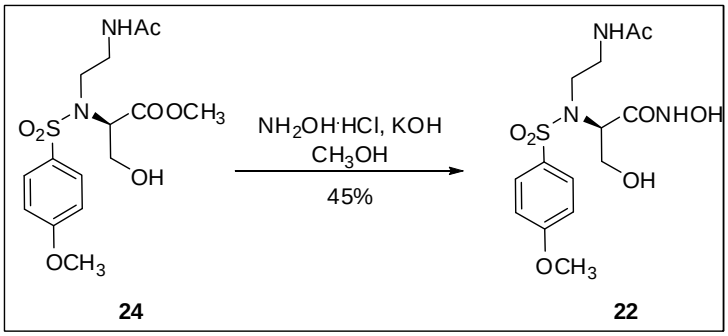

A suspension of KOH (96.0 mg, 1.71 mmol) in 560 µL of CH_3OH and a suspension of $NH_2OH{\cdot}HCl$ (79.0 mg, 1.14 mmol) in 1.00 mL of CH_3OH were refluxed for 15', then the solution of KOH was added to the solution of $NH_2OH{\cdot}HCl$ and the suspension was stirred at 40 °C for 10'. This suspension was cooled to room temperature and added to **22** (70.0 mg, 0.19 mmol). The reaction mixture was stirred for 1.5 h then was filtered and concentrated to dryness. The crude product which

was purified by a flash column chromatography on silica gel (from CH_2Cl_2/CH_3OH 7:1) to afford **22** (32.0 mg, 45%) as an oil.

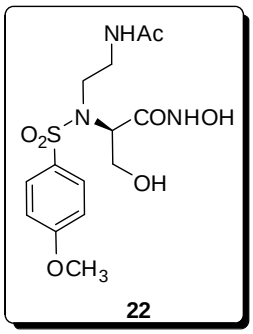

22

^{1}H NMR (200 MHz, $CDCl_3$): δ 7.83-7.75 (AA' part of an AA'MM' system, J_{AM} = 8.8 Hz, 2H), 7.07-7.04 (MM' part of an AA'MM' system, J_{AM} = 8.8 Hz, 2H), 4.39-4.30 (m, 1H), 3.89-3.36 (m, 6H), 3.87 (s, 3H), 1.92 (s, 3H). **^{13}C NMR** (50 MHz, $CDCl_3$): δ 171.2, 166.1, 162.3, 129.8, 128.4, 113.0, 59.3, 58.4, 53.9, 42.9, 38.8, 20.3.

Synthesis of compound 23.

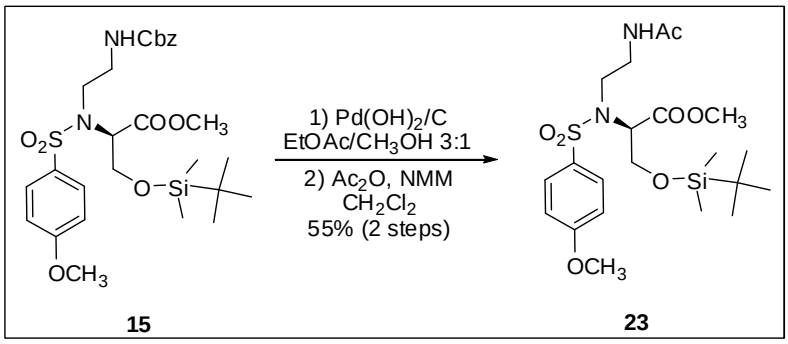

15 **23**

To a solution of **15** (320 mg, 0.55 mmol) in $EtOAc/CH_3OH$ 3:1 (4 mL) $Pd(OH)_2/C$ 20% wt. was added (160 mg, 50% wt.). The mixture was stirred at room temperature for 2 h, then was filtrated on Celite®. Evaporation of the solvent under reduced pressure gave the crude product that was used without further purification. The crude was redissolved in CH_2Cl_2 (3 mL) and then NMM (120 µL, 1.10 mmol) and Ac_2O (104 µL, 1.10 mmol) were added at room temperature. The mixture was stirred overnight, then it was diluted with CH_2Cl_2 (100 mL) and washed with H_2O (2x). The organic layer was dried over anhydrous Na_2SO_4 and the solvent was removed in vacuo to give a crude product (220 mg) that was purified by a flash column chromatography on silica gel (Petroleum ether/EtOAc 1:1 then 2:3) to afford **23** (145 mg, 55% yield in two steps) as an oil.

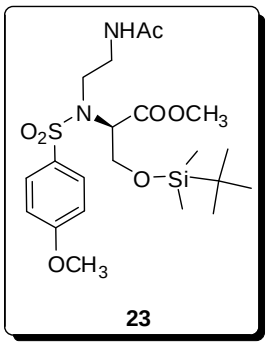

23

^{1}H NMR (200 MHz, $CDCl_3$): δ 7.74-7.67 (AA' part of an AA'MM' system, J_{AM} = 9.2 Hz, 2H), 6.97-6.90 (MM' part of an AA'MM' system, J_{AM} = 9.2 Hz, 2H), 6.60-6.71 (m, 1H), 4.66-4.61 (dd, *J* = 3.6 Hz, *J* = 6.6 Hz, 1H), 4.05-3.91 (m, 2H), 3.84 (s, 3H), 3.60 (s, 3H), 3.57-3.25 (m, 4H), 1.96 (s, 3H), 0.81 (s, 9H), 0.04 (s, 3H), 0.01 (s, 3H). **^{13}C NMR** (50 MHz, $CDCl_3$): δ 170.4, 170.0, 162.9, 130.9, 129.4, 114.1, 62.2, 61.8, 55.7, 52.4, 45.7, 39.4, 25.8, 23.5, 18.2, -5.3, -5.6.

Synthesis of compound 24.

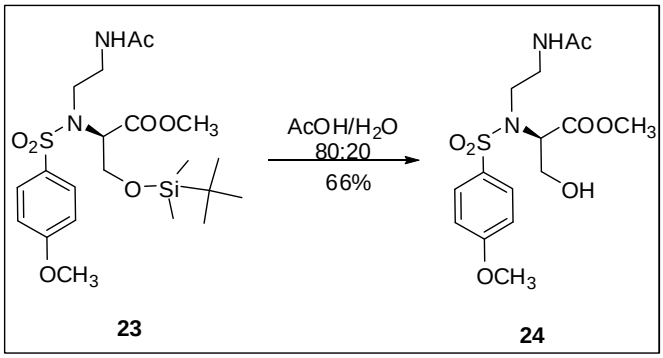

23 **24**

A solution of **23** (143 mg, 0.29 mmol) in 3.5 mL of a mixture AcOH/H_2O 80:20 was left to stir at 60°C for 4 h then toluene (10 mL) was added. Concentration of the solvent under vacuum gave a crude product (160 mg) which was purified by a flash column chromatography on silica gel (EtOAc) to afford **24** (73.0 mg, 66% yield) as a colourless oil.

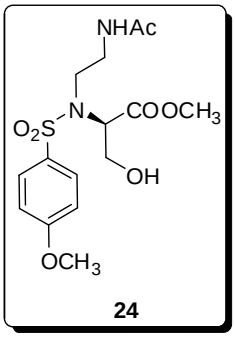

24

^{1}H NMR (200 MHz, $CDCl_3$): δ 7.75-7.67 (AA' part of an AA'MM' system, J_{AM} = 8.8 Hz, 2H), 6.98-6.91 (MM' part of an AA'MM' system, J_{AM} = 8.8 Hz, 2H), 6.80-6.71 (m, 1H), 4.63-4.58 (m, 1H), 4.12-3.92 (m, 2H), 3.85 (s, 3H), 3.65-3.32 (m, 4H), 3.51 (s, 3H), 1.97 (s, 3H). **^{13}C NMR** (50 MHz, $CDCl_3$): δ 171.5, 169.5, 163.0, 130.4, 129.5, 114.1, 62.2, 61.9, 55.7, 52.5, 45.8, 40.2, 23.3.

Synthesis of compound 25.

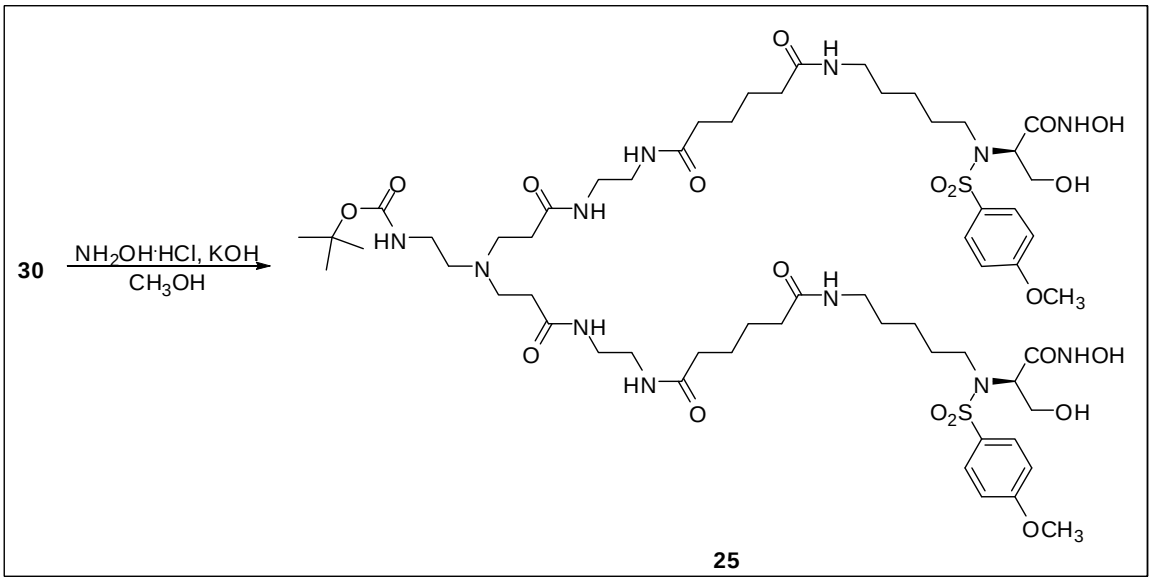

A suspension of KOH (60.0 mg, 1.06 mmol) in 350 µL of CH_3OH and a suspension of $NH_2OH{\cdot}HCl$ (49.0 mg, 0.71 mmol) in 590 µL of CH_3OH were refluxed for 15', then the solution of KOH was added to the solution of $NH_2OH{\cdot}HCl$ and the suspension was stirred at 40 °C for 10'. This suspension was cooled to room temperature and added to **30** (80.0 mg, 0.06 mmol). The reaction mixture was stirred for 7 h then was filtered and concentrated to dryness. The crude product which was purified by reversed-phase semi-preparative HPLC (from CH_3OH/H_2O 55:35 to 70:30) to afford **25** (18.0 mg, 24%) as a white solid.

HRMS: calcd. for $C_{59}H_{99}N_{12}O_{20}S_2$ 1359.6535. Found 1359.6534.

Synthesis of compound 26.

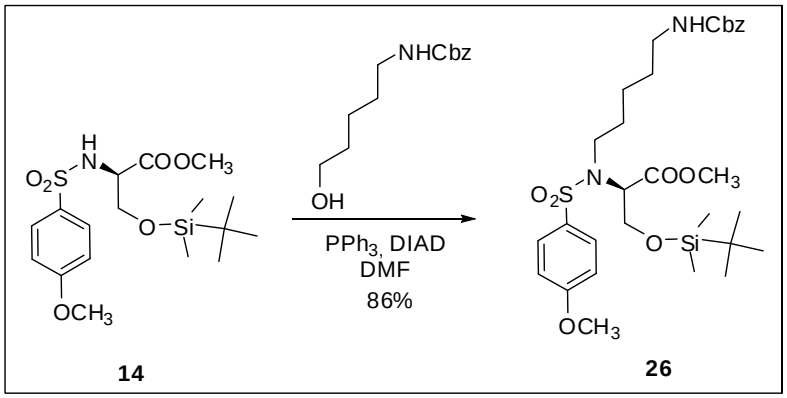

To a solution of **14** (700 mg, 1.73 mmol), N-Z-pentanolamine (494 mg, 2.08 mmol) and triphenilphosphine (546 mg, 2.08 mmol) in 12 mL of dry THF, 0.41 mL of DIAD (2.08 mmol) were

added drop-wise, in 1 h. The reaction was stirred at room temperature for 21 h, and then the solvent was removed in vacuo to give an yellow oil. After crystallization of the betainic side product (EtOAc/ciclohexane 1:8) the filtrate was concentrated in vacuum and the residue (1.35 g) was purified twice by flash column chromatography on silica gel ($CHCl_3$/EtOAc 15:1) to give pure **26** as an oil (931 mg, 86% yield).

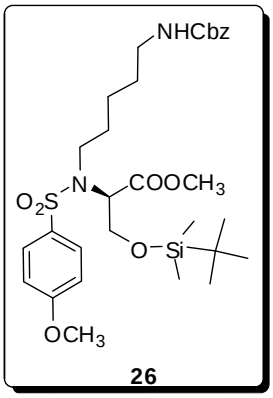

26

$[\alpha]^{25}_D$ +21.9 (c 0.80, $CHCl_3$). **ESI-MS**. $[M+Na]^+$ calcd 645.26. Found 645.25. $[M+K]^+$ calcd. 661.24. Found 661.08. **^{1}H NMR** (200 MHz, $CDCl_3$): δ 7.78-7.70 (AA' part of an AA'MM' system, J_{AM} = 9.2 Hz, 2H), 7.38-7.30 (m, 5H), 6.97-6.90 (MM' part of an AA'MM' system, J_{AM} = 9.2 Hz, 2H), 5.10 (A_2 system, 2H), 4.82-4.70 (m, 1H), 4.62-4.57 (dd, J = 4.6 Hz, J = 5.6 Hz, 1H), 4.14-3.90 (m, 2H), 3.85 (s, 3H), 3.55 (s, 3H), 3.32-3.12 (m, 4H), 1.85-1.14 (m, 6H), 0.83 (s, 9H), 0.03 (s, 3H), 0.02 (s, 3H). **^{13}C NMR** (50 MHz, $CDCl_3$): δ 169.6, 162.6, 156.2, 136.6, 131.7, 129.4, 128.4, 128.0, 113.9, 66.7, 63.3, 61.4, 55.6, 52.1, 47.0, 41.1, 30.8, 29.8, 25.8, 24.3, 18.2, -5.4, -5.5.

Synthesis of compound 27.

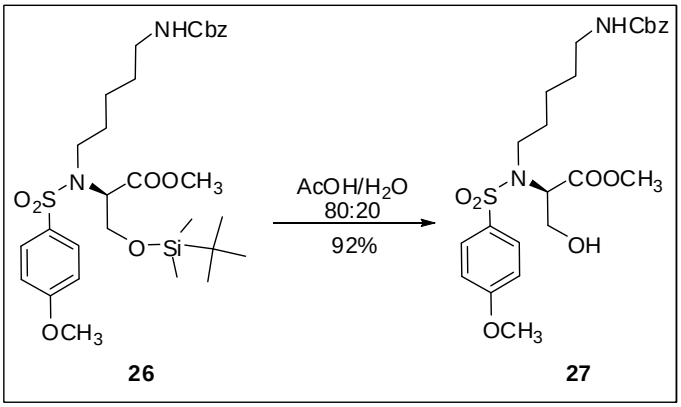

26 **27**

A solution of **26** (530 mg, 0.85 mmol) in 10 mL of a mixture AcOH/H_2O 80:20 was left to stir at 60°C for 8 h then toluene (20 mL) was added. Concentration of the solvent under vacuum gave a crude product (530 mg) which was purified by a flash column chromatography on silica gel (Petroleum ether/EtOAc 1:2) to afford **27** (400 mg, 92% yield) as a colourless oil.

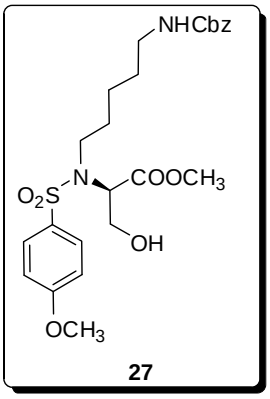

27

[α]$^{25}_{D}$ +33.9 (c 0.18, $CHCl_3$). **ESI-MS**. $[M+Na]^+$ calcd 531.18. Found 531.25. $[M+K]^+$ calcd. 547.15. Found 547.08. **^{1}H NMR** (200 MHz, $CDCl_3$): δ 7.82-7.75 (AA' part of an AA'MM' system, J_{AM} = 8.8 Hz, 2H), 7.40-7.33 (m, 5H), 7.00-6.94 (MM' part of an AA'MM' system, J_{AM} = 8.8 Hz, 2H), 5.10 (A_2 system, 2H), 4.82-4.74 (m, 1H), 4.56-4.49 (m, 1H), 4.14-4.03 (m, 1H), 3.95-3.82 (m, 1H), 3.88 (s, 3H), 3.61 (s, 3H), 3.40-3.00 (m, 4H), 2.55-2.48 (m, 1H), 1.78-1.18 (m, 6H). **^{13}C NMR** (50 MHz, $CDCl_3$): δ 170.1, 162.8, 156.5, 136.5, 131.3, 129.5, 128.5, 128.0, 114.0, 66.7, 61.8, 61.5, 55.7, 52.4, 47.3, 40.8, 30.0, 29.6, 23.9.

Synthesis of compound 28.

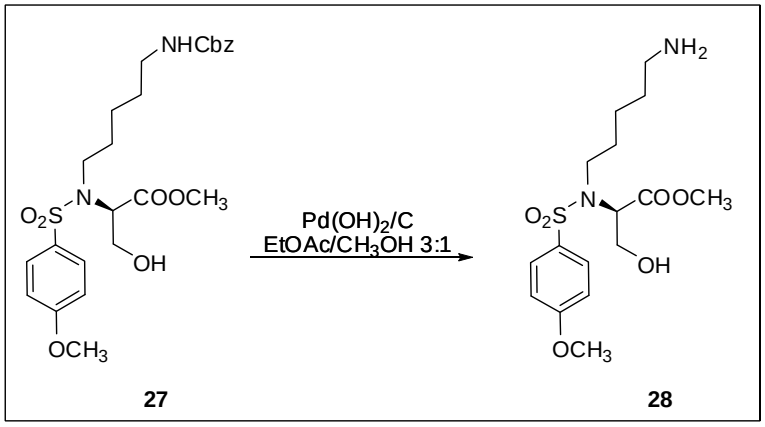

27 28

To a solution of **27** (184 mg, 0.36 mmol) in EtOAc/CH_3OH 3:1 (4 mL) $Pd(OH)_2$/C 20% wt. was added (92.0 mg, 50% wt.). The mixture was stirred at room temperature for 19 h, then it was filtrated on Celite®. Evaporation of the solvent under reduced pressure gave the crude product **28** that was used without further purification (quantitative yield).

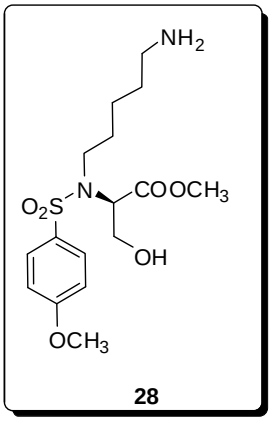

28

^{1}H NMR (200 MHz, CD_3OD): δ 7.78-7.72 (AA' part of an AA'MM' system, J_{AM} = 8.8 Hz, 2H), 7.10-7.02 (MM' part of an AA'MM' system, J_{AM} = 8.8 Hz, 2H), dd (*J* = 4.6 Hz, *J* = 6.6 Hz, 1H), 3.98-3.81 (m, 2H), 3.88 (s, 3H), 3.55 (s, 3H), 3.40-3.25 (m, 2H), 2.91 (t, *J* = 7.4 Hz), 1.79-1.24 (m, 6H). **^{13}C NMR** (50 MHz, CD_3OD): δ 169.1, 162.3, 130.4, 128.3, 112.8, 60.7, 59.9, 53.9, 50.3, 38.3, 28.9, 25.9, 22.3.

Synthesis of compound 29.

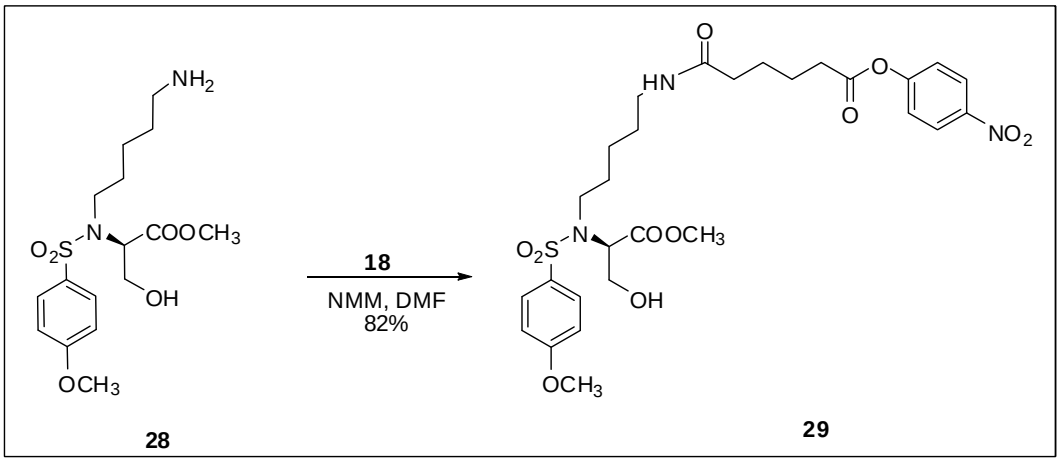

To a solution of the crude **28** (0.78 mmol) in DMF (30 mL), NMM (171 µL, 1.56 mmol) and **18** (1.51 g, 3.90 mmol) were added. The yellow solution was left to stir for 18 h, then DMF was removed. The crude product was redissolved in CH_2Cl_2 (100 mL) and washed with a saturated solution of $NaHCO_3$ (3 x 20 mL) and then with water (1x). The organic layer was dried over anhydrous Na_2SO_4 and the solvent was removed in vacuo to give a crude product that was purified by a flash column chromatography on silica gel ($CHCl_3$ then $CHCl_3/CH_3OH$ 15:1) to afford **29** (397 mg, 82%) as a pale yellow oil.

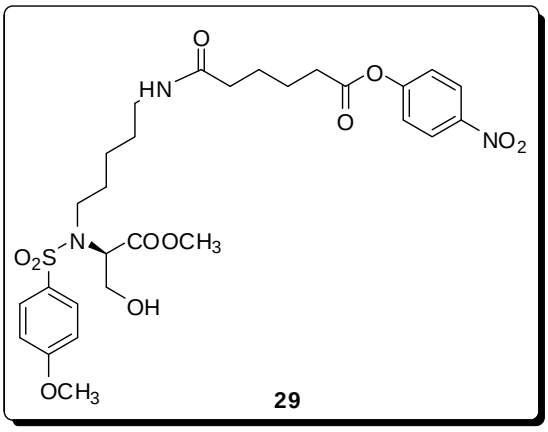

$[\alpha]^{25}_D$ +37.6 (c 0.21, $CHCl_3$). **ESI-MS**. $[M+Na]^+$ calcd 646.20. Found 646.25. $[M+K]^+$ calcd. 662.18. Found 662.17. **^{1}H NMR** (200 MHz, $CDCl_3$): δ 8.30-8.22 (AA' part of an AA'MM' system, J_{AM} = 9.2 Hz, 2H), 7.80-7.72 (AA' part of an AA'MM' system, J_{AM} = 8.8 Hz, 2H), 7.32-7.24 (MM' part of an AA'MM' system, J_{AM} = 9.2 Hz, 2H), 7.00-6.92 (MM' part of an AA'MM' system, J_{AM} = 8.8 Hz, 2H), 5.74-5.64 (m, 1H), 4.54-4.48 (m, 1H), 4.33-4.00 (m, 1H), 3.96-3.84 (m, 1H), 3.87 (s, 3H), 3.57 (s, 3H), 3.39-3.04 (m, 4H), 2.74-2.61 (m, 3H), 2.28-2.21 (m, 2H), 1.81-1.24 (m, 10H). **^{13}C NMR** (50 MHz, $CDCl_3$): δ172.6, 170.8, 169.9, 162.8, 155.2, 129.4, 126.1, 125.1, 122.4, 114.0, 62.0, 61.5, 55.7, 52.4, 47.2, 39.1, 36.3, 34.1, 31.8, 29.8, 29.0, 25.1, 24.4, 23.7.

Synthesis of compound 30

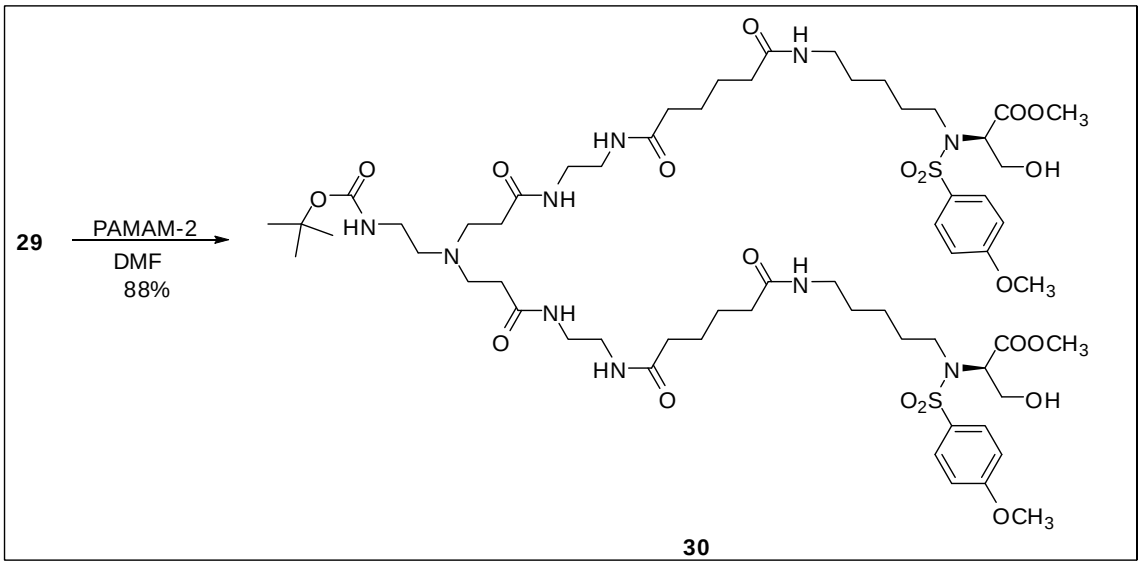

To a solution of **29** (105 mg, 0.168 mmol) in 1.5 mL of DMF was added dropwise a solution of PAMAM-2 (33.0 mg, 0.08 mmol) in 1 mL of DMF. The yellow solution was left to stir for 16 h, then DMF was removed in vacuo. The crude product (180 mg) was purified by a flash column chromatography on silica gel ($CHCl_3$/CH_3OH 10:1 then 4:1) to afford **30** (90 mg, 88%) as a colourless oil.

^{1}H NMR (400 MHz, CD_3OD): δ 7.78 (bs, 2H), 7.73-7.71 (AA' part of an AA'MM' system, J_{AM} = 8.8 Hz, 4H), 7.30 (bs, 2H), 6.94-6.93 (MM' part of an AA'MM' system, J_{AM} = 8.8 Hz, 4H), 6.73 (bs, 2H), 5.66 (bs, 1H), 4.55 (at, *J* = 6.0 Hz, 2H), 4.15 (bs, 2H), 4.03-3.99 (m, 2H), 3.91-3.87 (m, 2H), 3.84 (s, 6H), 3.51 (s, 6H), 3.37-3.09 (m, 18H), 2.74-2.14 (m, 18H), 1.72-1.54 (m, 12H), 1.50-1.38 (m, 13H), 1.30-1.23 (m, 4H). **^{13}C NMR** (50 MHz, CD_3OD): δ 173.9, 174.0, 173.3, 169.9, 162.8, 156.2, 131.2, 129.4, 114.0, 79.3, 61.7, 55.7, 52.3, 50.2, 47.0, 39.7, 39.5, 39.2, 36.1, 36.0, 33.8, 30.2, 29.0, 28.6, 25.3, 24.0.

Synthesis of compounds 31 and 32

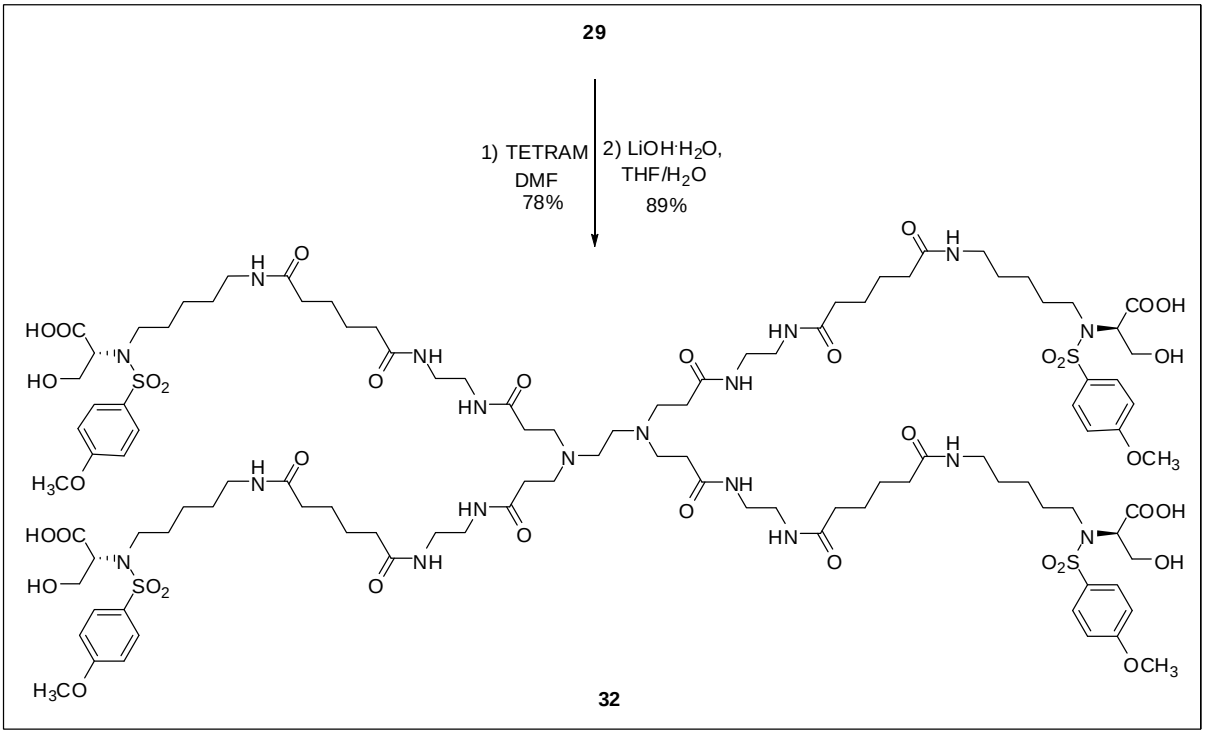

To a solution of **29** (96.0 mg, 0.15 mmol) in 1.40 mL of DMF was added dropwise a solution of TETRAM (18.0 mg, 0.04 mmol) in 800 µL of DMF. The yellow solution was left to stir for 18 h, then DMF was removed in vacuo. The crude product (110 mg) was purified by a column chromatography on Sephadex LH-20 resin (CH_3OH) to afford **31** (67.0 mg, 78%) as a colourless oil.

^{1}H NMR (200 MHz, CD_3OD): δ 7.79-7.74 (AA' part of an AA'MM' system, J_{AM} = 8.8 Hz, 8H), 7.07-7.03 (MM' part of an AA'MM' system, J_{AM} = 8.8 Hz, 8H), 4.57-4.51 (m, 4H), 3.99-3.79 (m, 8H), 3.87 (s, 12H), 3.55 (s, 12H), 3.34-2.70 (m, 36H), 2.52-2.10 (m, 32H), 1.72-1.20 (m, 40H). **^{13}C NMR** (50 MHz, CD_3OD): δ 174.5, 174.1, 173.0, 170.0, 163.1, 131.5, 129.2, 113.8, 61.6, 60.9, 55.0, 51.3, 39.0, 38.7, 35.5, 32.4, 30.0, 28.7, 25.3, 25.2, 24.0.

To a solution of **31** (36.0 mg, 0.02 mmol) in a mixture THF/H_2O 1:1 (1.2 mL), $LiOH{\cdot}H_2O$ (5.00 mg, 0.12 mmol) was added. The reaction mixture was stirred at room temperature for 6.5 h. The pH was adjusted to 4 with a H_3PO_4 solution (1M, H_2O) and the solvent was removed in vacuo. The crude product (40.0 mg) was purified by a column chromatography on Sephadex LH-20 resin (CH_3OH) to afford **32** (32.0 mg, 89%) as a colourless oil.

^{1}H NMR (200 MHz, CD_3OD): δ 7.77-7.7 (AA' part of an AA'MM' system, J_{AM} = 8.8 Hz, 8H), 6.94-6.93 (MM' part of an AA'MM' system, J_{AM} = 8.8 Hz, 8H), 3.90-3.75 (m, 8H), 3.83 (s, 12H), 3.40-2.99 (m, 44H), 2.68-2.57 (m, 8H), 2.25-2.18 (m, 16H), 1.90-1.18 (m, 40H).

Synthesis of compound 33

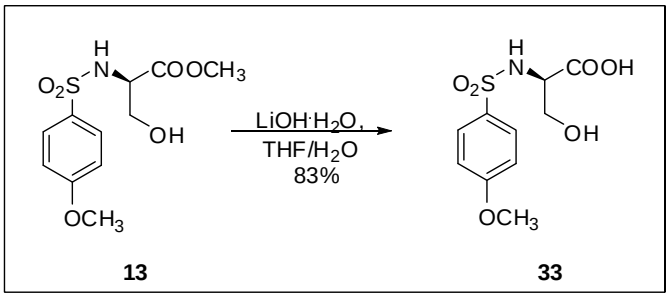

To a solution of **13** (150 mg, 0.52 mmol) in a mixture THF/H_2O 1:1 (12 mL), LiOH·H_2O (44.0 mg, 1.04 mmol) was added. The reaction mixture was stirred at room temperature for 1.5 h. The pH was adjusted to 3 with a H_3PO_4 solution (1M, H_2O) and the mixture was extracted with EtOAc. The organic phase was dried over Na_2SO_4 and the solvent was removed in vacuum. The crude product was used without further purification to afford **33** (118 mg, 83%) as a white solid.

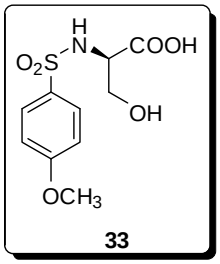

M.p.: dec. 217°C. **$[\alpha]^{25}_D$** -6.33 (c 0.30, CH_3OH). **Anal.** for $C_{10}H_{13}NO_6S$ calcd: C, 43.63; H, 4.76; N, 5.09. Found: C, 43.64; H, 4.80; N, 5.07. **^{1}H NMR** (200MHz, CD_3OD): δ 7.82-7.77 (AA' part of an AA'MM' system, J_{AM} = 9.2 Hz, 2H), 7.06-7.01 (MM' part of an AA'MM' system, J_{AM} = 9.2 Hz, 2H), 3.91-3.81 (m 1H), 3.86 (s, 3H), 3.80-3.64 (m, 2H). **^{13}C NMR** (50MHz, CD_3OD): δ 168.7, 162.9, 133.1, 128.9, 113.7, 62.9, 57.9, 54.8.

Synthesis of compound 34.

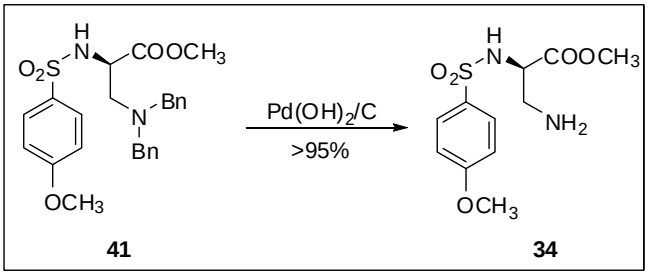

To a solution of **41** (703 mg, 1.50 mmol) in EtOAc/CH_3OH 4:1 (12.5 mL), $Pd(OH)_2$ (351 mg, 50% wt.) was added under inert atmosphere. The mixture was stirred under hydrogen atmosphere at room temperature for 19 h. The resulting mixture was then filtered and the solution was concentrated under pressure to give **34** (420 mg, >95%) as a pale yellow oil, that was used without any further purification.

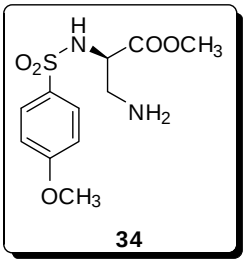

34

[α]$^{25}_{D}$ -1.67 (c 0.30, CH_2Cl_2). **^{1}H NMR** (200 MHz, CD_3OD); δ 7.82-7.78 (part AA' of an AA'MM' system, J_{AM} = 9.0 Hz, 2H), 7.10-7.06 (part MM' of an AA'MM' system, J_{AM} = 9.0 Hz, 2H), 4.23-4.16 (part A of an AXY system, J_{AX} = 4.8 Hz, J_{AY} = 9.2 Hz, 1H, CH aa), 3.88 (s, 3H, OCH_3), 3.47 (s, 3H, $COOCH_3$), 3.38-3.28 (m, 1H), 3.06 (part Y of an AXY system, J_{AY} = 9.2 Hz, J_{YX} = 13.2 Hz). **^{13}C NMR** (50 MHz, CD_3OD): δ 167.3, 162.4, 130.2, 128.3, 112.9, 54.0, 52.7, 51.1, 39.9.

Synthesis of compound 35.

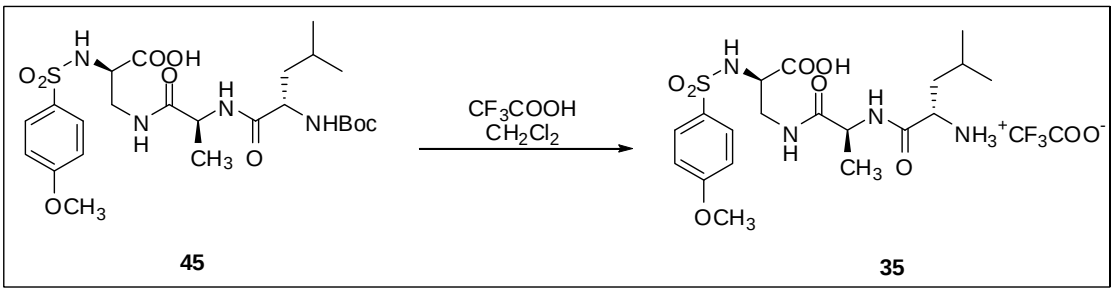

45 **35**

To a solution of **45** (193 mg, 0.35 mmol) in dry CH_2Cl_2 (5 mL) was added CF_3COOH (600 µL, 7.70 mmol). After 3 h 5 mL of toluene were added and solvent was removed in vacuum to give **35** as a glassy solid. The product was used without any further purification (quantitative yield).

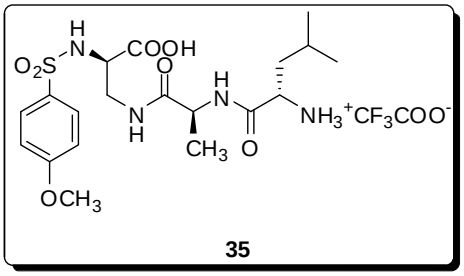

35

Anal. for $C_{21}H_{31}F_3N_4O_9S$ + 3 H_2O calcd: C, 40.25; H, 5.95; N, 8.94. Found: C, 40.32; H, 5.74; N, 8.80. **^{1}H NMR** (400 MHz, CD_3OD); δ 7.79-7.76 (part AA' of an AA'MM' system, J_{AM} = 8.8 Hz, 2H), 7.04-7.01 (part MM' of an AA'MM' system, J_{AM} = 8.8 Hz, 2H), 4.36 (q, J = 7.2 Hz, 1H), 4.03-3.98 (m, 1H), 3.91-3.86 (m, 2H), 3.85 (s, 3H), 3.50-3.42 (m, 2H), 1.82-1.64 (m, 3H), 1.36 (d, J = 7.2 Hz, 3H), 1.02-0.98 (m, 6H). **^{13}C NMR** (50 MHz, CD_3OD): δ 173.3, 171.1, 169.0, 163.1, 132.0, 129.0, 113.8, 55.1, 54.8, 51.5, 49.3, 41.2, 40.2, 23.9, 21.7, 20.5, 16.8.

Synthesis of compound 36: (S)-methyl 2-(dibenzylamina)-3-hydroxy propanoate.

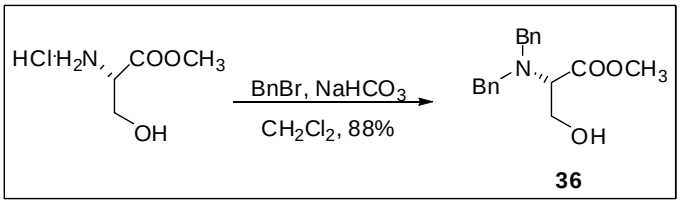

36

To a slurry of methyl-L-serine·HCl (2.00 g, 12.9 mmol) in DMSO/THF 1:4 were added at room temperature sodium hydrogenocarbonate (4.32 g, 51.44 mmol) and benzylbromide (3.36 mL, 28.3 mmol) and the resulting mixture was heated at reflux under nitrogen atmosphere for 17 h. The resulting slurry was diluted with water (2x) and extracted with EtOAc(2x). The organic layer was dried over anhydrous Na_2SO_4 and the solvent was removed in vacuo to give the crude product (4.20 g). Purification by flash chromatography on silica gel (Petroleum ether/EtOAc 8:1 then 5:1) gave **36** as a colourless oil (3.40 g, 88%).

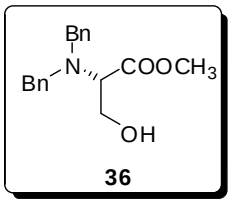

36

$[\alpha]^{25}_D$ -120.0 (c 0.90, CH_2Cl_2). **^{1}H NMR** (200 MHz, $CDCl_3$); δ 7.32-7.25 (m, 10H), 3.94-3.87 (part A of an AB system, J_{AB} = 13.2 Hz, 1H), 3.79 (s, 3H), 3.79-3.69 (m, 3H), 3.69-3.63 (part B of an AB system, J_{AB} = 13.2 Hz, 1H), 3.55 (t, *J* =7.6 Hz, 2H), 2.49-2.57 (m, 1H). **^{13}C NMR** (50 MHz, $CDCl_3$); δ 171.6, 138.6, 128.9, 128.5, 127.4, 62.0, 59.5, 55.0, 51.6.

Synthesis of compound 37: (S)-2-methoxycarbonyl-2-(dibenzylamino)ethyl methanesulphonate.

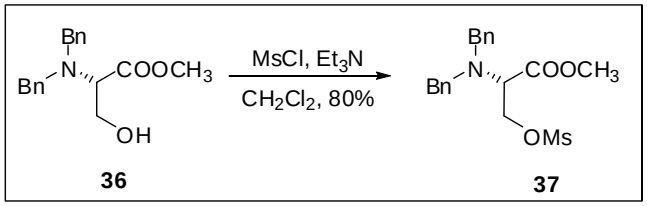

36 **37**

To a solution of **36** (1.93 g, 6.45 mmol) in 11 mL of CH_2Cl_2 were added at 0°C Et_3N (0.75 mL, 9.68 mmol) and MsCl (1.34 mL, 9.68 mmol). The reaction mixture was stirred for 5 h at room temperature, then was diluited with CH_2Cl_2 and washed with a saturated solution of NH_4Cl (2x). The organic layer was dried over anhydrous Na_2SO_4 and the solvent was removed in vacuo to give the crude product (2.40 g). The crude was purified by flash chromatography on silica gel (Petroleum ether/EtOAc 4:1) to give **37** as a colorless oil (1.95 g, 80%).

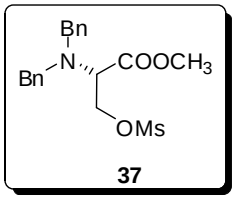

37

$[\alpha]^{25}_D$ -68.1 (c 0.26, CH_2Cl_2). **^{1}H NMR** (200 MHz, $CDCl_3$): δ 7.41-7.27 (m, 10H); 4.55-4.46 (dd, *J* = 9.2 Hz, *J* = 7.0 Hz, 1H); 4.39-4.31 (dd, *J* = 9.2 Hz, *J* = 6.0 Hz, 1H); 3.92-3.64 (m, 5H); 3.85 (s, 3H); 2.92 (s, 3H). **^{13}C NMR** (50 MHz, $CDCl_3$): δ 170.3, 138.5, 129.0, 128.8, 128.4, 67.4, 59.9, 55.4, 51.8, 37.3.

Synthesis of compound 38: (R)-methyl 2-azido-3-(dibenzylamino)propanoate.

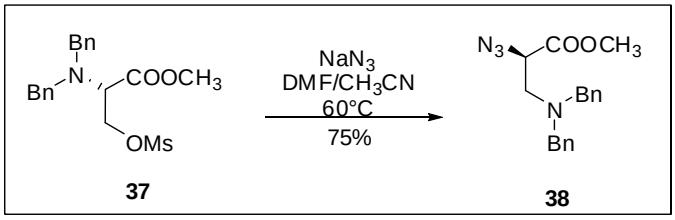

To a solution of **37** (890 mg, 2.36 mmol) in dry CH_3CN/DMF 4:1 (20 mL) was added at room temperature NaN_3 (422 mg, 7.15 mmol), and the mixture was heated at 60°C under a nitrogen atmosphere. After 18h EtOAc (80 mL) and water (80 mL) were added; the two layers were separated and the organic phase was washed with water (2x). The aqueous layer was extracted with EtOAc: the organic layers were combined and dried over anhydrous Na_2SO_4. The solvent was removed in vacuo to give the crude product (1.80 g). The crude was purified by flash chromatography on silica gel (Petroleum ether/EtOAc 7:1) to give **38** (583 mg, 75%) as a colourless oil.

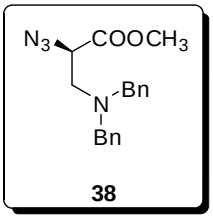

$[\alpha]^{25}_D$ +13.6 (c 0.22, CH_2Cl_2). **^{1}H NMR** (200 MHz, $CDCl_3$); δ 7.35-7.24 (m, 10H); 3.94 (t, *J* = 7.0 Hz, 1H), 4.82-3.55 (m, 4H); 3.70 (s, 3H); 2.95-2.91(m, 2H). **^{13}C NMR** (50 MHz, $CDCl_3$): δ 169.9, 138.5, 128.9, 128.3,127.2, 60.9, 58.8, 55.0, 52.5.

Synthesis of compound 40: (R)-methyl 3-(dibenzylamino)-2-aminopropanoate.

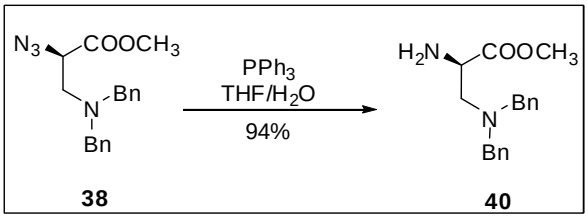

To a solution of **38** (590 mg, 1.81 mmol) in dry THF (12 mL) were added at room temperature PPh_3 (715 mg, 2.72 mmol) and water (324 µL, 18.1 mmol). The mixture was stirred at room temperature for 19 h and then was diluted with EtOAc. Water was added and the layers were separated. The aqueous phase was extracted with EtOAc (2x) and the combined organic layers were dried over anhydrous Na_2SO_4. The solvent was removed in vacuo to give the crude product (1.20 g). The crude was purified by flash chromatography on silica gel (Petroleum ether/EtOAc 1:2) to give **40** (507 mg, 94%) as a colourless oil.

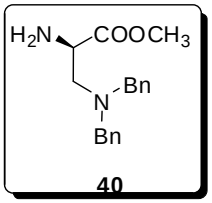

40

[α]$^{25}_{D}$ +8.66 (c 1.19, CH_2Cl_2). **^{1}H NMR** (200 MHz, $CDCl_3$); δ 7.34-7.21 (m, 10H), 3.70-3.51 (m, 5H), 3.68 (s, 3H); 2.83-2.74 (dd, *J* = 5.4, *J* = 12.8, 1H), 2.68-2.57 (dd, *J* = 8.0, *J* = 12.8, 1H). **^{13}C NMR** (50 MHz, $CDCl_3$): δ 174.9, 138.9, 129.0, 128.3, 127.1, 58.7, 58.2, 53.3, 51.0.

Synthesis of compound 41.

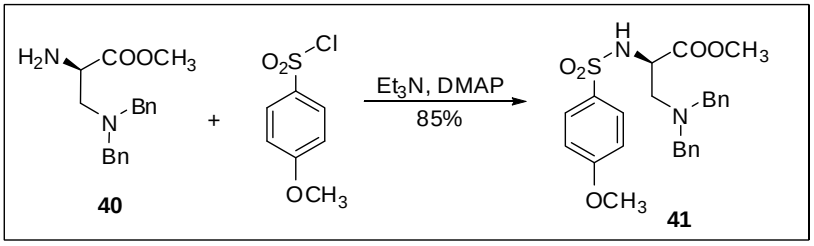

40 **41**

To a solution of **40** (140 mg, 0.47 mmol) in CH_2Cl_2 (3.5 mL) were added at room temperature Et_3N (130 µL, 0.94 mmol) and DMAP (catalytic). After 30 min 4-methoxybenzensulfonyl chloride (97.0 mg, 0.47 mmol) was added. After 18h the resulting mixture was diluted with CH_2Cl_2 and washed with HCl (3%, H_2O) and with water (2x). The organic layer was dried over anhydrous Na_2SO_4. The solvent was removed in vacuo to give **41** as a colourless product (185 mg, 85%), that was used without any further purification.

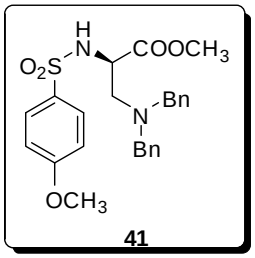

41

[α]$^{25}_{D}$ -5.20 (c 0.98, CH_2Cl_2). **^{1}H NMR** (200 MHz, $CDCl_3$); δ 7.72-7.68 (part AA' of an AA'MM' system, J_{AM} = 8.8 Hz, 2H), 7.37-7.23 (m, 10H), 6.93-6.89 (part MM' of an AA'MM' system, J_{AM} = 8.8 Hz, 2H), 5.10 (d, *J* = 7.6 Hz), 4.07-3.97 (m, 1H), 3.84 (s, 3H), 3.54 (as, 4H), 3.48 (s, 3H), 2.79-2.75 (dd, *J* = 1.8 Hz, *J* = 6.6 Hz, 2H). **^{13}C NMR** (50 MHz, $CDCl_3$): δ 171.3, 163.0, 138.2, 129.4, 129.0, 128.4, 127.3, 114.1, 58.3, 55.6, 55.0, 54.6, 52.3.

Synthesis of compound 42.

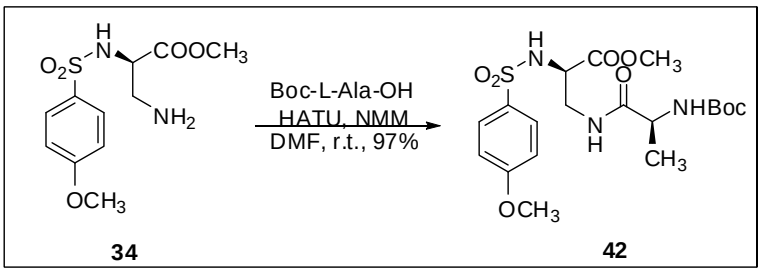

34 **42**

A solution of **34** (427 mg, 1.48 mmol), NMM (196 µL, 1.78 mmol) in dry DMF (5.5 mL) was added to a solution of Boc-Ala-OH (337 mg, 1.78 mmol) and NMM (196 µL, 1.78 mmol) in dry DMF (5.5 mL) and the mixture was stirred at room temperature for 30 min. HATU (677mg, 1.78 mmol) was added, and the mixture was stirred at room temperature for 17 h. The reaction mixture was diluited with 150 mL of CH_2Cl_2 and washed with brine (2x): the organic layer was dried over anhydrous Na_2SO_4 and the solvent was removed in vacuo to afford 1.20 g of a yellow pale solid. The crude material was purified by flash chromatography on silica gel (EtOAc/Petroleum ether 2:1) to afford **42** as a white glassy solid (635 mg, 93% yield).

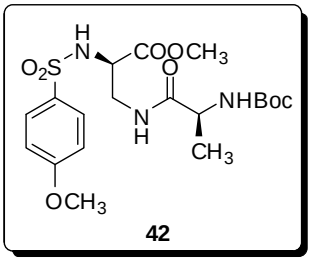

42

Anal. Calcd for $C_{19}H_{29}N_3O_8S$: C, 49.66; H, 6.36; N, 9.14. Found: C, 49.50; H, 6.32; N, 9.26. **^{1}H NMR** (200 MHz, $CDCl_3$); δ 7.78-7.74 (part AA' of an AA'MM' system, J_{AM} = 8.8 Hz, 2H), 6.99-6.94 (part MM' of an AA'MM' system, J_{AM} = 8.8 Hz, 2H), 6.74-6.66 (m, 1H, NH), 5.63 (d, J = 7.8 Hz, 1H, NH), 4.99 (d, J = 7.2 Hz, 1H, NH), 4.20-4.06 (m, 1H, CH aa), 4.14-3.93 (m, 1H, CH aa), 3.86 (s, 3H, OCH_3), 3.74-3.41 (m, 2H, CH_2N), 3.60 (s, 3H, $COOCH_3$), 1.46 (s, 9H, Boc), 1.36 (d, J = 7.4 Hz, 3H, CH_3 Ala). **^{13}C NMR** (50 MHz, $CDCl_3$): δ 173.2, 169.7, 162.8, 155.2, 130.2, 129.1, 114.0, 55.4, 54.9, 52.8, 50.0, 41.5, 28.1, 17.9.

Synthesis of compound 43.

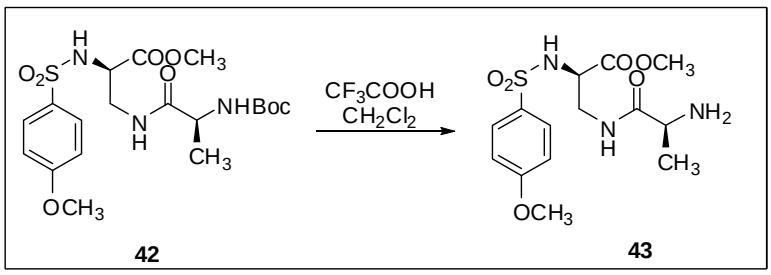

42 **43**

To a solution of **42** (620 mg, 1.35 mmol) in dry CH_2Cl_2 (25 mL) CF_3COOH (2.30 mL, 29.7 mmol) was added. After 1.5 h 20 mL of toluene were added and solvent was removed in vacuo to afford a yellow pale solid that was used without any further purification.

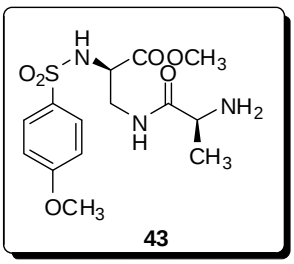

43

^{1}H NMR (200 MHz, CD_3OD); δ 7.78-7.73 (part AA' of an AA'MM' system, J_{AM} = 8.4 Hz, 2H), 7.06-7.02 (part MM' of an AA'MM' system, J_{AM} = 8.4 Hz, 2H), 4.08 (at, *J* = 6.2 Hz, 1H), 3.95-3.86 (m, 1H), 3.86 (s, 3H), 3.50-3.45 (m, 2H), 3.45 (s, 3H), 1.48 (d, *J* = 7.4 Hz, 3H). **^{13}C NMR** (50 MHz, CD_3OD): δ

170.2, 169.9, 163.2, 131.8, 129.0, 113.8, 55.0, 54.8, 51.5, 41.2, 16.2.

Synthesis of compound 44.

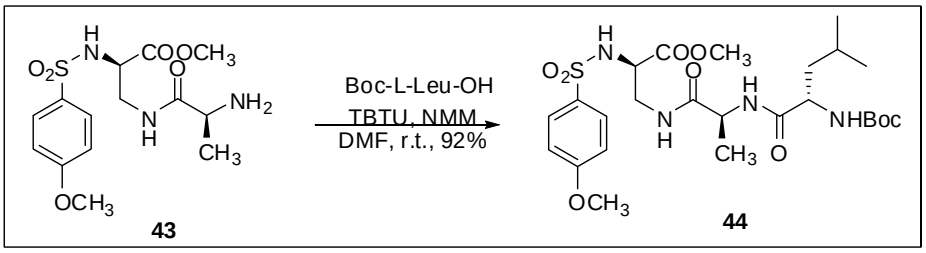

A solution of Boc-Leu-OH (530 mg, 2.29 mmol) and NMM (251 µL, 2.29 mmol) in dry DMF (7 mL) was added to a solution of **43** (985 mg, 2.08 mmol), NMM (251 µL, 2.29 mmol) in dry DMF (7 mL) and the mixture was stirred at room temperature for 20 min. TBTU (735 mg, 2.29 mmol) was added, and the mixture was stirred at room temperature for 20 h. The reaction mixture was diluited with 250 mL of CH_2Cl_2 and washed with HCl (1%, H_2O), $NaHCO_3$ sat. sol. and finally with water (2x). The organic layer was dried over anhydrous Na_2SO_4 and the solvent was removed in vacuo to afford 2.30 g of a yellow pale solid. The crude material was purified by flash chromatography on silica gel (EtOAc/Petroleum ether 3:1) to afford **44** as a white glassy solid (1.09 g, 92% yield).

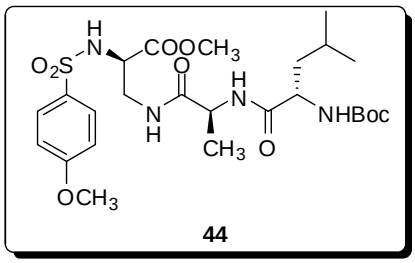

Anal. Calcd for $C_{25}H_{40}N_4O_9S$: C, 52.43; H, 7.04; N, 9.78. Found: C, 52.24; H, 7.35; N, 10.08. **^{1}H NMR** (200 MHz, $CDCl_3$); δ 7.80-7.72 (part AA' of an AA'MM' system, J_{AM} = 9.2 Hz, 2H), 7.03-6.92 (m, 3H), 6.57-6.62 (d, *J* = 7.4 Hz, 1H), 5.90-5.83 (m, 1H), 5.05-4.96 (m, 1H), 4.52-4.37 (m, 1H), 4.18-3.94 (m, 1H), 3.86 (s, 3H), 3.73-3.50 (m, 5H), 1.80-1.53 (m, 3H), 1.47 (s, 9H), 1.38 (d, *J* = 7.0 Hz, 3H), 0.98-0.94 (m, 6H). **^{13}C NMR** (50 MHz, $CDCl_3$): δ 173.3, 170.2, 163.1, 156.1, 131.0, 129.3, 114.2, 80.4, 55.6, 55.3, 52.9, 49.1, 40.7, 28.3, 24.7, 22.9, 21.6, 18.0.

Synthesis of compound 45.

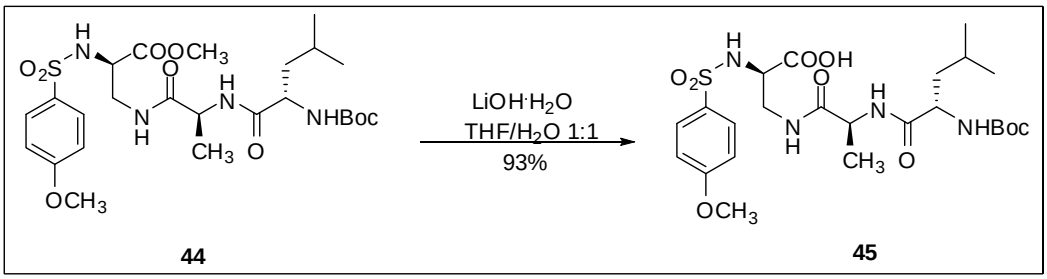

To a solution of **44** (250 mg, 0.44 mmol) in 14 mL of THF/H_2O 1:1, $LiOH \cdot H_2O$ (37.0 mg, 0.88 mmol) was added and the mixture was stirred for 2,4 h at rt, then H_3PO_4 1M was added (pH=4). EtOAc (40 mL) was added and the aqueous phase was separated and extracted 3x with EtOAc. The combined organic layer were dried over anhydrous Na_2SO_4 and the solvent was removed in vacuo to afford **45** (227 mg, 93% yield) of a white glassy solid.

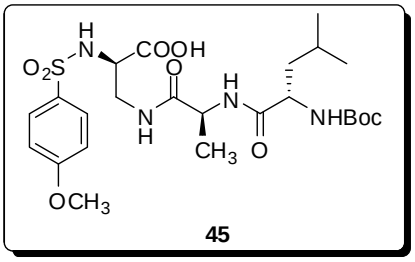

45

^{1}H NMR (200 MHz, CD_3OD): δ 7.80-7.74 (part AA' of an AA'MM' system, J_{AM} = 8.8 Hz, 2H), 7.03-6.99 (part MM' of an AA'MM' system, J_{AM} = 8.8 Hz, 2H), 4.35-4.24 (m, 1H), 4.15-4.0.8 (m, 1H), 3.84 (s, 3H), 3.75-3.69 (m, 1H), 3.50-3.44 (m, 2H), 1.77-1.1.45 (m, 3H), 1.45 (s, 9H), 1.34 (d, *J* = 7.0 Hz, 3H), 0.96-0.92 (m, 6H). **^{13}C NMR** (50 MHz, CD_3OD): δ 173.0, 172.7, 170.5, 162.1, 155.7, 131.0, 128.0, 112.9, 77.1, 53.9, 52.2, 48.1, 40.6, 39.6, 26.5, 23.6, 21.3, 19.5, 16.2.

Synthesis of compound 47.

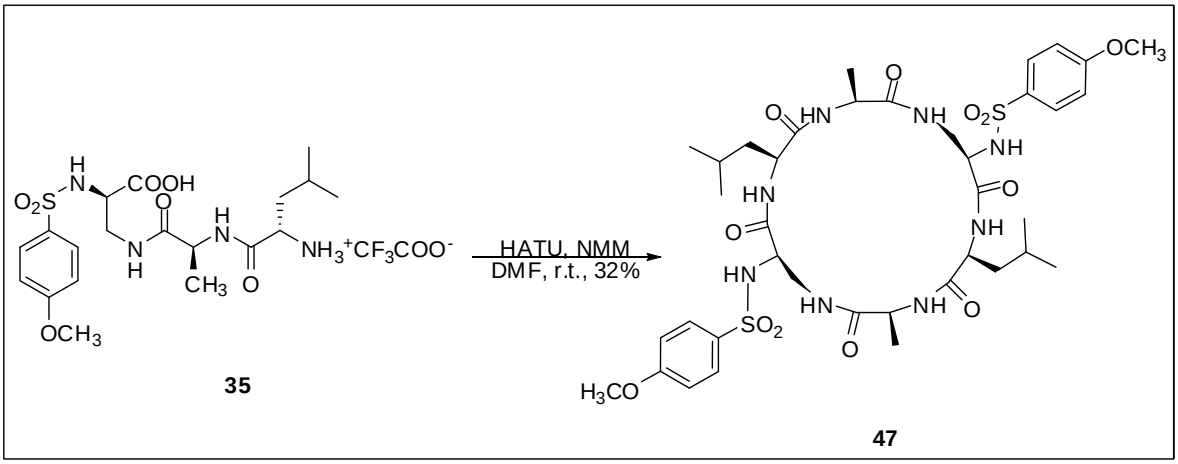

35 **47**

To solution of **35** (218 mg, 0.38 mmol) and NMM (100 µL, 0.91 mmol) in dry DMF (8 mL) was added HATU (175 mg, 0.46 mmol) was added, and the mixture was stirred at room temperature for 20 h. The reaction mixture was diluited with 100 mL of CH_2Cl_2 and washed with water (4x). The organic layer was dried over anhydrous Na_2SO_4 and the solvent was removed in vacuo to afford 280 mg of a crude product. The crude material was purified by flash chromatography on silica gel (EtOAc then EtOAc/CH_3OH 10:1) to afford **47** as a white solid (50.0 mg, 32% yield).

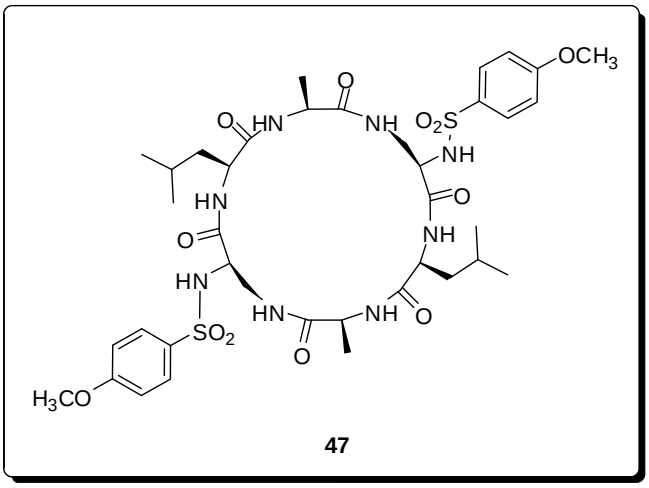

47

ESI-MS $[M+H]^+$ calcd 881.35. Found 881.45. $[M+Na]^+$ calcd. 903.34, Found 903.55. **^{13}C NMR** (50 MHz, DMSO): 174.5, 171.9, 169.5, 162.7, 131.9, 129.2, 128.9, 114.8, 114.6, 57.9, 56.1, 52.2, 49.2, 42.1, 40.7, 40.4, 24.4, 23.8, 23.6, 22.2, 22.0, 18.2.

Synthesis of compound 48.

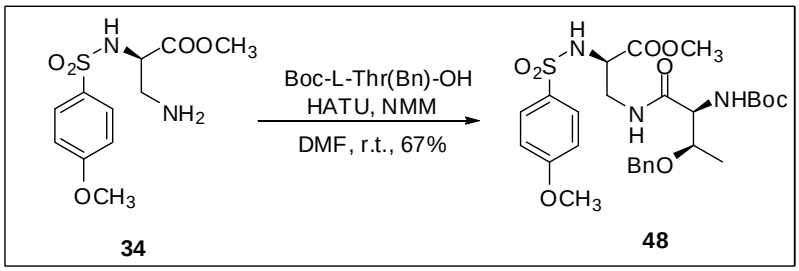

34 48

A solution of **34** (677 mg, 2.35 mmol), NMM (285 µL, 2.35 mmol) in dry DMF (7 mL) was added to a solution of Boc-Thr(OBn)-OH (727 mg, 2.35 mmol) and NMM (285 µL, 2.35 mmol) in dry DMF (6 mL) and the mixture was stirred at room temperature for 30 min. HATU (973 mg, 2.56 mmol) was added, and the mixture was stirred at room temperature for 17 h. The reaction mixture was diluited with 150 mL of EtOAc and washed with brine (2x): the organic layer was dried over anhydrous Na_2SO_4 and the solvent was removed in vacuo to afford 1.30 g of a yellow pale solid. The crude material was purified by flash chromatography on silica gel (EtOAc/Petroleum ether 1:1 then EtOAc) to afford **48** as a white glassy solid (912 mg, 67% yield).

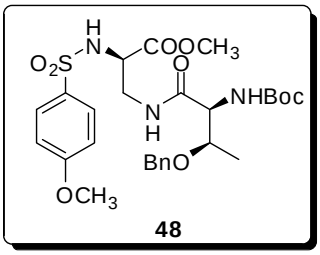

48

Anal. Calcd for $C_{27}H_{37}N_3O_9S$: C, 55.94; H, 6.43; N, 7.25. Found: C, 55.54; H, 6.44; N, 7.33. **^{1}H NMR** (200 MHz, $CDCl_3$): δ 7.76-7.68 (part AA' of an AA'MM' system, J_{AM} = 8.8 Hz, 2H), 7.37-7.26 (m, 5H), 6.97-6.85 (m, 3H), 5.51-5.42 (m, 2H), 4.66-4.60 (part A of an AB system, J_{AB} =11.4, 1H), 4.57-4.51 (part B of an AB system, J_{AB} =11.4, 1H), 4.22-4.10 (m, 2H), 3.96-3.89 (m, 1H), 3.85 (s, 3H), 3.74-3.46 (m, 2H), 3.57 (s, 3H), 1.47 (s, 9H), 1.16 (d, *J* = 6.2 Hz, 3H). **^{13}C NMR** (50 MHz, $CDCl_3$): δ 170.6, 169.9, 163.0, 129.3, 128.5, 127.8, 127.7, 114.3, 74.5, 71.7, 57.2, 55.7, 55.5, 53.1, 42.0, 28.5, 15.7.

Synthesis of compound 49.

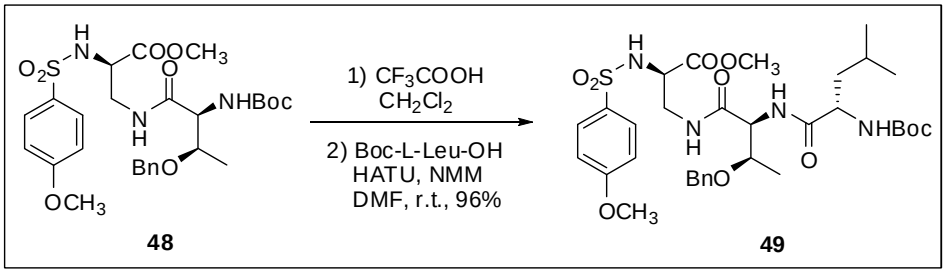

To a solution of **48** (700 mg, 1.21 mmol) in dry CH_2Cl_2 (20 mL) CF_3COOH (2.05 mL, 26.6 mmol) was added. After 2 h 10 mL of toluene were added and solvent was removed in vacuo to afford a yellow pale solid that was used without any further purification.

A solution of the crude product, NMM (145 µL, 1.33 mmol) in dry DMF (4 mL) was added to a solution of Boc-Leu-OH (336 mg, 1.45 mmol) and NMM (145 µL, 1.33 mmol) in dry DMF (4 mL) and the mixture was stirred at room temperature for 30 min. HATU (551 mg, 1.45 mmol) was added, and the mixture was stirred at room temperature for 17 h. The reaction mixture was diluited with 100 mL of CH_2Cl_2 and washed with water (3x), and the aqueous phase was extracted with CH_2Cl_2 (1x): the combined organic layer were dried over anhydrous Na_2SO_4 and the solvent was removed in vacuo to afford 1.40 g of a yellow pale solid. The crude material was purified by flash chromatography on silica gel (EtOAc/Petroleum ether 2:1) to afford **49** as a white glassy solid (860 mg, 97% yield).

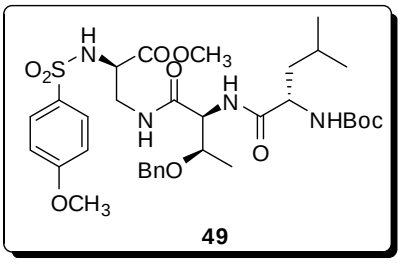

Anal. Calcd for $C_{33}H_{48}N_4O_{10}S$: C, 57.21; H, 6.98; N, 8.09. Found: C, 57.25; H, 7.06; N, 8.05. **^{1}H NMR** (200 MHz, $CDCl_3$): δ 7.78-7.71 (part AA' of an AA'MM' system, J_{AM} = 9.2 Hz, 2H), 7.40-7.28 (m, 5H), 7.17-7.10 (m, 1H), 6.97-6.88 (m, 3H), 5.88 (bd, *J* = 8.0 Hz, 1H), 4.92 (bd, *J* = 5.2 Hz, 1H), 4.62-4.57 (part A of an AB system, J_{AB} =11.4, 1H), 4.52-4.46 (part B of an AB system, J_{AB} =11.4, 1H), 4.38-4.22 (m, 2H), 4.12-3.59 (m, 3H), 3.59 (s, 3H), 3.56 (s, 3H), 3.44-3.31 (m, 1H), 1.75-1.44 (m, 3H), 1.41 (s, 9H), 1.16 (d, *J* = 6.6 Hz, 3H), 0.98 (ad, *J* = 5.2 Hz, 6H). **^{13}C NMR** (50 MHz, $CDCl_3$): δ 172.5, 170.2, 169.6, 162.8, 156.0, 137.8, 131.1, 129.3, 128.4, 127.7, 127.6, 114.1, 81.05, 73.9, 71.8, 57.3, 55.7, 55.4, 54.3, 53.0, 42.5, 40.9, 28.3, 25.1, 23.3, 21.8, 16.5.

Synthesis of compound 50.

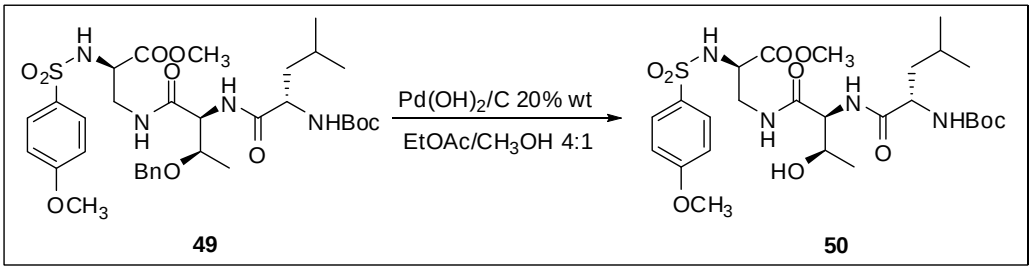

To a solution of **49** (400 mg, 0.58 mmol) in EtOAC/CH_3OH 4:1 (5 mL) $Pd(OH)_2/C$ 20% wt. was added (200 mg, 50% wt.). The mixture was stirred at room temperature for 17 h, then was filtrated on Celite® and the solvent was removed in vacuo to afford **50** (345 mg, quantitative yield) of a white glassy solid, that was used without any further purification.

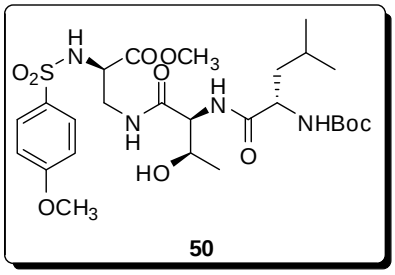

^{1}H NMR (200 MHz, CD_3OD): δ 7.78-7.73 (part AA' of an AA'MM' system, J_{AM} = 8.8 Hz, 2H), 7.06-7.02 (part MM' of an AA'MM' system, J_{AM} = 8.8 Hz, 2H), 4.20-4.04 (m, 4H), 3.45-3.34 (m, 2H), 3.47 (s, 3H), 1.78-1.43 (m, 3H), 1.46 (s, 9H), 1.14 (d, J = 6.2 Hz, 3H), 0.98-0.92 (m 6H).

Synthesis of compound 51.

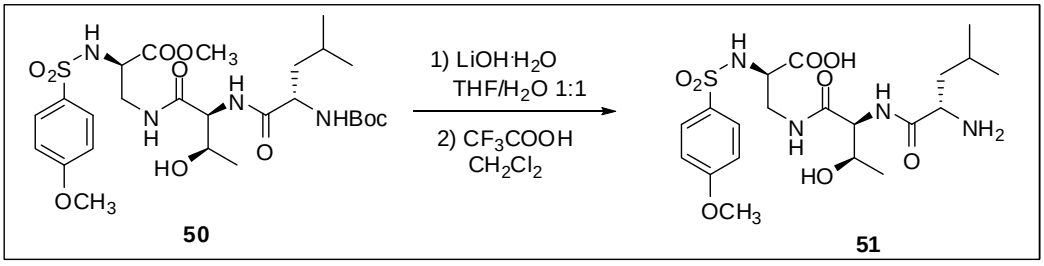

To a solution of **50** (150 mg, 0.25 mmol) in 4 mL of THF/H_2O, $LiOH{\cdot}H_2O$ (21.0 mg, 0.50 mmol) was added and the mixture was stirred for 2,3 h at rt, then H_3PO_4 1M was added (pH=2). EtOAc (40 mL) was added and the aqueous phase was separated and extracted 2x with EtOAc. The combined organic layer were dried over anhydrous Na_2SO_4 and the solvent was removed in vacuo. The crude was re-dissolved in dry CH_2Cl_2 (4 mL) and then CF_3COOH was added (420 µL, 5.50 mmol). The mixture was stirred at room temperature for 2 h, then toluene (10 mL) was added and the solvent was removed in vacuo. The crude was purified by reversed-phase semi-preparative HPLC to give of compound **51** (73.0 mg, 60 % yield).

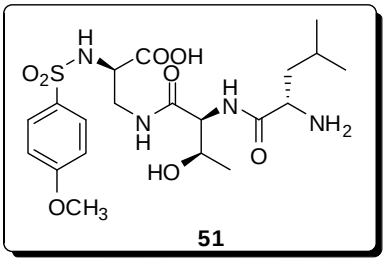

51

Anal. Calcd for $C_{20}H_{32}N_4O_8S + H_2O$: C, 47.42; H, 6.77; N, 11.06. Found: C, 47.68; H, 6.98; N, 10.57. **^{1}H NMR** (200 MHz, CD_3OD): δ 7.82-7.74 (part AA' of an AA'MM' system, J_{AM} = 9.2 Hz, 2H), 7.06-6.99 (part MM' of an AA'MM' system, J_{AM} = 9.2 Hz, 2H), 4.35 (d, *J* = 4.0 Hz, 1H), 4.25-4.12 (m, 1H), 4.06-3.99 (m, 1H), 3.85 (s, 3H), 3.64-3.59 (m, 1H), 3.57-3.41 (m, 2H), 1.87-1.65 (m, 3H), 1.20 (d, *J* = 6.2 Hz, 3H), 1.024-0.98 (m, 6H). **^{13}C NMR** (50 MHz, CD_3OD): δ 169.5, 168.7, 162.1, 130.3, 128.1, 112.9, 66.1, 58.2, 55.7, 53.8, 50.8, 41.6, 39.2, 23.2, 21.0, 19.6, 17.8.

Synthesis of compound 52.

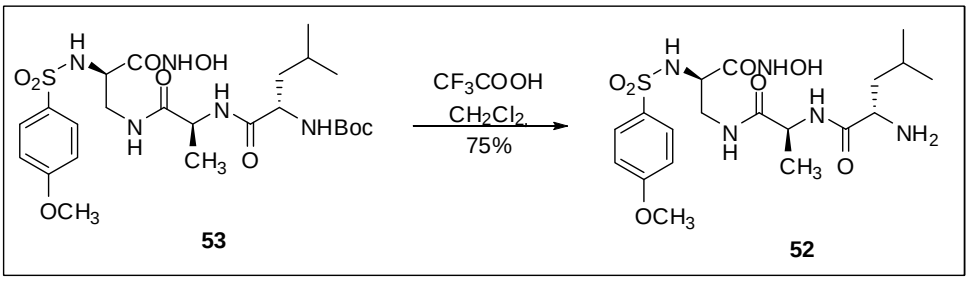

53 **52**

To a solution of compound **53** (42.0 mg, 0.07 mmol) in CH_2Cl_2 (1.25 mL), CF_3COOH (124 µL, 1.61 mmol) was added. The mixture was stirred at room temperature for 1 h, then toluene (5 mL) was added and the solvent was removed in vacuo. The crude was purified by reversed-phase semi-preparative HPLC to give of compound **52** (25.0 mg, 75% yield).

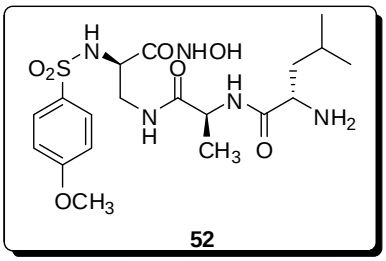

52

ESI-MS $[M+H]^+$ calcd 474.20. Found 474.25. $[M+Na]^+$ calcd 496.18. Found 496.25. **^{1}H NMR** (200 MHz, CD_3OD): δ 7.81-7.74 (part AA' of an AA'MM' system, J_{AM} = 9.2 Hz, 2H), 7.08-7.00 (part MM' of an AA'MM' system, J_{AM} = 9.2 Hz, 2H), 4.32 (q, *J* = 7.00 Hz, 1H), 3.92-3.81 (m, 2H), 3.87 (s, 3H), 3.33-3.29 (m, 2H), 1.82-1.63 (m, 3H), 1.36 (d, *J* = 7.00 Hz, 3H), 1.04-0.99 (m, 6H). **^{13}C NMR** (50 MHz, CD_3OD): δ 173.4, 169.0, 166.5, 163.1, 131.8, 128.7, 113.9, 54.9, 53.8, 51.6, 49.4, 41.6, 40.4, 24.1, 21.9, 20.7, 16.9.

Synthesis of compound 53.

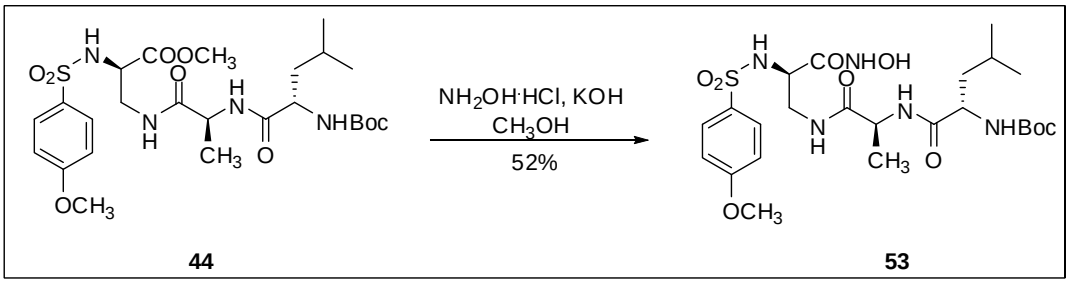

To a solution of $NH_2OH{\cdot}HCl$ (53.8 mg, 0.78 mmol) in 2 mL of CH_3OH was added a solution of KOH (87.0 mg, 1.56 mmol) in 1 mL CH_3OH and the suspension was stirred at room temperature for 30'. This suspension was to compound **44** (150 mg, 0.26 mmol). The reaction mixture was stirred for 24 h then a mixture of AcOH/H_2O 1:1 (10 mL) was added. The aqueous phase was separated and extracted 4x with EtOAc. The combined organic layer were dried over anhydrous Na_2SO_4 and the solvent was removed in vacuo. The crude product which was purified by a flash column chromatography on silica gel (from EtOAc to EtOAc/CH_3OH 5:1) to afford **53** (78.0 mg, 52% yield) as a pale yellow solid.

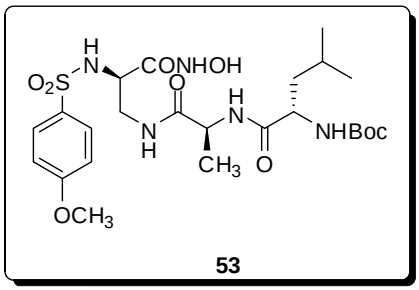

^{1}H NMR (200 MHz, CD_3OD): δ 7.77-7.72 (part AA' of an AA'MM' system, J_{AM} = 8.8 Hz, 2H), 6.99-6.95 (part MM' of an AA'MM' system, J_{AM} = 8.8 Hz, 2H), 4.26-4.02 (m, 2H), 3.84 (s, 3H), 3.84-3.74 (m, 1H), 3.35-3.28 (m, 2H), 1.74-1.24 (m, 15H), 0.94-0.90 (m, 6H). **^{13}C NMR** (50 MHz, CD_3OD): δ 174.1, 174.0, 166.5, 163.0, 156.5, 131.2, 128.9, 114.1, 80.3, 55.3, 54.2, 53.2, 41.7, 40.8, 28.0, 24.7, 22.8, 21.4, 21.2, 17.2.

Synthesis of compound 54.

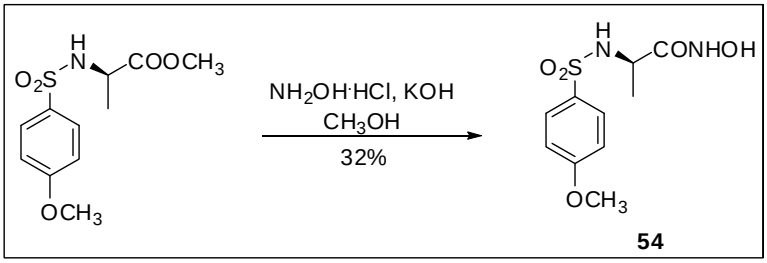

A suspension of KOH (307 mg, 5.49 mmol) in 2.5 mL of CH_3OH were refluxed for 15', then $NH_2OH{\cdot}HCl$ (252 mg, 3.66 mmol) was added. The suspension was stirred at 40 °C for 5' . This suspension was cooled to 0 °C and added to a solution of (R)-methyl 2-(4-

methoxyphenylsulfonamido)propanoate (250 mg, 0.91 mmol) in 1 mL of CH_3OH. The reaction mixture was stirred for 18 h then was diluted with EtOAc (15 mL), filtered and concentrated to dryness. The crude product (700 mg) was purified by a flash column chromatography on silica gel (from CH_2Cl_2/CH_3OH 13:1) to afford **34** (80.0 mg, 32%) as a white solid.

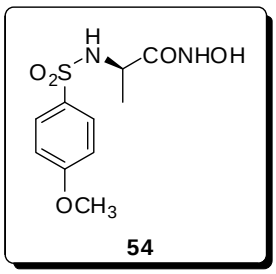

54

^{1}H NMR (200 MHz, CD_3OD): δ 7.81-7.75 (part AA' of an AA'MM' system, J_{AM} = 8.8 Hz, 2H), 7.08-7.03 (part MM' of an AA'MM' system, J_{AM} = 8.8 Hz, 2H), 3.87 (s, 3H), 3.68 (q, *J* = 7.00 Hz, 1H), 1.16 (d, *J* = 7.00 Hz, 3H). **^{13}C NMR** (50 MHz, CD_3OD): 169.6, 163.0, 131.9, 128.7, 113.9, 54.9, 50.3, 18.1.

Compound 57.

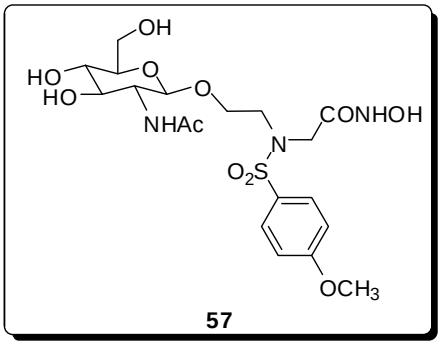

57

^{1}H NMR (200 MHz, CD_3OD): δ 7.82-7.78 (part AA' of an AA'MM' system, J_{AM} = 8.8 Hz, 2H), 7.10-7.06 (part MM' of an AA'MM' system, J_{AM} = 8.8 Hz, 2H), 4.37 (d, *J* = 8.4 Hz, 1H), 4.02- 3.60 (m, 7H), 3.88 (s, 3H), 3.49-3.20 (m, 5H), 2.00 (s, 3H). **^{13}C NMR** (50 MHz, CD_3OD): δ 172.7, 166.5, 163.3, 130.0, 129.3, 129.3, 114.0, 101.3, 76.6, 74.6, 70.5, 68.2, 61.2, 55.8, 55.0, 49.3, 21.9.

Compound 58.

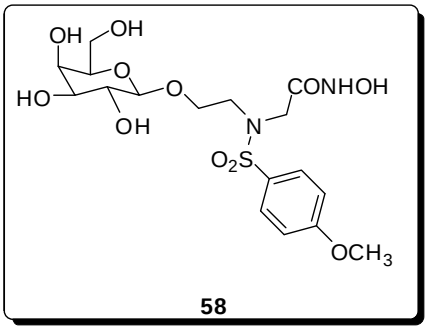

58

^{1}H NMR (200 MHz, CD_3OD): δ 7.84-7.79 (part AA' of an AA'MM' system, J_{AM} = 8.8 Hz, 2H), 7.11-7.07 (part MM' of an AA'MM' system, J_{AM} = 8.8 Hz, 2H), 4.20 (d, *J* = 6.6 Hz, 1H), 4.09-3.98 (m, 1H), 3.88 (m, 5H), 3.82-3.70 (m, 4H), 3.55-3.38 (m, 5H). **^{13}C NMR** (50 MHz, CD_3OD): δ 169.9, 163.3, 129.9, 114.0, 103.6, 75.4, 73.6, 71.2, 69.0, 68.0, 61.2, 54.9, 49.9, 49.5.

Compound 59.

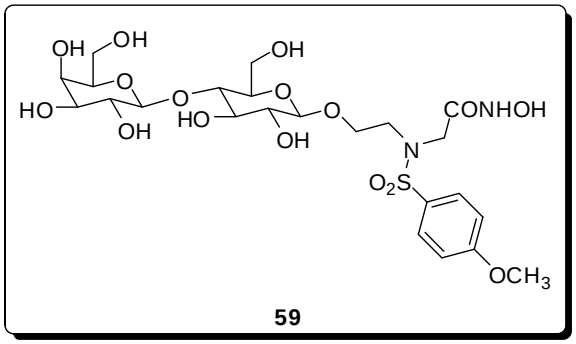

59

^{1}H NMR (200 MHz, CD_3OD): δ 7.78-7.72 (part AA' of an AA'MM' system, J_{AM} = 8.8 Hz, 2H), 7.07-7.02 (part MM' of an AA'MM' system, J_{AM} = 8.8 Hz, 2H), 4.32 (d, *J* = 8.0 Hz, 1H), 4.27 (d, *J* = 8.0 Hz, 1H), 3.88-3.76 (m, 3H), 3.80 (s, 3H), 3.72-3.14 (m, 15H).

Synthesis of compound 63.

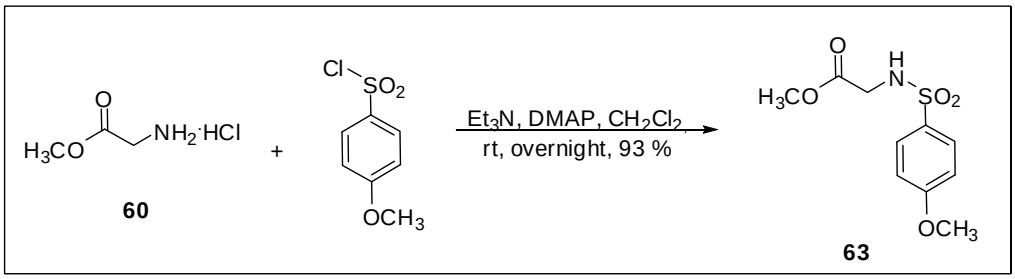

To a stirred suspension of glycine methyl esther hydrochloride **60** (300 mg, 2.39 mmol) in CH_2Cl_2 (5 mL) 1.00 mL of NEt_3 (7.17 mmol) were added at 0°C. The suspension was stirred at room temperature for 30', cooled to 0°C then *para*-toluen sulphonyl chloride (493 mg, 2.39 mmol) and DMAP (catalytic amount) were added. The reaction mixture was stirred at room temperature for 24 h then diluted with CH_2Cl_2. The mixture was neutralized with HCl (3%, H_2O). The organic phase was dried over Na_2SO_4 and the solvent was removed in vacuum. The crude product (650 mg) was purified by flash column chromatography on silica gel (petroleum ether/EtOAc 1:1) to afford **63** (580 mg, 93%) as a white solid.

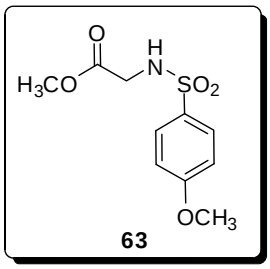

63

M.p.: 62-64 °C. **Anal.** for $C_{10}H_{13}NO_5S$ calcd: C, 46.32; H, 5.05; N, 5.40. Found: C, 46.21; H, 5.17; N, 5.51. **^{1}H NMR** (200MHz, $CDCl_3$): δ 7.81-7.77 (AA' part of an AA'MM' system, J_{AM} = 8.8 Hz, 2H), 6.99-6.95 (MM' part of an AA'MM' system, J_{AM} = 8.8 Hz, 2H), 5.08-5.06 (m, 1H), 3.86 (s, 3H), 3.77 (d, *J* = 5.4 Hz), 3.64 (s, 3H). **^{13}C NMR** (50MHz, $CDCl_3$): δ 169.3, 162.9, 130.6, 129.2, 114.1, 55.5, 52.4, 43.9.

Synthesis of compound 64.

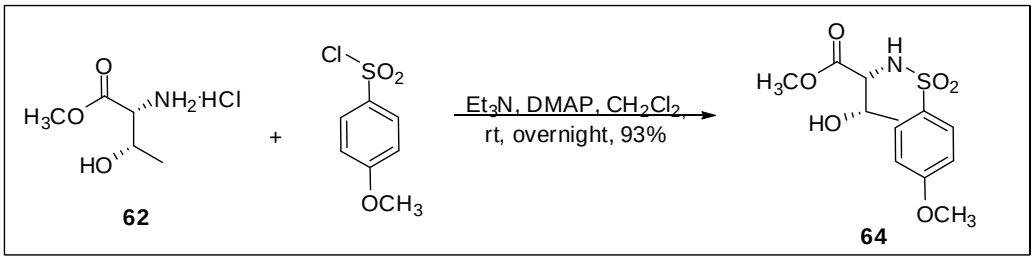

To a stirred suspension of **62** (1.00 g, 5.90 mmol), in CH_2Cl_2 (20 mL), 2.50 mL of NEt_3 (17.7 mmol) were added at 0°C. The suspension was stirred at room temperature for 30', cooled to 0°C then *para*-toluen sulphonyl chloride (1.22 g, 5.90 mmol) and DMAP (catalytic amount) were added. The reaction mixture was kept at room temperature for 18 h then diluted with CH_2Cl_2 and washed with a solution of HCl (3%, H_2O) (2x) and with brine (2x). The organic phase was dried over Na_2SO_4 and the solvent was removed in vacuum. The crude product was used without further purification to afford **64** (1.66 g, 93%) as a white solid.

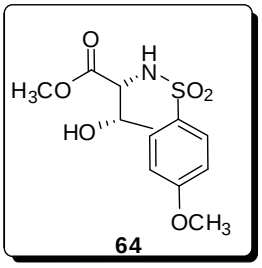

M.p.: 104-107 °C. **$[\alpha]^{25}_D$** +0.36 (c 0.60, $CHCl_3$). **Anal.** for $C_{12}H_{17}NO_6S$ calcd: C, 47.52; H, 5.65; N, 4.62. Found: C, 47.80; H, 6.09; N, 4.61. **^{1}H NMR** (200MHz, $CDCl_3$): δ 7.80-7.74 (AA' part of an AA'MM' system, J_{AM} = 8.8 Hz, 2H), 6.97-6.92 (MM' part of an AA'MM' system, J_{AM} = 8.8 Hz, 2H), 5.67 (d, *J* = 9.8, 1H), 4.20-4.08 (m, 1H), 3.88-3.76 (m, 1H), 3.53 (s, 3H), 2.48 (d, *J* = 5.6 Hz, 1H), 1.25 (d, *J* = 6.2 Hz, 1H), **^{13}C NMR** (50MHz, $CDCl_3$): δ 170.7, 162.8, 131.1, 129.3, 114.1, 68.4, 61.1, 55.7, 52.8, 20.1.

Synthesis of compound 65.

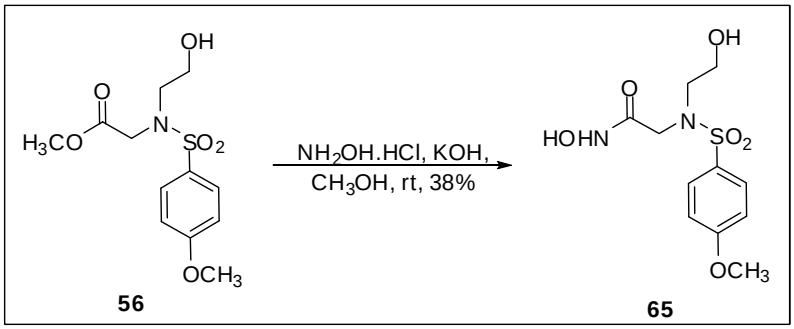

A suspension of KOH (244 mg, 4.35 mmol) and NH_2OH·HCl (240 mg, 3.48 mmol) in CH_3OH (1 mL) was stirred at room temperature for 1h, then a solution of **56** (300 mg, 0.87 mmol) in CH_3OH (2 mL) was added. The reaction mixture was stirred for 6 h, then diluted with EtOAc , washed with a

mixture AcOH/H_2O 1:1 and dried over Na_2SO_4. Concentration of the solvent under vacuum afford a crude product which was purified by flash column chromatography on silica gel (CH_2Cl_2/ CH_3OH 8:1) to afford **65** (114 mg, 38%) as a yellow solid.

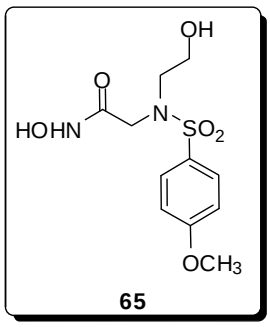

65

M.p.: 126-128 °C. **Anal.** for $C_{11}H_{16}N_2O_5S$ calcd: C, 43.41; H, 5.30; N, 9.21. Found: C, 43.57; H, 5.31; N, 9.51. **^{1}H NMR** (200MHz, CD_3OD): δ 7.81-7.77 (AA' part of an AA'MM' system, J_{AM} = 8.8 Hz, 2H), 7.10-7.06 (MM' part of an AA'MM' system, J_{AM} = 8.8 Hz, 2H), 3.87 (s, 3H), 3.81 (s, 2H), 3.68 (t, *J* = 5.4 Hz, 2H), 3.30-3.25 (m, 2H). **^{13}C NMR** (50MHz, CD_3OD): δ 168.7, 131.5, 131.2, 116.3, 116.2, 62.0, 57.0, 54.3, 45.4.

Synthesis of compound 67.

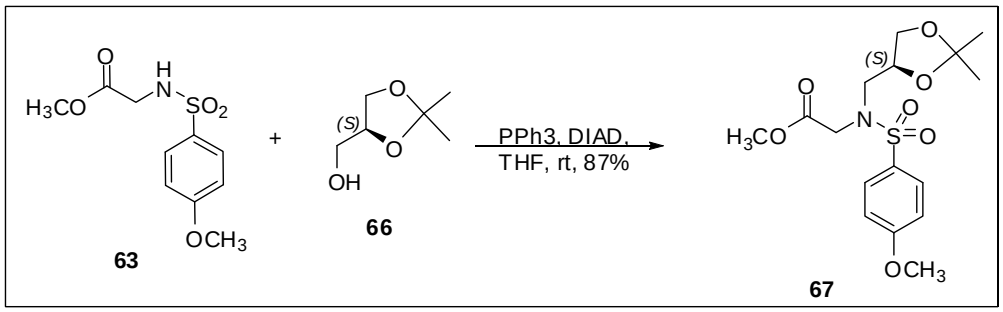

To a solution of **63** (1.04 g, 4.00 mmol), PPh_3 (1.37 g, 5.20 mmol) and **66** (0.69 g, 5.20 mmol) in dry THF (20 mL) DIAD (1.02 mL, 5.20 mmol) was slowly added. The reaction mixture was stirred overnight at room temperature then concentrated to dryness. 25 mL of a mixture cyclohexane/EtOAc 6:1 were added and the suspension was stirred for 30' at room temperature. The white solid was filtered off and the filtrate was concentrated to dryness. The crude product was purified by flash column chromatography on silica gel ($CHCl_3$/EtOAc 7:1) to afford **67** (1.30 g, 87%) as an oil.

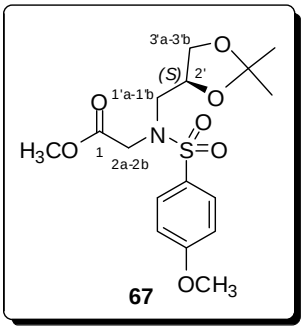

67

$[\alpha]^{25}_D$: +4.39 (c 0.41, $CHCl_3$). **HRMS** for $C_{16}H_{23}NO_7S$+H calcd: 374.1273. Found: 374.1268. **^{1}H NMR** (200MHz, $CDCl_3$) : δ 7.77-7.74 (AA' part of an AA'MM' system, J_{AM} = 9.2 Hz, 2H), 6.97-6.95 (MM' part of an AA'MM' system, J_{AM} = 9.2 Hz, 2H), 4.34-4.22 (m, 3H, H-2a, H-2', H-2b), 4.09-4.02 (A part of an ABX system, J_{AX} = 6.4 Hz, J_{AB} = 8.4 Hz, 1H, H-3'a), 3.87 (s, 3H, O*C*H_3), 3.68-3.64 (B part of an ABX system, J_{BX} = 6.8 Hz, J_{AB} = 8.4 Hz, 1H, H-3'b), 3.62 (s, 3H, COO*C*H_3), 3.62-3.52 (A part of an ABX system, J_{AX} = 4.0

Hz, J_{AB} = 14.8 Hz, 1H, H-1'a), 3.25-3.14 (B part of an ABX system, J_{BX} = 7.2 Hz, J_{AB} = 14.8 Hz, 1H, H-1'b), 1.35 (s, 3H, C(CH_3)$_2$), 1.30 (s, 3H, C(CH_3)$_2$). **^{13}C NMR** (50MHz, $CDCl_3$) : δ 169.7, 162.9, 131.0, 129.4, 114.1, 109.5, 75.4, 67.0, 55.5, 51.9, 50.4, 49.2, 26.6, 25.2.

Synthesis of compoundS 68 and 69.

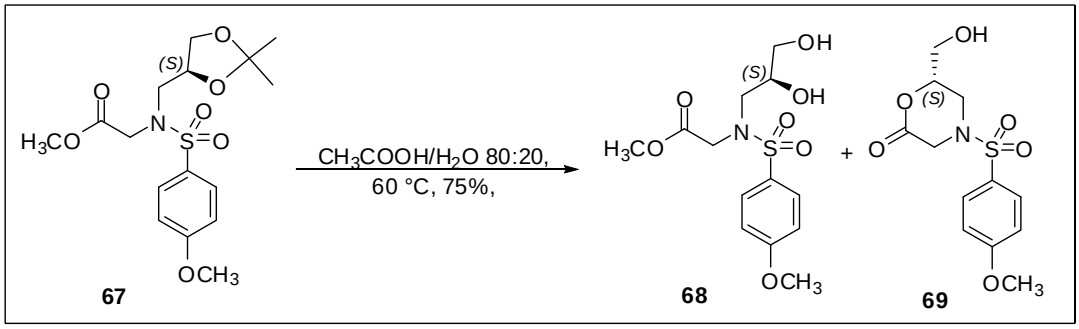

A solution of **67** (1.20 g, 3.21 mmol) in 18 mL of a mixture AcOH/H_2O 80:20 was left to stir at 60°C for 4 h then toluene (20 mL) was added. Concentration of the solvent under vacuum gave a crude product which was purified by a flash column chromatography on silica gel (EtOAc) to afford a mixture of **68** + **69** (total yield 75%) as an oil. An analytic amount of compound **68** has been purified for characterization.

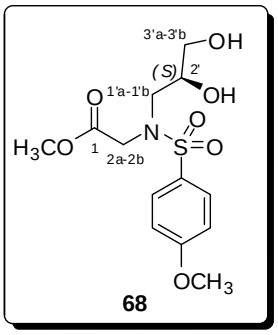

[α]$^{25}_D$: -7.00 (c 0.50, CH_3OH). **Anal.** for $C_{13}H_{19}NO_7S$ calcd: C, 46.84; H, 5.74; N, 4.20. Found: C, 47.07; H, 5.01; N, 4.66. **^{1}H NMR** (200MHz, $CDCl_3$): δ 7.78-7.73 (AA' part of an AA'MM' system, J_{AM} = 9.2 Hz, 2H), 7.00-6.96 (MM' part of an AA'MM' system, J_{AM} = 9.2 Hz, 2H), 4.12-4.08 (A part of an AB system, J_{AB} = 18.4 Hz, 1H), 4.02-3.97 (B part of an AB system, J_{AB} = 18.4 Hz, 1H), 3.92-3.85 (m, 1H), 3.87 (s, 3H), 3.76-3.56 (m, 1H), 3.72 (s, 3H), 3.39-3.28 (A part of an ABX system, J_{AX} = 7.6 Hz, J_{AB} = 14.6 Hz, 1H), 3.24-3.31 (B part of an ABX system, J_{BX} = 4.0 Hz, J_{AB} = 14.6 Hz, 1H), 2.42 (bs, 1H). **^{13}C NMR** (50MHz, $CDCl_3$): δ 170.6, 163.1, 130.1, 129.4, 114.3, 70.1, 63.4, 55.5, 52.4, 52.1, 50.2.

Synthesis of compound 70.

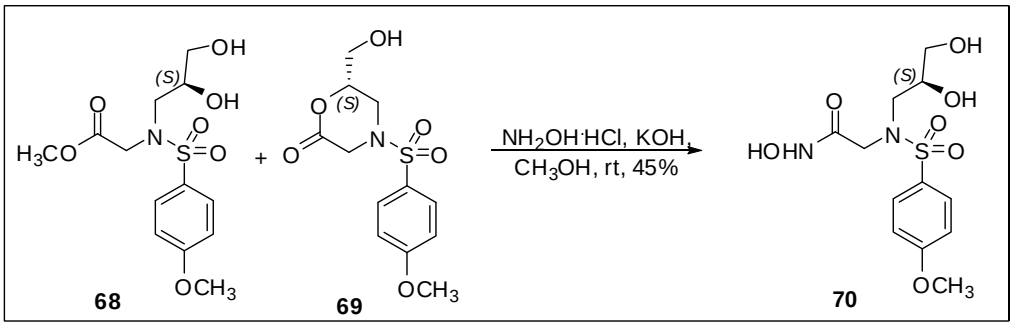

A suspension of KOH (168 mg, 3.00 mmol) and $NH_2OH \cdot HCl$ (167 mg, 2.40 mmol) in CH_3OH (2 mL) was stirred at room temperature for 1h, then a solution of **68** + **69** (0.60 mmol) in CH_3OH (2 mL) was added. The reaction mixture was stirred until no trace of starting material was revealed by TLC analysis (18 h), then concentrated to dryness. The crude product was dissolved in EtOAc, washed with a mixture AcOH/H_2O 1:1 and dried over Na_2SO_4. Concentration of the solvent under vacuum afford a crude product which was purified by HPLC (C_8 column Ultrasphere Beckman Coulter, AcCN/H_2O 10:90, AcCN/H_2O 30:70) to afford **70** (90.0 mg, 45%) as a pale yellow glassy solid.

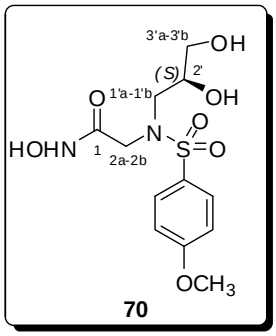

$[\alpha]^{25}_D$: -22.3 (c 0.48, CH_3OH). **HRMS** for $C_{12}H_{19}N_2O_7S$+H calcd: 335,0913. Found: 335.0909. **ESI-MS** $[M+H]^+$ calcd: 335.1. Found: 335.1. $[M+Na]^+$ calcd: 357.1. Found: 357.1. **^{1}H NMR** (400 MHz, CD_3OD) : δ 7.73-7.70 (AA' part of an AA'MM' system, J_{AM} = 8.8 Hz, 2H), 7.05-7.03 (MM' part of a AA'MM' system, J_{AM} = 8.8 Hz, 2H), 3.90-3.78 (m, 3H, CH_2-2, H-2'), 3.88 (s, 3H, OCH_3), 3.52-3.51 (m, 2H, CH-3'), 3.35-3.30 (m, 1H, H-1'a), 3.17-3.11 (B part of an ABX system, J_{BX} = 8.8 Hz, J_{AB} = 14.4 Hz, 1H, H-1'b). **^{13}C NMR** (50 MHz, CD_3OD) : δ 167.3, 163.3, 129.7, 129.3, 114.0, 70.5, 63.6, 54.9, 53.4, 50.0.

Synthesis of compound 71.

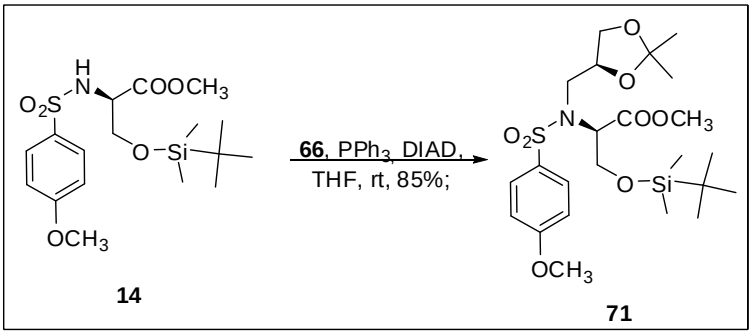

A solution of **14** (815 mg, 2.02 mmol), PPh_3 (692 mg, 2.63 mmol) and **66** (348 mg, 2.63 mmol) in dry THF (8 mL) was cooled to 0°C, then DIAD (0.52 mL, 2.63 mmol) was slowly added. The reaction mixture was heated to room temperature and stirred overnight then concentrated to dryness. 8 mL of a mixture cyclohexane/EtOAc 8:1 were added and the suspension was stirred for 30' at room temperature. The white solid was filtered off and the filtrate was concentrated to dryness. The crude product was purified by flash column chromatography on silica gel ($CHCl_3$/EtOAc 8:1) to afford **71** (890 mg, 85%) as a colourless oil.

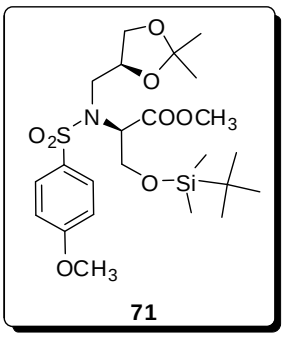

71

$[\alpha]^{25}_D$: +5.85 (c 0.41, $CHCl_3$). **Anal.** for $C_{23}H_{39}NO_8S$ calcd: C, 53.36; H, 7.49; N, 2.71. Found: C, 53.28; H, 7.18; N, 2.88. **^{1}H NMR** (200MHz, $CDCl_3$): δ 7.81-7.77 (AA' part of a AA'MM' system, J_{AM} = 8.8, 2H), 6.96-6.92 (MM' part of a AA'MM' system, J_{AM} = 8.8, 2H), 4.65 (t, J = 5.8, 1H), 4.47-4.34 (m, 1H), 4.13-4.01 (m, 2H), 3.86 (s, 3H), 3.77-3.70 (B part of a ABX system, J_{BX} = 6.6 Hz, J_{AB} = 8.4 Hz, 1H), 3.63 (s, 3H), 3.56-3.27 (m, 2H), 1.38 (s, 3H), 1.30 (s, 3H), 0.83 (s, 9H), 0.04 (s, 3H), 0.02 (s, 3H). **^{13}C NMR** (50 MHz, $CDCl_3$): δ 169.8, 162.7, 131.3, 129.6, 114.0, 109.3, 75.1, 67.6, 61.7, 61.2, 55.7, 52.3, 48.3, 27.0, 25.9, 25.6, 18.3, -5.3, -5.4.

Synthesis of compounds 72 and 73.

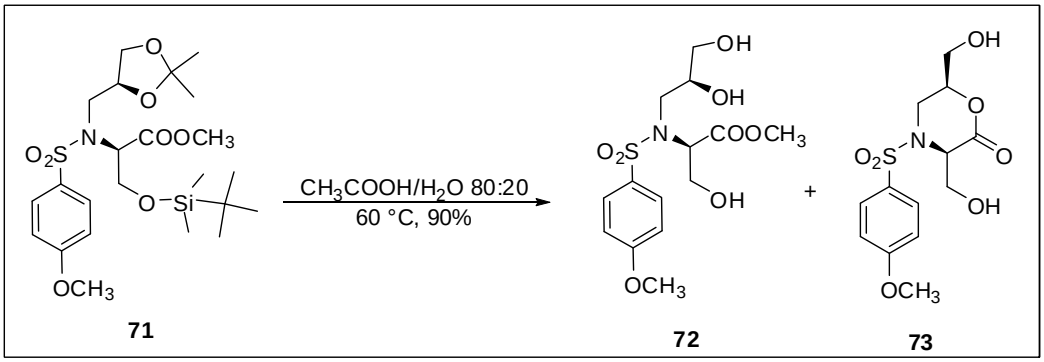

71 **72** **73**

A solution of **71** (300 mg, 0.58 mmol) in a mixture AcOH/H_2O 80:20 (5 mL) was heated at 60°C and stirred for 4 h, then toluene (5 mL) was added. Evaporation of the solvent under reduced pressure gave the crude product that was used without further purification (**72** + **73**) (total yield 90%).

Synthesis of compound 74.

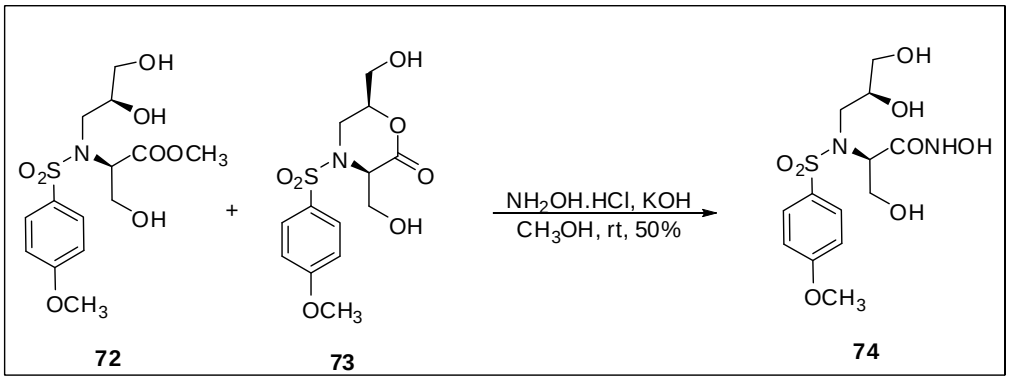

A suspension of KOH (151 mg, 2.70 mmol) and $NH_2OH{\cdot}HCl$ (150 mg, 2.18 mmol) in CH_3OH (2 mL) was stirred at room temperature for 1h, then a solution of a crude mixture of **72** + **73** (0.54 mmol) in CH_3OH (2 mL) was added. The reaction mixture was for 15 h then concentrated to dryness. The crude product was dissolved in EtOAc, washed with a mixture $AcOH/H_2O$ 1:1 and dried over Na_2SO_4. Concentration of the solvent under vacuum afford a crude product which was purified by HPLC (C_8 column Ultrasphere Beckman Coulter, $AcCN/H_2O$ 10:90, $AcCN/H_2O$ 20:80) to afford **74** (99.0 mg, 50%) as a white solid.

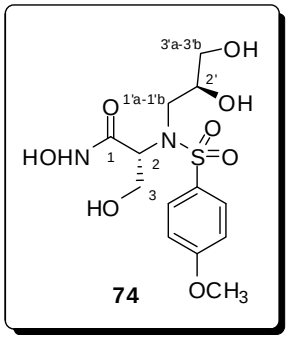

$[\alpha]^{25}_D$: -11.0 (c 0.25, CH_3OH). **HRMS:** calcd. for $C_{13}H_{20}N_2O_8S$+H: 365.1019; found: 365.1013. **ESI-MS** $[M+H]^+$ calcd: 365.1. Found: 365.1. **ESI-MS** $[M-H]^-$ calcd: 363.1. Found: 363.1. **^{1}H NMR** (400 MHz, CD_3OD): δ 7.86-7.83 (AA' part of an AA'MM' system, J_{AM} = 9.2 Hz, 2H), 7.11-7.09 (MM' part of a AA'MM' system, J_{AM} = 9.2 Hz, 2H), 4.41-4.37 (A part of a AXY system, J_{AX}= 8.0 Hz, J_{AY} = 5.5 Hz, 1H, H-2), 4.14-4.08 (m, 1H, H-2'), 3.91 (s, 3H, -OC*H*$_3$), 3.88-3.83 (X part of a AXY system, J_{AX} = 8.0 Hz, J_{XY} = 11.9 Hz, 1H, H-3a), 3.80-3.79 (Y part of a AXY system, J_{AY} = 5.6 Hz, J_{XY} = 12.0 Hz, 1H, H-3b), 3.65-3.60 (A part of a ABX system, J_{AX} = 3.6 Hz, J_{AB} = 15.6 Hz, 1H), 3.58-3.57 (A part of an AB system, J_{AB} = 4.0 Hz, 1H), 3.57-3.56 (B part of an AB system, J_{AB} = 4.0 Hz, 1H), 3.31-3.25 (B part of a ABX system, J_{BX} = 8.8 Hz, J_{AB} = 15.6 Hz, 1H). **^{13}C NMR** (50 MHz, CD_3OD): δ 169.1, 164.5, 131.6, 130.6, 115.2, 72.9, 64.9, 62.2, 60.7, 56.2, 49.7.

Synthesis of compound 75.

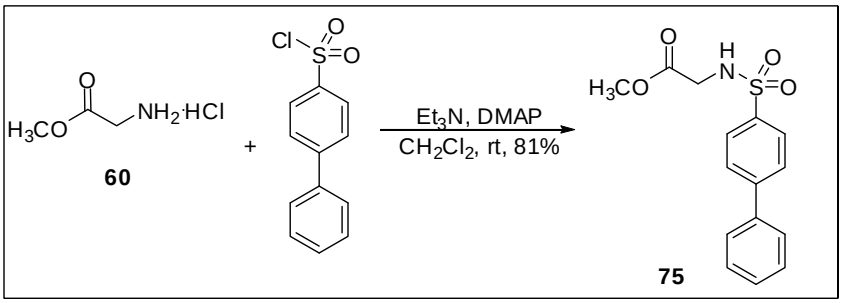

To a stirred suspension of **60** (500 mg, 4.00 mmol) in CH_2Cl_2 (5 mL), 1.66 mL of NEt_3 (12.0 mmol) were added at 0°C. The suspension was stirred at room temperature for 30', cooled to 0°C then *para*-biphenyl sulphonyl chloride (1.01 g, 4.00 mmol) and DMAP (catalytic amount) were added. The reaction mixture was kept at room temperature for 18 h then diluted with CH_2Cl_2. The mixture was neutralized with HCl (3%, H_2O) and washed with brine (3x). The organic phase was dried over Na_2SO_4 and the solvent was removed in vacuum. The crude product was purified by flash column chromatography on silica gel (petroleum ether/EtOAc 2:1) to afford **75** (990 mg, 81%) as a white solid.

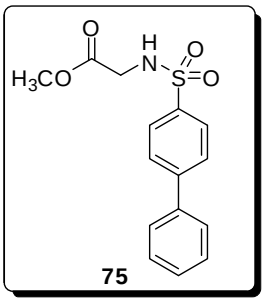

M.p.: 128-131 °C. **Anal.** for $C_{15}H_{15}NO_3S$ calcd: C, 59.00; H, 4.95; N, 4.59. Found: C, 59.26; H, 4.68; N, 4.32. **^{1}H NMR** (200MHz, $CDCl_3$): δ 7.95-7.91 (AA' part of an AA'MM' system, J_{AM} = 8.4 Hz, 2H), 7.74-7.70 (MM' part of an AA'MM' system, J_{AM} = 8.4 Hz, 2H), 7.68-7.41 (m, 5H), 5.15 (t, *J* = 5.4 Hz, 1H, NH), 3.84 (d, *J* = 5.4 Hz, 1H), 3.64 (s, 3H). **^{13}C NMR** (50MHz, $CDCl_3$): δ 169.3, 145.8, 139.1, 137.7, 128.0, 128.5, 127.5, 127.3, 52.6, 44.1.

Synthesis of compound 76.

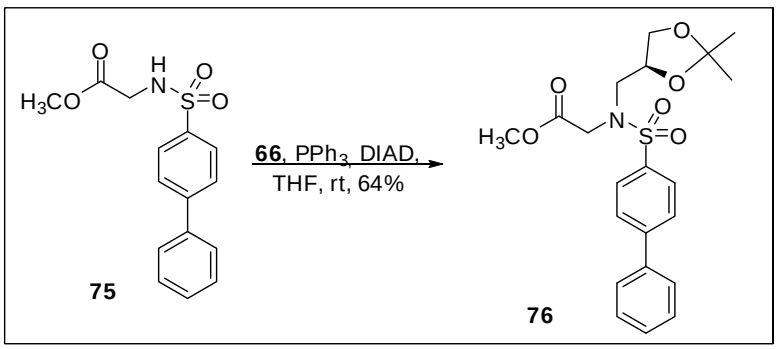

To a solution of **75** (700 mg, 2.29 mmol), PPh_3 (784 mg, 2.98 mmol) and **66** (394 mg, 2.98 mmol) in dry THF (9 mL) DIAD (586 µL, 2.98 mmol) was slowly added. The reaction mixture was stirred overnight at room temperature then concentrated to dryness. 10 mL of a mixture cyclohexane/EtOAc 8:1 were added and the suspension was stirred for 30' at room temperature. The white solid was filtered off and the filtrate was concentrated to dryness. The crude product (1.70 g) was purified by flash column chromatography on silica gel ($CHCl_3$/EtOAc 20:1) to afford **76** (617 mg, 64%) as an oil.

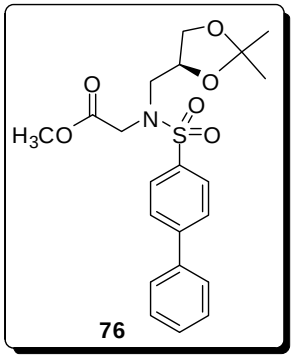

76

^{1}H NMR (200MHz, $CDCl_3$): δ 7.92- 7.86 (m, 2H), 7.74-7.60 (m, 2H), 7.53-7.41 (m, 5H), 4.40-4.18 (m, 3H), 4.12-4.04 (m, 1H), 3.74-3.59 (m, 2H), 3.61 (s, 3H), 3.31-3.20 (m, 1H), 1.37 (s, 3H), 1.31 (s, 3H). **^{13}C NMR** (50MHz, $CDCl_3$): δ 169.2, 145.6, 139.2, 138.0, 129.0, 128.4, 127.8, 127.5, 127.2, 109.7, 75.6, 67.2, 52.2, 50.8, 49.5, 26.9, 25.5.

Synthesis of compounds 77 and 78.

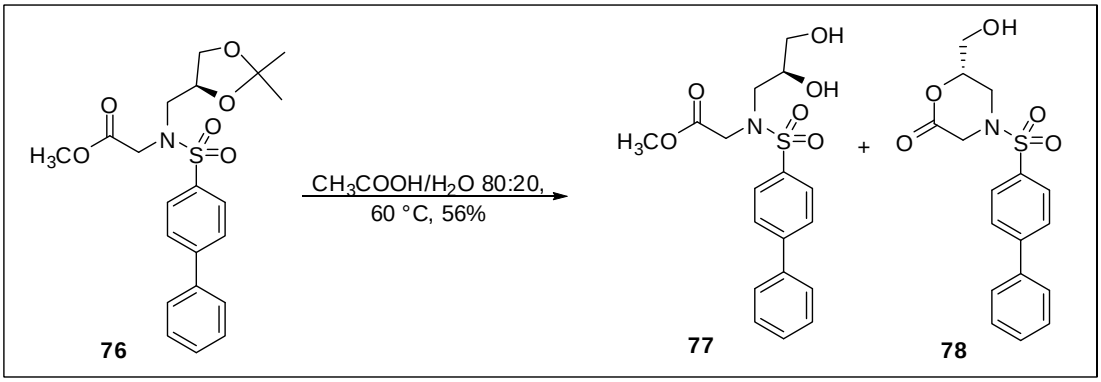

76 **77** **78**

A solution of **76** (550 mg, 1.31 mmol) in 17 mL of a mixture AcOH/H_2O 80:20 was left to stir at 60°C for 4 h then toluene (20 mL) was added. Concentration of the solvent under vacuum gave a crude product which was purified by a flash column chromatography on silica gel (CH_2Cl_2/CH_3OH 20:1) to afford a mixture of **77** + **78** (total yield 56%) as a white solid. An analytic amount of compound **77** has been purified for characterization.

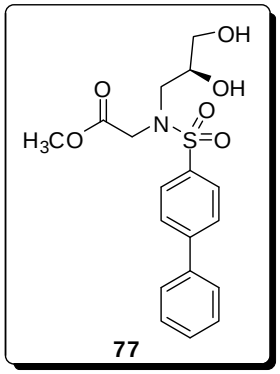

77

^{1}H NMR (200MHz, CD_3OD): δ 7.93-7.89 (m, 2H), 7.82-7.78 (m, 2H), 7.70-7.65 (m, 2H), 7.52-7.39 (m, 3H), 4.34-4.24 (A part of an AB system, J_{AB} = 18.4 Hz), 4.23-4.14 (B part of an AB system, J_{AB} = 18.4 Hz), 3.88-3.77 (m, 1H), 3.61 (s, 3H), 3.61-3.48 (m, 3H), 3.26-3.15 (m, 1H). **^{13}C NMR** (50MHz, CD_3OD): δ 169.2, 144.6, 138.2, 137.1, 127.8, 127.2, 126.7, 126.3, 125.9, 70.0, 62.6, 50.4, 48.8.

Synthesis of compound 79.

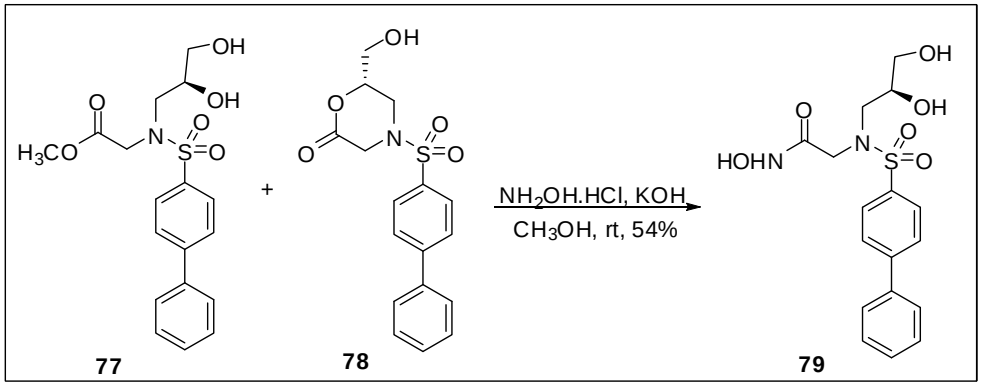

77 78 79

A suspension of KOH (195 mg, 3.48 mmol) in 1.10 mL CH_3OH and a suspension of $NH_2OH{\cdot}HCl$ (161 mg, 2.32 mmol) in 2.00 mL of CH_3OH were refluxed for 15', then the solution of KOH was added to the solution of $NH_2OH{\cdot}HCl$ and the suspension was stirred at 40 °C for 10'. This suspension was cooled to room temperature and added to **77** + **78** (0.58 mmol). The reaction mixture was stirred for 2 h then was filtered and concentrated to dryness. The crude product which was purified by a flash column chromatography on silica gel (from CH_2Cl_2/CH_3OH 7:1 to 3:1) to afford **79** (120 mg, 54%) as a white solid.

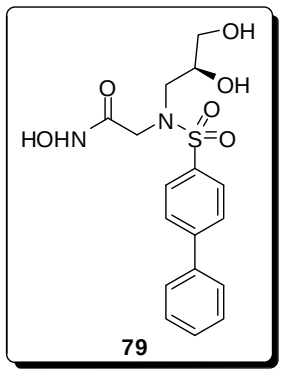

79

ESI-MS $[M-H]^-$ calcd: 379.10. Found: 378.98. **^{1}H NMR** (200MHz, DMSO): δ 7.90-7.71 (m, 5H), 7.55-7.38 (m, 4H), 3.87-3.60 (m, 3H), 3.33-2.90 (m, 6H). **^{13}C NMR** (50MHz, DMSO): δ 169.8, 144.5, 138.8, 138.1, 129.5, 128.9, 128.2, 127.7, 127.5, 70.7, 64.1, 53.7, 49.9.

Synthesis of compound 80.

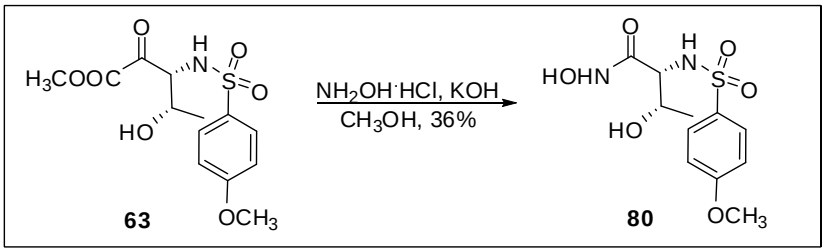

A suspension of KOH (280 mg, 5.00 mmol) and $NH_2OH{\cdot}HCl$ (276 mg, 4.00 mmol) in CH_3OH (2 mL) was stirred at room temperature for 1h, then a solution of **63** (303 mg, 1.00 mmol) in CH_3OH (2 mL) was added. The reaction mixture was stirred for 18 h, then concentrated to dryness. The crude product was dissolved in EtOAc , washed with a mixture $AcOH/H_2O$ 1:1 and dried over Na_2SO_4. Concentration of the solvent under vacuum afford a crude product which was purified by flash column chromatography on silica gel (CH_2Cl_2/CH_3OH 6:1) to afford **80** (110 mg, 36%) as a pale yellow solid.

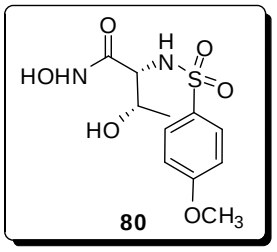

M.p.: 105-107 °C**. $[\alpha]^{25}_D$:** +23.0 (c 0.30, CH_3OH). **ESI-MS** $[M+Na]^+$ calcd. 327.1. Found: 327.1. **ESI-MS** $[M-H]^-$ calcd. 303.1. Found: 303.1. **^{1}H NMR** (200MHz, CD_3OD): δ 7.81-7.76 (AA' part of an AA'MM' system, J_{AM} = 9.2 Hz, 2H), 7.06-7.01 (MM' part of an AA'MM' system, J_{AM} = 9.2 Hz, 2H), 3.96-3.86 (m, 1H), 3.90 (s, 3H), 3.51 (d, J = 4.8 Hz, 1H), 1.04 (d, J = 6.2 Hz, 3H). **^{13}C NMR** (50MHz, CD_3OD): δ 168.8, 164.5, 133.2, 130.3, 115.2, 68.9, 61.5, 56.1, 19.5.

Synthesis of compound 81.

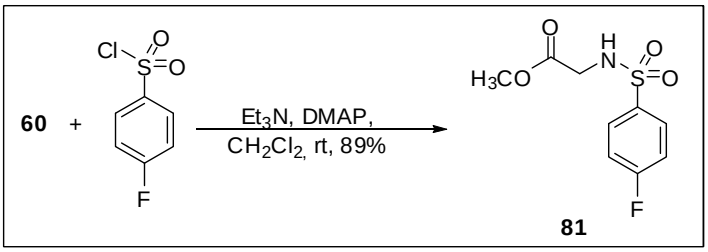

To a stirred suspension of **60** (1.00 g, 8.00 mmol), in CH_2Cl_2 (30 mL), 3.20 mL of NEt_3 (16.0 mmol) were added at 0°C. The suspension was stirred at room temperature for 30', cooled to 0°C then *para*-fluorobenzensulphonyl chloride (1.55 g, 8.00 mmol) and DMAP (catalytic amount) were added. The reaction mixture was kept at room temperature for 18 h then diluted with CH_2Cl_2 and washed with a solution of HCl (3%, H_2O) and with a saturated solution of $NaHCO_3$ (3x). The organic

phase was dried over Na_2SO_4 and the solvent was removed in vacuum. The crude product was purified by flash column chromatography on silica gel (petroleum ether/EtOAc 1:1) to afford **81** (1.85 g, 89%) as a white solid.

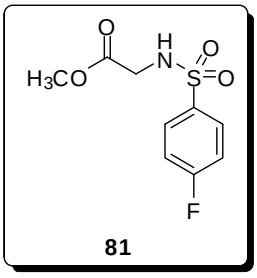

81

M.p.: 125-128 °C. **Anal.** for $C_9H_{10}FNO_4S$ calcd: C, 43.72; H, 4.08; N, 5.67. Found: C, 43.52; H, 4.11; N, 5.58. **^{1}H NMR** (200MHz, $CDCl_3$): δ 7.92-7.85 (q, $J_{H,H}$ = 8.6 Hz, $^4J_{H,F}$ = 5.0 Hz, 2H, H_{orto} *p*-F- C_6H_4), 7.26-7.14 (q, $J_{H,H}$ = 8.2 Hz, $^3J_{H,F}$ = 8.4 Hz, 2H, H_{meta} *p*-F-C_6H_4), 5.27 (bs, 1H), 3.8 (s, 2H), 3.60 (s, 3H). **^{13}C NMR** (50MHz, $CDCl_3$): δ 167.7, 162.6, 130.0, 129.8, 116.5, 116.1, 52.6, 43.9.

Synthesis of compound 82.

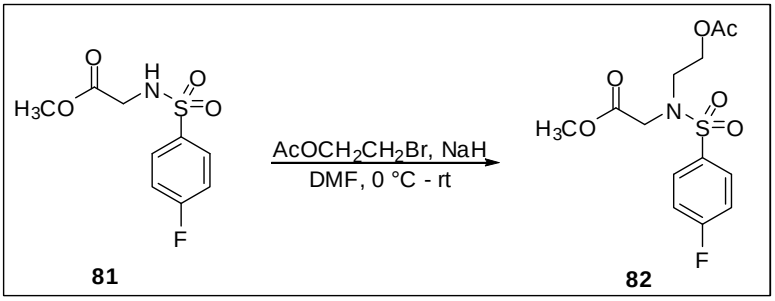

81 **82**

To a stirred solution of **81** (600 mg, 2.43 mmol) in DMF dry (2 mL), NaH (64.0 mg, 2.67 mmol) was added at 0°C under a nitrogen atmosphere. The reaction mixture was kept at 0°C for 20', then 2-bromoethyl acetate (0.27 mL, 2.43 mmol) was added. The mixture was stirred at room temperature for 18 h then diluted with CH_2Cl_2 (15 mL) and washed with a saturated solution of NH_4Cl (3x), with water (2x) and dried over Na_2SO_4. Evaporation of the solvent under vacuum afford a crude product which was purified by flash column chromatography on silica gel (petroleum ether/CH_2Cl_2/EtOAc 2:1:1) to afford **82** (480 mg, 60%) as a white solid.

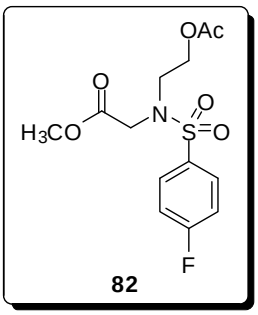

82

M.p.: 67-69 °C. **Anal.** for $C_{13}H_{16}FNO_6S$ calcd: C, 46.84; H, 4.84; N, 4.20. Found: C, 46.65; H, 4.80; N, 4.37. **^{1}H NMR** (200MHz, $CDCl_3$): δ 7.84 (bq, $J_{H,H}$ = 8.8 Hz, $^4J_{H,F}$ = 5.0 Hz, 2H, H_{orto} *p*-F- C_6H_4), 7.19 (bq, $J_{H,H}$ = 8.8 Hz, $^3J_{H,F}$ = 8.4 Hz, 2H, H_{meta} *p*-F-C_6H_4), 4.19 (d, *J* = 5.6 Hz, 2H), 4.16 (s, 3H), 3.62 (s, 3H), 3.50 (t, *J* = 5.6 Hz, 2H). **^{13}C NMR** (50MHz, $CDCl_3$): δ 170.5, 169.2, 165.2 (d, $^1J_{C,F}$ = 254.2 Hz, Cq-F), 135.6 (d, $^4J_{C,F}$ = 3[illegible] Hz, Cq-SO_2), 130.1 (d, $^3J_{C,F}$ = 9.85 Hz, C_{orto} *p*-F-C_6H_4), 116.2 (d, $^2J_{C,F}$ = 22.75 Hz, C_{meta} *p*-F- C_6H_4), 62.2, 52.2, 48.7, 46.9, 20.7.

Synthesis of compound 82a.

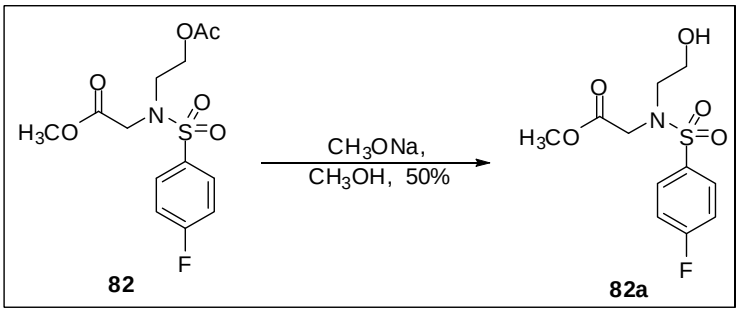

To a stirred solution of **27** (450 mg, 1.35 mmol) in CH_3OH (12 mL), CH_3ONa (15.0 mg, 0.27 mmol) was added at room temperature. The mixture was stirred for 1 h, then the pH was adjusted to 7.0 with HCl (10%, CH_3OH). Evaporation of the solvent under vacuum gave a crude product which was purified by flash column chromatography on silica gel (petroleum ether/CH_2Cl_2/EtOAc 1:1:1) to afford **27a** (150 mg, 50%) as white solid.

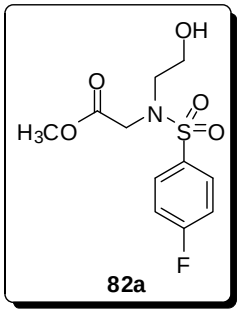

M.p.: 91-95 °C. **Anal.** for $C_{13}H_{16}FNO_6S$ calcd: C, 45.35; H, 4.84; N, 4.81. Found: C, 45.05; H, 4.53; N, 4.67. **^{1}H NMR** (200MHz, $CDCl_3$): δ 7.85 (bq, $J_{H,H}$ = 8.8 Hz, $^4J_{H,F}$ = 5.0 Hz, 2H, H_{orto} *p*-F- C_6H_4), 7.18 (bq, $J_{H,H}$ = 8.8 Hz, $^3J_{H,F}$ = 8.6 Hz, 2H, H_{meta} *p*-F-C_6H_4), 4.10 (s, 2H), 3.71 (m, 5H), 3.36 (t, *J* = 5.2 Hz, 3H), 2.99 (s, 1H). **^{13}C NMR** (50MHz, $CDCl_3$): δ 170.7, 164.2 (d, $^1J_{C,F}$ = 253.4 Hz, Cq -F), 135.2, 130.1 (d, $^3J_{C,F}$ = 9.1 Hz, C_{orto} p-F- C_6H_4), 118.2 (d, $^2J_{C,F}$ = 22.75 Hz, C_{meta} *p*-F- C_6H_4), 62.1, 51.2.

Synthesis of compound 83.

To a stirred solution of **75** (500 mg, 1.64 mmol) in DMF dry (2 mL), NaH (43.0 mg, 1.80 mmol) was added at 0°C under a nitrogen atmosphere. The reaction mixture was warmed to room temperature and stirred for 30', then 2-bromoethyl acetate (0.18 mL, 1.64 mmol) was added. The

mixture was stirred for 36 h and the pH was adjusted to 7 with a saturated solution of NH_4Cl. After the extraction with CH_2Cl_2 the organic layer was dried over Na_2SO_4. Evaporation of the solvent under vacuum afford a crude product which was purified by flash column chromatography on silica gel (petroleum ether/CH_2Cl_2/EtOAc 2:1:1) to afford **83** (310 mg, 48%) as a colourless oil.

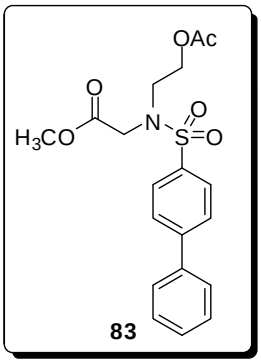

83

Anal. for $C_{19}H_{21}NO_6S$ calcd: C, 58.30; H, 5.41; N, 3.58. Found: C, 57.56; H, 5.50; N, 3.39. **^{1}H NMR** (200MHz, $CDCl_3$): δ 7.92-7.87 (m, 2H), 7.73-7.69 (m 2H), 7.63-7.58 (m, 2H), 7.51-7.44 (m, 3H), 4.23 (t, *J* = 5.6 Hz, 2H), 4.20 (s, 2H), 3.63 (s, 3H), 3.58 (t, *J* = 5.6 Hz, 2H), 2.00 (s, 3H). **^{13}C NMR** (50MHz, $CDCl_3$): δ 170.5, 169.2, 145.7, 139.1, 138.0, 129.0, 128.5, 127.8, 127.5, 127.3, 62.3, 52.1, 48.9, 47.0, 20.7.

Synthesis of compound 83a.

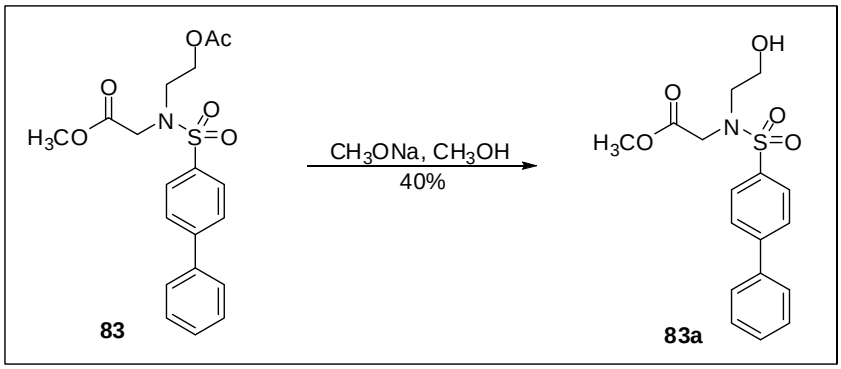

83 **83a**

To a stirred solution of **83** (280 mg, 0.72 mmol) in CH_3OH (12 mL), 150 µL of a solution of CH_3ONa (1M, CH_3OH) were added at 0°C. The mixture was stirred at room temperature for 4 h, then the pH was adjusted to 7.0 with HCl (10%, CH_3OH). Evaporation of the solvent under vacuum gave a crude product (450 mg) which was purified by flash column chromatography on silica gel (petroleum ether/CH_2Cl_2/EtOAc 2:1:1) to afford **83a** (100 mg, 40%) as white vitreous solid.

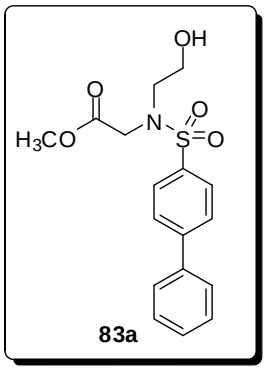

83a

^{1}H NMR (200MHz, $CDCl_3$): δ 7.93-7.88 (m, 2H), 7.74-7.70 (m 2H), 7.61-7.58 (m, 2H), 7.48-7.44 (m, 3H), 4.11 (s, 2H), 3.79-3.60 (m, 5H), 3.40 (t, *J* = 4.6 Hz, 2H). **^{13}C NMR** (50MHz, $CDCl_3$): δ 170.8, 145.8, 139.1, 137.5, 129.0, 128.5, 127.8, 127.6, 127.2, 60.7, 52.6, 52.3, 49.8.

Synthesis of compound 84.

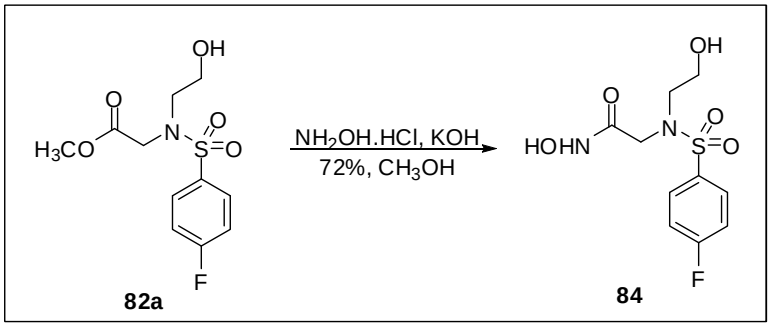

82a **84**

A suspension of KOH (121 mg, 2.15 mmol) and $NH_2OH{\cdot}HCl$ (120 mg, 1.72 mmol) in CH_3OH (1.5 mL) was stirred at room temperature for 1h, then a solution of **82a** (125 mg, 0.43 mmol) in CH_3OH (2 mL) was added. The reaction mixture was stirred for 18 h, then concentrated to dryness. The crude product was dissolved in EtOAc , washed with a mixture AcOH/H_2O 1:1 and dried over Na_2SO_4. Concentration of the solvent under vacuum afford a crude product which was purified by flash column chromatography on silica gel (CH_2Cl_2/CH_3OH 5:1) to afford **84** (90.0 mg, 72%) as a white solid.

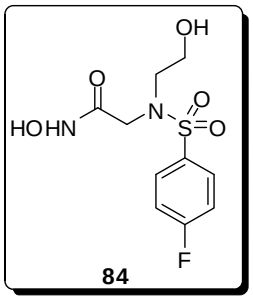

84

M.p.: 118-119 °C. **Anal.** for $C_{10}H_{13}FN_2O_5S$ calcd: C, 41.09; H, 4.48; N, 9.58. Found: C, 40.74; H, 4.19; N, 9.30. **^{1}H NMR** (200MHz, CD_3OD): δ 7.99-7.92 (q, $J_{H,H}$ = 8.8 Hz, $^{4}J_{H,F}$ = 5.2 Hz, 2H, H_{orto} *p*-F- C_6H_4), 7.38-7.30 (q, $J_{H,H}$ = 8.8 Hz, $^{3}J_{H,F}$ = 8.4 Hz, 2H, H_{meta} *p*-F-C_6H_4), 3.91 (s, 2H), 3.72 (t, *J* = 5.4 Hz, 3H), 3.37 (t, *J* = 5.4 Hz, 2H), 3.34 (s, 1H). **^{13}C NMR** (50MHz, CD_3OD) : δ 169.4, 167.6 (d, $^{1}J_{C,F}$ = 244.6 Hz, Cq -F), 137.4, 132.4 (d, $^{3}J_{C,F}$ = 9.1 Hz, C_{orto} *p*-F- C_6H_4), 118.2 (d, $^{2}J_{C,F}$ = 22.75 Hz, C_{meta} *p*-F- C_6H_4), 60.6, 52.6, 52.0, 49.6.

Synthesis of compound 85.

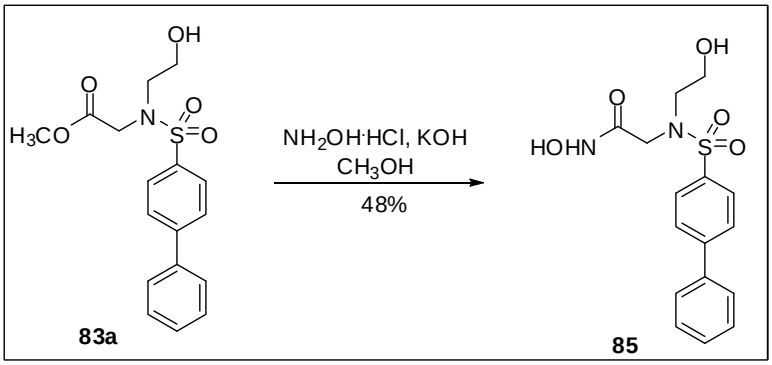

A suspension of KOH (65.0 mg, 1.15 mmol) and $NH_2OH{\cdot}HCl$ (64.0 mg, 0.92 mmol) in CH_3OH (1 mL) was stirred at room temperature for 1h, then a solution of **83a** (80.0 mg, 0.23 mmol) in CH_3OH (1 mL) was added. The reaction mixture was stirred for 18 h, then diluted with EtOAc and washed with a mixture AcOH/H_2O 1:1. The organic layer was dried over Na_2SO_4: concentration of the solvent under vacuum afford a crude product (110 mg) which was purified by flash column chromatography on silica gel (CH_2Cl_2/CH_3OH 8:1) to afford **85** (38.0 mg, 48%) as a light yellow solid.

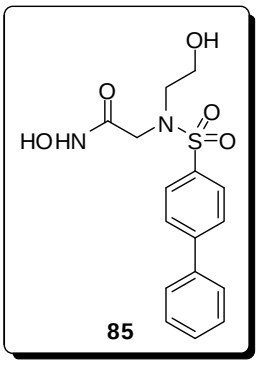

M.p.: 142 °C. **Anal.** for $C_{16}H_{18}N_2O_5S$ calcd: C, 54.84; H, 5.18; N, 7.99. Found: C, 55.37; H, 5.30; N, 8.32. **^{1}H NMR** (200MHz, DMSO-d_6): δ 7.94-7.82 (m, 4H), 7.81-7.77 (m, 2H), 7.59-7.48 (m, 3H), 3.84 (s, 2H), 3.58 (at, *J* = 6.6 Hz, 2H), 3.38 (s, 3H), 3.28 (t, *J* = 5.8 Hz, 3H). **^{13}C NMR** (50MHz, DMSO-d_6): δ 165.5, 144.5, 138.7, 138.0, 129.4, 128.8, 128.0, 127.6, 127.4, 79.5, 59.6, 51.6.

Reference List

[1.] Leslie, A. G. W. Molecular data processing . Moras, D., Podjarny, A. D., and Thierry, J.-C. 50-61. 1991. Oxford, Oxford University Press.
Ref Type: Serial (Book,Monograph)

[2.] P. R. Evans, *Joint CCP4 and ESF-EACBM Newsletter* **1997,** *33* 22-24.

[3.] M. G. Rossmann, D. M. Blow, *Acta Cryst.* **1962,** *15* 24.

[4.] Crowther, R. A. The Molecular Replacement Method. 1972. New York, Gordon & Breach.
Ref Type: Edited Book

[5.] A. Vagin, A. Teplyakov, *J.Appl.Crystallogr.* **1997,** *30* 1022-1025.

[6.] A. Vagin, A. Teplyakov, *Acta Crystallogr.,Sect.D: Biol.Crystallogr.* **2000,** *56* 1622-1624.

[7.] G. N. Murshudov, A. Vagin, E. Dodson, *J.Acta Cryst.D53* **1997,** 240-255.

[8.] D. E. McRee, *J.Mol.Graphics* **1992,** *10* 44-47.

[9.] V. S. Lamzin, *Acta Crystallogr.,Sect.D: Biol.Crystallogr.* **1993,** *49* 129-147.

[10.] R. A. Laskowski, M. W. MacArthur, D. S. Moss, J. M. Thornton, *J.Appl.Crystallogr.* **2009,** *26* 283-291.

[11.] V. Lukacova, Y. Zhang, M. Mackov, P. Baricic, S. Raha, J. A. Calvo, S. Balaz, *J.Biol.Chem.* **2004,** *279* 14194.

Publications

1. Dragoni, E.; Calderone, V.; Fragai, M.; Jaiswal, R.; Luchinat, C.; Nativi, C. Biotin-Tagged Probes for MMP Expression and Activation: Design, Synthesis, and Binding Properties. *Bioconjugate Chemistry* **2009,** *20* (4), 719-727.

2. Altamura, M.; Dragoni, E.; Infantino, A. S.; Legnani, L.; Ludbrook, S. B.; Menchi, G.; Toma, L.; Nativi, C. Cyclic glycopeptidomimetics through a versatile sugar-based scaffold. *Bioorganic & Medicinal Chemistry Letters* **2009,** *19* (14), 3841-3844.

3. Jimenez-Barbero, J.; Dragoni, E.; Venturi, C.; Nannucci, F.; Ardà, A.; Fontanella, M.; Andrè, S.; Canada, F. J.; Gabius, H.-J.; Nativi, C. a-O-Linked Glycopeptide Mimetics: Synthesis, Conformation Analysis, and Interactions with Viscumin, a Galactoside-Binding Model Lectin. *Chemistry-A European Journal* **2009,** *15*, 10423-10431.

4. High-Affinity, Water soluble Inhibitors of Matrix Metalloproteinases (MMPIs). In preparation.

Biotin-Tagged Probes for MMP Expression and Activation: Design, Synthesis, and Binding Properties

Elisa Dragoni, Vito Calderone, Marco Fragai, Rahul Jaiswal, Claudio Luchinat,* and Cristina Nativi*

Magnetic Resonance Center (CERM) - University of Florence, Via L. Sacconi 6, 50019 Sesto Fiorentino, Italy, Department of Organic Chemistry, University of Florence, Via della Lastruccia 13, 50019 Sesto Fiorentino, and Department of Agricultural Biotechnology, University of Florence, Via Maragliano, 75-77, 50144 Florence, Italy. Received September 8, 2008; Revised Manuscript Received January 24, 2009

The design and synthesis of biotin chain-terminated inhibitors (BTI) showing high affinity for matrix metalloproteinases (MMPs) on one side and high affinity for avidin through the biotinylated tag on the other are reported. The affinity of the designed BTI toward five different MMPs has been evaluated and the simultaneous formation of a highly stable ternary system Avidin-BTI-MMP clearly assessed. This system will permit the development of new approaches to detect, quantify, or collect MMPs in biological samples, with potential applications in vivo.

INTRODUCTION

The design of molecular probes able to selectively bind biomolecular targets is gaining importance not only for their applications in molecular biology, but also for the development of new techniques for the early stage diagnosis and therapy of several pathologies (*1*). Rational drug design driven by structural data is currently applied to speed up the design of new candidate drugs in pharmaceutical research (*2*−*5*). The same approach is even more important to design molecular probes where, besides classical requirements, additive structural and functional features are required.

Matrix metalloproteinases (MMPs), also known as matrixins, are proteinases that participate in extracellular matrix (ECM) degradation (*6*) and in several extracellular processes (*7*−*10*). Under normal physiological conditions, the activity of MMPs is strictly regulated by transcription/activation of zymogens precursors, interaction with specific ECM components, and inhibition by endogenous inhibitors (TIMPs) (*11*−*14*). An imbalance of these activities may results in diseases such as atherosclerosis, thrombosis, or heart failure (*15, 16*). As a matter of fact, expression and activation of MMPs are increased in these pathologies, as well as in almost all human cancers, compared to physiological conditions (*17*). Indeed, ECM degradation by MMPs does promote tumor invasiveness. Furthermore, it has been recently demonstrated that MMPs carry out functions other than promotion of invasion, and that they likely take part in the development of cancer even before invasion. Noteworthy, the degree of overexpression of MMPs in cancer tissues is strictly associated with the level of tumor invasiveness and with its tendency to form metastasis. It is therefore apparent that the development of efficient molecular devices designed to reveal the overexpression of MMPs may be a powerful tool for the early detection of tumors and the assessment of their aggressiveness, as well as of cardiocirculatory problems (*18*).

* Prof. Claudio Luchinat, Magnetic Resonance Center (CERM), University of Florence, Via L. Sacconi 6, 50019 Sesto Fiorentino, Italy, e-mail: luchinat@cerm.unifi.it, Tel.: +390554574262, Fax: +390554574253; Prof. Cristina Nativi, Department of Organic Chemistry, University of Florence, Via della Lastruccia 13, 50019 Sesto Fiorentino, Italy, e-mail: cristina.nativi@unifi.it, Tel.: +390554573540, Fax: +390554573531.

Studies focused on the detection of overexpression of MMPs have already been reported (*19*) and probes to profile MMPs in tissues synthesized and tested (*20, 21*). In particular, hydrolyzable, near-infrared fluorescent molecules have been successfully tested in mice to detect fibrosarcoma (*22*). Unfortunately, this innovative technique suffers from the serious limitation represented by the limited penetration of light (a few millimeters); such a degree of penetration is only sufficient for the readout of superficial subcutaneous tumors (<10 mm).

An interesting approach to detect overexpression of MMP in atherosclerosis has also been published. Low molecular weight inhibitors, able to interact with the active site of MMPs involved in atherosclerotic plaque disruption, have been targeted with nuclear agents and tested in vivo (*23*−*25*). Although the results reported were extremely encouraging, the approach presented a scarce flexibility, due to experimental difficulties in preparing the targeted inhibitors and to limited availability of suitable nuclear agents.

A significant improvement in the development of MMP-conjugated probes to detect pathological events may be the rational design of biotin-labeled inhibitors (*26*), capable of binding to MMPs exclusively and with high affinity. These tagged molecules rely on the well-known avidin−biotin molecular recognition system and could be used in conjunction with commercially available biotin-labeled probes (i.e., radionuclide chelates) to efficiently detect pathological tissues by imaging the local overexpression of MMPs. The use of such molecules is not limited to in vivo imaging but can be extended to in vitro applications such as MMP purification by using avidin columns or devices.

Capitalizing on our expertise on expression and structural characterization of MMPs (*27*−*29*) and on the rational design and synthesis of MMP inhibitors (*30*−*35*), in the present paper we report the design and synthesis of carboxylic-containing, biotinylated inhibitors able to show high affinity for MMPs and at the same time able to strongly interact with avidin through the biotinylated tag.

In clinical therapy, selectivity of inhibitors for a specific MMP is dramatically important, so much so that the lack of selectivity is believed to have been the main reason for failures of clinical trials in the past. Often, the failure of clinical trials, due to the severity of the side-effects, was related to the chronic adverse

10.1021/bc8003827 CCC: $40.75
Published on Web 03/10/2009

effects of nonselective inhibitors. On the other hand, for the molecules proposed here, selectivity is not an issue as chronic use is not required. Indeed, ideal probes to detect overexpression of MMPs must not be selective inhibitors vs a specific MMP, but they should instead selectively recognize MMPs among other proteins. These new biotinylated molecules designed to bind to MMPs and to be recognized by avidin might therefore be successfully used in the in vitro collection/purification of MMPs, in the visualization of pathological tissues where MMPs are overexpressed, and to evaluate the aggressiveness of the pathology by monitoring, e.g., radioactivity. Moreover, it might be possible to test in vivo the efficacy of clinical treatments against a specific disease by just monitoring the level of MMPs produced during the therapy. In addition, such molecules can be easily employed for collecting and purifying MMPs from biological samples.

EXPERIMENTAL PROCEDURES

General. All reagents were commercially available and used as received. Dry solvents were prepared before use. The catalytic domain of the MMP-12 (G106-G263) was cloned into the pET21a (Novagen) using the restriction enzymes *Nde I* and *Xho I* (New England BioLabs). NMR spectra were recorded using a Varian Gemini 200, Varian Mercury 400 spectrometer, and a Brucker 700 spectrometer (HSQC). HPLC purification was performed using Althech Ultrasphere C-18 column (250 × 10 mm) and monitored with a Dionex photodiode array detector. SPR data were obtained using a BioRad ProteOn XPR36.

(*R*)-Methyl 2-(*N*-(bromomethyl)biphenyl-4-ylsulfonamido)-4-methylpentanoate (8). To a solution of **3** (600 mg, 1.66 mmol), 6-bromo-1-hexanol (450 mg, 2.49 mmol), and triphenylphosphine (872 mg, 3.32 mmol) in 17 mL of dry THF, 0.65 mL of DIAD (1.66 mmol) was added dropwise, in 1 h. The reaction was stirred at rt for 43 h, and then the solvent was removed in vacuo to give a yellow oil. After crystallization of the betainic side product (EtOAc/cyclohexane 1:8), the filtrate was concentrated in vacuum and the residue (3.20 g) was purified twice by flash column chromatography on silica gel (hexane/EtOAc 6:1, then CH_2Cl_2) to give pure **8** as a white solid (515 mg, 60% yield).

$[\alpha]^{25}_D$ +47.4 (c 1.13, $CHCl_3$). MP: 59−61 °C. ^{1}H NMR (200 MHz, $CDCl_3$) δ 7.90−7.86 (part AA′ of an AA′MM′ system, J_{AM} = 8.8 Hz, 2H), 7.72−7.68 (part MM′ of an AA′MM′ system, J_{AM} = 8.8 Hz, 2H), 7.65−7.40 (m, 5H), 4.63−4.55 (dd, 1H, J = 5.6 Hz, J = 6.0 Hz), 3.46 (s, 3H), 3.40 (t, J = 6.8 Hz, 2H), 3.30−3.06 (m, 2H), 1.97−1.17 (m, 11H), 0.99−0.94 (m, 6H). ^{13}C NMR (50 MHz, $CDCl_3$) δ 171.66, 145.27, 139.23, 138.26, 128.97, 128.38, 127.88, 127.26, 127.20, 58.09, 51.96, 45.95, 39.59, 33.86, 32.75, 31.19, 27.86, 26.36, 24.63, 22.99, 21.73. ESI-MS $[M + H]^+$ calcd 524.14. Found 524.11.

***tert*-Butyl (5-((4*S*)-2-oxohexahydro-1*H*-thieno[3,4-*d*]imidazol-4-yl)pentanamido)methylcarbamate (6).** A suspension of *N*-Boc-1,6-diaminohexane hydrochloride **5** (310 mg, 1.23 mmol) and NMM (0.14 mL, 1.23 mmol) in dry DMF (3 mL) was added to a slurry of D-biotin (300 mg, 1.23 mmol) and NMM (0.14 mL, 1.23 mmol) in dry DMF (10 mL), and the mixture was stirred at rt for 10 min. A solution of HATU (468 mg, 1.23 mmol) in dry DMF (3 mL) was added, and the mixture was stirred for 3.5 h. The reaction mixture was diluted with 20 mL of CH_2Cl_2 and washed with water: the organic layer was dried over anhydrous Na_2SO_4, and the solvent was removed in vacuo to give a yellow pale oil. Part of DMF was removed in vacuum to give 2.20 g of a yellow solid. The crude material was purified by flash column chromatography on silica gel (CH_2Cl_2/CH_3OH 6:1) to give **6** as a white solid (500 mg, 92% yield).

MP: 174−175 °C. ^{1}H NMR (200 MHz, $CDCl_3$) δ 6.17−6.07 (m, 2H), 4.70−4.56 (m, 1H), 4.55−4.49 (part A of an ABMN system, J_{AB} = 8.0 Hz, J_{AM} = 4.4 Hz, 1H), 4.36−4.29 (part B of ABX system, J_{AB} = 8.0 Hz, J_{BX} = 4.6 Hz, 1H), 3.24−3.10 (m, 5H), 2.97−2.71 (part MN of an AMN system, J_{MN} = 12.4 Hz, J_{AM} = 4.4 Hz, 2H), 2.22 (t, J = 7.0 Hz, 2H), 1.48−1.25 (m, 23H). ^{13}C NMR (50 MHz, $CDCl_3$) δ 173.80, 163.62, 155.91, 62.11, 60.56, 55.56, 40.56, 39.70, 35.65, 30.06, 29.87, 29.27, 28.61, 28.18, 28.09, 26.39, 26.25, 25.84. Anal. ($C_{16}H_{28}N_4O_4S$) C, 51.69; H, 7.62; N, 15.00.

(5-((4*S*)-2-Oxohexahydro-1*H*-thieno[3,4-*d*]imidazol-4-yl)pentanamido)methanaminium (7). A solution of CF_3COOH (1.9 mL, 23.8 mmol) in dry CH_2Cl_2 (6.2 mL) was added to a suspension of **6** (480 mg, 1.08 mmol) in dry CH_2Cl_2 (4.6 mL). After 1.5 h, 10 mL of toluene was added and solvent was removed under vacuum to give a pale yellow oil. The oil was repeatedly washed with CH_3OH and $CHCl_3$; the compound **7** (490 mg, >90%) so obtained was used without any further purification.

^{1}H NMR (200 MHz, CD_3OD) δ 4.53−4.47 (part A of an ABMN system, J_{AB} = 8.0 Hz, 1H), 4.33−4.27 (part B of an ABX system, J_{AB} = 8.0 Hz, J_{BX} = 4.4 Hz, 1H), 3.23−3.14 (m, 3H), 3.00−2.87 (m, 5H), 2.73−2.67 (part M of an AMN system, J_{MN} = 12.4 Hz, 1H), 2.20 (t, J = 7.2 Hz, 2H), 1.72−1.40 (m, 12H). ^{13}C NMR (50 MHz, CD_3OD): 174.45, 164.54, 159.90, 62.07, 60.32, 55.74, 39.77, 39.40, 38.79, 35.54, 28.87, 28.53, 28.27, 27.24, 26.12, 25.75, 25.69.

(2*R*)-Methyl-4-methyl-2-(*N*-(((5-((4*S*)-2-oxohexahydro-1*H*-thieno[3,4-*d*]imidazol-4-yl)pentanamido)methylamino)methyl)biphenyl-4-ylsulfonamido)pentanoate (9). To a solution of **7** (236 mg, 0.69 mmol) in dry DMF (4 mL) were added 4 Å activated pellets molecular sieves (400 mg). The mixture was stirred at rt for 1 h. Cesium hydroxide monohydrate previously dried at 120 °C for 24 h (116 mg, 0.69 mmol) was added, and the solution was allowed to stir for 30 min. TBAI (250 mg, 0.69 mmol) and compoud **8** (360 mg, 0.69 mmol) was finally added and the mixture was stirred for 48 h. The crude material was purified by flash column chromatography on silica gel (CH_2Cl_2/CH_3OH 6:1) to give **9** (300 mg, 55%) as a pale yellow solid.

MP: 129−131 °C. ^{1}H NMR (200 MHz, CD_3OD) δ 7.91−7.41 (m, 9H), 4.58−4.48 (m, 2H), 4.34−4.28 (part B of an ABX syst, J_{AB} = 7.8 Hz, J_{BX} = 4.4 Hz, 1H), 3.43 (s, 3H), 3.26−3.14 (m, 4H), 3.04−2.74 (m, 6H), 2.21 (t, J = 7.0 Hz, 2H), 1.73−1.29 (m, 25H), 0.95 (ad, 6H, J = 5.4 Hz). ^{13}C NMR (50 MHz, $CDCl_3$) δ 174.45, 171.45, 164.47, 145.45, 138.97, 138.03, 128.71, 128.15, 127.70, 127.05, 126.80, 62.07, 60.32, 58.13, 55.72, 51.14, 47.60, 45.71, 39.79, 39.26, 38.73, 35.54, 30.97, 28.94, 28.50, 28.27, 26.18, 26.06, 25.94, 25.84, 25.69, 24.42, 21.93, 20.58. ESI-MS $[M + H]^+$ calcd 786.42. Found 786.50.

(2*R*)-4-Methyl-2-(*N*-(((5-((4*S*)-2-oxohexahydro-1*H*-thieno[3,4-*d*]imidazol-4yl)pentanamido)methylamino)methyl)biphenyl-4-ylsulfonamido)pentanoic acid (4). To a solution of **9** (143 mg, 0.18 mmol) in 2.8 mL of THF/H_2O (1:1 v/v) LiOH·H_2O (15.1 mg, 0.36 mmol) was added and the mixture was stirred for 6 h at rt, then H_3PO_4 1 M was added (pH = 5); the solvent was removed in vacuum, and the solution was lyophilized. The solid obtained was redissolved in AcCN/H_2O 3:1 and purified by a reversed-phase semipreparative HPLC to give compound **4** (76 mg, 55%).

$[\alpha]^{25}_D$ +38.19 (c 0.33, CH_3OH). MP: 119−121 °C. ^{1}H NMR (400 MHz, CD_3OD) δ 7.96−7.38 (m, 9H), 4.49−4.46 (part A of an ABMN system, J_{AB} = 8.0 Hz, J_{AM} = 4.4 Hz, 1H), 4.41−4.37 (m, 1H), 4.30−4.27 (part B of an ABX system, J_{AB} = 8.0 Hz, J_{BX} = 4.6 Hz, 1H), 3.49−3.38 (m, 1H), 3.29−3.14 (m, 4H), 2.93−2.88 (m, 5H), 2.71−2.68 (part N of an AMN system, J_{MN} = 12.8 Hz, 1H), 2.19 (t, J = 7.2 Hz, 2H), 1.88−1.22 (m, 25H), 0.93 (at, J = 6.4 Hz, 6H). ^{13}C NMR (50 MHz, CD_3OD) δ 176.04, 174.39, 164.51, 144.75, 139.22,

128.64, 127.94, 127.79, 126.80, 126.76, 62.07, 61.02, 60.31, 55.72, 47.51, 45.04, 40.31, 39.77, 38.79, 35.54, 30.38, 28.96, 28.51, 28.27, 26.12, 25.92, 25.68, 25.56, 24.81, 22.17, 21.16. ESI-MS $[M + H]^+$ calcd 772.41. Found 772.54. Anal. ($C_{31}H_{45}N_5O_6S_2$) C, 57.43; H,7.08; N, 10.61.

(2*R*)-Methyl-2-(4-methoxy-*N*-(((5-((4*S*)-2-oxohexahydro-1*H*-thieno[3,4-*d*]imidazol-4-yl) pentanamido)methylamino)methyl)phenylsulfonamido)propanoate (12). To a solution of **7** (170 mg, 0.50 mmol) in dry DMF (2 mL), 4 Å activated pellets molecular sieves (280 mg) were added, and the mixture was gently stirred at rt for 1 h. Cesium hydroxide monohydrate, previously dried at 120 °C for 24 h, (84 mg, 0.50 mmol) was added, and the reaction mixture was stirred for 30 min. A solution of **11** (218 mg, 0.50 mmol) and TBAI (182 mg, 0.50 mmol) in DMF (1 mL) were finally added, and the mixture was stirred for 48 h at rt. The crude material obtained was purified by flash column chromatography on silica gel (CH_2Cl_2/CH_3OH 6:1) to give **12** (200 mg, 58%) as a pale yellow solid.

MP: 93−94 °C. ^{1}H NMR (200 MHz, CD_3OD) δ 7.78−7.70 (part AA′ of an AA′MM′ system, $J_{AM} = 9.2$ Hz, 2H), 6.95−6.94 (part MM′ of an AA′MM′ system, $J_{AM} = 9.2$ Hz, 2H), 4.58−4.47 (m, 2H), 4.38−4.32 (part B of an ABX system, $J_{AB} = 7.8$ Hz, $J_{BX} = 4.4$ Hz, 1H), 3.88 (s, 3H), 3.55 (s, 3H), 3.26−3.14 (m, 5H), 3.03−2.87 (m, 5H), 2.72−2.69 (part N of an AMN system, $J_{MN} = 12.6$ Hz, 1H), 2.20 (t, $J = 7.0$ Hz, 2H), 1.72−1.29 (m, 25 H). ^{13}C NMR (50 MHz, CD_3OD) δ 173.27, 171.80, 163.50, 162.71, 131.39, 129.28, 114.03, 68.21, 61.99, 60.22, 55.72, 55.18, 52.49, 52.26, 45.45, 40.70, 38.06, 35.78, 30.84, 29.85, 28.94, 28.15, 28.07, 26.33, 26.25, 26.03, 25.80, 23.16, 16.83. ESI-MS $[M + H]^+$ calcd 698.35. Found 698.30.

(2*R*)-2-(4-Methoxy-*N*-(((5-((4*S*)-2-oxohexahydro-1*H*-thieno[3,4-*d*]imidazol-4-yl)pentanamido)methylamino)methyl)phenylsulfonamido)propanoic Acid (10). To a solution of **12** (229 mg, 0.33 mmol) in 4.8 mL of CH_3OH/H_2O 1:1, $LiOH \cdot H_2O$ (28.0 mg, 0.66 mmol) was added and the mixture was stirred for 19 h at rt. A solution of H_3PO_4 (1 M, H_2O) was added (pH = 5), the solvent was removed under vacuum, and the crude product was lyophilized. The solid obtained was redissolved in AcCN/ H_2O 3:1 and purified by a reversed-phase semipreparative HPLC to give compound **10** (53 mg, 23%) as a white solid.

MP: 70−72 °C. ^{1}H NMR (400 MHz, CD_3OD) δ 7.80−7.77 (part AA′ of an AA′MM′, $J_{AM} = 9.2$ Hz, 2H), 7.04−7.02 (part MM′ of an AA′MM′ system, $J_{AM} = 9.2$ Hz, 2H), 4.50−4.47 (m, 1H), 4.36 (q, $J = 7.2$ Hz, 1H), 4.31−4.28 (m, 1H), 3.86 (s, 3H), 3.32−3.26 (m, 1H), 3.21−3.15 (m, 4H), 2.98−2.90 (m, 5H), 2.72−2.68 (part N of an AMN system, $J_{MN} = 12.4$ Hz, 1H), 2.19 (t, $J = 7.2$ Hz, 2H), 1.70−1.30 (m, 22H), 1.20 (d, $J = 7.2$ Hz, 3H). ^{13}C NMR (50 MHz, CD_3OD) δ 176.67, 174.39, 164.51, 162.68, 132.33, 129.02, 113.65, 62.07, 60.31, 57.73, 55.74, 54.83, 47.60, 44.68, 39.80, 38.80, 35.54, 29.84, 29.00, 28.51, 28.29, 26.13, 25.95, 25.70, 25.59, 25.53, 25.37, 16.16. ESI-MS: $[M + H]^+$ calcd 684.34. Found 684.30. Anal. ($C_{23}H_{37}N_5O_7S_2$) C, 49.47; H, 6.60; N, 12.70.

RESULTS AND DISCUSSION

Aryl-sulfonamide derivatives have been largely exploited to synthesize broad-spectrum MMP inhibitors. These scaffolds present different positions which can be easily functionalized by introducing new functional groups. This feature and their easy synthetic accessibility make sulfonamide derivatives suitable candidates to design biotin-tagged probes for MMPs. As zinc binding groups (ZBG), the carboxylic acid was selected despite its relatively weak affinity for the metal ion (*36*−*38*). The choice of a carboxylic acid to replace the most commonly used hydroxamic acid warrants higher stability of the inhibitor under physiological conditions (*39*) and provides better bioavailability (*40*).

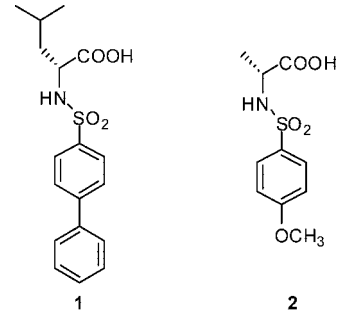

1 2

Figure 1. Structure of the selected scaffolds **1** and **2**.

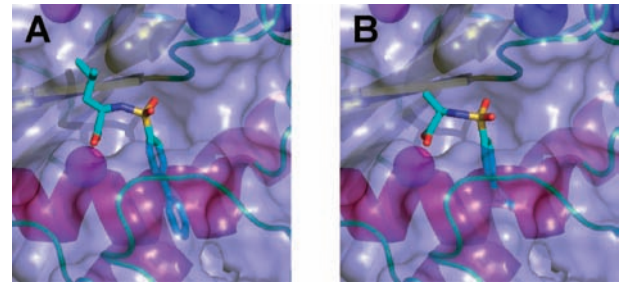

Figure 2. X-ray structure of the catalytic domain of MMP-12 complexed with **1** (A) and with **2** (B). Only the ligand binding site is shown for clarity.

In all MMPs, the flexibility of the protein loops forming the active site makes these enzymes able to modify the shape of the catalytic pocket to accommodate ligands with different structures (*41*−*44*). In particular, analyzing the structures available on the protein data bank, it is apparent that the volume of the S_1' cavity can be changed to host ligands bearing lipophilic groups of different size. However, in MMP-1 and MMP-7 the S_1' cavity is narrow as well as short "trucked" (MMP-7) such that bulky groups generally do not fit. Therefore, in order to probe all members of the MMP family, two scaffolds, bearing either a linear biphenyl moiety or a shorter methoxyphenyl group, were considered as possible bases for the synthesis of BTIs.

Among all the scaffolds evaluated, molecules **1** and **2** (Figure 1) were selected for their low K_i values against five different MMPs (see Table 1). Noteworthy, the two scaffolds exhibit a sizably different selectivity and affinity for the MMPs chosen. In particular, inhibitor **1**, due to the presence of a biphenyl moiety on the sulfonamide sulfur, showed inhibition constants in the nanomolar range. Only for MMP-1 and MMP-7 was the affinity in the low-micromolar range due to the relatively slim size of the S_1' pocket (*45*). Although still good, **2** is a weaker MMP inhibitor with micromolar values of K_i for all the MMPs tested.

Matrix metalloproteinase 12 (MMP-12) performs proteolysis of several ECM components including elastin, laminin, and type IV collagen. The stability of the active MMP-12 catalytic domain in the presence of weak inhibitors, the relatively large S_1' pockets, and the high yield of the ^{15}N-enriched protein in minimal medium make this enzyme an ideal model to evaluate BTI candidates.

To explore the binding mode of the two scaffolds and to properly design the biotin tag derivatives, the two inhibitors were soaked in crystals of MMP-12 and the structure of the complexes solved by X-ray crystallography. Analysis of the crystal structures (see Figure 2) revealed that the inhibitors share a similar binding mode, with the catalytic zinc ion coordinated by the oxygens of the free carboxylate, the sulfonyl oxygen H-bonded with the NH of the Ala 182, and the liphophilic

Table 1. Inhibition Constants (K_i) of the Considered Compounds toward the Considered MMPs

compound	MMP-1	MMP-7	MMP-8	MMP-12	MMP-13
1	18 ± 2 μM	56 ± 6 μM	31 ± 4 nM	25 ± 2 nM	108 ± 12 nM
2	302 ± 25 μM	80 ± 9 μM	4.6 ± 5 μM	1.4 ± 0.2 μM	2.6 ± 0.3 μM
4	25 ± 3 μM	450 ± 50 nM	4 ± 0.5 nM	5 ± 0.6 nM	0.7 ± 0.2 nM
10	295 ± 40 μM	73 ± 7 μM	8 ± 1 μM	1.6 ± 0.2 μM	1.2 ± 0.1 μM

Scheme 1. Synthesis of BTI 4 and Bromosulfenamide 8

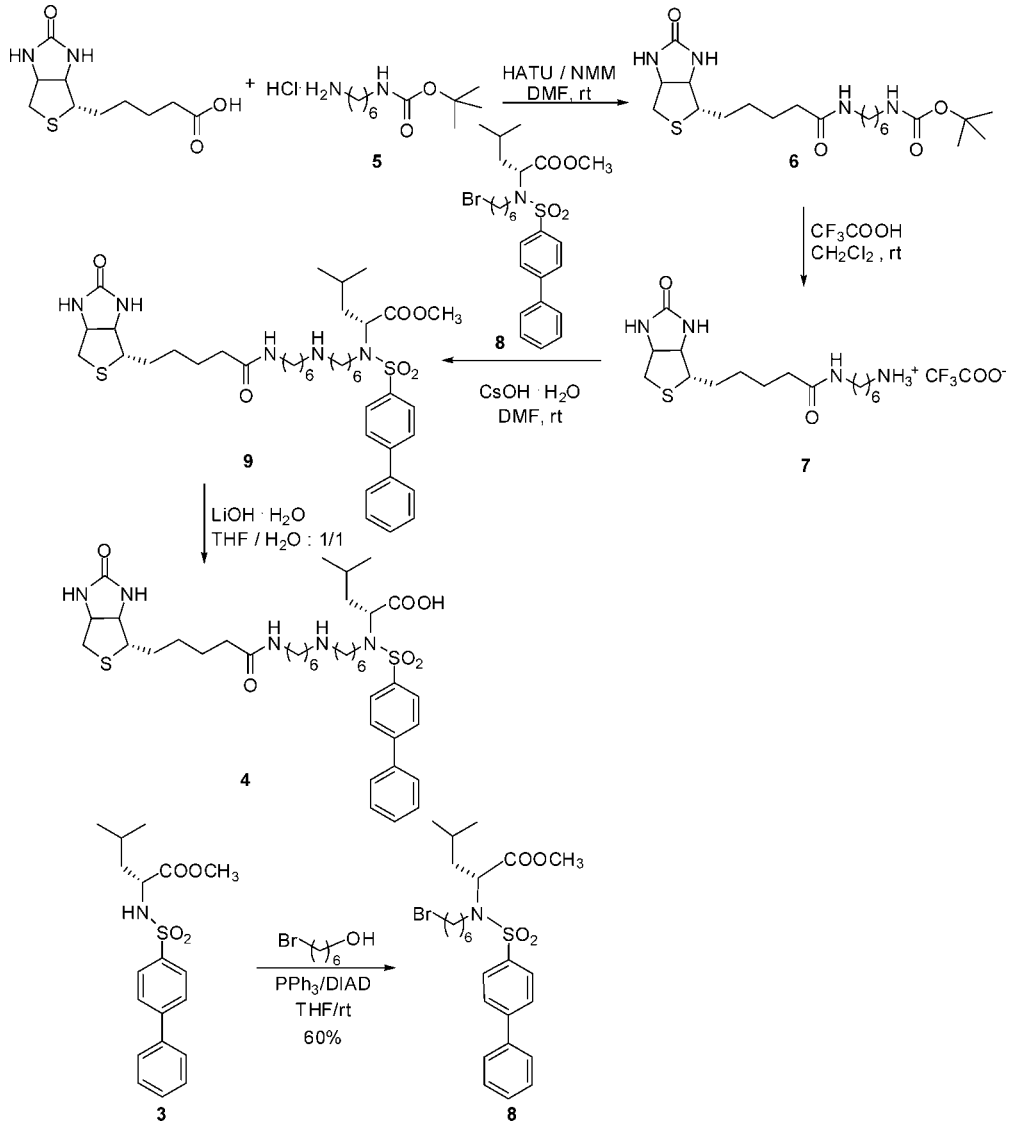

groups nested inside the S_1' pocket. The structural analysis accounts for the larger affinity of **1** for MMP-12 with respect to scaffold **2**, as observed in the enzymatic assays. Indeed, in the MMP-12−**1** complex, larger hydrophobic interactions result from the larger surface-to-surface contact area due to the presence of the biphenyl moiety. More important for the biotin tag inhibitor design was the solvent exposure of the sulfonamide nitrogen revealed by the crystal structures for both ligands. These structural data address the question related to the identification of the position where the tag can be inserted without spoiling the binding affinity.

A further critical point in developing efficient biotinylated probes for in vivo and in vitro applications is represented by the choice of a suitable linker able to prevent any steric clashes between avidin and the target biomolecule. While a too-short spacer may impair the ability of the probe to bind both MMP and avidin, the use of a too-long spacer could affect the bioavailability, stability, and solubility of the whole molecule. In particular, a too-long linker can increase the susceptibility of the probe to be split by enzymes such as the biotinidase that can degrade the molecule in vivo (*46*). Once more, the availability of the three-dimensional structure of both avidin−biotin complex (present in protein data bank, PDB code: 2avi) and **1**−MMP-12 complex has provided the background information needed for a rational molecular design of the biotin-tagged inhibitors we conceived (see Supporting Information).

A fourteen-membered spacer was designed to link the biotin residue to the carboxylic-methyl ester sulfonamide **3** (Scheme 1), that is the shorter, synthetically convenient linker allowing the probe to bind both MMP and avidin binding sites.

The biotinylated inhibitor **4** was obtained as shown in Scheme 1. Biotin was first reacted under known procedures (*46*) with the N-Boc-1,6-diaminohexane **5** to give the amido derivative **6** which, after removal of *tert*-butyloxy carbonyl protecting group, gave the trifluoroacetylammonium salt **7**. Compound **7** was treated with the bromosulfonamide **8** in the presence of cesium

Scheme 2. Synthesis of BTI 10

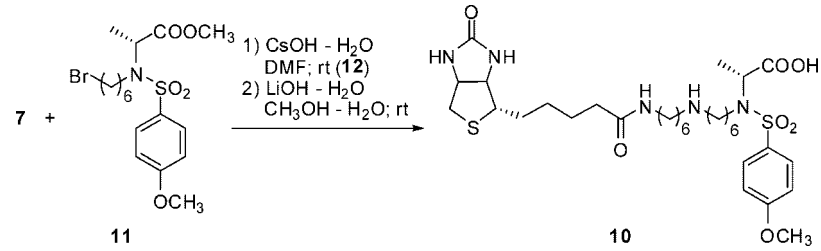

hydroxide, in dimethylformamide as solvent, to give the diastereomerically pure ester **9** in 55% yield. Removal of the methyl ester with lithium hydroxide/water from the latter afforded BTI **4** as a diastereomerically pure compound in 55% yield (Scheme 1). Following the synthetic pathway reported for **4**, the biotin-tagged MMP-12 inhibitor **10** was also prepared from **7** and bromosulfonamide **11**, as a diasteromerically pure compound (Scheme 2).

The affinity properties of the two BTI derivatives toward the selected MMPs were first evaluated by fluorimetric assay (see Supporting Information). The K_i values are reported in Table 1. While BTI **4** had lower K_i values as compared to the corresponding precursor **1**, BTI **10** exhibited comparable affinity with respect to its precursor **2**. The micromolar K_i of BTI **10** for all the tested MMPs unambiguously demonstrated that the latter is less interesting as a probe to detect these enzymes in vivo, though it might be suitable to collect and purify MMPs from biological samples. Conversely, BTI **4** exhibited a nanomolar affinity for all the MMPs considered (including MMP-7) except for MMP-1, for which the K_i was, however, still in the low micromolar range. The molecular details for the observed improved affinity were analyzed by investigating the BTI **4** -MMP-12 complex.

Several attempts aimed at obtaining the X-ray structure of the biotin tag inhibitors in complex with MMP-12, either by soaking or cocrystallization, failed, probably for steric reasons owing to the tag. Therefore, interaction of compound **1** and of its biotin tag derivative **4** with the catalytic domain of MMP-12 was further investigated following the chemical shift perturbations on $^{15}N-^{1}H$ HSQC spectra using ^{15}N-labeled protein samples. The chemical shift is a sensitive indicator of protein−ligand interactions and can be used to identify the binding site when the resonance assignment is available (*47*). The complete assignment of the catalytic domain of MMP-12 complexed with the weak inhibitor acetohydroxamic acid is available in our laboratory. Increasing amounts of **1** and **4** were added to 200 μM solutions of the protein up to an equimolar concentration. Although several NH signals were shifted by adding the inhibitors, as many as 134 and 129 cross-peaks belonging to protein adducts with **1** and **4**, respectively, were easily reassigned. The intensity of signals belonging to NH groups perturbed by the addition of the ligands decreased linearly, while new cross-peaks corresponding to the BTI-bound form of the protein appeared and gradually increased their intensity, in agreement with the effect produced by a slow-exchanging ligand.

The binding mode of ligands **1** and **4**, respectively, was analyzed and compared by reporting Garrett values [$\Delta\delta$(NH)] on a surface representation of the MMP-12 structure (Figure 3). As is evident from Figure 3, for both inhibitors, the region with significant $^{15}N-^{1}H$ HSQC spectral perturbations involves the catalytic pocket. The analysis of Garrett values rules out relevant additive interactions of the biotinylated tail present in BTI **4** with protein regions outside the catalytic pocket, suggesting a different origin for the observed improved affinity. In addition, a hypothetical binding mode with the biotinylated tail of BTI **4** fitting in the S_1' cavity can be completely excluded by the chemical shift perturbations on the $^{15}N-^{1}H$ HSQC spectra that are similar for **1** and **4** as well as by the K_i values of the BTI **10**, which, although biotinylated, showed a low affinity for the enzyme. Likely, extra interactions related to a better fit of **4** into the active site of the enzyme become possible when the fourteen-membered spacer is introduced on BTI **4**. These extra interactions are particularly evident for MMP-7 (Table 1) where the affinity increases by 2 orders of magnitude upon the introduction of the linker.

Although a high affinity for the target protein is a basic requirement for the proposed bifunctional ligand to play its role, only the ability of the latter to bind MMP and avidin simultaneously could prove its real efficacy as effective BTI.

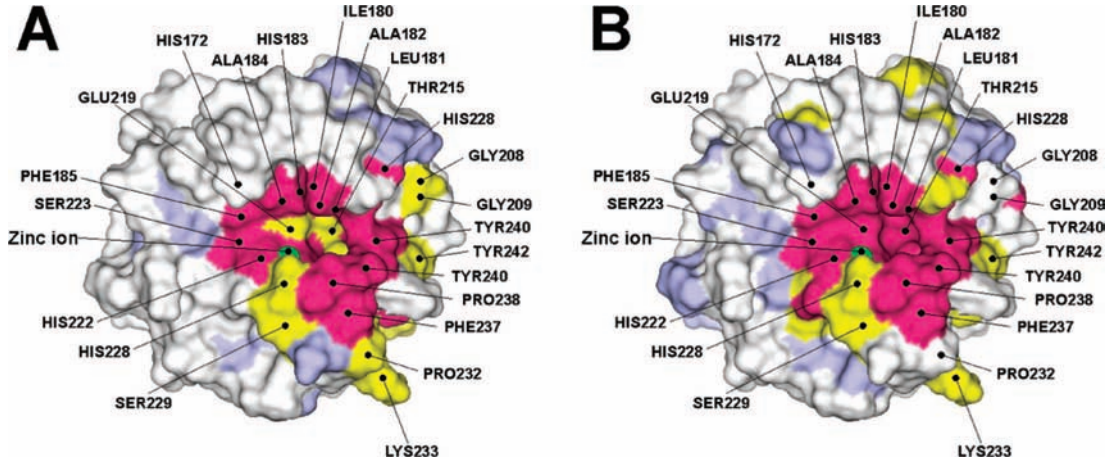

Figure 3. Surface representation of the residues of the catalytic domain of MMP-12 affected by chemical shift perturbation upon the addition of **1** (A) and of **4** (B). Areas of interaction with significant $^{15}N-^{1}H$ HSQC spectra perturbations are colored-coded according to the Garret values. Magenta, $\Delta\delta$(NH) > 0.1 ppm; Yellow, 0.1 > $\Delta\delta$(NH) > 0.05; Cyan, 0.05 > $\Delta\delta$(NH) > 0.03.

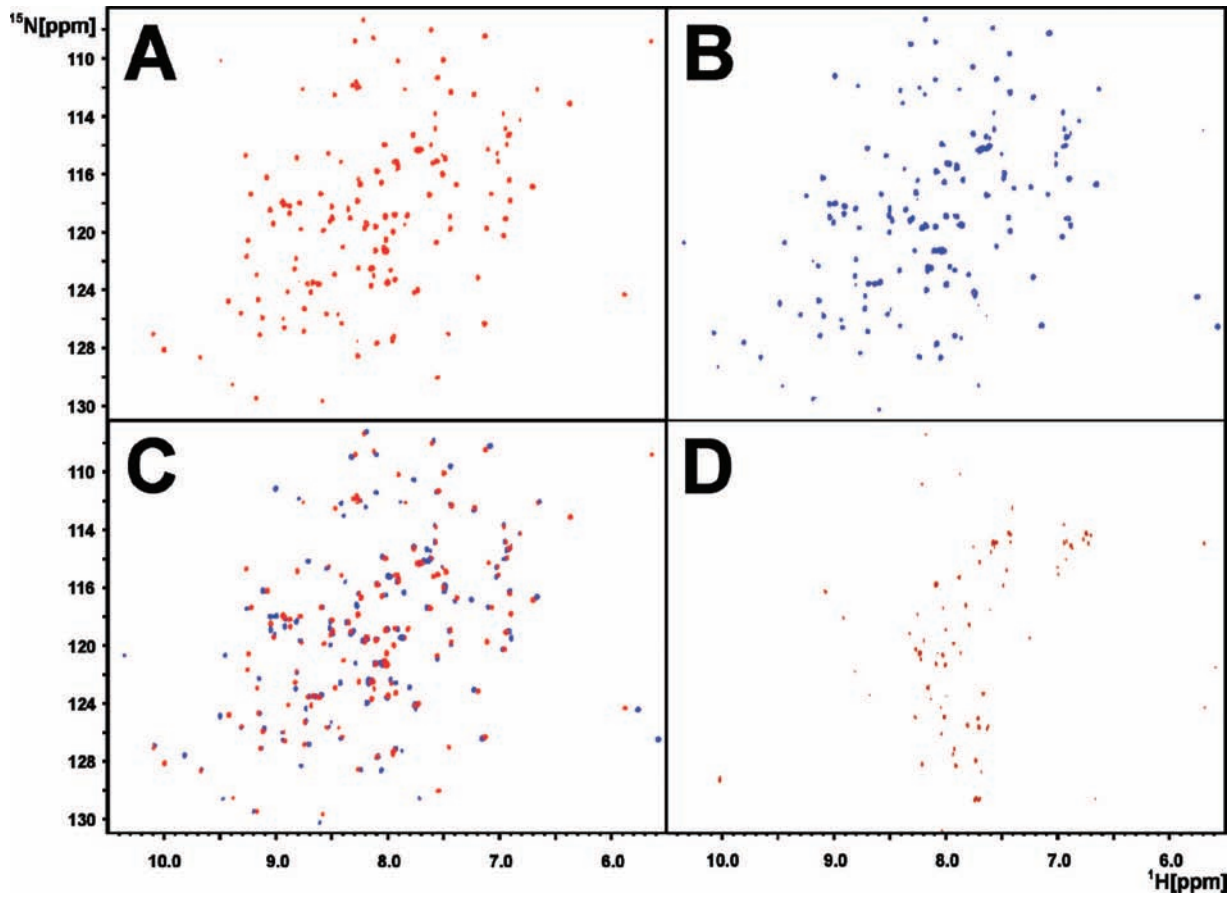

Figure 4. ^{15}N−^{1}H HSQC spectrum of MMP-12 catalytic domain in the absence (A) and in the presence (B) of compound **4** (equimolar concentration). The two spectra are superimposed to highlight the cross-peak shifts (C). The ternary complex formation Avidin-BTI-MMP is seen in panel D where most of the cross-peaks disappeared.

Two different approaches based on NMR spectroscopy and on surface plasmon resonance (SPR) were followed to demonstrate the ternary Avidin-BTI-MMP interaction. Several NMR parameters are strongly influenced by the molecular weight and by the dynamical properties of the investigated macromolecules. Classical NMR experiments such as ^{15}N−^{1}H HSQC usually performed to investigate biomolecules up to 30−40 kDa are inefficient for larger systems due to the fast transverse relaxation rate that broaden the signals beyond the detection threshold (*48*). Therefore, NH resonances can act as probes to investigate the formation of large protein−protein complexes (*49*). In the present case, the evolution of the NH signals of the ^{15}N MMP-12 catalytic domain complexed with the BTI **4** in ^{15}N−^{1}H HSQC spectra was exploited to monitor the interaction with nonlabeled avidin, given that the binding of the biotin moiety to one of the four binding sites on the tetrameric avidin should provide a 87 kDa complex. Since multiple binding for each avidin molecule may occur, even larger protein complexes are expected in solution. As shown in Figure 4 (panel D), the addition of an equimolar solution of the 65 kDa avidin to a solution of the ^{15}N-labeled catalytic domain of MMP-12 complexed with the BTI **4** caused the complete disappearance of all NH cross-peaks without any precipitation of the sample.

To exclude the presence of aspecific protein−protein interactions, avidin was added to a solution containing 200 μM of NNGH-inhibited-MMP-12 catalytic domain: in this case, no changes were detected in the HSQC spectra. Therefore, we can reasonably conclude that the strong protein−protein interaction, monitored by the ^{15}N−^{1}H HSQC experiments, is mediated by the BTI **4** which is able to bind MMP-12 and avidin and to prevent, at the same time, an extensive reciprocal reorientation of the complex subunits. Although NMR data allowed us to ascertain that **4** does bind both avidin and MMP-12 simultaneously, the micromolar concentrations used for these experiments do not provide information on how this simultaneous interaction may affect the nanomolar affinity of the inhibitor to MMP-12. Indeed, possible steric effects related to the presence of the hemopexin domain need to be evaluated to understand the real binding capability of the probe toward functionally active enzymes (*50*). In this respect, the availability of the active full-length MMP-12 allowed us to ascertain the efficiency of the biotinylated inhibitor to bind simultaneously avidin and the physiologically active enzyme and to quantify the effect of the hemopexin domain on the affinity constant.

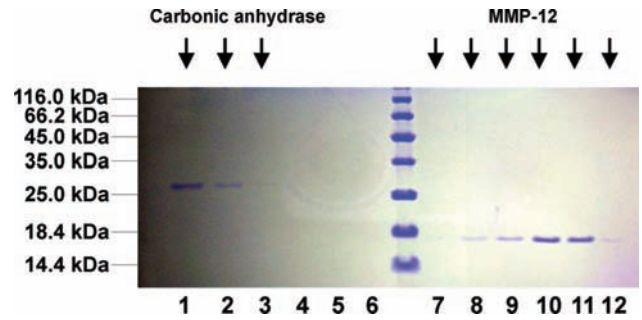

Figure 5. SDS PAGE analysis of the fractions shows an effective chromatographic separation of MMP-12 and carbonic anhydrase loaded on a monomeric avidin-bound column.

Surface plasmon resonance (SPR) is widely applied to investigate protein−protein and protein−ligand interactions. Information on affinity constant, on binding kinetics, as well as on binding enthalpy can be quickly obtained by using small

amounts of protein samples. In particular, the sensitivity of the SPR technique permits the investigation of high-affinity interactions and monitoring the formation of ternary complexes. SPR analysis was carried out using a ProteOn XPR36 parallel array biosensor equipped with avidin sensor chips (NLC). This chip has an avidin-coated surface that can be used to immobilize biotinylated molecules and macromolecules (*51*). In our study, BTI **4** was immobilized on channels 1−5 of the chip by injecting PBS-T buffered solutions of the biotinylated molecule at different concentrations. The sixth channel was left blank. The assay was performed by injecting solutions of the full-length MMP-12 on the chip channels and fitting the sensorgrams at four different concentrations. The measured K_D (4.6 ± 0.3 nM) (Supporting Information Figure S2) was comparable to the fluorimetric K_i measured for **4** vs the isolated catalytic domain of MMP-12 (BTI **4**−MMP-12 complex).

The employment of bifuctional ligand BTI **4** for the selective collection of matrix metalloproteinases from biological fluids has been evaluated by using a monomeric avidin-bound column (Pierce). An amount of 2.5 mg of BTI **4** was dissolved in 8.1 mL of Tris-buffer, and the solution (50 uL) was mixed with the same volume of an equimolar sample of MMP-12 (0.4 mM) dissolved into Tris buffer; 25 uL of the mixture so obtained was added to 50 uL of a solution of carbonic anhydrase from erythrocytes (0.1 mM in Tris-buffer). A monomeric avidin-bound column (0.6 mL of settled gel) was loaded with the solution of BTI **4**, MMP-12, and carbonic anhydrase; then, it was first eluted with 1.4 mL of Tris-buffer and subsequently with a solution of NNGH (1 mM, Tris buffer). Relying on the strong avidin−biotin interaction, the column blocked BTI **4**−MMP-12 complex, while carbonic anhydrase was completely washed out. Addition of nanomolar inhibitor NNGH displaced BTI **4** complexed to MMP-12, and the latter was so eluted and separated from carbonic anhydrase (Figure 5).

In summary, the present structure-based design led to the development of a potent biotin probe to bind matrix metalloproteinases for possible application in vitro and in vivo. The structural requirements defined through the analysis of the X-ray structures allowed selection of the position on the scaffold where the linker could be introduced and the correct length of the biotinylated tag. As defined by NMR analysis, the origin of the larger affinity observed for BTI **4** is a better fit of the selected scaffold in the catalytic pocket rather than additive interactions of the linker on the protein surface. The enzymatic assay demonstrated a nanomolar to low micromolar (MMP-1) affinity of **4** not only for MMP-12 but also for all the MMPs investigated. Furthermore, the evolution of the $^{15}N-^{1}H$ HSQC spectra upon the addition of unlabeled avidin to solution of ^{15}N MMP-12 clearly showed that the fourteen-member spacer used to link the biotin unit to carboxylic aryl sulfonamide inhibitor **1** ensures the simultaneous binding of the two proteins without permitting large interprotein mobility. SPR analyses clearly showed the ability of **4** to bind the functional active enzyme MMP-12 and avidin side-by-side. This simultaneous interaction did not affect negatively the nanomolar affinity of inhibitor **4** for MMP-12, given that the SPR data nicely reproduced the fluorimetric values measured for the BTI **4**−MMP-12 complex.

ACKNOWLEDGMENT

This work was supported by EC (Projects: MEST-CT-2004-504391, Integrated Project - SPINE2-COMPLEXES no 031220, Nano4Drugs no LSHB-CT-2005-019102; SFMET no 201640), by MIUR (FIRB Prot. RBLA032ZM7; FIRB Prot. RBIP06LSS2), Ente Cassa di Risparmio di Firenze, Genexpress.

Supporting Information Available: Protein cloning, expression and purification, X-ray data, details of fluorimetric assays and synthesis and characterization of compounds **1**−**3** and **11** are included. This material is available free of charge via the Internet at http://pubs.acs.org.

LITERATURE CITED

(1) Giepmans, B. N. G., Adams, S. R., Ellisman, M. H., and Tsien, R. Y. (2006) The fluorescent toolbox for assessing protein location and function. *Science 312*, 217–224.

(2) Blundell, T. L., Jhoti, H., and Abell, C. (2002) High-throughput crystallography for lead discovery in drug design. *Nat. Rev. Drug Discoery 1*, 45–54.

(3) Johnson, S. L., and Pellecchia, M. (2006) Structure- and fragment-based approaches to protease inhibition. *Curr. Top. Med. Chem. 6*, 317–329.

(4) Heckmann, D., Meyer, A., Marinelli, L., Zahn, G., Stragies, R., and Kessler, H. (2007) Probing integrin selectivity: rational design of highly active and selective ligands for the α 5β1 and α5β3 integrin receptor. *Angew. Chem., Int. Ed. 46*, 3571–3574.

(5) Jahnke, W., Blommers, M. J., Fernandez, C., Zwingelstein, C., and Amstutz, R. (2005) Strategies for the NMR-based identification and optimization of allosteric protein kinase inhibitors. *ChemBioChem 6*, 1607–1610.

(6) Page-McCaw, A., Ewald, A. J., and Werb, Z. (2007) Matrix metalloproteinases and the regulation of tissue remodelling. *Nat. Rev. Mol. Cell Biol. 8*, 221–233.

(7) Parks, W. C., Wilson, C. L., and Lopez-Boado, Y. S. (2004) Matrix metalloproteinases as modulators of inflammation and innate immunity. *Nat. Rev. Immunol. 4*, 617–629.

(8) D'Alessio, S., Fibbi, G., Cinelli, M., Guiducci, S., Del Rosso, A., Margheri, F., Serrati, S., Pucci, M., Kahaleh, B., Fan, P. S., Annunziato, F., Cosmi, L., Liotta, F., Matucci-Cerinic, M., and Del Rosso, M. (2004) Matrix metalloproteinase 12-dependent cleavage of urokinase receptor in systemic sclerosis microvascular endothelial cells results in impaired angiogenesis. *Arthritis Rheum. 50*, 3275–3285.

(9) Boire, A., Covic, L., Agarwal, A., Jacques, S., Sherifl, S., and Kuliopulos, A. (2005) PAR1 is a matrix metalloprotease-1 receptor that promotes invasion and tumorigenesis of breast cancer cells. *Cell 120*, 303–313.

(10) Fragai, M., and Nesi, A. (2007) Substrate specificities of matrix metalloproteinase 1 in PAR-1 exodomain proteolysis. *ChemBioChem 8*, 1367–1369.

(11) Knauper, V., Will, H., Lopez-Otin, C., Smith, B., Atkinson, S. J., Stanton, H., Hembry, R. M., and Murphy, G. (1996) Cellular mechanisms for human procollagenase-3 (MMP-13) activation. Evidence that MT1-MMP (MMP-14) and gelatinase a (MMP-2) are able to generate active enzyme. *J. Biol. Chem. 271*, 17124–17131.

(12) Morrison, C. J., and Overall, C. M. (2006) TIMP Independence of matrix metalloproteinase (MMP)-2 activation by membrane type 2 (MT2)-MMP is determined by contributions of both the MT2-MMP catalytic and hemopexin C domains. *J. Biol. Chem. 281*, 26528–26539.

(13) Ra, H. J., and Parks, W. C. (2007) Control of matrix metalloproteinase catalytic activity. *Matrix Biol. 26*, 587–596.

(14) Overall, C. M., Tam, E., McQuibban, G. A., Morrison, C., Wallon, U. M., Bigg, H. F., King, A. E., and Roberts, C. R. (2000) Domain interactions in the gelatinase A· TIMP-2· MT1-MMP activation complex: the ectodomain of the 44-kDa form of membrane type-1 matrix metalloproteinase does not modulate gelatinase A activation. *J. Biol. Chem. 275*, 39497–39506.

(15) Fingleton, B. (2007) Matrix metalloproteinases as valid clinical targets. *Curr. Pharm. Des. 13*, 333–346.

(16) Skiles, J. W., Gonnella, N. C., and Jeng, A. Y. (2004) The design, structure, and clinical update of small molecular weight matrix metalloproteinase inhibitors. *Curr. Med. Chem. 11*, 2911–2977.

(17) Egeblad, M., and Werb, Z. (2002) New functions for the matrix metalloproteinases in cancer progression. *Nat. Rev. Cancer 2*, 161–174.

(18) Bremer, C., Tung, C. H., Bogdanov, A., and Weissleder, R. (2002) Imaging of differential protease expression in breast cancers for detection of aggressive tumor phenotypes. *Radiology 222*, 814–818.

(19) Lepage, M., Dow, W. C., Melchior, M., You, Y., Fingleton, B., Quarles, C. C., Pepin, C., Gore, J. C., Matrisian, L. M., and McIntyre, J. O. (2007) Non invasive detection of matrix metalloproteinase activity in vivo using a novel magnetic resonance imaging contrast agent with a solubility switch. *Mol. Imaging 6*, 393–403.

(20) David, A., Steer, D., Bregant, S., Devel, L., Makaritis, A., Beau, F., Yiotakis, A., and Dive, V. (2007) Cross-linking yield variation of a potent matrix metalloproteinase photoaffinity probe and consequences for functional proteomics. *Angew. Chem., Int. Ed. 46*, 3275–3277.

(21) Saghatelian, A., Jessani, N., Joseph, A., Humphrey, M., and Cravatt, B. F. (2004) Activity-based probes for the proteomic profiling of metalloproteases. *Proc. Natl. Acad. Sci. U.S.A. 101*, 10000–10005.

(22) Bremer, C., Tung, C. H., and Weissleder, R. (2001) In vivo molecular target assessment of matrix metalloproteinase inhibition. *Nat. Med. 7*, 743–748.

(23) Faust, A., Waschkau, B., Waldeck, J., Holtke, C., Breyholz, H. J., Wagner, S., Kopka, K., Heindel, W., Schafers, M., and Bremer, C. (2008) Synthesis and evaluation of a novel fluorescent photoprobe for imaging matrix metalloproteinases. *Bioconjugate Chem. 19*, 1001–1008.

(24) Wagner, S., Breyholz, H. J., Law, M. P., Faust, A., Holtke, C., Schroer, S., Haufe, G., Levkau, B., Schober, O., Schafers, M., and Kopka, K. (2007) Novel fluorinated derivatives of the broad-spectrum MMP inhibitors N-hydroxy-2(R)-[[(4-methoxyphenyl)sulfonyl](benzyl)- and (3-picolyl)-amino]-3-methyl-butanamide as potential tools for the molecular imaging of activated MMPs with PET. *J. Med. Chem. 50*, 5752–5764.

(25) Wagner, S., Breyholz, H. J., Faust, A., Holtke, C., Levkau, B., Schober, O., Schafers, M., and Kopka, K. (2006) Molecular imaging of matrix metalloproteinases in vivo using small molecule inhibitors for SPECT and PET. *Curr. Med. Chem. 13*, 2819–2838.

(26) Uttamchandani, M., Wang, J., Li, J. Q., Hu, M. Y., Sun, H. Y., Chen, K. Y. T., Liu, K., and Yao, S. Q. (2007) Inhibitor fingerprinting of matrix metalloproteases using a combinatorial peptide hydroxamate library. *J. Am. Chem. Soc. 129*, 7848–7858.

(27) Bertini, I., Calderone, V., Fragai, M., Luchinat, C., and Maletta, M. (2006) Snapshots of the reaction mechanism of matrix metalloproteinases. *Angew. Chem., Int. Ed. 45*, 7952–7955.

(28) Bertini, I., Calderone, V., Fragai, M., Luchinat, C., Mangani, S., and Terni, B. (2003) X-ray structures of binary and ternary enzyme-product-inhibitor complexes of matrix metalloproteinases. *Angew. Chem., Int. Ed. 42*, 2673–2676.

(29) Bertini, I., Calderone, V., Fragai, M., Luchinat, C., Mangani, S., and Terni, B. (2004) Crystal structure of the catalytic domain of human matrix metalloproteinase 10. *J. Mol. Biol. 336*, 707–716.

(30) Bertini, I., Calderone, V., Fragai, M., Giachetti, A., Loconte, M., Luchinat, C., Maletta, M., Nativi, C., and Yeo, K. (2007) Exploring the subtleties of drug-receptor interactions: the case of matrix metalloproteinases. *J. Am. Chem. Soc. 129*, 2466–2475.

(31) Bertini, I., Fragai, M., Lee, Y.-M., Luchinat, C., and Terni, B. (2004) Paramagnetic metal ions in ligand screening: The CoII matrix metalloproteinase 12. *Angew. Chem., Int. Ed. 43*, 2254–2256.

(32) Calderone, V., Fragai, M., Luchinat, C., Nativi, C., Richichi, B., and Roelens, S. (2006) A high-affinity carbohydrate-containing inhibitor of matrix metalloproteinases. *ChemMedChem 1*, 598–601.

(33) Bertini, I., Fragai, M., Giachetti, A., Luchinat, C., Maletta, M., Parigi, G., and Yeo, K. J. (2005) Combining in silico tools and NMR data to validate protein−ligand structural models: application to matrix metalloproteinases. *J. Med. Chem. 48*, 7544–7559.

(34) Fragai, M., Nativi, C., Richichi, B., and Venturi, C. (2005) Design in silico, synthesis and binding evaluation of a carbohydrate-based scaffold for structurally novel inhibitors of matrix metalloproteinases. *ChemBioChem 6*, 1345–1349.

(35) Mannino, C., Nievo, M., Machetti, F., Papakyriakou, A., Fragai, M., and Guarna, A. (2006) Synthesis of bicyclic molecular scaffolds (BTAa): An investigation towards new selective MMP-12 inhibitors. *Bioorg. Med. Chem. 14*, 7392–7403.

(36) Agrawal, A., Romero-Perez, D., Jacobsen, J. A., Villarreal, F. J., and Cohen, S. M. (2008) Zinc-binding groups modulate selective inhibition of MMPs. *ChemMedChem 3*, 812–820.

(37) Puerta, D. T., and Cohen, S. M. (2004) A bioinorganic perspective on matrix metalloproteinase inhibition. *Curr. Top. Med. Chem. 4*, 1551–1573.

(38) Pikul, S., Ohler, N. E., Ciszewski, G., Laufersweiler, M. C., Almstead, N. G., De, B., Natchus, M. G., Hsieh, L. C., Janusz, M. J., Peng, S. X., Branch, T. M., King, S. L., Taiwo, Y. O., and Mieling, G. E. (2001) Potent and selective carboxylic acid-based inhibitors of matrix metalloproteinases. *J. Med. Chem. 44*, 2499–2502.

(39) Wang, X. Q., Choe, Y. C., Craik, C. S., and Ellman, J. A. (2002) Design and synthesis of novel inhibitors of gelatinase B. *Bioorg. Med. Chem. Lett. 12*, 2201–2204.

(40) Auge, F., Hornebeck, W., Decarme, M., and Laronze, J. Y. (2003) Improved gelatinase a selectivity by novel zinc binding groups containing galardin derivatives. *Bioorg. Med. Chem. Lett. 13*, 1783–1786.

(41) Bertini, I., Calderone, V., Cosenza, M., Fragai, M., Lee, Y.-M., Luchinat, C., Mangani, S., Terni, B., and Turano, P. (2007) Solution structure of inhibitor-free human metalloelastase (MMP-12) indicates an internal conformational adjustment. *J. Mol. Biol. 374*, 1333–1344.

(42) Bhaskaran, R., Palmier, M. O., Bagegni, N. A., Liang, X. Y., and Van Doren, S. R. (2007) Solution structure of inhibitor-free human metalloelastase (MMP-12) indicates an internal conformational adjustment. *J. Mol. Biol. 374*, 1333–1344.

(43) Devel, L., Rogakos, V., David, A., Makaritis, A., Beau, F., Cuniasse, P., Yiotakis, A., and Dive, V. (2006) Development of selective inhibitors and substrate of matrix metalloproteinase-12. *J. Biol. Chem. 281*, 11152–11160.

(44) Tochowicz, A., Maskos, K., Huber, R., Oltenfreiter, R., Dive, V., Yiotakis, A., Zanda, M., Bode, W., and Goettig, P. (2007) Crystal structures of MMP-9 complexes with five inhibitors: contribution of the flexible Arg424 side-chain to selectivity. *J. Mol. Biol. 371*, 989–1006.

(45) Lovejoy, B., Welch, A. R., Carr, S., Luong, C., Broka, C., Hendricks, R. T., Campbell, J. A., Walker, K. A. M., Martin, R., Van Wart, H., and Browner, M. F. (1999) Crystal structures of MMP-1 and -13 reveal the structural basis for selectivity of collagenase inhibitors. *Nat. Struct. Biol. 6*, 217–221.

(46) Sabatino, G., Chinol, M., Paganelli, G., Papi, S., Chelli, M., Leone, G., Papini, A. M., De Luca, A., and Ginanneschi, M. (2003) A new biotin derivative-DOTA conjugate as a candidate for pretargeted diagnosis and therapy of tumors. *J. Med. Chem. 46*, 3170–3173.

(47) Canales-Mayordomo, A., Fayos, R., Angulo, J., Ojeda, R., Martin-Pastor, M., Nieto, P. M., Martin-Lomas, M., Lozano, R., Gimenez-Gallego, G., and Jimenez-Barbero, J. (2006) Backbone dynamics of a biologically active human FGF-1 monomer, complexed to a hexasaccharide heparin-analogue, by 15N NMR relaxation methods. *J. Biomol. NMR 35*, 225–239.

(48) Pellecchia, M., Sebbel, P., Hermanns, U., Wuthrich, K., and Glockshuber, R. (1999) Pilus chaperone FimC-adhesin FimH interactions mapped by TROSY-NMR. *Nat. Struct. Biol. 6*, 336–339.

(49) D'Silva, L., Ozdowy, P., Krajewski, M., Rothweiler, U., Singh, M., and Holak, T. A. (2005) Monitoring the effects of antagonists

on protein-protein interactions with NMR spectroscopy. *J. Am. Chem. Soc. 127*13220–13226.
(50) Bertini, I., Calderone, V., Fragai, M., Jaiswal, R., Luchinat, C., Melikian, M., Mylonas, E., and Svergun, D. (2008) Evidence of reciprocal reorientation of the catalytic and hemopexin-like domains of full-length MMP-12. *J. Am. Chem. Soc. 130*, 7011–7021.
(51) Bravman, T., Bronner, V., Lavie, K., Notcovich, A., Papalia, G. A., and Myszka, D. G. (2006) Exploring "one-shot" kinetics and small molecule analysis using the ProteOn XPR36 array biosensor. *Anal. Biochem. 358*, 281–288.

BC8003827